



LIBRARY
COPY

THE MECHANISM OF LIQUID PHASE RESISTANCE
TO GAS ABSORPTION IN A PACKED COLUMN

by

CARY JUDSON KING, III

B.E., Yale University (1956)

S.M., Massachusetts Institute of Technology (1958)

SUBMITTED IN PARTIAL FULFILLMENT OF THE
REQUIREMENTS FOR THE DEGREE OF
DOCTOR OF SCIENCE

at the

MASSACHUSETTS INSTITUTE OF TECHNOLOGY

(1960)

Signature redacted

Signature of Author:

Department of Chemical Engineering
April 21, 1960

Signature of Professor in
Charge of Research:

Signature redacted

J. Edward Vivian

Signature of Chairman,
Departmental Committee on
Graduate Students:

Glenn C. Williams

✓

THE MECHANISM OF LIQUID PHASE RESISTANCE
TO GAS ABSORPTION IN A PACKED COLUMN

by

CARY JUDSON KING, III

Submitted for the degree of Doctor of Science in the Department of
Chemical Engineering, April 21, 1960.

ABSTRACT

Desorption of five slightly soluble gases from water into air was carried out on 1-1/2 inch Raschig rings for five different sets of flow conditions. Since water and air flow rates and temperatures at all points in the column were held constant during a given set of runs, it was possible to determine the effect of solute liquid phase diffusivity alone on the mass transfer process.

The results showed that the liquid phase volumetric mass transfer coefficient varies with liquid phase diffusivity to the 0.5 power, as best as can be determined experimentally, at typical industrial flow conditions corresponding to air rates from 26 to 91% of flooding. This indicates that penetration theory provides the mechanism of the liquid phase resistance to mass transfer at these flow conditions. An important consequence of this finding is that short wetted wall columns and laminar jets may be taken as appropriate models of the liquid phase behavior for laboratory study of complex absorption processes.

Before carrying out the packed column study it was necessary to measure the diffusivities in water solution of the five solute gases: Helium, hydrogen, oxygen, carbon dioxide, and propylene. The gases were found to vary by a factor of 4.4 in diffusivity, which was sufficient for the purpose of the experiment.

The penetration theory behavior of the liquid phase, and also possible unsteady-state behavior of the gas phase, throw doubt on the applicability of two film additivity to a packed column. The additivity concept serves as a means of predicting the absorption rate of a gas of intermediate solubility from independent studies of a liquid phase controlled process and a gas phase controlled one. Iterative mathematical solutions for simplified countercurrent cases show that the two film additivity relation is reliable to within 10% for a single surface lifetime. A much greater effect comes from the distribution of liquid surface lifetimes in a packed column. In many cases it is possible for

analysis to divide the liquid surface into two portions: One active, engaged in reaching a certain lifetime, and obeying two film additivity; the other dead, and inactive for any sort of liquid phase transfer.

A dimensional equation for the liquid phase mass transfer coefficient of the active surface was derived, based on the mechanism of penetration behavior and a knowledge of the hydrodynamics of falling films:

$$\frac{k_L^*}{D_L} = \alpha \left(\frac{4L}{a_e \mu} \right)^{0.6} \left(\frac{\mu}{\rho D_L} \right)^{0.5} \left(\frac{\rho^2 g}{\mu^2} \right)^{1/6}$$

In order to use the equation one must know a_e , the active interfacial area, from an independent source.

Department of Chemical Engineering
Massachusetts Institute of Technology
Cambridge 39, Massachusetts

April 21, 1960

Professor Philip Franklin
Secretary of the Faculty
Massachusetts Institute of Technology
Cambridge 39, Massachusetts

Dear Sir:

In accordance with the regulations of the Faculty, I herewith submit a thesis, entitled "The Mechanism of Liquid Phase Resistance to Gas Absorption in a Packed Column," in partial fulfillment of the requirements for the degree of Doctor of Science in Chemical Engineering from the Massachusetts Institute of Technology.

Respectfully submitted,

Signature redacted

Cary Judson King, (III)

ACKNOWLEDGMENT

I wish to thank Professor J. Edward Vivian for his interest and advice throughout the course of this thesis. Messrs. Henry Chasen and Al Merrill of the Department of Chemical Engineering were of great assistance in the construction and maintenance of the equipment. Messrs. James Donovan and James Baird of Artizan Metals, Inc., of Waltham, Massachusetts, kindly donated the packed column. Fellowship aid was supplied throughout the entire course of the study by the General Electric Educational & Charitable Fund.

I am particularly grateful to Mr. Allan Whitney who performed the final typing.

Finally, I should like to acknowledge the very real contributions of my wife, Jeanne, who put up with strange and long working hours, painstakingly typed the draft, and sustained me over the rougher stretches.

TABLE OF CONTENTS

	<u>Page</u>
Chapter 1	SUMMARY. 1
Chapter 2	INTRODUCTION 12
2.1	Theoretical Background 13
2.1.1	Two Film Theory 13
2.1.2	Penetration Theory. 19
2.1.3	Other Theories for Liquid Phase Mechanism 23
2.1.4	Packed Tower Design 28
2.2	Experimental Background. 29
2.2.1	Liquid Phase Resistance 30
2.2.2	Peaceman's Criticism. 32
2.2.3	Gas Phase Resistance. 33
2.2.4	Models of the Liquid Phase Absorption Process 34
2.2.5	Additivity of Resistances 36
2.2.6	Equilibrium at the Interface. 38
2.3	Purpose of This Thesis 39
Chapter 3	APPARATUS AND PROCEDURE. 42
3.1	Choice of Experiment 42
3.2	Design of Apparatus. 43
3.3	Experimental Procedure 50
Chapter 4	EXPERIMENTAL RESULTS 52
4.1	Diffusivity Measurements 52
4.2	Packed Tower Data. 52
4.2.1	Desorption Results. 52
4.2.2	Pressure Drop Results 58
Chapter 5	DISCUSSION AND APPLICATION OF RESULTS. 60
5.1	Analysis of Experimental Conditions and Calculational Assumptions. 60
5.1.1	Degree of Subordination of Gas Phase Resistance 60
5.1.2	Coefficient of Desorption vs. Coefficient of Absorption. 63
5.1.3	Effects of Pool Height, Repacking, and Packed Height. 68
5.1.4	Other Sources of Error. 77

	<u>Page</u>
5.2 Analysis of Experimental Results	78
5.2.1 Regimes of Operation	79
5.2.2 Agreement with Previous Work	81
a. Effect of Diffusivity	81
b. Effect of Bulk Liquid and Gas Flow Rates	85
c. Effect of Temperature	87
5.2.3 Effect of One Solute Gas Upon Another	90
5.3 Mechanism of Liquid Phase Resistance	90
5.4 Applications of Experimental Results	94
5.4.1 Chemical Reaction Systems	95
5.4.2 Additivity of Resistances	99
5.4.3 Dimensionless Correlation	103
5.4.4 Mechanisms of Models	104
Chapter 6 CONCLUSIONS	106
Chapter 7 RECOMMENDATIONS	108

APPENDIX

Chapter 8 ADDITIVITY OF RESISTANCES	111
8.1 Theoretical Survey of Nature of Additivity in Penetration Systems	111
8.1.1 Single Lifetime - Constant Stagnant Film Gas Resistance	115
8.1.2 Single Lifetime - Countercurrent Problem	121
a. Laminar Boundary Layer	135
b. Highly Turbulent Boundary Layer	150
8.1.3 Single Lifetime - Co-current Cases	156
8.1.4 Distribution of Lifetimes	158
8.2 Re-examination of Literature Studies of Additivity	168
8.2.1 Stirred Flask	168
8.2.2 Packed Towers	175
Chapter 9 DIMENSIONLESS CORRELATION	200
a. Short Wetted Wall Column	204
b. Packed Tower	210
Chapter 10 INTEGRATION OF SECOND ORDER, INFINITELY FAST, IRREVERSIBLE REACTION OVER PACKED TOWER HEIGHT	231
Chapter 11 MECHANISM OF STIRRED FLASK ABSORPTION	234

	<u>Page</u>
Chapter 12	EFFECT OF ONE SOLUTE GAS UPON ANOTHER. 238
Chapter 13	DETAILS OF APPARATUS AND PROCEDURE 249
13.1	Apparatus. 249
13.1.1	Tower and Water System 249
13.1.2	Air System 256
13.1.3	Auxiliaries. 258
13.2	Procedure. 259
Chapter 14	DIFFUSIVITY MEASUREMENTS 263
	Outline. 263
Chapter 15	ANALYTICAL TECHNIQUES. 330
15.1	Difficulties in Analyzing Solutions of Sparingly Soluble Gases in Water 330
15.2	Oxygen 331
15.3	Carbon Dioxide 335
15.4	Helium, Hydrogen, and Propylene. 340
15.4.1	Separation Apparatus 342
15.4.2	Chromatographic Analysis 347
15.5	Potassium Chloride 353
Chapter 16	METHOD OF TREATMENT OF DATA. 356
16.1	Method of Calculating Transfer Coefficients. 356
16.1.1	Helium, Hydrogen, and Propylene. 358
16.1.2	Oxygen 359
16.1.3	Carbon Dioxide 368
16.1.4	Temperature Correction 371
16.2	Method of Averaging and Plotting Results 371
16.2.1	Plots of $(H.T.U.)_{OL}$ vs. D_L 371
16.2.2	Plots of $\log (H.T.U.)_{OL}$ vs. T 378
16.3	Sample Calculations. 379
16.3.1	Diffusivity. 379
16.3.2	Helium $(H.T.U.)_{OL}$ 381
16.3.3	Oxygen $(H.T.U.)_{OL}$ 383
16.3.4	Carbon Dioxide $(H.T.U.)_{OL}$ 385

	<u>Page</u>
16.3.5	Least Squares Fit of Log (H.T.U.) vs. Log D_L Plot 388
16.3.6	Air Flow Rates 391
	a. General Formulae 391
	b. Calculation of Desired Air Manometer Pressure Drop for a Specific Run. 393
Chapter 17	SUMMARIZED DATA AND CALCULATED RESULTS. 396
Chapter 18	RE-EXAMINATION OF THE OXYGEN DATA OF HOLLOWAY 410
Chapter 19	MISCELLANEOUS PLOTS 424
	a. Temperature Correction to $(H.T.U.)_L$ 424
	b. Oxygen Solubility. 425
	c. Calibration of Water Orifices. 426
Chapter 20	NOMENCLATURE. 427
Chapter 21	REFERENCES. 436
Chapter 22	BIOGRAPHICAL NOTE 446

LIST OF FIGURES

<u>Figure No.</u>		<u>Page</u>
3.1	Packed Column Assembly	47
3.2	Flow Diagram of Apparatus	48
4.1	(H.T.U.) _{OL} vs. D_L at $G = 900$: Best Slopes	53
4.2	(H.T.U.) _{OL} vs. D_L at $L = 2100$: Best Slopes	53
4.3	(H.T.U.) _{OL} vs. D_L at $G = 900$: Best 0.5 Slope	54
4.4	(H.T.U.) _{OL} vs. D_L at $L = 2100$: Best 0.5 Slope	54
4.5	K_{La} vs. D_L at $G = 900$	55
4.6	K_{La} vs. D_L at $L = 2100$	55
4.7	(H.T.U.) _{OL} vs. T	56
4.8	Loading and Flooding Rates in Column	59
5.1	Average k_L over Short Column	74
5.2	Hold-up On 1-1/2 Inch Ceramic Raschig Rings	82
5.3	Agreement With Data Of Sherwood & Holloway: Effect of Diffusivity	84
5.4	Agreement With Data Of Sherwood & Holloway: Effect of Air Rate	84
5.5	Agreement With Data Of Sherwood & Holloway: Effect of Water Rate	86
5.6	Agreement With Other Authors: Effect of Temperature	88
8.1	Additivity Deviation For Liquid Penetration And Stagnant, No Hold-up Gas Film	120
8.2	Local Variation of k_L' For Liquid Penetration And Stagnant, No Hold-up Gas Film	122
8.3	Variation of Local Heat Transfer Coefficient in Flow Through Tubes	129
8.4	Additivity Solution: Liquid Penetration & Insensitive Laminar Gas Boundary Layer; $R = 1$	137
8.5	Variation of Local Coefficients: Liquid Penetration & Insensitive Laminar Gas Boundary Layer; $R = 1$	140
8.6	Variation of Local Coefficients: Liquid Penetration & Insensitive Laminar Gas Boundary Layer; $R = 1$	141
8.7	Additivity Solution: Liquid Penetration & Insensitive Laminar Gas Boundary Layer; $R = 2$	148
8.8	Additivity Solution: Liquid Penetration & Insensitive Laminar Gas Boundary Layer; $R = 0.5$	148
8.9	Additivity Solution: Liquid Penetration & Insensitive Laminar Gas Boundary Layer; $R = 0.2$	149
8.10	Additivity Solution: Liquid Penetration & Insensitive Turbulent Gas Boundary Layer; $R = 2$	149
8.11	Additivity Solution: Liquid Penetration & Insensitive Turbulent Gas Boundary Layer; $R = 1$	151
8.12	Additivity Solution: Liquid Penetration & Insensitive Turbulent Gas Boundary Layer; $R = 0.5$	151

8.13	Additivity Solution: Countercurrent Insensitive Laminar Boundary Layers; $R = 1$	154
8.14	j_D Correlation For Mass Transfer From Packing To Gas Phase.	177
8.15	Comparison Of One Inch Carbon Ring Data	184
8.16	Data of Houston & Walker.	187
8.17	Values of f Derived From Data Of Houston & Walker	191
8.18	Vaporization & Absorption Data for One Inch Ceramic Rings .	193
8.19	Shulman Correlation Of f vs. Hold-up.	196
9.1	Correlation of Data of Holloway	221
9.2	Shulman Correlation for Data of Holloway.	222
12.1	Concentration Profile Near Interface In Case Of Low Diffusivity Desorbing Solute.	241
3.1	Packed Column Assembly.	250
3.2	Flow Diagram of Apparatus	251
14.1	Diaphragm Cell For Measuring Diffusivities.	277
14.2	Data Of Gertz and Loeschke Plotted vs. Present Diffusivity Values.	321
15.1	Gas Separation Apparatus.	343
15.2	Sampling Facilities for Chromatograph	349
15.3	Typical Peak for Helium & Hydrogen	354
15.4	Typical Peak for Propylene.	354
16.1	Driving Force Profile for Oxygen Run.	362
16.2	N.T.U. Integral for Oxygen Runs	363
17.1	Logarithmic Plot of Tower Pressure Drop vs. Air Rate.	405
18.1	Heat Effects from Humidification & Heat Transfer.	416
18.2	Driving Force Profile for Holloway Run No. 47	418
18.3	N.T.U. Integral for Holloway Run No. 47	419
19.1	Temperature Correction to $(H.T.U.)_{OL}$	424
19.2	Oxygen Solubility, Data of Winkler.	425
19.3	Calibration of Water Orifices	426

LIST OF TABLES

<u>Table No.</u>		<u>Page</u>
2.1	Theoretical Predictions Concerning the Effect of Solute Diffusivity on the Liquid Phase Coefficient of Absorption.	27
2.2	Constants Found by Sherwood and Holloway for Equation 2.2.1	31
4.1	Diffusivity Measurements.	52
4.2	Effects of Varying Column Height and Pool Height, and of Redumping Packing on (H.T.U.) _{OL} at 25°C	57
5.1	Summary of Literature Data for Oxygen Solubility in Water at 25°C	66
5.2	Corrections to be Applied to Oxygen (H.T.U.) _{OL} Results Corresponding to a -1% Error in Solubility Data	67
5.3	Conditions of Tower Operation	81
8.1	Numerical Solution of Countercurrent Insensitive Laminar Boundary Layer - Penetration Case for R = 1	138
8.2	Summary of Calculations of δ for Cases of Countercurrent Insensitive Laminar Boundary Layer.	150
8.3	Summary of Calculations of δ for Cases of Countercurrent Insensitive Highly Turbulent Boundary Layer	152
8.4	Deviations from Two Film Additivity Predicted by Two Lifetime Theory	165
8.5	Values of K_{La}/K_{Lfa} From Two Lifetime Theory For $\lambda = 5, 10,$ and ∞ (f Constant at 0.7).	167
8.6	Diffusivities of Various Solutes.	170
8.7	Recalculated Results of Goodgame & Sherwood	171
8.8	Recalculated Results of Whitman & Davis	174
8.9	Summary of Literature Studies of the Gas Phase Resistance for Common Packings, and Sources of Liquid Phase Coefficients (Air-Water System)	179
9.1	Values of α for Use in Equation 9.19.	226
14.1	Magnitude of Terms in Equation 14.5.23.	290
14.2	Determination of λ	295
14.3	Calibration of Cells.	296
14.4	Recalibration of Cells.	297
14.5	Experimental Diffusivity Determinations	298
14.6	Summary of Experimental Determinations.	300
14.7	Agreement of Diffusivities with the Literature.	302
14.8	ΔT_{max} And Lag As A Function Of Radius In An Infinitely Long Cell	308

<u>Table No.</u>		<u>Page</u>
14.9	Contact Time Ranges In Various Studies	325
17.1	Summary of Packed Column Desorption Data & Calculated Results	397
17.2	"Best" Values of Data	403
17.3	Least Squares Slopes of Plots	404
18.1	Re-calculation of Holloway's Part I Oxygen Data	420
18.2	Possible Corrections of Holloway's Oxygen Data for -1.0% Error Present In Winkler Data	421

CHAPTER I

SUMMARY

Background

Successful analysis of large scale mass transfer processes has to date been gained only through empirical means. Empirical correlations are useful and desirable when theoretical knowledge is absent, but they do have several shortcomings. One is completely sure of the effects of only those variables that have been varied independently of all others, and there are usually uncertainties in geometrical scale-up.

Many industrial absorption processes are carried out in packed columns in which a gas stream is contacted with a liquid that is flowing in layers over an irregular bed of solids. All existing correlations for mass transfer behavior in such a column are empirical. A knowledge of the actual mechanism of the transfer would be valuable for the two reasons mentioned above. Also when a complex absorption such as one involving simultaneous chemical reaction is to be accomplished, it is desirable to carry out either a mathematical analysis or a study on a small, laboratory scale model before building the final large scale equipment. The transfer mechanism of a model must be the same as that in the packed column. A mathematical analysis is, of course, also dependent on mechanism.

Several models of liquid phase absorption behavior in a packed

tower have been proposed, among them falling laminar or turbulent jets, short or long wetted wall columns, and stirred flasks. Each of these models is sufficiently different from the packed tower so that the liquid phase transfer mechanism may also be different. Laminar jets and short wetted wall columns have recently been shown conclusively to be representations of penetration theory (99, 155). A stirred flask or any more turbulent model on the other hand may possibly give more of a film or boundary layer behavior, corresponding to there being less motion and/or agitation at the liquid surface than in the bulk of the liquid. Indeed, recent Russian work has apparently shown that it is possible to obtain a liquid phase controlled process in a stirred flask that is completely independent of liquid phase diffusivity (74). It has frequently been claimed in the Russian literature that such a behavior is exactly that which occurs in a packed column at conditions of loading or near-flooding.

There exists, however, only one purported indication of the mechanism of liquid phase resistance to absorption in a packed column. Sherwood and Holloway (131), studying the desorption of various slightly soluble gases from water at different flow rates and temperatures, ascertained that the Nusselt mass transfer coefficient group varied with the Schmidt group to the 0.5 power, thus placing an exponent of 0.5 on the diffusivity in so far as it affects the coefficient of absorption. This would indicate that penetration theory applies to liquid phase

resistance, since other feasible mechanisms predict other exponents (between 0 and 1) on the diffusivity, or at least exponents that should vary with changing liquid or gas flow rates.

Peaceman (107), however, showed that Holloway's exponent on the Schmidt group was determined more by the effect of temperature than by the effect of diffusivity alone. He then showed that Holloway's data, when plotted at constant flow rates and temperature against Holloway's diffusivity values, gave an exponent of 0.37, known only at one very low set of flow conditions and reliant entirely upon his limited hydrogen desorption data. The exponent of 0.5 on Holloway's Schmidt group might not give the true effect of diffusivity if, for example, certain necessary variables such as surface tension or gravity acceleration had been left out of his dimensional analysis. The 0.37 exponent, in turn, depends greatly on the value of diffusivity used for hydrogen, and a range of nearly 100% exists in the literature for that value.

The experiment of desorbing slightly soluble gases from water remains a powerful tool for determining the effect of diffusivity on the liquid side resistance to gas absorption, and thus indicating the mechanism. The absorption or desorption of slightly soluble gases should be entirely liquid phase controlled. Slightly soluble gases in solution do not perceptibly affect the physical flow or spreading qualities of the solvent. They also give such low rates of transfer that, for reasonable values

of the ratio of gas to liquid stream flow rate, there should be no perceptible build-up of solute in the bulk gas phase. Thus a comparison of the mass transfer coefficients for desorption of various gases on the same packing at the same liquid and gas flow rates and at the same temperature should give the effect of only the liquid phase diffusivity of the solute. That then was the experiment chosen for this thesis: The desorption of solute gases of widely varying diffusivities from water into air in flow over commercial sized packing.

Experimental Procedure and Apparatus

There are few reliable values of diffusivities available in the literature for slightly soluble gases in water. It was therefore necessary to set up an apparatus for their determination. A glass diaphragm cell was chosen as the most reliable and proven method, even though the use of one necessitates that analyses be made of the solutions. Values of diffusivity in water at 25°C were obtained for propylene, carbon dioxide, oxygen, hydrogen and helium, with the following results:

<u>Gas</u>	<u>Diffusivity in Water at 25°C</u>
Propylene	$1.44 \times 10^{-5} \text{ cm}^2/\text{sec}$
Carbon Dioxide	2.00×10^{-5}
Oxygen	2.41×10^{-5}
Hydrogen	4.8×10^{-5}
Helium	6.3×10^{-5}

From this it may be seen that the solute gases exhibited a factor of 4.4 difference in diffusivity.

It was also necessary to establish analytical techniques for the five gases in water. Standard chemical analyses were employed for two: The Winkler method for oxygen and the barium hydroxide absorption technique for carbon dioxide. For the other three gases an apparatus was constructed which separated all the dissolved gas from a water sample through repeated spraying of the sample into a vacuum chamber. The extracted gas was then passed into a gas chromatograph. A nitrogen carrier was used for helium and hydrogen analyses, whereas a helium carrier was used for propylene analyses.

The packed tower employed for the study (Figure 3.1) was made of standard twelve inch pipe, so arranged that packed heights of either one or two feet could be attained. One and one-half inch ceramic Raschig rings were placed in the tower. All corrosible surfaces both in the tower and in the auxiliary equipment were coated with Tygon paint. Water was circulated continuously through copper tubing and rubber hose, while air was passed through once, with galvanized stovepipe conduits (Figure 3.2). The air was treated with steam and/or water in a spray tower to give a stream saturated at 25°C. It entered the bottom of the packing through four notched and capped brass pipes, discharging just above the level of a water pool kept in the bottom of the packing. The water entered

the top of the packing through 23 sealed downcomer tubes so arranged as to cover equal areas. These precautions were taken in order to minimize end transfer effects.

An experimental run was made by allowing the system to come to steady-state operation and then taking at least two sets of samples of the inlet and outlet water streams. These samples were analyzed as described above.

Seventy runs were made in all. Five different sets of flow conditions were studied in detail; they corresponded to different liquid to gas flow rate ratios and various percentages of the flooding gas rates (between 26% and 91%). By far the most runs were made at 25°C, although some were made at other temperatures. Runs were also made to check the effect of the height of packing and of the water pool, and to determine the effects of simultaneous transfer of two gases.

Experimental Results

Logarithmic plots of mass transfer coefficient versus solute diffusivity were made for each set of flow conditions (Figures 4.1 and 4.2). The points on the plots were each the median of the several results obtained for the particular solute at those flow conditions. The slopes presented below are those of the correlating straight lines on the

logarithmic plots. They were determined by a weighted least squares technique.

<u>Water Rate</u> (lb./hr.-sq.ft.)	<u>Air Rate</u> (lb./hr.-sq.ft.)	<u>% Of Flooding Air Rate</u>	<u>Slope</u>
2,100	900	56	0.50
5,000	900	73	0.54
10,000	900	91	0.53
2,100	285	26	0.48
2,100	1,400	80	0.53

The flow rates are on a basis of empty tower cross-sectional area.

The data of Sherwood and Holloway at a water rate of 2,000 lb./hr.-sq.ft., an air rate of 230 lb./hr.-sq.ft. and on one and one-half inch ceramic rings give a slope of 0.48 when plotted against the present diffusivities. Thus it appears that, within experimental error, the mass transfer coefficient for a liquid phase controlled desorption or absorption process in a packed tower varies with the 0.5 power of diffusivity. There is no evident confirmation of the Russian claim that the diffusivity has a lesser effect as flooding is approached.

The results, then, lend strong support to the application of penetration theory to the liquid phase transfer behavior in a packed tower. All liquid phase transfer is unsteady state with no apparent turbulences coming close enough to the liquid-gas interface to affect the diffusive process during the short lifetimes of liquid surface elements. To the extent that the exponent on diffusivity is constant

and equal to one-half, it is unlikely that any other feasible mechanical picture can predict the same results.

The apparent applicability of penetration theory also indicates that the short wetted wall column and the laminar jet are the most realistic of the present models of liquid phase behavior.

The effect of temperature on the volumetric liquid phase mass transfer coefficient ($k_L a$) was indicated by oxygen runs to be representable by

$$k_L a \sim e^{0.019T}$$

where T is Centigrade temperature. Hydrogen runs, which were much less accurate, placed the coefficient in the exponent at 0.016. An examination of these results along with recalculated values from Holloway's data and other literature results places the most reliable coefficient at 0.020.

Further Applications of Results

Classical two film theory gives for an absorption system in which the resistances of both phases are important

$$\frac{1}{K_L a} = \frac{1}{k_L a^*} + \frac{1}{H k_G a^*}$$

where $K_L a$ is the overall volumetric mass transfer coefficient based on liquid concentration driving forces, and $k_L a^*$ and $k_G a^*$ are the individual

volumetric coefficients of the liquid and gas phases respectively, measured independently of each other or with the resistance of the other phase suppressed. H is the Henry's Law solubility coefficient.

This equation, in order to be rigorously true, requires that there be a constant ratio of $Hk_G a^*$ to $k_L a^*$ at each and every point of interface. This obviously is not true for a system in which the liquid phase obeys penetration theory.

Numerical, iterative solutions were made for the transfer rate in several cases of a liquid obeying penetration theory in contact with a countercurrent gas phase showing a laminar or turbulent unsteady state behavior. For purposes of simplification the gas phase was considered to behave as a boundary layer with negligible hold-up (insensitive to past history) or, equivalently, as a thin stagnant film of varying thickness. Surprisingly enough the results show that the above additivity of resistances equation is always obeyed during a single contacting to within 10% for these cases. Similarly an analytical solution for a penetration theory liquid phase in contact with a gas phase showing stagnant film behavior (with constant film thickness) gives agreement to within 5%.

The greater deviation from additivity comes, however, from the wide distribution of surface lifetimes that occur in a packed tower.*

*Lifetime is defined as the age of a liquid surface element when it is (or will be) mixed back into the liquid bulk.

As an extreme of the actual situation the liquid surface may be divided into two portions: A fraction, f , all engaged in reaching a certain constant lifetime, and the remaining fraction, $1-f$, which is infinitely old, or "dead." The ratio of the true value of $K_L a$ to that predicted by the two film additivity equation above is then

$$\frac{f}{1} + \frac{fR}{fR},$$

where R is equal to $Hk_{Ga}^*/k_L a^*$.

Examination of applicable literature data (62) shows that this dead surface approach is just as valid for most flow conditions as one postulating two finite liquid surface lifetimes. The conclusion, then, is that a certain fraction of the actual liquid surface may be considered dead at any given flow conditions and two film additivity may be taken to apply to the rest. For any gas of intermediate solubility the overall transfer coefficient may be predicted by two film additivity from ammonia and oxygen data, but not from vaporization data and oxygen data.

The other major application made of the experimental data was the derivation of a dimensional equation,

$$\frac{k_L^*}{D_L} = \alpha \left(\frac{4L}{a_e \mu} \right)^{0.6} \left(\frac{\mu}{\rho D_L} \right)^{0.5} \left(\frac{\rho^2 g}{\mu^2} \right)^{1/6},$$

derived through dimensional analysis and based on the penetration model

of the liquid phase and present knowledge of the hydrodynamic and absorption properties of falling liquid films. Here D_L is diffusivity, L is liquid flow rate per unit empty tower cross-sectional area, a_e is the active portion of the interfacial area, μ is viscosity, ρ is density, g is the acceleration of gravity, and α is a dimensional constant dependent upon the packing size and nature, with units of length^{-1/2}.

Values for a_e , in light of the above mentioned reliability of the dead surface concept, are best obtained in the case of ceramic packings from ammonia data, as has been done by Shulman, et al (137).

The utility of this equation is limited by the present knowledge of values of a_e , and can be tested for general applicability only when there is a greater knowledge of the effect of other variables on a_e .

CHAPTER 2

INTRODUCTION

The transfer of a substance from a gaseous stream to a liquid stream or vice versa is a common process in the chemical industry. When the substance or substances actually undergoing the transfer from the one state of matter to the other are major components of the bulk gas and liquid streams themselves and a sizeable heat addition or removal accomplishes the evaporation or condensation process, the name given to the operation is distillation. On the other hand, when the more isothermal process of transfer of a component from or to a relatively nonvolatile liquid or a relatively noncondensable gas through the approach of solubility equilibria is carried out, the operation is known as absorption or desorption, depending upon whether the solute transfer is from the gas to the liquid or vice versa.

Many commercial absorption processes occur in the chemical and petroleum industries. Examples are the absorption of carbon dioxide and/or hydrogen sulfide in ethanolamine solutions or caustic-carbonate solutions, the absorption of nitrogen oxides in nitric acid production, the recovery of natural gasoline components or liquid petroleum gas from lighter refinery gases by absorption into a heavier hydrocarbon stream, and the absorption of acetylene in acetone. It should be noticed that the first two processes involve an actual chemical reaction of the absorbed solute with the solvent, whereas the latter two examples are presumably cases of purely physical absorption, where there is no important chemical reaction of the solute occurring upon absorption.

The equilibrium solute distribution between the gas and liquid phases treated in such an operation may be measured readily in various types of solubility apparatus. Solubilities of gases in reacting and nonreacting liquids have been correlated successfully often through the techniques of thermodynamics.

The rate at which thermodynamic equilibrium is attained in the absorption apparatus is, however, equally as important and often more so, in so far as it affects the size and design of equipment used to carry out an interphase transfer.

Perhaps the most commonly used absorption apparatus is the packed tower, in which the liquid stream passes by gravity flow over dispersed solids, such as ceramic or carbon Raschig rings, Berl saddles, coke, or even broken stone. The solids distribute the liquid stream over a large interfacial area of contact between the liquid and the gas stream, which is usually forced upward through the tower, countercurrent to the direction of liquid flow.

It is, then, the rate of absorption in a packed tower of this sort that is the subject of this thesis. More specifically, the transfer through the liquid phase near the gas-liquid interface is studied to determine the mechanism which accomplishes the transfer of the absorbing solute.

2.1 Theoretical Background

2.1.1. Two Film Theory

The first successful approach to analysis of the rate of mass transfer in a packed tower was the two-film theory of Whitman (83, 158), first

proposed in a complete form in 1923. The major contribution of the theory was a realization that potential resistances to the mass transfer process in an absorption system exist in both the liquid and gas phases on either side of the gas-liquid interface.

The two-film theory postulates that stagnant "films" or very thin regions of no solute hold-up occur in both the gas and liquid phases on either side of the interface, and offer the controlling resistance to mass transfer. This concept was based to an extent upon observation, for the gas film at least, since it was known that gases or liquids flowing past a solid surface have their sharpest velocity gradient in the immediate vicinity of the solid surface, and consequently this relatively more stagnant fluid region offers the bulk of the resistance to a convectational heat transfer process (81, 108), which is similar in nature to a mass transfer process. These films are assumed to have certain thicknesses, x_G and x_L , constant throughout the tower, and the transfer through them is taken to occur by molecular diffusion alone. An additional assumption of the theory is that complete equilibrium is rapidly attained between the phases at the interface between them.

The rate of mass transfer is, then

$$N_A = \frac{D_V}{x_G} (C_G - C_{G1}) = \frac{D_L}{x_L} (C_1 - C_L) \quad (2.1.1.)$$

- where N_A = rate of absorption per unit area (moles/area time)
 C_G = concentration of solute in the bulk gas phase (moles/volume)
 C_{G1} = concentration of solute in the gas phase at the interface (moles/volume)
 C_1 = concentration of solute in the liquid phase at the interface (moles/volume)

- C_L = concentration of solute in the bulk liquid phase
 (moles/volume)
- D_L = diffusivity of solute in liquid (area/time)
- D_V = diffusivity of solute in gas (area/time)
- x_G = thickness of gas film (length)
- x_L = thickness of liquid film (length)

The absorption is a steady-state process at all points, since there is no solute hold-up in the film.

Applying the perfect gas law to the gas phase to obtain the more common unit of pressure, we have

$$N_A = \frac{D_V}{RTx_G} (p_G - p_i) \quad (2.1.2.)$$

where p_G and p_i are solute partial pressures in the bulk and at the interface, respectively.

In the analysis of rate processes it has always proved useful to retain the "distance from equilibrium" in concentration or pressure units* as a driving force, to be multiplied by a rate coefficient in order to obtain the transfer rate. Thus, defining

$$k_G = \frac{N_A}{p_G - p_i} \quad (2.1.3.)$$

*There has been some question as to whether fugacities or partial pressures and concentrations are the proper driving forces. The problem, however, does not enter at atmospheric pressures and for dilute concentrations.

and

$$k_L = \frac{N_A}{C_i - C_L}, \quad (2.1.4.)$$

we have, from (2.1.1.) and (2.1.2.)

$$k_G = \frac{D_G}{RTx_G} \quad (2.1.5.)$$

and

$$k_L = \frac{D_L}{x_L} \quad (2.1.6.)$$

To obtain the total amount of absorption occurring in a packed column, it is necessary to add the area over which the absorption is taking place; hence

$$N = N_A a = k_G a (p_G - p_i) = k_L a (C_i - C_L), \quad (2.1.7.)$$

since N_A , k_G , and k_L are taken to be constant at all points of interface.

Here a is the interfacial area per unit tower volume across which absorption occurs. $k_G a$ and $k_L a$ are called "volumetric" coefficients of absorption, since they refer to transfer rates per unit tower volume.

The assumption of rapid and complete interfacial equilibrium requires

$$C_i = m(p) p_i \quad (2.1.8.)$$

where $m(p)$ is the solubility of the solute gas at pressure, p . For the case of dilute solutions for which Henry's law holds, m is a constant equal to $1/H$, where H is the Henry's law constant.

$$p_i = H C_i \quad (2.1.9.)$$

It is usually impossible to measure concentrations and pressures at the exact interface. Hence overall coefficients of absorption are often defined:

$$K_L = \frac{N_A}{C_e - C_L} \quad (2.1.10.)$$

$$K_G = \frac{N_A}{P_G - P_e} \quad (2.1.11.)$$

Here p_e is the partial pressure of solute in equilibrium with the bulk concentration in the liquid and C_e is the concentration in equilibrium with the partial pressure in the bulk gas.

For systems obeying Henry's Law,

$$p_e = HC_L \quad (2.1.12.)$$

and

$$HC_e = P_G \quad (2.1.13.)$$

Combining these equations with (2.1.3.), (2.1.4.), (2.1.10.), and (2.1.11.), there results, at a point of interface

$$1/K_L = 1/HK_G = 1/k_L + 1/Hk_G, \quad (2.1.14.)$$

or, since k_L and k_G are taken constant at all points of interface,

$$1/K_L a = 1/HK_G a = 1/k_L a + 1/Hk_G a. \quad (2.1.15.)$$

This is the well-known equation for additivity of resistances. Equations (2.1.14.) and 2.1.15.) may take on two different limiting conditions. For a solute of very high solubility or for a case in which the liquid phase resistance is artificially minimized in some way (gas phase resistance controlling),

$$\frac{1}{Hk_G} \gg \frac{1}{k_L}.$$

Therefore

$$\frac{1}{K_L} = \frac{1}{HK_G} \approx \frac{1}{Hk_G} \quad (2.1.16.)$$

and

$$\frac{1}{K_L a} = \frac{1}{HK_G a} \cong \frac{1}{HK_G a} \quad (2.1.17.)$$

Similarly, for a very low solubility or for a case in which gas phase resistance is artificially eliminated (liquid phase resistance controlling),

$$\frac{1}{k_L} \gg \frac{1}{HK_G}$$

Therefore

$$\frac{1}{K_L} = \frac{1}{HK_G} \cong \frac{1}{k_L}, \quad (2.1.18.)$$

and

$$\frac{1}{K_L a} = \frac{1}{HK_G a} \cong \frac{1}{k_L a} \quad (2.1.19.)$$

It should be noted at this point that the possibility of the occurrence of a chemical reaction in the liquid film has not been considered. The field of absorption with chemical reaction is a large one in itself, and present knowledge is covered well elsewhere (10, 107, 133h). The effect of chemical reaction will be mentioned later (Section 5.4.1 and Chapter 10), but in this chapter only "physical" absorption systems are considered.

The two-film theory has proved useful in attacking the problems of absorption rates. It does, however, involve the assumption of a pair of stagnant, no hold-up films, which are known now to be contrary to experimental evidence in simpler liquid-gas flow systems. A more reasonable approach to the gas phase transport behavior near solid or liquid surfaces is afforded by laminar or turbulent boundary layer theory (see, e.g., Knudsen and Katz (75); however, in the case of the liquid phase behavior

it is difficult to conceive of any stagnation near the gas-liquid interface except for the case of an extremely high air drag.

2.1.2. Penetration Theory

A more realistic approach to the behavior of the liquid phase was adopted by Higbie (59) in 1935, in what has come to be known as the penetration theory. In a packed tower, Higbie pictured absorption as occurring in a series of short time exposures of liquid surfaces during each of which exposures unsteady-state mass transfer takes place into the liquid. Thus, liquid would arrive at a particular piece of packing from an essentially well-mixed pool of liquid above, flow down the packing in smooth flow and become mixed into the bulk liquid again at the next point of discontinuity in the packing surface (possibly at the bottom of that particular piece of packing). Assuming that the liquid near the interface acts as if it were near a free surface (that is, a surface where there is no air drag and hence might as well be the surface between a liquid and a vacuum), there is no velocity gradient in the liquid near the interface. If there is no turbulence near enough to the interface to affect the absorption process during the time of exposure, transfer will be accomplished by liquid molecular diffusion alone. Diffusion in liquids is an extremely slow process, and, for a large enough thickness of the liquid layer flowing over the packing, the transfer process can therefore be assumed as equivalent to unsteady-state transfer into a semi-infinite stagnant region of liquid.* This concept is facilitated if one views the liquid from a Lagrangian standpoint, that is if one "rides" down the piece of packing with the liquid.

*It was found, mathematically, by Johnstone and Pigford (69) that this is a valid assumption even for free gravity flow of water down a wetted wall some one or two feet in height, at common flow rates.

The problem thus reduces to one of solving an equation analogous to that for transient heat conduction into a semi-infinite slab,

$$D_L \frac{\partial^2 C}{\partial y^2} = \frac{\partial C}{\partial t} \quad (2.1.20.)$$

with the boundary conditions

$$\begin{aligned} C &= C_L \text{ at } y > 0, & t &= 0 \\ C &= C_L \text{ as } y \rightarrow \infty, & t &> 0 \\ C &= C_i \text{ at } y = 0, & t &> 0 \end{aligned} \quad (2.1.21.)$$

Here C = concentration in liquid at any point, y , and at any time, t

C_L = concentration of bulk liquid before exposure

C_i = concentration at interface

D_L = solute diffusivity

For $C_1 = p_G/H = \text{constant}$, or liquid phase resistance controlling (see Equations (2.1.10.) and (2.1.18.)), the solution to this equation is known (13a). The rate of absorption at any time, t , after birth is

$$N_A^1 = \sqrt{\frac{D_L}{\pi t}} (C_1 - C_L) \quad (2.1.22.)$$

and the concentration, C , at any distance, y , from the interface is

$$\frac{C - C_L}{C_1 - C_L} = \text{erfc} \left(\frac{y}{2\sqrt{D_L t}} \right) \quad (2.1.23.)$$

Over the entire exposure time, θ , the average rate of absorption is

$$N_A = \frac{1}{\theta} \int_0^\theta N_A^1 dt$$

or

$$N_A = 2 \sqrt{\frac{D_L}{\pi \theta}} (C_i - C_L) \quad (2.1.24.)$$

Consequently at any time, t , k_L^1 , the instantaneous coefficient of absorption is

$$k_L^1 = \sqrt{\frac{D_L}{\pi t}} \quad (2.1.25.)$$

and the average absorption coefficient, k_L , is defined by

$$k_L = 2 \sqrt{\frac{D_L}{\pi \theta}} \quad (2.1.26.)$$

If the theory is applied to a packed tower and it is assumed that, (a) all times of exposure duration ("lifetimes") of liquid surface throughout the column are equal and, (b) that the duration of an exposure is so short that only an infinitesimal amount of change in average liquid phase concentration occurs in the course of the exposure, then k_L in Equation (2.1.26.) above, compounded with the interfacial area per unit tower volume, a , gives the effective volumetric transfer coefficient for a liquid phase resistance controlled system.

For situations in which the liquid phase does not control and there is an appreciable gas phase resistance, C_i will be a function of t , since an unsteady state process is occurring, and the problem becomes more complex. This is so because the value of k_L^1 as a function of time depends upon the time history of C_i in a nonsimple way (resulting from the solution of (2.1.20.) coupled with the first two boundary conditions of (2.1.21.) and a third boundary condition where C_i becomes a function of time).

Thus, while Equation (2.1.14.) holds at a given point of interface through definition alone, there is no assurance that Equation (2.1.15.) for the overall combination of individual resistances over the interface holds at all.

The case of mass transfer obeying penetration theory in a liquid coupled with a constant stagnant, no hold-up film resistance in the gas phase has been solved and presented in the literature for the analogous heat transfer case (13b) and has been used by Emmert (36) to test the applicability of Equations (2.1.14.) and (2.1.15.) considered on an overall basis. He found for a given single liquid surface lifetime that the two-film theory additivity prediction would be obeyed to a maximum deviation of 5% of K_L . This solution and the whole problem of the additivity of resistances in general are investigated further in this thesis (Section 5.4.2. and Chapter VIII).

It is of interest to note at this point that Danckwerts (21) has proposed that a penetration mechanism applies to most free surface mass transfer processes, if not to all. Thus, he extends the theory to surfaces other than those of smooth falling liquid layers, for example the liquid surface in a stirred flask. He suggests that in such a system the concept that all surface elements exist for a constant lifetime before being mixed back into the liquid bulk is unrealistic, and that a more reasonable one would be for there to be a certain random renewal rate of surfaces, characterized by a renewal rate constant, s , the reciprocal of which then replaces θ in the expression for the overall liquid phase absorption coefficient, Equation (2.1.26.). Such a renewal process does not seem in line with the picture of liquid flow over regular pieces of packing, however.

2.1.3. Other Theories for Liquid Phase Mechanism

Another somewhat similar mechanism has been proposed by Kishinevsky (71, 72), who used it to derive predictions for chemical reaction systems. His view, as is common in the Russian literature, is that transfer processes at gas-liquid interfaces in commercial equipment tend to occur through a "free turbulence" mechanism* in such a way that the transfer rate is independent of solute diffusivity and controlled only by hydrodynamic conditions. Possibly this would happen because the surface renewal rate is so rapid that the solute does not diffuse appreciably away from the first few molecular layers, which are saturated by the process of attainment of equilibrium at the interface (see also Chapter 11). Whether or not this latter is Kishinevsky's intended physical picture is difficult to determine from his writings. It is more probable that he and Kafarov (70) picture some sort of turbulent eddy transfer mechanism which retains an eddy "diffusivity" level higher than that afforded by molecular diffusion up to and, essentially, at the interface. Such a picture seems to be in discord with the concept of a damping effect of surface tension at the interface.

It is possible, however, that turbulence in the liquid layer could come close enough to the interface to affect the mass transfer process, probably much in the same way as it affects the transfer in a fluid near a solid interface. Much theoretical and experimental study has been made of this latter process. Perhaps the most successful approach for mass transfer near solid surfaces has been that of Deissler (29), who pictures an eddy diffusivity extending within the so-called laminar sub-layer

*See also a review article by Kafarov (70) on this sort of thinking.

but damped out to zero at the wall in such a way that

$$\epsilon = n^2 u y \left(1 - e^{-\frac{n^2 u y}{\nu}} \right) \quad (2.1.27.)$$

where ϵ = eddy diffusivity
 u = velocity in the direction of flow
 y = distance from the solid interface
 ν = kinematic viscosity
 n = a constant

For fully developed flow (steady-state) this gives a variation of transfer coefficient with solute diffusivity to the $3/4$ power in liquid systems where Schmidt Number is high (29). In the entrance regions in tubes or over plates there is some deviation from this $3/4$ power variation, but not enough to alter the power of variation greatly (see Figure 6 of reference 29). For the analogous nonturbulent system, laminar boundary layer flow, there is a variation of transfer coefficient with diffusivity to the $2/3$ power (120). The net influence of the introduction of turbulence in Deissler's manner into the unsteady-state boundary layer system for liquid flow is then to raise the power of variation of transfer coefficient with respect to diffusivity slightly. Strictly, this raising of the exponent occurs only for cases of liquid diffusion (Schmidt Number above 100). For gas phase transfer the situation is different (see Section 8.2.2.).

Since laminar boundary layer theory differs from penetration theory mathematically and physically only in the presence or absence of a velocity gradient near the interface, it would be anticipated that a turbulence dying out near the gas-liquid interface in the liquid layer flowing over packing would, in a liquid phase controlled absorption process,

increase the power of variation of transfer coefficient with respect to solute diffusivity to a power greater than the $1/2$ predicted by penetration theory.

If, however, the turbulence maintained a relatively high^{er} eddy diffusivity up closer to the interface than predicted by analogy to Deissler's relationship for solid interfaces, the situation described above as a second possible explanation of the Russian authors' hypothesis would be approached, and the transfer coefficient would become less and less dependent upon solute diffusivity. This could be possible since surface tension would exert less of a damping influence than would an actual solid surface. Hence for some certain turbulent flow conditions the power of variation might appear to be $1/2$; however, since the magnitude of eddy diffusivity should change strongly with flow rate in a falling film, it is unlikely that a $1/2$ power of variation would be apparent over a very wide range of flow conditions.

Still another possible mechanism of transfer within the liquid phase that has some basis in the literature should be mentioned. It has heretofore been postulated in the discussion of penetration theory and related theories that there is no velocity gradient in the liquid near the gas-liquid interface. This seems to be a logical assumption since the relative kinematic viscosities of a typical gas and a typical liquid are such that a drag force capable of influencing the velocity profile in the gas greatly will have a much lesser influence on the velocity profile in the liquid. At 20°C the ratio of the kinematic viscosity of air to that of water is 15.

Howkins and Davidson (60) conclude from studies made recently of countercurrent gas flow against a liquid flowing down a string of spheres inside a tube that "loading" (the first point of sudden increase in slope

of the logarithmic pressure drop versus gas flow rate curve) in a packed column occurs because of the exertion of a very large air drag on the liquid at points of contraction in the path of gas flow. This drag becomes comparable to or even greater than that of a solid surface and tends to prevent the liquid layer from falling along the packing. One would conclude from this that, as loading conditions are approached and exceeded in a packed tower, there would be an increasing portion of liquid interfacial surface that behaves transfer-wise as if it were in contact with a solid surface; that is there would be a laminar boundary layer behavior of sorts in these portions of the liquid, with the consequent increased influence of solute diffusivity on the transfer process ($2/3$ power for a solid surface (120)). The foregoing discussion regarding the effects of turbulences near the interface could then be superimposed on this.

For purposes of a simple-minded physical picture, it can be said that the occurrence of boundary layer behavior or Deissler-type damped turbulence represents an intermediate case of sorts between penetration theory behavior and an unsteady-state view of stagnant no hold-up film theory behavior. A model of unsteady-state penetration into a stagnant film of finite hold-up has been proposed by Toor and Marchello (151) as a transitional model approaching penetration theory for short exposure times and film theory for long exposure times. As a consequence the variation with diffusivity changes smoothly from $1/2$ power to first power as exposure time increases. Because of the apparent unlikeliness of the existence of any such truly stagnant film (even one of finite hold-up) the above suggestions for deviations from simple penetration behavior seem to have a stronger physical basis than does a model of penetration into a stagnant film of finite hold-up. In justice to Toor and Marchello it

should be stated that their model was not developed with an eye to packed tower behavior but more with reference to transfer near liquid-liquid and liquid-solid interfaces. For those cases their theory is somewhat more plausible but still questionable as to physical basis.

In summary of this section, Table 2.1 gives the predictions of the various theories and theoretical modifications discussed herein concerning the effect of solute diffusivity on the coefficient of absorption for a liquid phase controlled system.

TABLE 2.1

Theoretical Predictions Concerning The Effect Of
Solute Diffusivity On The Liquid Phase Coefficient Of Absorption

<u>Theory</u>	<u>Effect Of Diffusivity</u>
1. Two film	$k_L \sim D_L^{1.0}$
2. Penetration	$k_L \sim D_L^{0.5}$
3. Free turbulence	$k_L \sim D_L^0$
4. Turbulence damped near the free surface	$k_L \sim D_L^n$ where n varies from 0 to 0.6, changing with flow conditions
5. Large air drag - no effect of turbulence	$k_L \sim D_L^n$ where n varies from 0.5 to 0.67, increasing with gas rate
6. Large air drag - turbulence also effective	$k_L \sim D_L^n$ where n varies from 0 to 0.75, changing with flow conditions
7. Penetration into stagnant film of finite hold-up	$k_L \sim D_L^n$ where n varies from 0.5 to 1.0 changing with flow conditions

2.1.4. Packed Tower Design (133d)

If $K_L a$, the "overall" volumetric coefficient, is known at every point in a tower, the height of a tower necessary to increase the liquid concentration of solute from C_1 to C_2 may be found from a material balance on the liquid phase and Equation (2.1.10.)

$$\frac{L}{\rho_L} \frac{dC_L}{dh} = N = K_L a (C_e - C_L) \quad (2.1.28.)$$

where h = column height

L = weight liquid flow rate per empty tower cross section

ρ_L = liquid density

The assumption of plug flow of gas and liquid through the packing is built into the material balance. Integrating,

$$\int_{C_B}^{C_T} \frac{dC_L}{(C_e - C_L)} = \int_0^h \frac{\rho_L K_L a}{L} dh \quad (2.1.29.)$$

where C_T = C_L at liquid inlet (top) and

C_B = C_L at liquid outlet (bottom)

From two film theory, for a case where solubility is a function of concentration, $K_L a$ is not constant, even though $k_L a$ and $k_G a$ may be (Equation 2.1.15.). Also L and ρ_L may vary throughout the column. In cases where solutions are dilute (and L , ρ_L , and temperatures remain constant) and Henry's Law is obeyed (and $K_L a$ is constant by two film theory), $C_e - C_L$ is linear in C_L and Equation (2.1.29.) becomes

$$h = \frac{L}{\rho_L K_L a} \int_{C_B}^{C_T} \frac{dC_L}{C_e - C_L} = \frac{L (C_T - C_B)}{\rho_L K_L a \Delta C_{L \text{ l.m.}}} \quad (2.1.30.)$$

where $\Delta C_{L \text{ l.m.}}$ is defined in the same way as $\Delta T_{\text{l.m.}}$ in heat transfer analyses (see Section 13.1). Similar equations may be derived for $K_G a$ (133d).

The integral
$$\int_{C_B}^{C_T} \frac{dC_L}{C_e - C_L}$$

is often referred to as the number of transfer units in the tower $(N.T.U.)_{OL}$. The height of a transfer unit $(H.T.U.)_{OL}$ is defined as

$$(H.T.U.)_{OL} = \frac{h}{(N.T.U.)_{OL}} \quad (2.1.31.)$$

For dilute systems, therefore,

$$(H.T.U.)_{OL} = \frac{L}{\rho_L K_L a} \quad (2.1.32.)$$

Similarly $(H.T.U.)_L$ is defined in terms of $k_L a$. Expressions for $(H.T.U.)_{OG}$ and $(H.T.U.)_G$ may also be obtained (133d).

2.2 Experimental Background

In the experimental determination of rate data in packed towers it has been considered desirable to study systems in which either the gas phase resistance or liquid phase resistance controls, that is, systems in which the resistance offered by one phase to the mass transfer process is negligible compared to that of the other. Thus, as discussed in

Section 2.1.1., the absorption of a gas of low solubility approaches the case of liquid resistance controlling; whereas the absorption of a gas of very high solubility approaches the case of gas resistance controlling. According to the two-film theory, then, data obtained in this manner could be combined by Equation (2.1.15.) to give the transfer rate for a gas of intermediate solubility.

2.2.1. Liquid Phase Resistance

The most extensive and systematic study of liquid phase resistance to physical absorption in a packed column has been that of Sherwood and Holloway (131), published in 1940. In this work the authors studied the desorption of oxygen from water into air extensively at 25°C on several packings in order to determine the effects of flow rates and of packing size and shape. From dimensional analysis, and an observed lack of effect of gas flow rate on the transfer coefficient, they concluded that the transfer coefficient, $k_L a$, coupled into a Nusselt group $\left(\frac{k_L d}{D_L}\right)$, where d would be a length dimension, should be a function of a Reynolds group $\left(\frac{dL}{\mu}\right)$ and a Schmidt group $\left(\frac{\mu}{\rho D_L}\right)$ alone. Thus they correlated their results in a semi-dimensionless form

$$\frac{k_L a}{D_L} = \alpha \left(\frac{L}{\mu}\right)^{1-n} \left(\frac{\mu}{\rho D_L}\right)^{1-s} \quad (2.2.1.)$$

The values of α and n for various kinds of packing were determined from the above-mentioned oxygen runs, and are shown in Table 2.2. Values of α are valid only when units of feet, hours, and pounds are used, since the equation is dimensional.

TABLE 2.2

Constants Found By Sherwood and Holloway, (131)
For Equation 2.2.1. (25°C)

<u>Packing</u>	<u>α</u>	<u>n</u>
2 inch ceramic Raschig rings	80	0.22
1.5 inch ceramic Raschig rings	90	0.22
1 inch ceramic Raschig rings	100	0.22
0.5 inch ceramic Raschig rings	280	0.35
3/8 inch ceramic Raschig rings	550	0.46
1.5 inch ceramic Berl saddles	160	0.28
1 inch ceramic Berl saddles	170	0.28
0.5 inch ceramic Berl saddles	150	0.28
3 inch Spiral Tile	110	0.28

The value of s was fixed at 0.5, based upon the results of a series of measurements made before the extensive oxygen runs. In these first runs the desorption of carbon dioxide, oxygen, and hydrogen (all relatively insoluble gases) was studied in a tower packed with 1.5 inch rings to a height of 8 inches. Temperature and flow conditions were varied over wide ranges. Unfortunately an amount of end transfer below the packing equivalent to six inches of packed height was also measured because of the sampling techniques in these first runs.

To obtain a value of s from these results, the authors first determined the effect of temperature on the transfer coefficient for each gas at constant flow rates, and then determined the value of n for carbon dioxide and oxygen desorption by plotting the transfer coefficients, corrected to 25°C, against liquid flow. There was, as has been mentioned before, no

observed effect of air flow rate on the liquid phase transfer coefficient below loading conditions. Once n had been determined as 0.25 (the different value from that found in the later oxygen runs may have been caused by the end effect), $(\frac{k_L a}{D_L})$ divided by $(\frac{L}{\mu})^{1-n}$ was plotted against $(\frac{\mu}{\rho D_L})$ for all runs. This correlation gave s equal to 0.53, which was taken as essentially equal to 0.50, thus affording agreement with Higbie's penetration theory.

Subsequent investigations of liquid phase behavior have either confirmed Holloway's oxygen data, correlated data for new packings in this manner, or studied cases of simultaneous chemical reaction. Among those who have confirmed Holloway's data for various packings are Molstad, et al, (92), Vivian and Whitney (156), Whitney and Vivian (162), Deed, Schutz, and Drew (27), and Landau, et al (80). The only other study in which physical absorption or desorption of solute gases of widely varying liquid phase diffusivity has been examined is the recently published work of Onda, et al (102), who absorbed hydrogen and carbon dioxide on 6 mm. ceramic Raschig rings and found $k_L a$ to vary with D_L to the 0.42 power.

2.2.2. Peaceman's Criticism

Peaceman (107c) has offered a valid criticism of the 0.5 value found for s by Sherwood and Holloway (131). He pointed out that their method of plotting $k_L a/D_L$ divided by $(L/\mu)^{1-n}$ against the Schmidt group gives more the effect of temperature than the effect of diffusivity alone, since the Schmidt group in liquid systems is highly temperature sensitive. Peaceman replotted the transfer coefficient for each of the three gases

against diffusivity at constant flow rates and constant temperature, using the values of diffusivity employed by Holloway (the best available at the time and in Peaceman's time). This yielded an exponent of 0.37. This indicates that either (1) the values of D_L utilized were incorrect, or (2) there were not enough variables brought into the dimensional analysis to account for the effect of temperature completely. It is also true that the end transfer may have a different mechanism from the transfer on the packing and hence the power found from Holloway's data may not be indicative of the transfer process on the packing.

In any event, the correct exponent on the Schmidt number rests completely on Sherwood and Holloway's hydrogen data, only three coefficients for which were obtained - at constant flow rate and varying temperature. This is so because oxygen and carbon dioxide, their other two solutes, have essentially the same diffusivity as one another.

2.2.3. Gas Phase Resistance

Measurements and correlations of gas phase resistance in packed towers have in general been less successful than liquid phase studies. For one thing, it has been difficult to find gases of high enough solubility to give a case of gas phase resistance controlling in accordance with Equation (2.1.15.), although for methanol and ethanol absorption such a situation is approached. As a result, liquid phase resistance has often been eliminated artificially, either (1) by studying the absorption of ammonia into strong acid solution or of acid gases into strong alkali, or (2) by vaporizing water into air (86, 89, 130, 146, 154). Such experiments

give very high transfer rates with the result that very short packed heights with contingent large relative end effects and uncertainties of flow distribution have been necessary to enable one to measure the driving forces ($p_G - p_e$) at either end of the packing, and thereby calculate $K_G a$ by the equation analogous to (2.1.29.).

Values of $k_G a$ obtained from physical absorption measurements (and corrected by Equation (2.1.15.) for $k_L a$) have generally been lower than $k_G a$ values obtained from vaporization factors by as much as a factor of two (35, 38, 62, 93, 94, 119). There is also disagreement as to the dependence of $k_G a$ upon liquid and gas flow rates. Then, finally, there is disagreement between investigators on the magnitude of coefficients for the same system at the same conditions.

Further discussion of the gas phase problem is delayed until Section 5.4.2. and Chapter 8, where it is considered in more detail in the light of the results of this thesis.

2.2.4. Models of the Liquid Phase Absorption Process

Because of the shortcomings of the various theoretical and empirical approaches to packed column design many recent workers have felt it desirable to study small scale models of the absorption process. This has been especially true for the study of cases of absorption accompanied by liquid phase chemical reaction, where the interaction between chemical kinetics and diffusion predicted by two-film or penetration theory is often complex, and often complicated by the absence of reliable chemical

kinetic data. Anomalies and internal disagreement within the literature have often been found for the study of these systems in packed columns (133h), so the general feeling is that it is best to obtain a basic understanding of these systems in the simplest models before tackling the problem of chemical reaction - diffusion interaction in the more complex forms of industrial apparatus. Aside from gaining basic understanding, it is also desirable to have some sort of model of a packed column so a new reaction system may be examined on a small scale before the packed tower or other apparatus to carry it out industrially is constructed.

The most obvious small-scale model is a bench-sized packed column, which is often used for the latter purpose mentioned above. There is, however, a scaling problem for packed columns, occasioned by uncertainties in interfacial area, variation of liquid surface exposure times with packing size, and surface tension bridging of liquid between pieces of packing, which occurs proportionately more for small packings than for large ones. As far as a basic understanding of the diffusion-reaction mechanism is concerned, a small packed column is no simpler to analyze than a large one.

The more simplified models that have been studied are laminar liquid jets (15, 18, 114, 124), short wetted wall columns (43, 87, 99, 155, 157), wetted spheres (23, 88, 168), and stirred flasks (46, 68, 74). The first three of these have been proven to be simulations of the penetration theory, and, in two cases (23, 99), have been felt to obey it so reliably that they have been used for the actual measurement of diffusivities (see also Sections 14.2.1 and 14.8). Although the short wetted wall column and the sphere column were originally designed as models

of the packed column rather than as simulations of the penetration theory, it appears there is no reason to accept them per se as valid models of the flow over packing without evidence of the applicability of penetration theory to liquid phase behavior in a packed column. In light of Peaceman's criticism of Sherwood and Holloway's conclusions, this has not heretofore been successfully proven.

The other common model, the stirred flask, bears less similarity to the flow in a packed column. It is possible, however, that a penetration mechanism applies here, too, following Danckwerts' random surface renewal picture (Section 2.1.2.). There is, though, no experimental evidence to confirm this. The only mechanisml study of physical absorption in a stirred flask has been that of Kishinevsky and Serebryansky (74), who absorbed oxygen, nitrogen, and hydrogen into water in a very rapidly stirred flask with consequent high transfer rates and found no evident influence of solute diffusivity in the process. They mention that at lower stirring rates (and 1/5 the transfer rate) there was some effect of molecular diffusivity. Their results are examined in more detail in Chapter 11.

2.2.5. Additivity of Resistances

The problem of additivity of resistances, it should be stressed, is not whether Equation (2.1.14.) holds at each and every point of interfacial area. It obviously does, by definition. The problem is whether Equation (2.1.15.) can be applied to calculate $K_L a$ from data taken for separate cases where each of the individual phase resistances is measured in the absence of resistance of the other phase. Thus the "additivity" equation might better be rewritten

$$\frac{1}{K_L a} = \frac{1}{HK_G a} = \frac{1}{k_L a^*} + \frac{1}{Hk_G a^*} \quad (2.2.2.)$$

where $k_L a^*$ = $K_L a$ measured in absence of gas phase resistance.

$k_G a^*$ = $K_G a$ measured in absence of liquid phase resistance.

The only two studies of the additivity of resistances in absorption as such have been that of Goodgame and Sherwood (46) and that of Whitman and Davis (159). The former vaporized water, and absorbed carbon dioxide (liquid phase controlled), ammonia, and acetone in water in a stirred flask. They found that the acetone and ammonia absorption rates tended to agree within 4% with values calculated from the vaporization rate and the carbon dioxide rate by the additivity equation (2.2.2.). In order to obtain this agreement, however, it was necessary for them to assume that k_L and k_g varied with solute diffusivities to the 1/2 power (penetration models in both gas and liquid). Their work is discussed further in Section 8.2.1., along with the data of Whitman and Davis from a similar stirred flask experiment, which were originally calculated assuming all solutes had the same liquid and gas phase diffusivities, the maximum deviation from additivity being reported as 15%.

Gordon and Sherwood (48) in analyzing the water-isobutanol liquid-liquid extraction system in a stirred flask found there to be some question of the validity of computing overall coefficients by additivity from measured individual coefficients, but the difficulty seemed to be more a question of what diffusivity values to believe (129).

Unfortunately no packed tower studies of both vaporization and gas-phase influenced absorption have been made together in the same apparatus.

As was mentioned previously, however, most absorption data for highly soluble gases, measured as K_{Ga} and corrected by (2.2.2.) to k_{Ga} , tend to give lower coefficients than those from vaporization studies.

2.2.6. Equilibrium at the Interface

The derivation given previously in Section 2.1.1. for the two-film theory (and also, incidentally, that mentioned in Section 2.1.2. for penetration theory coupled with a constant stagnant, no-holdup gas film resistance) contained the assumption of complete and rapid thermodynamic equilibrium between the phases at the gas-liquid interface. It is conceivable that this may not be, possibly because of the accumulation of large molecules at the interface which would only let a very small fraction of the solute molecules arriving at an interface pass on through. Thus an added resistance would be presented in series between those of the gas and liquid phases. A separate concept could also be the case where the rate of net solute transfer across the interface rivals in magnitude the normal rate of molecular interchange through thermal motion. In this situation the "dynamic" equilibrium would differ from the "static" equilibrium measured at lower rates of transfer. A calculation (121) shows that such a high rate of transfer is, however, unlikely in commercial equipment, at pressures other than very low ones.

Recent studies made of absorption in falling laminar jets (15, 18, 114, 124) have shown that at the rates of mass transfer employed in commercial apparatus there is apparently no interfacial resistance. In one case (15) there is a possible resistance at a very high rate of

mass transfer (exposure times less than 0.01 second) reported. There is also evidence that a concentration of any of several commercial surface active agents adequate to reduce the liquid gas surface tension significantly reduces the rate of liquid phase mass transfer in some way both in jets and wetted wall columns (18, 37) and in packed columns (130). Even here, though, there may not be so much an interfacial resistance as a reduced solute diffusivity in the liquid near the interface or regions of hydrodynamically stagnated interface (see Chapter 9).

Thus, in the absence of unusual surfactant concentrations, the assumption of rapid and complete equilibrium at the gas-liquid interface seems to be (for packed tower absorption rates) one of the most reliable of those built into the various derivations of the first portion of this chapter.

2.3 Purpose of this Thesis

The desorption of relatively insoluble gases from water into air in a packed column presents an opportunity rare in chemical engineering studies, namely, the investigation of the effect of one single variable while all others are held constant. If air and water flow rates over a given type of packing are held constant and the temperature of the whole system is maintained constant, the single remaining variable which is believed to affect the mass transfer process is the diffusivity of the solute gas in water. This is true because solute concentration in both air and water will be extremely low and since liquid phase resistance will control.

If a wide range of solute gas diffusivities is studied then the mode of variation of $k_L a$ with D_L will be known at all gas and liquid flow rates investigated. The theoretical predictions of Section 2.1 may then be compared with the results and the liquid phase mechanism or possible mechanisms will be indicated.

The mechanism of the liquid phase transfer process is of importance for a fourfold reason:

1. A knowledge of the mechanism will indicate what are reliable laboratory scale models to use.
2. The liquid phase mechanism is important in evaluating the effect of reaction kinetics on the mass transfer process in the case of absorption with chemical reaction (and the models may be used for studying this effect).
3. The effects of all pertinent variables upon the liquid phase resistance can be predicted.
4. A knowledge of the transfer mechanism would contribute to our knowledge of mass transfer near fluid-fluid interfaces in general.

The primary purpose of this thesis, then, was to carry out the experiment for solute gases of widely varying diffusivities and to perform it at several different flow conditions with a view to shedding light on liquid phase mechanism.

Since the effect of the diffusivity of the solute gas in water was being examined, it was also necessary, as a secondary objective, to carry out a program of diffusivity measurements, since insufficient reliable literature data were available.

Finally, as another secondary objective, if, as was to be expected, a mechanism other than film theory applied in the liquid phase, it was desirable to determine the implications of this mechanism as far as the additivity of resistances or the gas phase resistance problem in general were concerned.

CHAPTER 3

APPARATUS AND PROCEDURE

3.1 Choice of Experiment

A desorption system was chosen rather than an absorption system for three reasons. First, and most important, one of the prime objects of the thesis is to maintain the hydrodynamics of the system constant as those of the air-water system, for all solute gases. This would not be accomplished if a large enough solute gas concentration were included in the air stream to give a driving force ($C_e - C_L$) sufficient to produce a readily measureable amount of mass transfer.

Secondly, a much lesser amount of solute gas consumption is necessary in a desorption system. This is so since, in order to attain a driving force as large in magnitude as that for desorption from an initially saturated water solution, it would be necessary to operate with a gas phase of pure solute gas. On the large scale of the present experiment this would be prohibitive.

Finally, the coefficient of absorption is equal to that of desorption, as is predicted by all theoretical approaches and has been confirmed by Allen (4, 131), Carlson (12), and Sherwood and Killgore (132).

The solute gases employed were chosen to be sparingly soluble, to give as wide a range of diffusivity as possible and, as a secondary requirement, to be relatively inexpensive. Hydrogen and helium, being the lightest gases, have high diffusivities in water. Oxygen and carbon dioxide have been studied extensively before, affording an opportunity

for comparison of data, and have lower diffusivities. Propylene has a still lower diffusivity and hence was chosen as the fifth gas. It was originally felt that ethylene would have a diffusivity intermediate between propylene and carbon dioxide; however, preliminary diffusivity measurements (Chapter 14) indicated its diffusivity was close to that of carbon dioxide and so ethylene was discarded as an experimental solute. All five gases have sufficiently low solubilities to afford cases of liquid phase resistance completely controlling when desorbed, and yet have high enough solubilities to be analyzed in solution with sufficient accuracy by the analytical techniques which were developed and are set forth in Chapter 15.

3.2 Design of Apparatus

Correct nature and sizing of the packing and packed column were of prime importance for fulfilling the objectives of this study. For this reason the column design was set first, and then all piping and auxiliary apparatus were designed to meet with the requirements thereby imposed.

Eight primary requirements had to be met by the packed tower and auxiliary system.

- 1) The size and type of packing should be representative of that used in industry. This was especially so because of the problems already discussed (Section 2.2.4.) encountered in scaling from one size packing to another. Ceramic Raschig rings were selected as the most common industrial packing, and a packing dimension of 1 1/2 inches was taken as large enough to be a usual industrial size. Choice of 1 1/2 inch Raschig rings also would allow for

a comparison of common data points with Sherwood and Holloway (131), who used 1 1/2 inch rings for their carbon dioxide, oxygen, and hydrogen studies.

- 2) The diameter of the column had to be sufficiently large to make the wall surface a negligible portion of the total packing surface and to prevent other wall effects such as preferential flow of water toward the wall. A ratio of tower diameter to packing diameter of eight has been recommended as being adequate for this latter purpose by Baker, Chilton and Vernon (5), who studied maintenance of flow distribution in flow over dumped packing. Since flow concentration towards the wall becomes more pronounced as tower height increases, and the recommendation of Baker, et al, is based on a tower height of several feet, a factor of 8 (corresponding to a one-foot tower diameter) was taken as a reliable compromise between maintenance of flow distribution and reduction of excessive power requirements for the pump and blower. For a one-foot diameter column filled with 1 1/2 inch Raschig rings the wall contributes only 10% of the total surface area.

- 3) The height of packing had to be short enough so that there would still be enough solute remaining in the effluent water to allow an accurate analytical determination of the driving force there. The height also had to be great enough so that it, itself, could be measured with accuracy and so that end transfer effects would be minimized. The actual measurement of the height does

not, however, enter into the investigation of mechanism through comparative absorption coefficients, as it does into the determination of absolute coefficient of absorption.

A packed height of either one or two feet was taken as a compromise between these two requirements. In this respect it was not possible to represent typical conditions in industry, where a much greater height is generally employed.

- 4) Water and air flows equivalent to loading and flooding in the tower had to be provided for, since many industrial columns operate at flow rates equivalent to 70 or 80% of flooding. Also, because of the higher flow rates, a much different transfer mechanism could control in this range (70). To give flooding at liquid to gas weight flow ratios between 2 and 10, it was necessary to design for a maximum water flow of 13,000 lbs. per hr. per sq. ft. and an air flow of 1,600 lbs. per hr. per sq. ft., both based on the empty tower cross sectional area.
- 5) To give temperature control and thus allow the single variable of solute diffusivity to be investigated, the column had to be operated with the water temperature held constant from run to run at 25°C. Thus a steam injection device was provided for the water stream.
- 6) To ensure isothermal conditions in a run a provision had to be made for saturating the air stream with water at the water stream temperature of 25°C, and thus eliminating the heat effect

of humidification on the packing. This took the form of a separate spray tower, equipped with both steam and water injection.

- 7) In order to avoid excessive water consumption at high flow rates, the water stream had to be made recirculatory.
- 8) The entire water circulation system had to be protected from corrosion, since the collection of corrosion products could well alter surface transfer conditions of the water and also alter the nature of the packing surface.

With these factors in mind the packed column system shown in Figure 3.1 and the auxiliary equipment shown in Figure 3.2 were constructed.

The tower consisted of four sections of 12 inch steel pipe. The normal operation was with a one foot packed height and with the section labeled "optional" omitted; however, this section could be used to give either a second foot of packing height or an additional head on the inlet water at the top of the column.

The interior of the column and the interior of the two water storage drums were given three coats of Series K, self-priming Tygon paint to guard against corrosion. Similarly the rest of the water system was made of copper piping, or rubber hose where flexible joints were necessary.

A bypass arrangement allowed for water flow rate control, and one of three calibrated orifices measured the flow. Steam and the solute gas were injected through two injection tees, located prior to a valve, several elbows, and the orifice in the flow scheme. Flow through these

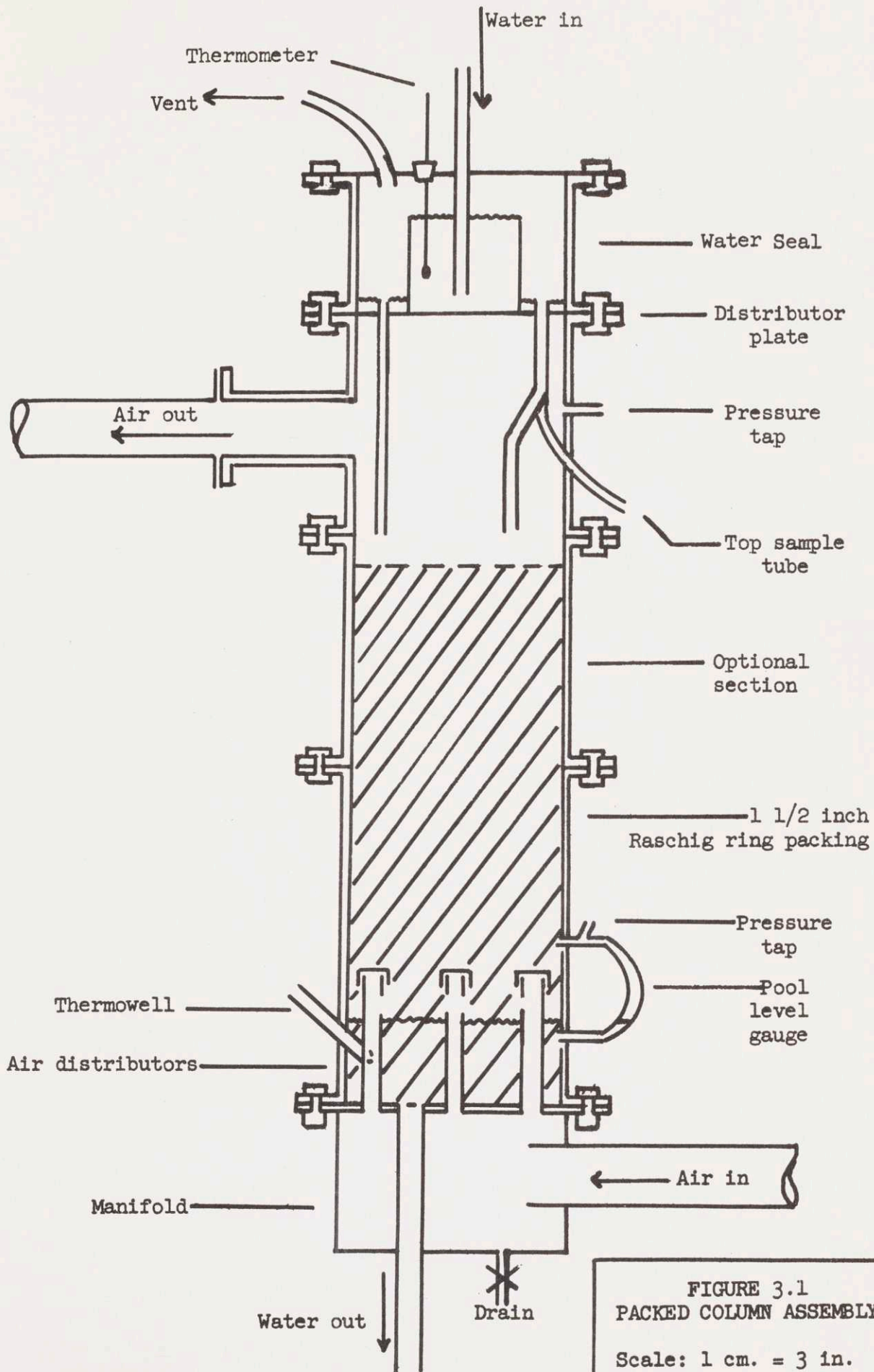


FIGURE 3.1
 PACKED COLUMN ASSEMBLY
 Scale: 1 cm. = 3 in.

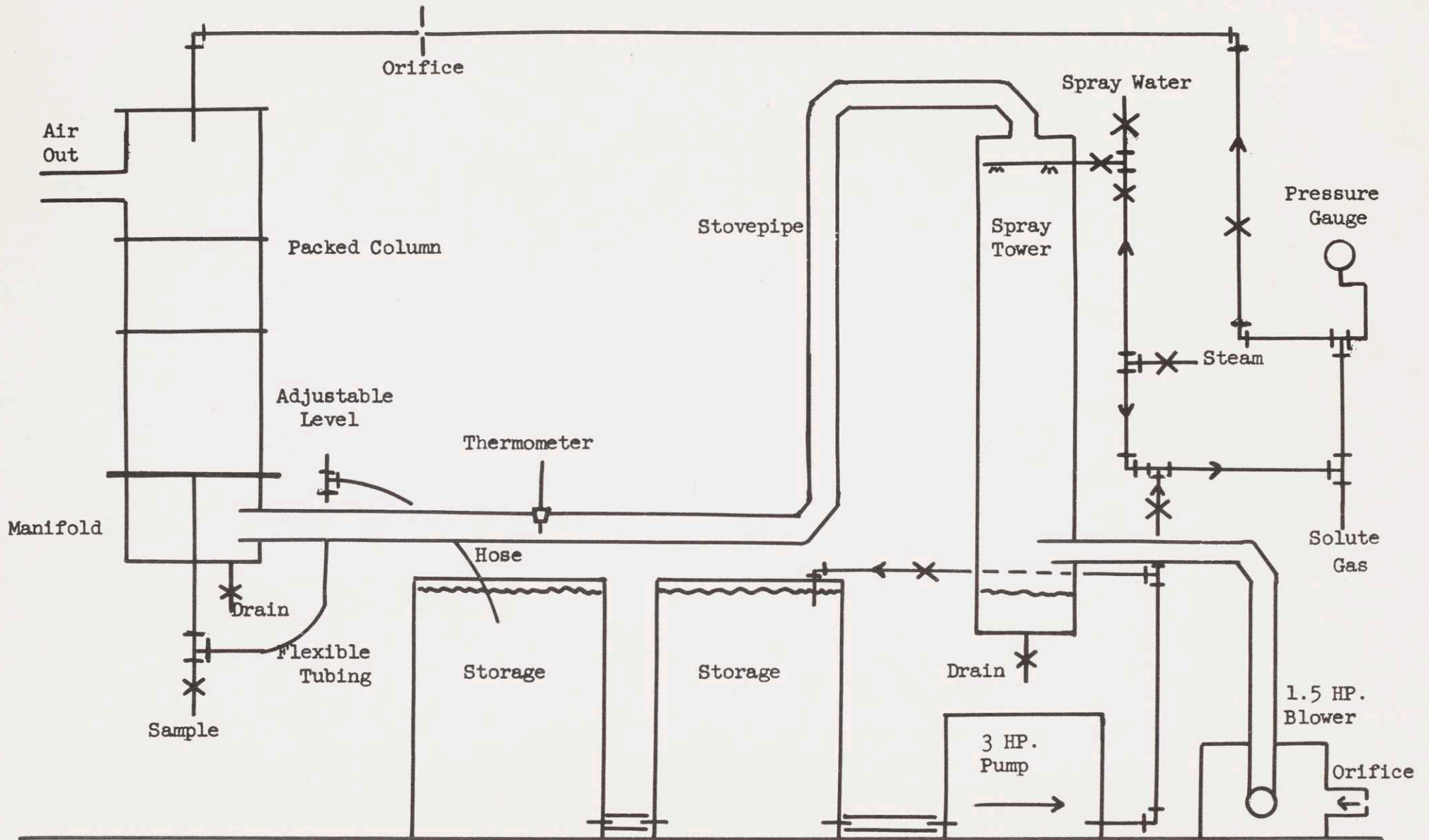


FIGURE 3.2 FLOW DIAGRAM OF APPARATUS

fittings gave effective absorption of the gas and the steam into the water. The rate of solute gas injection was roughly metered by one of two capillary flow meters.

Upon entering the top of the tower the solute-bearing water flowed over a liquid seal and on to the packing through a distribution system, consisting of some 23 lengths of copper tubing. At the bottom of the packing the water fell into a pool, from which it flowed back to the storage drums. A levelling tee arrangement in this line made it possible to hold the pool height constant, just below the air inlet openings. The distribution and take-off system was quite similar to that employed by Vivian (154) and by Whitney (160).

A 3 horsepower centrifugal pump was used to circulate the water. Most of the water line was made of 1 1/4 inch copper tubing, although 2 inch brass pipe was used for the exit line.

Air was drawn into the system by a 1 1/2 horsepower, D.C., variable speed rotary blower. Sharp edge orifices were butt-mounted on the air inlet, and flow rates computed from standard data (109c). The air lines consisted entirely of 4 inch galvanized stove pipe.

From the blower the air passed through a six-foot high eight-inch diameter spray tower, equipped for both steam and water injection, and from there into a manifold distributor at the bottom of the tower. Upon leaving the tower at the top the air was drawn into a chimney through another blower.

Complete details of the apparatus are given in Chapter 13 of the Appendix. The apparatus used for measuring diffusivities is discussed

in Chapter 14 of the Appendix. It consisted of a pair of sintered glass diaphragm cells.

3.3 Experimental Procedure

A series of seventy runs was made, investigating the transfer of the five solute gases at five different flow conditions and the constant temperature of 25°C. A few runs were made examining the effects of temperature, of packed height, of redumping the packing, and of using deaerated water.

Before solute gas was injected in a run, the tower was operated for 15 minutes at the desired air flow rate and a water flow 25 to 50% higher than that desired for the run. This established the water hold-up in the tower. The need for it was shown experimentally (Runs 2 and 3) and has also been shown by Shulman, et al (136) who studied hold-up on packing.

The water flow rate was then brought back to the desired value, and temperatures, air humidity, and pool height were adjusted to the operating conditions. After ten minutes samples of the inlet and exit water streams were taken through the devices provided for this (see Figure 3.1, Figure 3.2, and Section 13.1). At least one more set of samples was taken in each run, at least five minutes later. Pressures and temperatures were recorded at each sampling time.

These samples were then analyzed by the various procedures described in Chapter 15 of the Appendix and from the resulting water

concentrations values of the transfer coefficient, $K_L a$, were computed. Details of the calculational methods and the treatment of the data are given in Chapter 16 of the Appendix.

At all flow conditions at least two duplicate runs were made for each solute gas (in addition to the duplicate samplings within a run). For conditions where data tended to scatter, still more runs were made.

In addition to the mass transfer runs pressure drop measurements were made in the regions of the various flow conditions, to indicate the occurrence of loading or flooding. A more amplified description of the experimental procedure is given in Section 13.2 of the Appendix. The procedure for diffusivity measurements is covered in detail in Chapter 14 of the Appendix.

CHAPTER 4EXPERIMENTAL RESULTS4.1 Diffusivity Measurements

Table 4.1 summarizes the values of diffusivity found experimentally for the five solute gases by the diaphragm cell technique described in detail in Chapter 14 of the Appendix, where an evaluation of the accuracy of the measurements may also be found.

TABLE 4.1

<u>Solute Gas</u>	<u>Diffusivity at 25°C in Water</u>
Propylene	1.44×10^{-5} cm. ² /sec.
Carbon Dioxide	2.00
Oxygen	2.41
Hydrogen	4.8
Helium	6.3

4.2 Packed Tower Data4.2.1. Desorption Results

Figures 4.1 and 4.2 give weighted least squares correlations of $(H.T.U.)_{OL}$ vs. D_L at 25°C and various constant flow conditions. The diffusivities listed in Table 4.1 are used in these plots. Figures 4.3 and 4.4 give the same data, correlated by the best log-log line of -0.50 slope. Figures 4.5 and 4.6 present the results plotted as $K_L a$ against D_L , the correlating lines being the best of +0.50 log-log slope.

Figure 4.7 presents the experimental results for the variation of

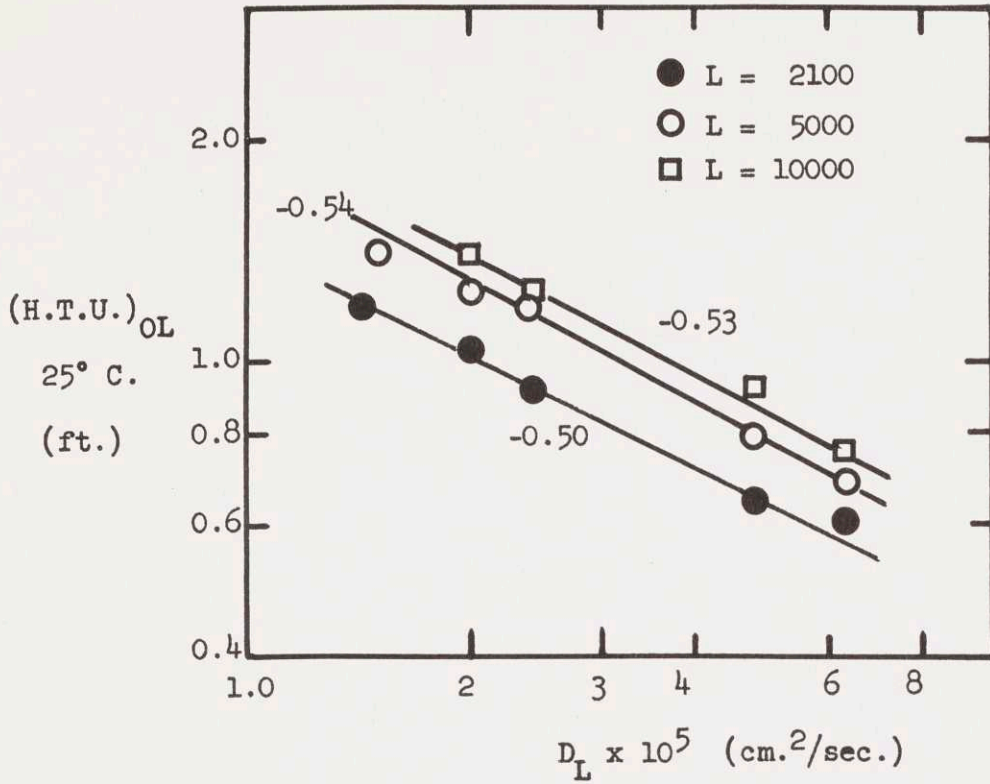


FIGURE 4.1 $(H.T.U.)_{OL}$ VS. D_L AT $G = 900$:
BEST SLOPES

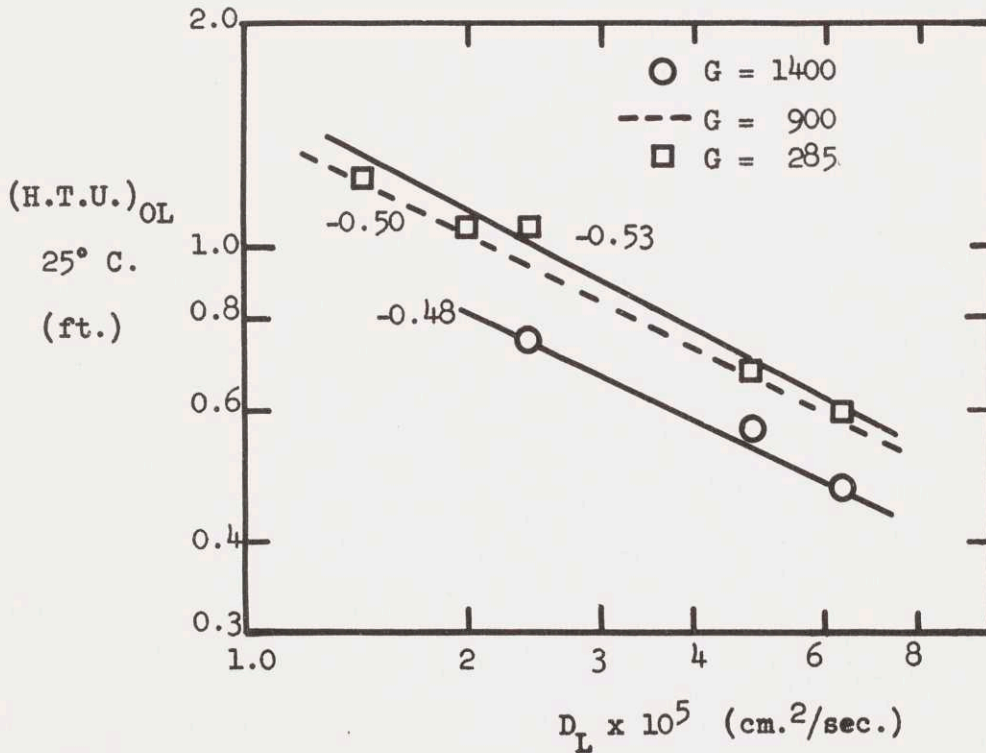


FIGURE 4.2 $(H.T.U.)_{OL}$ VS. D_L AT $L = 2100$:
BEST SLOPES

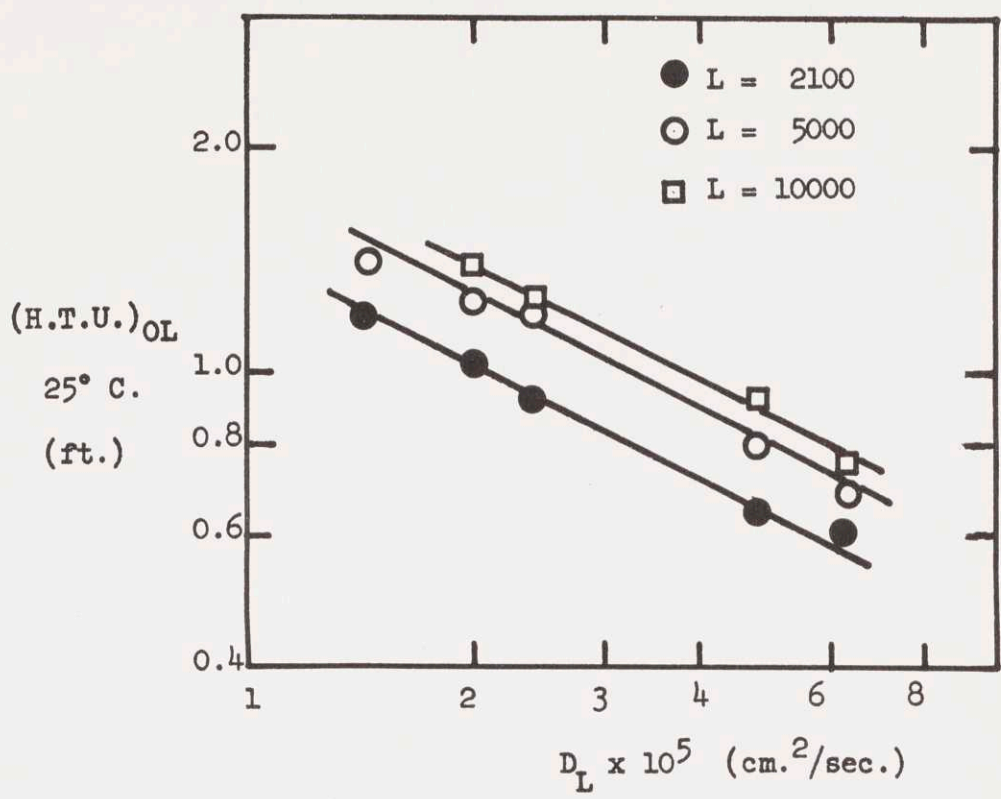


FIGURE 4.3 $(H.T.U.)_{OL}$ VS. D_L AT $G = 900$:
BEST 0.5 SLOPE

- -

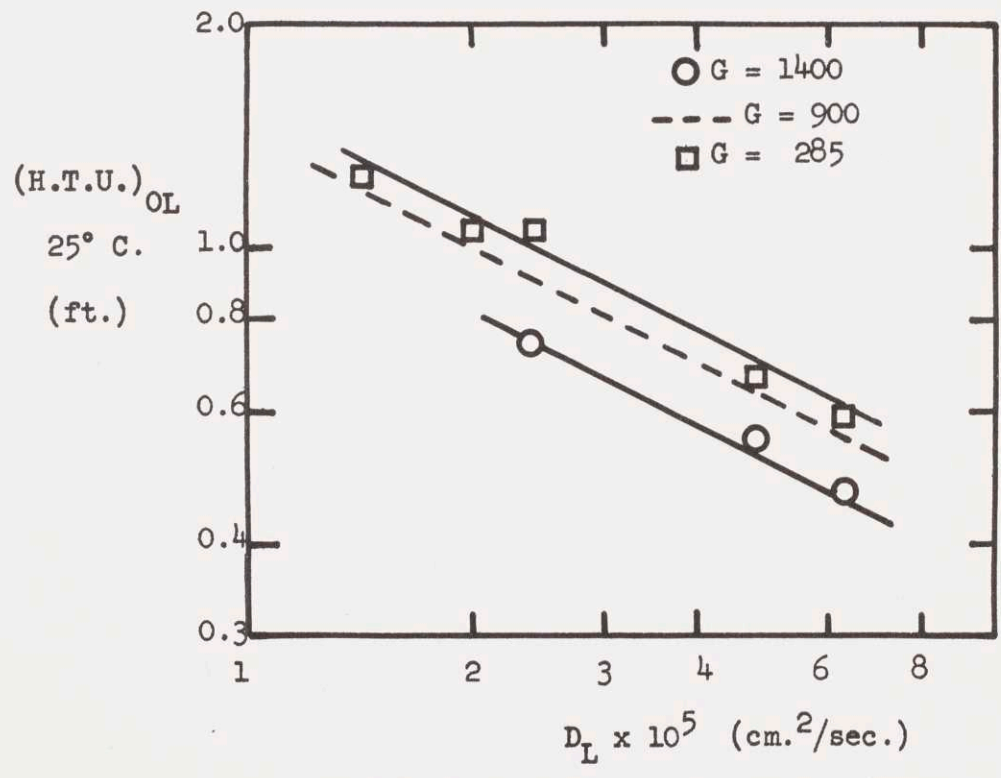
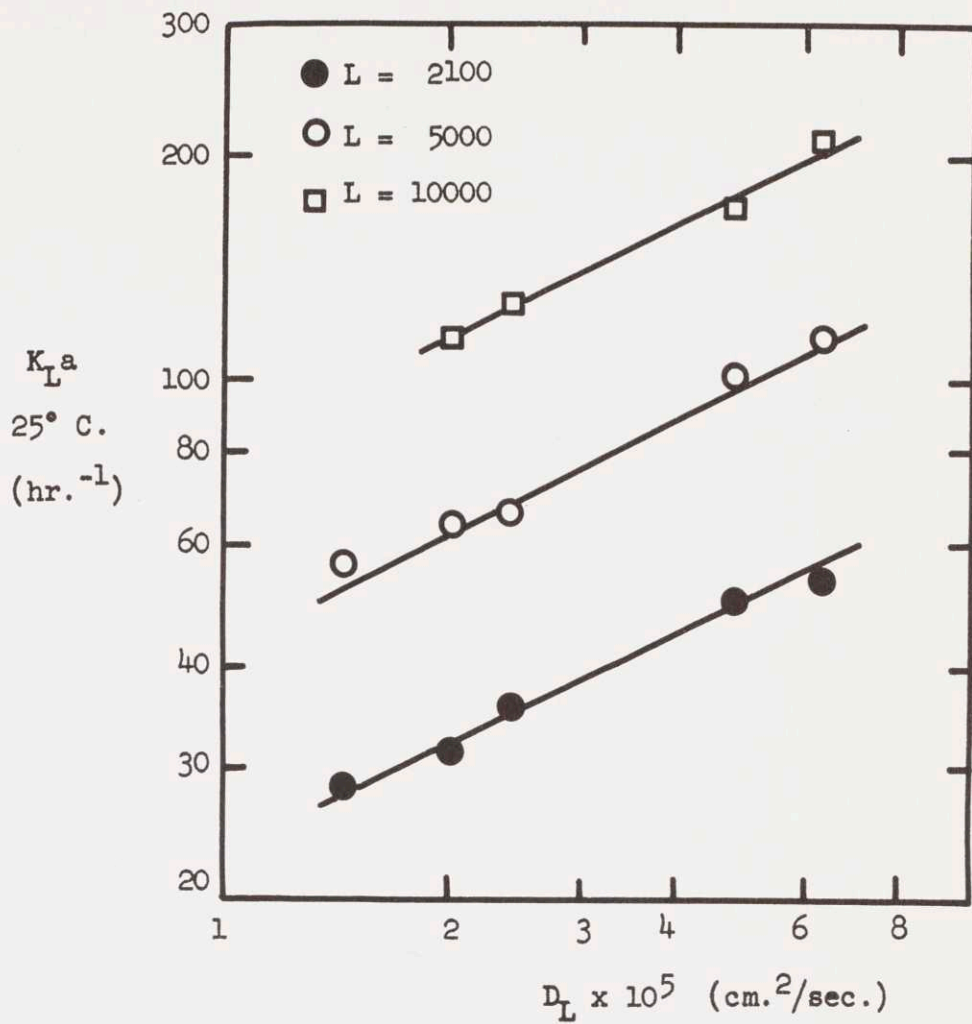
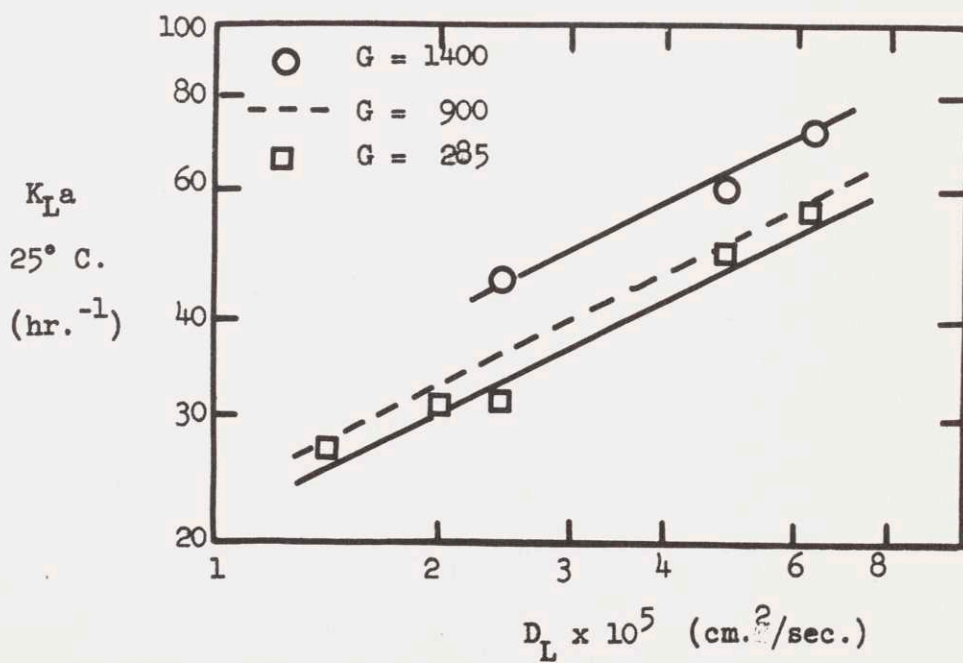


FIGURE 4.4 $(H.T.U.)_{OL}$ VS. D_L AT $L = 2100$:
BEST 0.5 SLOPE


 FIGURE 4.5 $K_L a$ VS. D_L AT $G = 900$

 FIGURE 4.6 $K_L a$ VS. D_L AT $L = 2100$

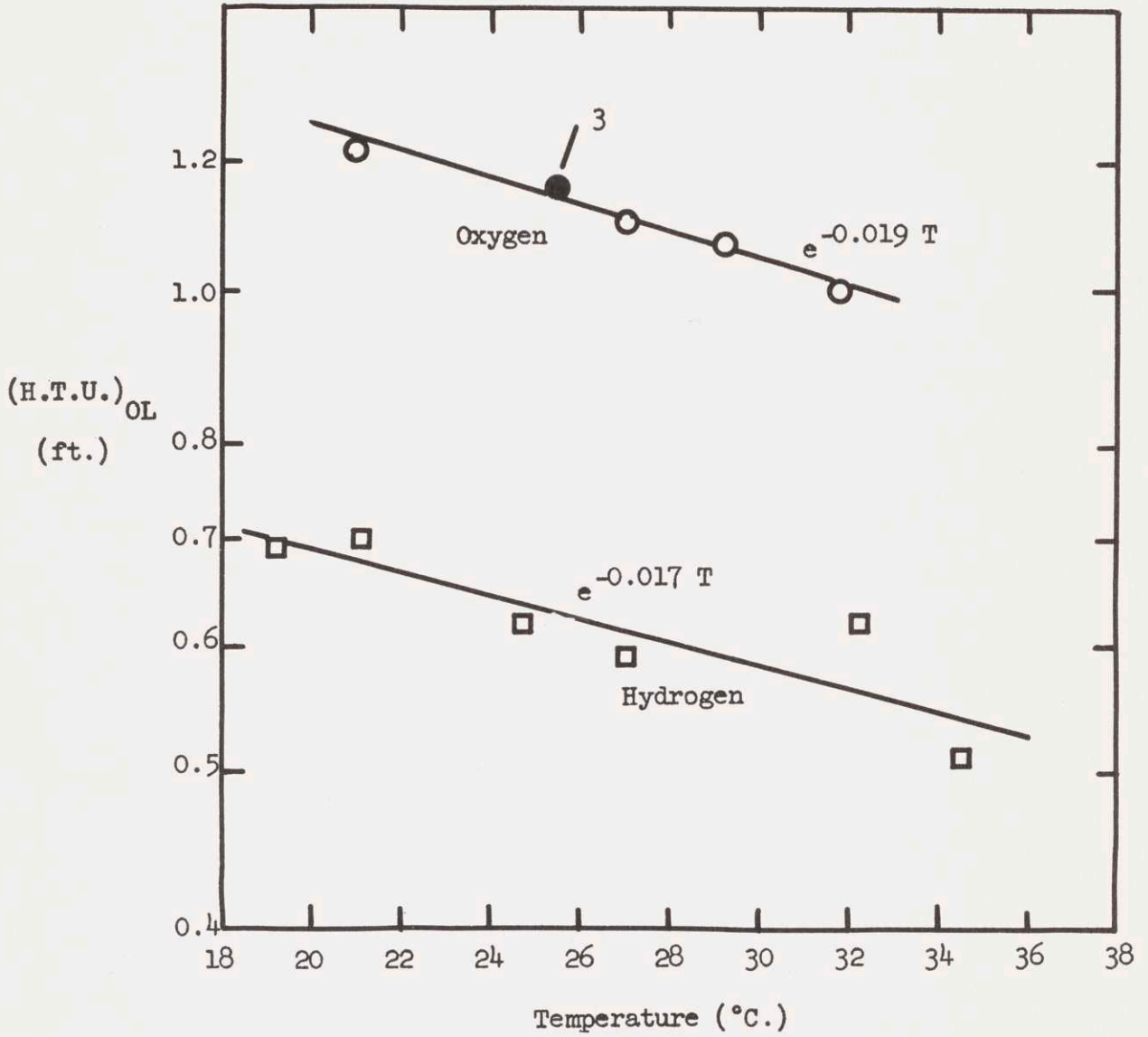


FIGURE 4.7 $(H.T.U.)_{OL}$ VS. TEMPERATURE

$(H.T.U.)_{OL}$ with temperature, for the two cases studied.

Table 4.2 summarizes the effects of varying column height and pool height, and of redumping the packing.

TABLE 4.2

Effects Of Varying Column Height And Pool Height, And Of Redumping Packing On $(H.T.U.)_{OL}$ At 25°C

		----- $(H.T.U.)_{OL}$ -----							
		-----Original Dump-----				-----Redump-----			
		----High Pool----		-----Low Pool----		-----Low Pool----			
<u>Solute</u>	<u>L</u>	<u>G</u>	<u>2.04 Ft.</u>	<u>1.07 Ft.</u>	<u>1.17 Ft.</u>		<u>1.17 Ft.</u>	<u>2.13 Ft.</u>	
		Lb/Hr.Ft. ²		--Meas.--		-Smooth-			
O ₂	2,100	900	1.02 Ft.	0.93 Ft.	0.93 Ft.	0.93 Ft.	-	1.11 Ft.	
O ₂	5,000	900	-	-	1.20	1.18	1.17 Ft.	1.24	
H ₂	2,100	900	-	-	0.66	0.67	0.63*	0.75	

*Smoothed from temperature variation measurements.

Three other results should be mentioned:

- 1) The use of steam deaerated water for oxygen desorption at $L = 5,000$, $G = 900$ with the original dump, low pool height, and a packed height of 1.17 feet gave $(H.T.U.)_{OL}$ at 25°C equal to 1.20 feet, in agreement with the result for non-deaerated water at the same conditions.
- 2) For the absorption of oxygen at $L = 2,100$ and $G = 1,400$, with the redumped packing, low pool height, and a packed height of 1.17 feet, $(H.T.U.)_{OL}$ at 25°C was 0.70 feet, a lower value than obtained for desorption at the same conditions.

3) Propylene desorption rates at three of the flow conditions were open to question (see Section 5.2.3.). Therefore these results were not included in the final correlation of data.

A complete summary of the experimental data and calculations is given in Chapter 17. Chapter 16 explains the calculational methods.

4.2.2. Pressure Drop Results

Figure 4.8 presents the results of pressure drop measurements, so plotted as to give G vs. L at incipient loading, complete loading, and flooding (see Section 5.2.1.). Plots of pressure drop vs. G , from which Figure 4.8 is obtained are presented in Figure 17.1 of the Appendix.

The dotted portion of the flooding curve is extrapolated by analogy to Figure 96 of Reference 133.

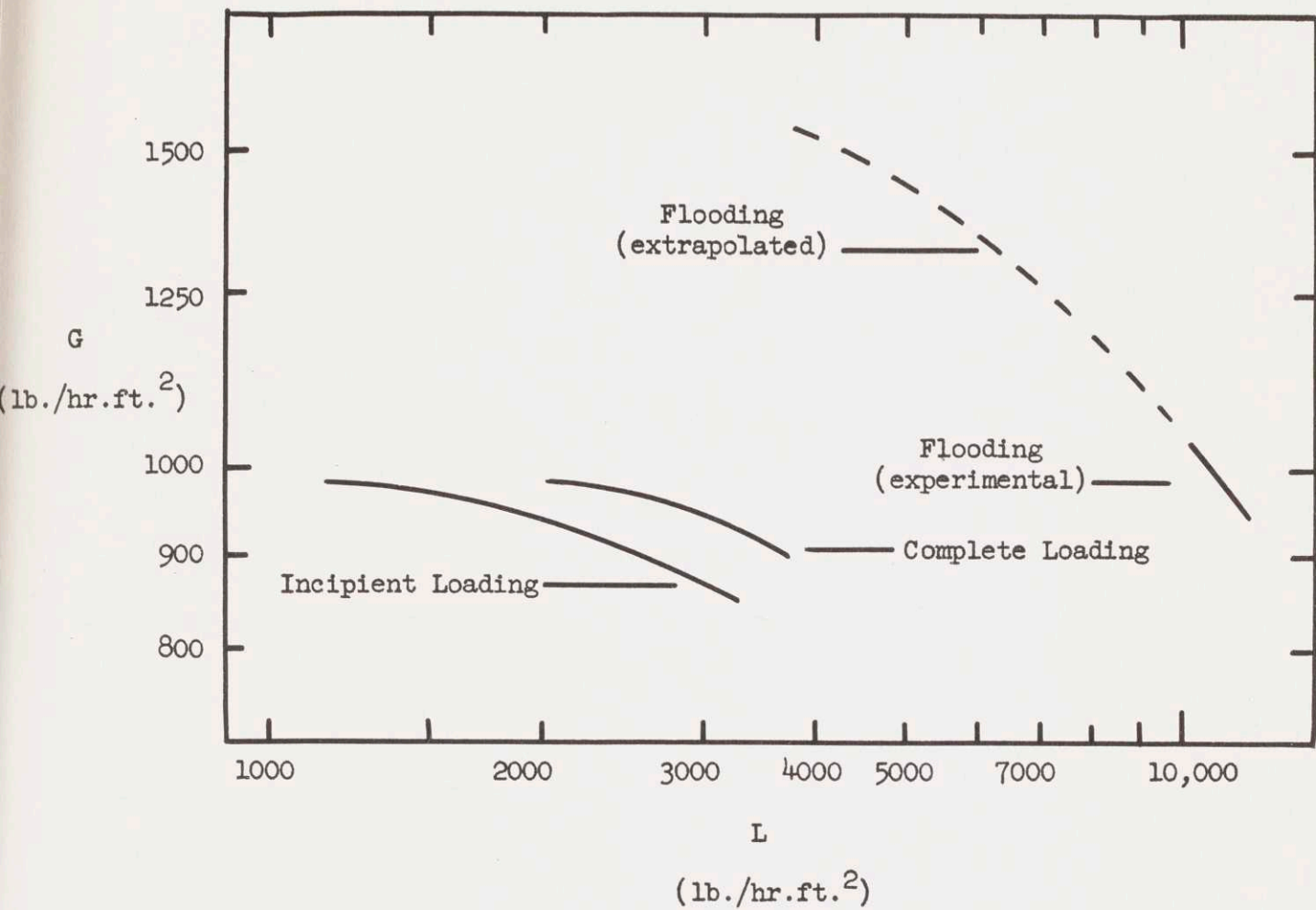


FIGURE 4.8 LOADING AND FLOODING RATES IN COLUMN

CHAPTER 5

DISCUSSION AND APPLICATION OF RESULTS

5.1 Analysis of Experimental Conditions and Computational Assumptions

5.1.1. Degree of Subordination of Gas Phase Resistance

The experiment as designed was intended to take advantage of the very low solubilities of the five solute gases in order to suppress gas phase resistance. The rates of mass transfer found would then be attributable to liquid phase transfer alone. In the terminology of Section 2.1, $K_L a$ would be equal to $k_L a$.

The additivity of resistances, predicted by two-film theory,

$$\frac{1}{K_L a} = \frac{1}{H k_G a^*} + \frac{1}{k_L a^*}, \quad (2.2.2.)$$

may be used to indicate the degree of subordination of gas phase resistance. The asterisks, it should be recalled, indicate coefficients measured in the absence of significant transfer resistance in the other phase.

The gas phase resistance should have the greatest effect in the case of a low air flow rate, a high water flow rate, and the most soluble gas, as may be verified by an examination of Equation (2.2.2.). Carbon dioxide is, by a factor of ten, the most soluble gas; therefore the carbon dioxide data at $L = 10,000$, $G = 900$ should show the greatest effect of gas phase resistance. Sherwood and Holloway (130) give $k_G a^*$ equal

to 33 lb. mol./hr.cu.ft.atm. for this case, based on their study of the vaporization of water at 25°C from 1-1/2 inch Raschig rings. This value has been corrected for their 3 inches of equivalent end transfer effect in 8 inches of packing height. A correction for the difference in molecular diffusivities between water vapor and carbon dioxide would serve to lower this by 25% to 25 lb. mol./hr.cu.ft.atm., if $K_G a$ is assumed to vary with D_V to the 0.5 power, the most extreme probable correction, (116b)(see Section 8.2.2).

From the results of this thesis $K_L a$ at these conditions is 115 hr.⁻¹. Taking H for carbon dioxide at 25°C equal to 30 l.atm./g - mol., from the data of Bohr (125),

$$\begin{aligned} \frac{1}{Hk_G a^*} &= \left(\frac{1}{25} \frac{\text{hr.ft.}^3 \text{atm.}}{\text{lb. mol.}} \right) \left(\frac{1}{30} \frac{\text{g.mol.}}{\text{l.atm.}} \right) \left(28.3 \frac{\text{l.}}{\text{ft.}^3} \right) \left(\frac{1 \text{ lb.mol.}}{454 \text{ g.mol.}} \right) \\ &= 8.3 \times 10^{-5} \text{ hr.} \end{aligned}$$

whereas

$$\begin{aligned} \frac{1}{K_L a} &= \frac{1}{115} \text{ hr.} \\ &= 8.7 \times 10^{-3} \text{ hr.} \end{aligned}$$

Thus at the extreme conditions, the gas phase, by two film theory additivity, presents only one per cent of the total resistance to desorption. This is small enough to be negligible. (Furthermore, the fraction active surface is near unity. See Section 8.2.2).

It has also been mentioned previously (Section 2.1.2.) that it is possible to make a penetration theory additivity "correction" to the two-film theory of additivity assuming a constant thin-film gas phase resistance in contact with a liquid surface during its lifetime. For the extreme case of CO_2 desorption at $L = 10,000$, $G = 900$, this correction is less than 0.3% (see Figure 8.1). Such other theories of additivity (i.e., turbulent gas phase boundary layer coupled with penetration, etc.) as are presented in Chapter 8 also predict a negligible correction for gas phase resistance.

All these theories, however, do not allow for the occurrence of relatively stagnant air pockets in contact with water surfaces active for transfer. Such stagnant portions of air could present a sizeable gas phase resistance at those portions of the interface. The occurrence of stagnant pools in the water phase in contact with moving air, is not at all unlikely (Section 8.1.4.); however, it is difficult to conceive of portions of the much more mobile air phase being stagnant in the presence of active, moving liquid surface. Also the lack of any consistent tendency for the carbon dioxide $K_L a$ transfer coefficients to be low in relation to the coefficients for the other, ten times or more less soluble, gases indicates the absence of any significant gas phase resistance. This is confirmed, too, by Sherwood and Holloway's observed lack of influence of air flow rate on carbon dioxide desorption rates (61, 131).

The $K_L a$ values obtained in this thesis may thus be taken as true $k_L a$ (or $k_L a^*$) coefficients for liquid phase resistance in the absence

of significant gas phase resistance. Similarly $(H.T.U.)_{OL} = (H.T.U.)_L$.

5.1.2. Coefficient of Desorption vs. Coefficient of Absorption

The H.T.U. for oxygen absorption at $L = 2,100$, $G = 1,400$ comes out to be lower (higher $K_L a$) than that for oxygen desorption by some 7%. Since this 7% is significantly larger than the estimated standard deviation of the data (3% for absorption and 1% for desorption), the indication is either that the coefficient for desorption is in reality not equal to the coefficient for absorption in this case or that there was an error in either the analytical or calculational technique.

It is difficult to conceive theoretically of a realistic transfer mechanism in a packed column for which $k_L a$ (or $(H.T.U.)_L$) for desorption should not equal $k_L a$ (or $(H.T.U.)_L$) for absorption under the same hydrodynamic and temperature conditions. The concepts of concentration gradients and driving forces involved are completely analogous for the two processes, and the transfer rates encountered are certainly not great enough to affect the interfacial equilibrium (121) or the hydrodynamics. There is also experimental proof in the literature (4, 12, 131, 132) indicating that the coefficients for desorption and absorption are equal under similar conditions to these.

The more obvious reason for the discrepancy would be an error in the analytical or calculational techniques. The standardization of the thiosulfate solutions used for oxygen analyses against weighed phthalate sample was reproducible to 0.2% (Section 15.2); however, it was also

necessary to employ oxygen solubility data in the calculational process (Section 16.1.2), and these may well not have had the 0.2% accuracy of the solution standardizations.

The effect of an error in the oxygen solubility data (which would present itself as an error in C_E in the calculational equations of Section (16.1.2) may be estimated using the approximate equation

$$(N.T.U.)_{OL} = \ln \frac{(C_L - C_E)_T}{(C_L - C_E)_B} \quad (16.1.6)$$

The nomenclature used here is defined in Section 16.1.2 and in Chapter 20. C_E may, to an approximation, be taken equal at tower top and tower bottom. If the equation is differentiated with respect to C_E , and use is made of the fact that $(N.T.U.)_{OL} = h/(H.T.U.)_{OL}$, we have

$$\frac{d(N.T.U.)_{OL}}{d C_E} = \frac{C_T - C_B}{(C_T - C_E)(C_B - C_E)} \quad (5.1.1)$$

and, taking $d(N.T.U.)_{OL}$ equal to $\Delta(N.T.U.)_{OL}$ and $d C_E$ equal to ΔC_E ,

$$\begin{aligned} \frac{\Delta(N.T.U.)_{OL}}{(N.T.U.)_{OL}} &= - \frac{\Delta(H.T.U.)_{OL}}{(H.T.U.)_{OL}} = \frac{(C_T - C_B) C_E}{(C_T - C_E)(C_B - C_E)(N.T.U.)_{OL}} \cdot \frac{\Delta C_E}{C_E} \\ &= \frac{(C_T - C_B) C_E (H.T.U.)_{OL}}{(C_T - C_E)(C_B - C_E) h} \cdot \frac{\Delta C_E}{C_E} \end{aligned} \quad (5.1.2)$$

or

$$\% \text{ error in } (H.T.U.)_{OL} = - \frac{(C_T - C_B) C_E (H.T.U.)_{OL}}{(C_T - C_E)(C_B - C_E) h} \cdot \% \text{ error in } C_E \quad (5.1.13)$$

Substituting data for oxygen desorption run 64 (sample set 1), there results

$$\% \text{ error in } (H.T.U.)_{OL} = 6.1 (\% \text{ error in } C_E).$$

Data for oxygen absorption run 63 (sample set 1) give

$$\% \text{ error in } (H.T.U.)_{OL} = -1.7 (\% \text{ error in } C_E).$$

Since these are errors in opposite directions the 7% discrepancy between $(H.T.U.)_{OL}$ for absorption and $(H.T.U.)_{OL}$ for desorption could have come from an error of -1% in the oxygen solubility.

Table 5.1 gives the various data for oxygen solubility given by Seidell (125), and also another more recent value. The data of Winkler were used for calculational purposes because Holloway had checked them fairly closely (see below) and they were intermediate between the more recent measurements.

The range of these literature solubility values is 3%, so it is not at all unlikely that the Winkler data are 1% too low; as a matter of fact, such a correction would place the true value at the average of the seven literature values.

Holloway (61d) endeavored to check the Winkler data by bubbling both 99.5% pure oxygen and air "through distilled water and tap water in a 250 cc. glass-stoppered erlenmeyer ..., at a constant known temperature for an hour or more." His calculated partial pressures of oxygen taking humidity into account, were 0.972 and

0.979 atm. for saturation with oxygen, and 0.2095 and 0.2120 atm. for saturation with air. He attributed the low values for pure oxygen (2% low) to loss of oxygen; however, one could as well take a -1% error in the Winkler data and attribute a 3% too low value for pure oxygen and the slight ($< 1\%$) error for air to analytical error and incomplete saturation, in addition to loss of oxygen during an analysis for the case of pure oxygen.

TABLE 5.1

Summary of Literature Data for Oxygen Solubility
in Water at 25°C

<u>Investigator</u>	<u>Solubility (g - mol./liter atm.)</u>
Winkler (1891)	0.00126
Bohr and Bock (1891)	0.00129
Geffcken (1904)	0.00126
Fox (1909)	0.00129
Orcutt and Seevers (1936)	0.00125
Morgan and Richardson (1930)	0.001275
Morrison and Billet (1948)(97)	0.00125

It is apparent that the effect of a solubility error is greater the lower the $C_L - C_E$ driving force at the bottom of the tower; thus the error in $(H.T.U.)_{OL}$ for absorption is greater than that in $(H.T.U.)_{OL}$ for desorption (because the oxygen concentration initially was nearer equilibrium), and the error for 2 feet packed height is greater than that for 1 foot packed height.

The corrected $(H.T.U.)_{OL}$ at $L - 2,100$, $G - 1,400$ for oxygen

absorption and desorption corresponding to this possible -1% solubility error would be 0.74 ft., a small change from the desorption value based on the Winkler data. Table 5.2 summarizes the corrections, calculated by Equation (5.1.3.), necessary in the various other measured oxygen (H.T.U.)_{OL} values for a -1% error in the Winkler solubility data.

TABLE 5.2

Corrections to be Applied to Oxygen (H.T.U.)_{OL} Results
Corresponding to a -1% Error in Solubility Data

Packed Height Ft.	L Lb./Hr.Sq.Ft.	G Lb./Hr.Sq.Ft.	(H.T.U.) _{OL} Calc. Ft.	Correction %	(H.T.U.) _{OL} Corr. Ft.
1.17	2,100	1,400	0.75	-1.7	0.74
1.17	2,100	1,400	0.69*	+6.1	0.74
1.17	2,100	900	0.93	-1	0.92
1.17	2,100	285	1.06	-1	1.05
1.17	5,000	900	1.20	-1	1.16
1.17	10,000	900	1.27	-0.7	1.26
2.04	2,100	900	1.02	-2.3	1.00
2.13	5,000	900	1.24	-1.2	1.23
2.13	2,100	900	1.11	-1.9	1.09

*Absorption

The effect is small in all cases, having about a 1% effect in lowering the slopes of the log (H.T.U.)_{OL} vs. log D_L plots, and tending to bring the values of (H.T.U.)_{OL} at 2 ft. packed height slightly closer to the values at 1 ft. packed height.

The effect of this possible error in the Winkler data on the calculated results of Holloway (61) is discussed in Chapter 18 of the Appendix.

Although the oxygen data tend to show much less internal scatter than the data for other solute gases, the discussion of this section indicates one serious limitation to the oxygen desorption technique that should be kept in mind. In instances when the concentration at the bottom of the tower becomes quite small, a slight error in oxygen solubility data may have a large effect on the calculated $(H.T.U.)_{OL}$ or $K_L a$.

5.1.3. Effects of Pool Height, Repacking, and Packed Height

The height of the water collection pool at the bottom of the packing was varied in the early runs in order to determine whether there was any perceptible added mass transfer rate at the higher pool height from turbulence or additional interfacial air-water contact area caused by mixing or by the momentum of the air emanating from the air distribution ports. The results in Table 4.2 indicate there was no such effect detectable.

Half of the original packing dump was removed after Run 4. The remaining one foot of packing was removed and redumped after Run 49, and then an additional foot of packing was added after Run 67. Table 4.2 indicates a possible 3% lower $(H.T.U.)_{OL}$ for the redumped one foot height than for the original dump, based on the $L = 5,000$, $G = 900$

oxygen results. The $L = 2,100$, $G = 900$ hydrogen results indicate a similar effect. For a 2 ft. packed height there is some 10% discrepancy between dumps for the $L = 2,100$, $G = 900$ oxygen data.

Both of these could be attributed to different bed densities occasioned by inadvertent differences in packing loading technique. Any significant effect of bed settling as time went on may be discounted by an examination of the history of $L = 2,100$, $G = 900$ oxygen runs in the case of the first dump (Table 17.1).

In analyzing both the case of redumping the packing and the case of variation of packed height, the accuracy in measurement of the packed height should be kept in mind. This is probably on the order of half a packing diameter, or 6% of the one foot height and 3% of the two foot height. This could account almost completely for the observed effects of redumping.

The effect of varying the packed height is apparently slightly more severe. Accepting for the moment the -1% error in the Winkler solubility data indicated in Section 5.1.2, the $(H.T.U.)_{OL}$ for oxygen at $L = 2,100$ and $G = 900$ is some 8% higher at 2 ft. packed height than at 1 ft. packed height (first dump), and the $(H.T.U.)_{OL}$ for oxygen at $L = 5,000$ and $G = 900$ is some 7% higher at 2 ft. packed height than at 1 ft. packed height (second dump). The $(H.T.U.)_{OL}$ for hydrogen is 17% higher for 2 ft. packed height than for 1 ft. packed height (second dump). There is an indication that for oxygen at $L = 2,100$ and $G = 900$ in the second dump the $(H.T.U.)_{OL}$ at 2 ft. packed height is 16% higher

than for 1 ft. packed height. This rather large variation in the case of the second dump could be partially due to inaccurate height measurement and partially due to some other effect.

The hydrogen variation with height should not be given too much weight, first because of the greater scatter of hydrogen data in general, and, second because an analysis similar to Equation (5.1.3) shows that the deviation could have come from the presence of some 0.06% of hydrogen in laboratory air. This is not unlikely considering that the water storage tanks had open surfaces.

The possibility of poorer water distribution at the top of the tower in the instance of the second dump at 2 ft. packed height should also not be discounted.

Holloway (61) also noticed a 15 or 20% lower $(H.T.U.)_{OL}$ at the low packed heights (6.5 inches) than at higher packed heights (17 inches and 49 inches) for 1 and 1-1/2 inch Raschig rings. (see Figures 5.4 and 5.5) He discounted the effect of end transfer as being responsible for this in light of the agreement of his results in the cases of 17 inch and 49 inch packed heights for 1 inch Raschig rings. The re-examination of his data made in Chapter 18 indicates that his values of $(H.T.U.)_{OL}$ for 49 inches height may have been as much as 8% lower than those for 17 inches height. This operates in the opposite direction than to produce a trend with height and thus makes an end transfer effect even less probable.

In the present case the pool surface area was only 3% of the total packing surface in the instance of 1 ft. packed height. Allowing for only a fraction of the packing surface being wetted and effective for desorption, it is possible that the pool could produce an end effect sufficient to account for the observed effect of packed height; however it is unlikely that the pool surface is as "active" for desorption as that of the water in actual flow over the packing.

The presence of any end transfer at the top of the packing is unlikely in view of the elaborate water distribution system. Any significant effect of poor water distribution on the upper layers of packing is unlikely in view of the 23 downcomer tubes, and would also have acted to produce an opposite effect of packed height from that observed. Some effect in the observed direction might possibly have come from turbulence produced by the momentum of the jets of water emanating from the downcomer tubes or from turbulence in the water produced by the incoming air streams and not detected by the variation of water pool height at the bottom of the packing.

Another possible effect of packed height that could have a mechanisml significance should be mentioned. Assuming that an unsteady-state penetration effect holds, to the extent that the residence time of the water on the packing in flow over it is small compared to the average lifetime that an element of water surface would reach in flow through an infinitely high column, the indicated $K_L a$ will be high (or H.T.U. will be low) at a low packed height. This will be so because the surface in the "last" exposure will not reach its normal age. An approximate

analysis may be made of this possibility:

Assuming that there is one certain surface lifetime, θ , that would be reached by a water surface element and one certain residence time, τ , of water on the packing in flow over it, the distortion of the observed $k_L a$ from the $k_L a$ for an infinite packed height would be

$$\begin{aligned}
 k_L a &= \frac{a}{\tau} \int_0^{\tau} k_L(\tau) d\tau = \frac{a}{\tau} \left[n \int_0^{\theta} \sqrt{\frac{D_L}{\pi t}} dt + \int_{n\theta}^{\tau} \sqrt{\frac{D_L}{\pi t}} dt \right] \\
 &= \frac{a}{\tau} \left[2n \sqrt{\frac{D_L \theta}{\pi}} + 2 \sqrt{\frac{D_L (\tau - n\theta)}{\pi}} \right] \quad (5.1.4)
 \end{aligned}$$

taking k_L at any age, t , equal to $\sqrt{\frac{D_L}{\pi t}}$ by penetration theory (Equation 2.1.25). Now, since $k_L a_{\infty} = 2a \sqrt{\frac{D_L}{\pi \theta}}$ by penetration theory (Equation 2.1.26),

$$\frac{k_L a}{k_L a_{\infty}} = \frac{1}{\tau} \left[n\theta + \sqrt{\theta (\tau - n\theta)} \right] \quad (5.1.5)$$

where $n\theta \leq \tau \leq (n+1)\theta$

$k_L a$ = the measured $k_L a$

$k_L a_{\infty}$ = $k_L a$ for an infinitely high tower

n = an integer

τ = residence time of surface elements in tower

t = surface age

θ = surface lifetime in infinitely high tower

D_L = diffusivity

The first term in this expression comes from the absorption or desorption that has taken place in all the penetration before the last one the surface undergoes before leaving the tower. The second term gives the fraction of transfer occurring during this last penetration. $k_L a / k_L a_\infty$ is, for a non-integral value of τ/θ , greater than 1 because during this last penetration the surface does not reach the lifetime it would have, had it not suddenly left the column; thus the average $k_L a$ for this last penetration is greater than the $k_L a$ for the preceding complete penetrations, because the lifetime, $\tau - n\theta$, characterizing it is less than the lifetime, θ , characterizing the preceding penetrations. For τ being an integral number of lifetimes, obviously $k_L a = k_L a_\infty$.

This solution is shown graphically in Figure 5.1.

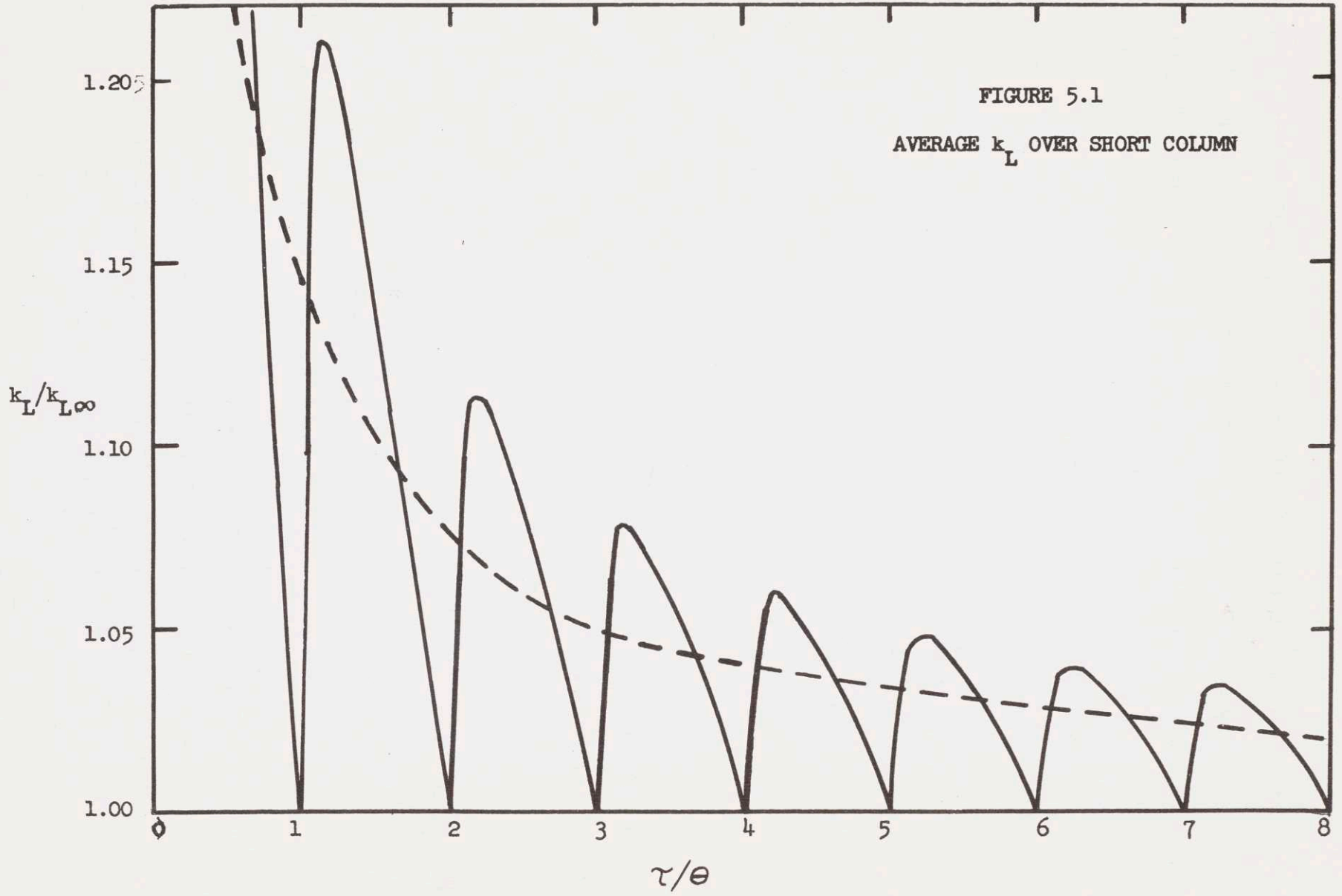
In reality there will be a distribution of lifetimes and a distribution of residence times, both of which will serve to smooth out the peaks in this single-lifetime, single-residence time curve. A smoothed curve, arbitrarily drawn so as to include the same area beneath it as under the original, peaked curve is also shown in Figure 5.1 as the dotted line.

An estimation of the average τ/θ ratio in the present packed column may be made by the following method:

For the case of $L = 2100$, $G = 900$, Shulman et al (136), give the water hold-up on 1-1/2 inch Raschig rings as 0.042 cu.ft. H_2O /cu.ft. packing. It is unreasonable, however, to credit all this hold-up to active flow through the tower. Shulman divides the hold-up into operating and static

FIGURE 5.1

AVERAGE k_L OVER SHORT COLUMN



hold-ups, the former being the amount of water that drains readily from the packing, and the latter being the amount retained for a longer time. For the present flow conditions he gives an operating hold-up equal to 0.033 cu.ft./cu.ft., or 80% of the total hold-up. This operating hold-up may be taken as the best available approximation of the hold-up present in the tower as active flow.

If one assumes that the surface hold-up time is 2/3 of the average hold-up time of the water in active flow (since the surface velocity for free gravity fall is 3/2 times the mean bulk velocity of the falling liquid film (107d), then the average hold-up time, τ , of surface elements in the tower is

$$\tau = \frac{2}{3} \frac{(0.033 \text{ cu.ft./cu.ft.})(62.4 \text{ lb/ft}^3)(3600 \text{ sec/hr})}{2100 \text{ lb/hr.sq.ft.}} \cdot h \text{ (ft)}$$

$$= 2.4 \text{ h sec.},$$

where h is the packed height in feet.

An estimate of the average surface lifetime during an exposure may be obtained by separating the a_e (see Chapter 9) from the measured value of $k_L a^*$ at these conditions by the use of the values given by Shulman et al (137). This yields an effective interfacial area of about 18 sq.ft./cu.ft. of packing for L = 2100, G= 900, and flow over 1-1/2 inch Raschig rings.

The value of $K_L a$ for oxygen desorption reported in Chapter 4 for these flow conditions is 36 hr⁻¹. If this is taken equal to $k_L a$, and

a is taken as 18 sq.ft./cu.ft., then

$$k_L = 36/18 = 2.0 \text{ ft./hr.}$$

By Equation (2.1.26) this is equal to $2 \sqrt{\frac{D_L}{\pi \theta}}$, from penetration theory,

with θ denoting an average lifetime of the effective liquid surface. Thus

$$\begin{aligned} \theta &= \frac{D_L}{\pi} \left(\frac{2}{k_L}\right)^2 \\ &= \frac{(2.41 \times 10^{-5} \text{ cm.}^2/\text{sec.})(4)}{\pi (4.0 \text{ ft.}^2/\text{hr.}^2)} \frac{1 \text{ ft.}^2}{(30.5)^2 \text{ cm.}^2} (3600)^2 \frac{\text{sec.}^2}{\text{hr.}^2} \\ &= 0.11 \text{ sec.} \end{aligned}$$

On this basis, then, at 1 ft. packed height τ/θ is 22, and at 2 ft. packed height τ/θ is 43. Figure 5.1 indicates that the difference between values of $k_L a$ at the two ft. height due to the effect of small τ/θ should be negligibly small.

This calculation, however, was based upon the assumptions of (1) plug flow of the active liquid through the packing, and (2) a hold-up time of surface liquid elements on the packing characterized by the operating hold-up. The first of these assumptions is probably valid; the second, however, may not be. To the extent that a much lesser liquid volume is involved in the active film flow over the packing, the τ/θ value will be lower, and this effect would come more into play, serving to produce a higher $k_L a$ (or lower $(\text{H.T.U.})_L$) at lower packed heights.

Because of this uncertainty and because of Holloway's aforementioned results for 1 inch Raschig rings (which indicate an effect of height other than end transfer at low heights) the H.T.U. results of this thesis have not been corrected for possible end transfer.

In conclusion, it should be stated that, to the extent that any transfer other than that attributable to flow over packing is minimized, a knowledge of the absolute values of $(H.T.U.)_{OL}$ is unnecessary for the purposes of this investigation, since only relative values for the various solute gases are indicative for determining the effect of solute diffusivity.

5.1.4 Other Sources of Error

The summarized data presented in Table 17.1 show that the experimental technique was such as to give about 5 to 6 per cent standard deviation in the H.T.U. values for solutes other than oxygen. Much of this apparently random scatter probably entered from the analytical techniques employed. Chapter 15 of the Appendix discusses analytical errors, which may amount to 10% for helium, hydrogen, and propylene, 4% or more for carbon dioxide, and about 1% for oxygen. Twice the error for a single analysis is possible, since two analyses are necessary for each H.T.U. computation. This is in actuality dependent on the N.T.U. value, being valid strictly for $N.T.U. = e$ (see Equation 16.1.4). For a lower N.T.U. the error could be greater, and for a higher N.T.U. the error would be less.

Although analytical errors could account for the bulk of the observed scatter, it is probable, too, that some arose from the sampling

procedure. All samples other than oxygen solutions required two minutes for collection (Chapter 13), and tower conditions could change enough during this time to produce a small effect.

The possible 5% error in water flow rate measurement mentioned in Chapter 13 could account for 1 to 2 per cent or more of the scatter in H.T.U.'s, since $(H.T.U.)_L$ varies as $L^{0.25}$ below loading and flooding and with L to a higher power as the loading and flooding regime is entered (131). The possible 5% error in air flow measurements should affect the H.T.U.'s less, since $(H.T.U.)_L$ is less dependent upon gas flow rate, G (131). Because it would enter as a consistent error, an air flow rate error would affect all values at the same G equally, whereas an error in L might not be constant.

The scatter of the data indicates the effect of random errors; it would not, however, point out consistent errors such as, for instance, the possible error in oxygen solubility mentioned in Section 5.12. The lack of a tendency for the points for any particular solute gas to deviate consistently in any one direction from the correlating $(H.T.U.)_{OL}$ vs. D_L line indicates there is probably no consistent error in the results for one gas and not for the others. Any consistent errors affecting the results for all solute gases in the same way would most probably be attributable to sampling technique or poor bulk stream flow rate measurements. The possible errors from these causes have been discussed above.

5.2 Analysis of Experimental Results

5.2.1 Regimes of Operation

The results of pressure drop measurements made in the vicinity of each of the five flow conditions that were studied are shown in Figure 4.8 and Figure 17.1. Also presented in Figure 17.1 are the results of Tillson (150), who studied pressure drops through packing, both below and at loading.

Tillson defined his loading point as the gas flow rate, G , at which a plot of $\log \Delta P/h$ (pressure drop per unit height of packing) versus $\log G$ developed a slope greater than 2.0. This corresponds to the curve marked "incipient loading" for the present data. In actuality, if one defines loading and flooding in a packed tower as the two sharpest break points in the $\log \Delta P/h$ vs. $\log G$ curve, then the greatest degree of change in slope per change in G in the loading region occurs between the curves marked "incipient loading" and "complete loading," where the slope changes in a more or less uniform manner with G (and L) from 2.0 to 2.5. The slope then will retain a value between 2.5 and 2.8 over a much larger G (or L) range extending up to the flooding point. Flooding is defined as the second sharp break point in the $\log \Delta P/h$ vs. $\log G$ curve (slope suddenly increasing above 3.0). A much sharper break point was observed for flooding than for the loading regime.

Tillson's loading points are somewhat below the present incipient loading points; however the disagreement is practically within the scatter of the present data. There may, in actuality, have been some

physical difference between the present column and Tillson's to account for this.

What is more striking is a comparison between the pressure drops at various flow rates for the present data and those of Tillson. Tillson's pressure drops are higher; at $L = 1750$ and $G = 900$ Tillson gives $\Delta P/h$ equal to 0.43 inches of water per foot of height, while the present data give 0.34 inches per foot. This may well be attributable to the fact that Tillson measured the pressure drop over the packing support in addition to that through the packing. He varied the packed height in his studies of 1/2 inch Raschig rings and claimed to find no "end effect," i.e., $\Delta P/h$ was the same at all heights for given flow conditions. The pressure drop through 1/2 inch Raschig rings is, however, about three times that through 1-1/2 inch Raschig rings, so an end effect significant in the case of 1-1/2 inch Raschig rings might not be apparent for 1/2 inch rings. This could account for the difference between the present data and those of Tillson.

The pressure drop for dry 1-1/2 inch Raschig rings packing given by Berl (8) is identical with that found in the present study, as shown in Figure ~~4.8~~^{17.1}. Together with the close agreement found with the results of Holloway (Section 5.2.2), this indicates that there was nothing untoward occurring through the tower.

The five flow conditions studied are presented in terms of L/G ratio and the regime of operation in relation to loading or flooding in Table 5.3. The conditions are also conveniently represented on a water

hold-up plot to show their relation to one another and to the hold-up in Figure 5.2. The hold-up data are those of Shulman et al, (136). The flooding values were extrapolated by analogy to the curves presented in reference (133), page 248.

TABLE 5.3

Conditions of Tower Operation

<u>L</u>	<u>G</u>	<u>L/G</u>	<u>Regime</u>	<u>G(% of Flooding at that L/G)</u>
2,100	285	7.4	Below loading	26
2,100	900	2.3	Near incipient loading	56
5,000	900	5.6	Above loading	73
10,000	900	11.1	Above loading	91
2,100	1,400	1.5	Above loading	80

5.2.2 Agreement with Previous Work

a. Effect of Diffusivity

The only previous investigations of the effect of solute diffusivity on liquid phase resistance to absorption or desorption in packed towers have been those of Sherwood and Holloway (61, 131) and Onda, et al (102). The latter studied only a small laboratory scale column.

As has been discussed in Sections 2.2.1 and 2.2.2, interpretation of the Sherwood and Holloway data is complicated somewhat by the facts that six inches of end effect were present with only eight inches of packed height and that temperature was not maintained constant in the runs made with different solute gases. Hydrogen, the only solute with a

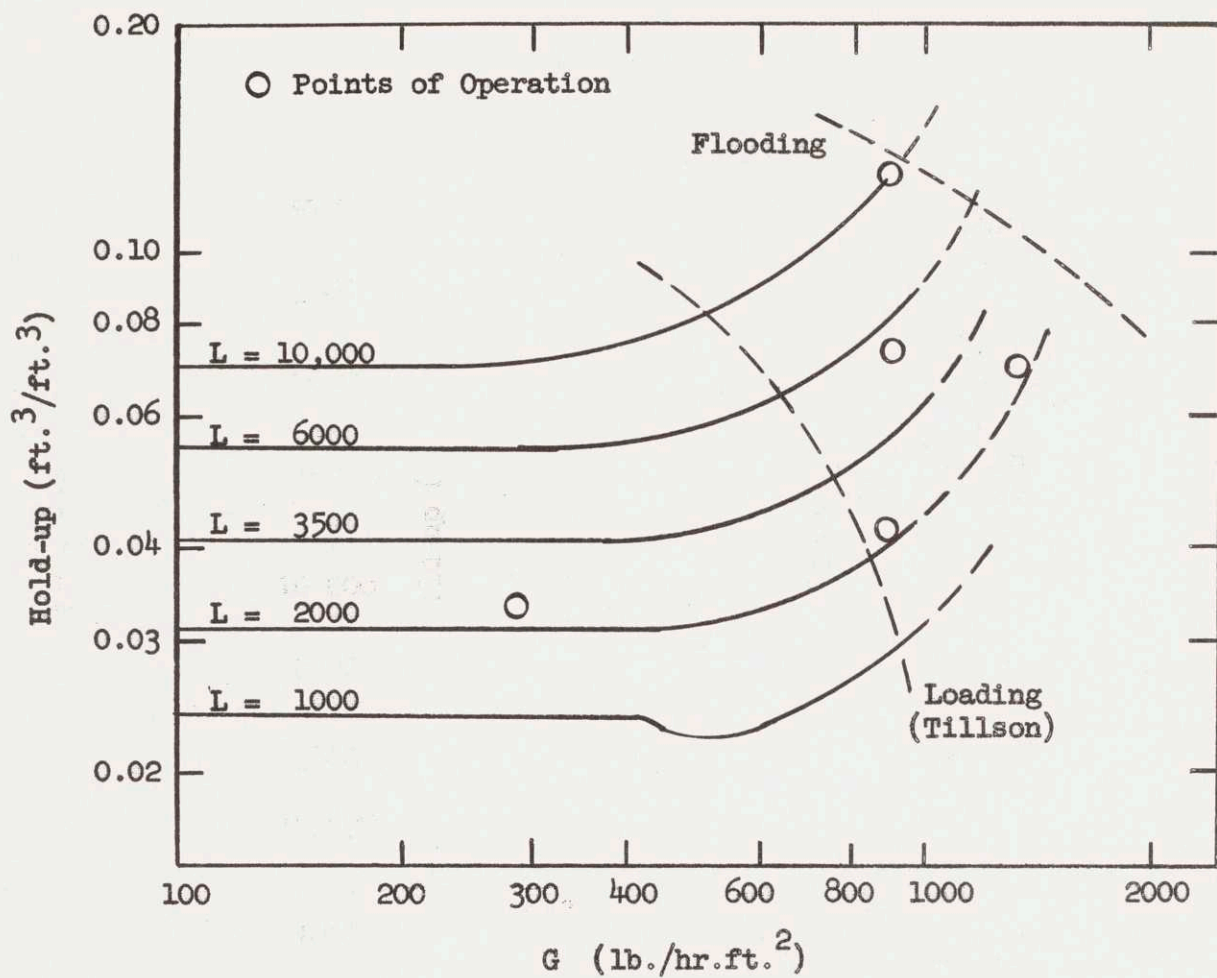


FIGURE 5.2 HOLD-UP ON 1 1/2 IN. CERAMIC RASCHIG RINGS

(from Shulman, Ullrich & Wells, A.I.Ch.E. Jour., 1, 247 (1955))

widely different diffusivity from the others, was only studied at one set of flow conditions which were relatively low rates for industrial application. Diffusivity values were also questionable at the time.

Their data for carbon dioxide, oxygen, and hydrogen are shown in comparison with the present data in Figure 5.3. Values at 25°C were taken by interpolation from their curves of $(H.T.U.)_L$ variation with temperature and have been corrected for the end effect by the ratio of their $(H.T.U.)_L$ found for oxygen desorption in Part II (with no apparent end effect).

The Sherwood and Holloway data agree well with the present values of diffusivity giving an exponent on diffusivity of 0.5 as was found in the present case. Apparently, therefore, the mechanism of the end transfer in Holloway's tower was also characterized by the 0.5 power of diffusivity.

Onda, et al, (102) studied the absorption of both carbon dioxide and hydrogen into water in a small column packed with 6 mm. (1/4 inch) Raschig rings, at conditions well below loading and L/G varying from 35 to 250 (relatively very high values, corresponding to the L/G employed industrially for sparingly soluble gases). They report a variation of k_L with $D_L^{0.42}$; however they used a value of hydrogen diffusivity in water equal to 6.3×10^{-5} cm.²/sec. at 25°C, a value quite different from the 4.8×10^{-5} cm.²/sec. found in this thesis. Their value for carbon dioxide, by back-calculation from their results, was 2.0×10^{-5} cm.²/sec., exactly equal to that found experimentally

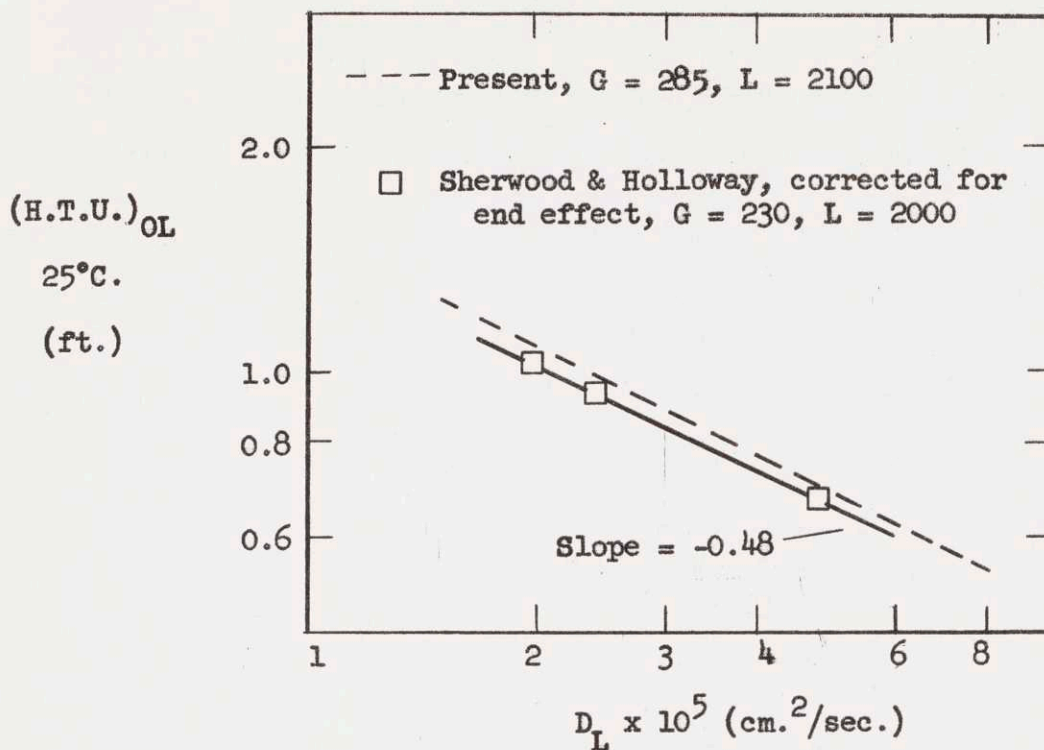


FIGURE 5.3 AGREEMENT WITH DATA OF SHERWOOD & HOLLOWAY:
EFFECT OF DIFFUSIVITY

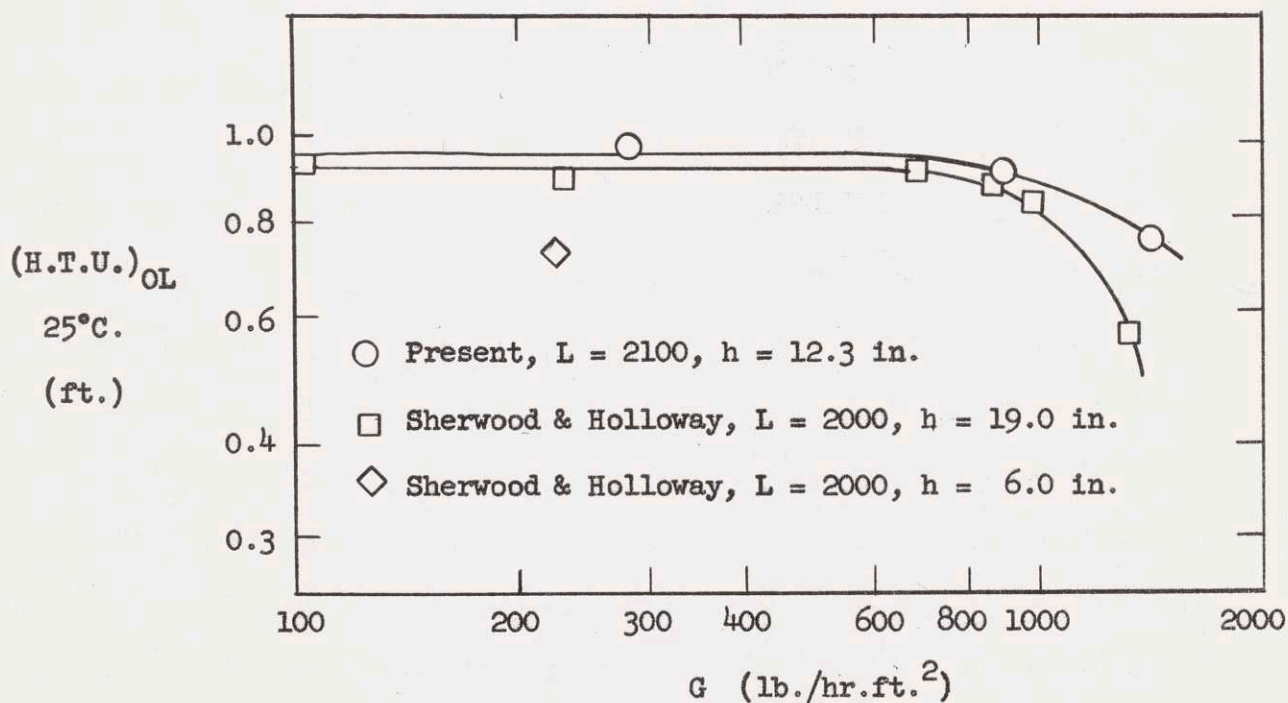


FIGURE 5.4 AGREEMENT WITH DATA OF SHERWOOD & HOLLOWAY: EFFECT OF AIR RATE

in this thesis. Use of the present hydrogen diffusivity value gives a $k_L a$ variation with $D_L^{0.55}$ from their results. The scatter of their data is such, however, that this slope could as well be 0.50. This would require that their $k_L a$ vs. L curve for hydrogen be placed 5% higher, which could readily be done.

b. Effect of Bulk Liquid and Gas Flow Rates

Figures 5.4 and 5.5 present the present data for the effects of G and L on $(H.T.U.)_L$ for oxygen desorption and also comparable data of Sherwood and Holloway (61, 131). Comparison at identical flow conditions is possible for the effect of G . Agreement is close, except at high air flow rates, where the effect is qualitatively the same: Above loading $k_L a$ tends to increase markedly (and $(H.T.U.)_L$ tends to decrease) with increasing G .

For the effect of L on the transfer rate comparison at identical flow conditions is not possible, since L was varied at $G = 900$ in the present instance and L was varied at $G = 230$ by Sherwood and Holloway.

Below loading, $(H.T.U.)_L$ was found to vary with $L^{0.22}$ by Sherwood and Holloway, an effect found qualitatively in the present values at $G = 285$ and $G = 900$. As loading is exceeded Sherwood and Holloway found the exponent on L to increase continually; however, the present data at $L = 10,000$ and $G = 900$ indicate that, as flooding is approached at this $L/G (= 11)$, the effect of G in reducing $(H.T.U.)_L$, mentioned in the preceding paragraph and shown in Figure 5.4, tends to offset

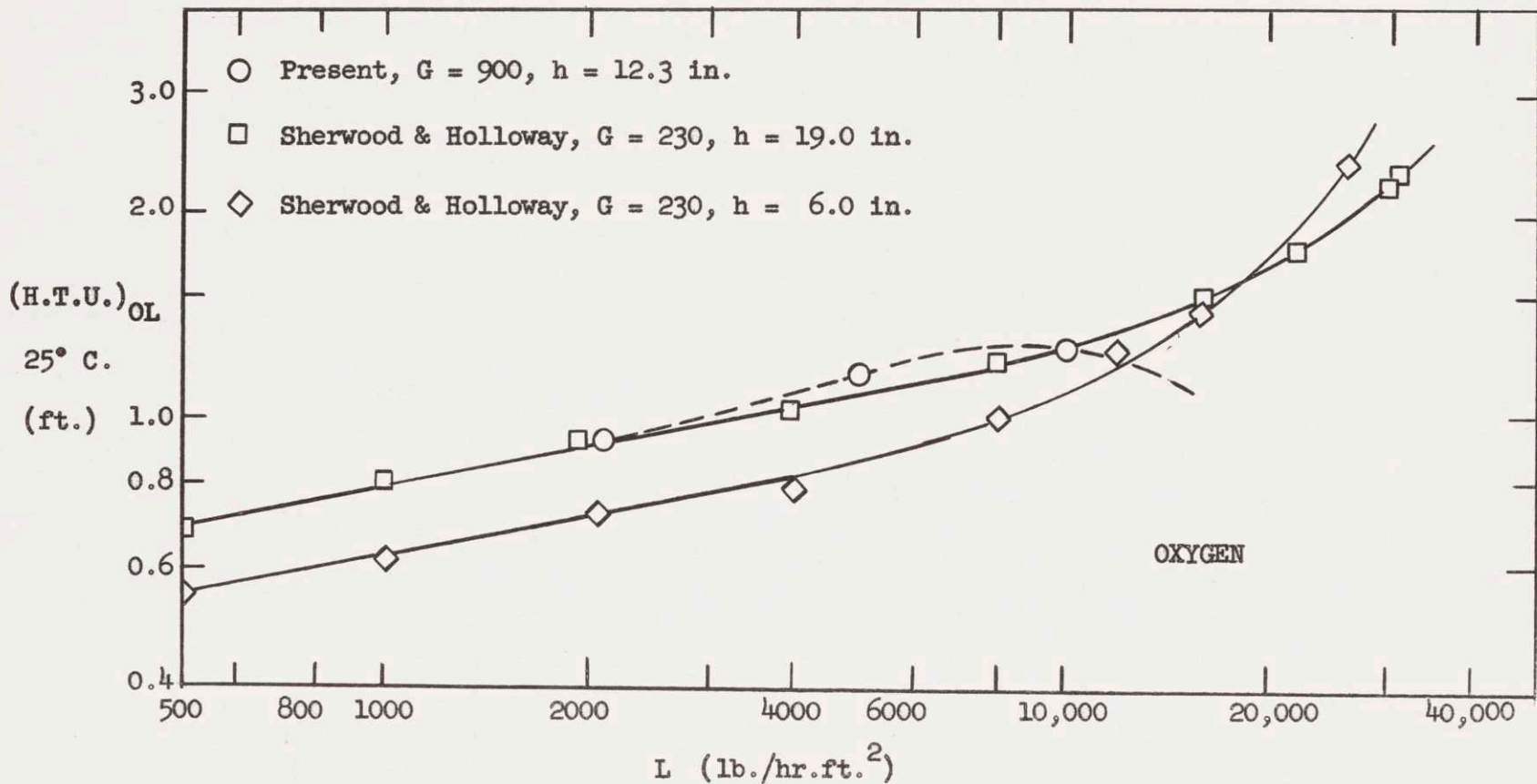


FIGURE 5.5 AGREEMENT WITH DATA OF SHERWOOD & HOLLOWAY: EFFECT OF WATER RATE

the effect of L to increase $(H.T.U.)_L$. The Sherwood and Holloway results do not approach so close to flooding ($G = 230$ is only 65% of the flooding G at their highest value of L) as do the present results (91% of the flooding G at $L = 10,000$ and $G = 900$).

c. Effect of Temperature

The most extensive past study of the effect of temperature on $k_L a$ and $(H.T.U.)_L$ is, again, that of Sherwood and Holloway (61, 131). From their Part I studies (with end effect) of the effect of temperature on $(H.T.U.)_L$ they correlated all their data with $(H.T.U.)$ varying as $e^{-0.023T}$, where T is Centigrade or Kelvin temperature. Their results for oxygen, however, were originally calculated using an equation for $(H.T.U.)_L$ that assumes no change in the solubility of oxygen in water throughout the column. In many cases, though, the oxygen solubility did vary significantly. A recalculation of their data for the effect of temperature on $(H.T.U.)_L$ for oxygen serves to lower somewhat in absolute magnitude the exponential temperature coefficient. The recalculated results are shown in Table 18.1 and, graphically, in Figure 5.6. The best curves through the recalculated data are characterized by $(H.T.U.)_L$ varies as $e^{-0.020T}$. This slope also provides a better representation of the hydrogen data than the original -0.023 , and the carbon dioxide data fits well if one point is neglected.

This variation with $e^{-0.020T}$ agrees closely with the -0.019 exponent which correlates the present oxygen temperature effect data. The

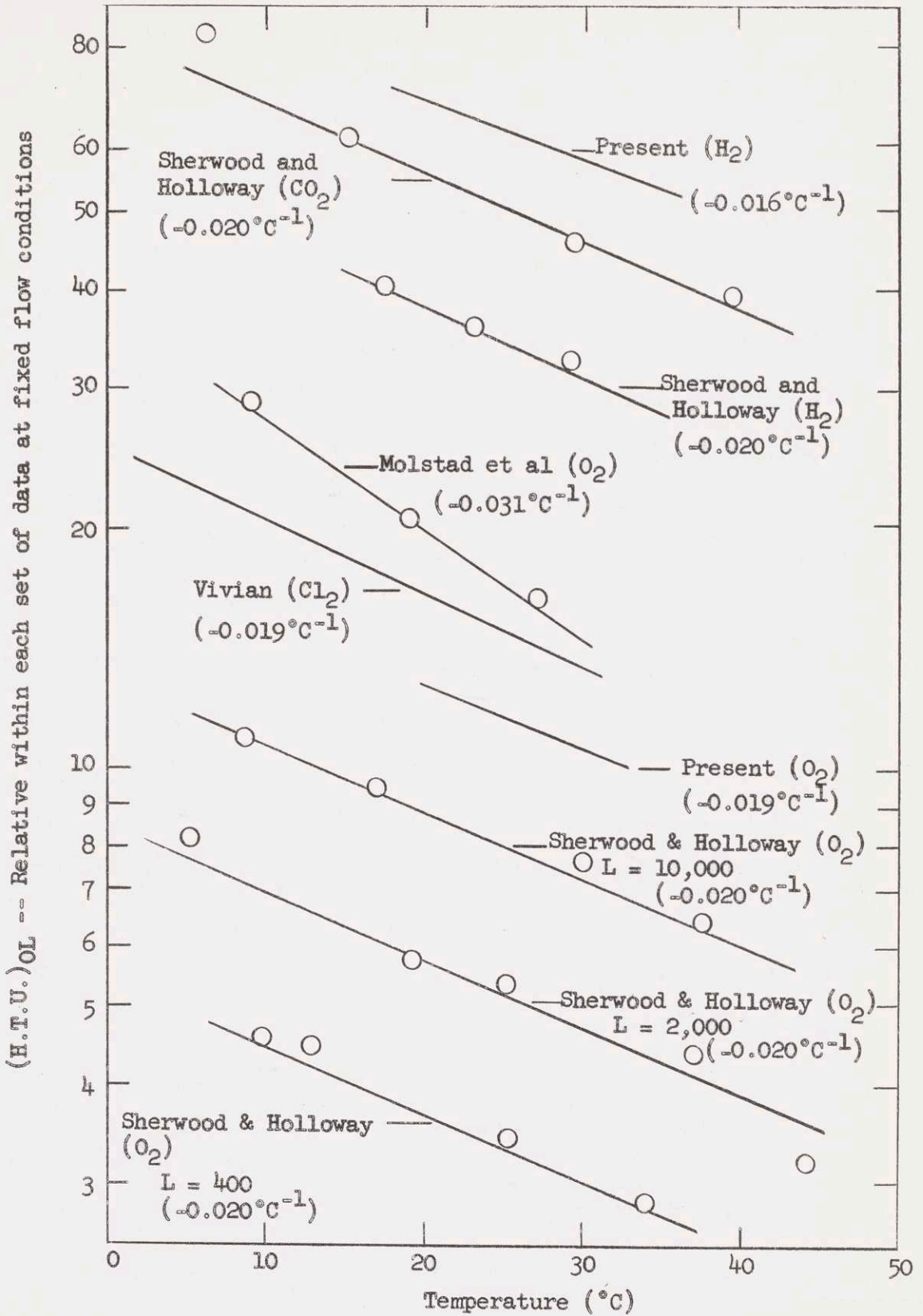


FIGURE 5.6 AGREEMENT WITH OTHER AUTHORS: EFFECT OF TEMPERATURE

present hydrogen data can also assume this slope within their scatter, and do so well if one point is neglected.

Vivian and Whitney (154, 156) examined the effect of temperature on $(H.T.U.)_L$ for chlorine absorption and found a good semi-logarithmic correlation with a slope of -0.021 over a wide temperature range (2 to $32^\circ C$). The chlorine system is, however, one involving a chemical reaction (hydrolysis), the equilibrium and kinetics of which may vary temperature, although Morris (96) indicates the influence of temperature on the hydrolysis is slight. Although the agreement of the slope of the correlation of Vivian and Whitney with the present slope and that of the Sherwood and Holloway data is good, it should not be expected to be exact because of the presence of the simultaneous chemical reaction.

Another investigation of the effect of temperature was that of Molstad, et al, (92), who studied drip point grid tile. From three points of $(H.T.U.)_L$ for oxygen desorption vs. temperature they found $(H.T.U.)_L$ to vary as $e^{-0.031T}$, as shown in Figure 5.6. They, however, computed their results using the same equation neglecting solubility changes that Sherwood and Holloway used, and the actual variation of equilibrium solubility because of temperature variation in their column may well account for the much higher slope they found. They present insufficient temperature data to permit a recalculation.

In summary, then, the present data, the re-analyzed data of Sherwood and Holloway (131), and the data of Vivian and Whitney (156) all indicate

an effect of temperature on liquid phase transfer rate given by

$$(\text{H.T.U.})_L \sim e^{-0.020T} \quad (5.2.1)$$

or

$$k_L a \sim e^{0.020T}, \quad (5.2.2)$$

where T is in degrees Centigrade or Kelvin.

5.2.3 Effect of One Solute Gas Upon Another

The problem of possible interactions between solute gases present in the water is discussed in detail in Chapter 12 of the Appendix. It is indicated there that the only serious effects of this kind apparently occurred in some cases of propylene desorption. There, because of the presence of dissolved air in the water in addition to the propylene, supersaturation tended to occur as the water passed through the column. This tendency, in turn, may have caused turbulences quite close to the interface and thus produced a deceptively low $(\text{H.T.U.})_{OL}$.

Propylene runs in which this took place are omitted from Figures 4.1 through 4.6.

5.3 Mechanism of Liquid Phase Resistance

The results shown in Figures 4.1 through 4.6 are well correlated by $(\text{H.T.U.})_L$ being proportional to $D_L^{-0.50}$ and $k_L a$ being proportional to $D_L^{0.50}$, at each of the five water and air flow conditions. The

range of least squares slopes of $\log (\text{H.T.U.})_L$ vs. $\log D_L$ is from -0.48 to -0.54, with the standard deviations of the slopes (determined by scatter of the individual points) being such as to make a uniform slope of -0.50 at all five flow conditions readily possible (see Table 17.3). Plots of the best -0.50 slope lines through the data (Figures 4.3 and 4.4) show as good a correlation of the data visually as do the best least squares slope lines (Figures 4.1 and 4.2).

There is no perceptible trend of the slope of $\log (\text{H.T.U.})_L$ vs. $\log D_L$ with changing water flow rate ($L = 2100, 5000, \text{ and } 10,000$) at a constant air flow rate ($G = 900$) as is shown in Figure 4.1. Although there is decreasing slope with decreasing air rate at a constant L of 2100 (-0.53 at $G = 285$, -0.50 at $G = 900$, and -0.48 at $G = 1400$), this is within the probable error of the slopes and cannot really be taken as any confirmation of a trend in slope.

Thus it may reasonably be concluded that $(\text{H.T.U.})_L$ varies as $D_L^{-0.50}$ and $k_L a$ varies as $D_L^{0.50}$ over the entire range of flow conditions studied. This result is in excellent agreement with the prediction of penetration theory (Section 2.1.2) that k_L varies as the square root of D_L . The square root variation characterizes the unsteady-state molecular diffusion of solute into a fluid with no velocity gradient. This agreement with penetration theory extends at least, by Table 5.3 from L/G of 1.5 to 11, and from 26 to 91% of flooding.

The data agree excellently with penetration theory, but do they confirm it? In response to this it may be queried whether absolute

confirmation of any theory is possible through scientific experimentation. The usual practice is to accept a theory if it has a reasonable physical foundation and if it agrees rather than disagrees with such data as are taken to test it. To this extent the concept of penetration, or its broader statement of unsteady-state diffusion into liquid with no velocity gradient or turbulence in the transfer zone, may be taken as the mechanism of liquid phase mass transfer for gas absorption in a packed tower.

Such other theories as have been suggested for liquid phase behavior (see Section 2.1.3 and Table 2.1) either do not predict an exponent of 0.50 on diffusivity (two-film, "turbulence controlled") or else suggest that the exponent should vary with flow conditions (boundary layer from air drag, turbulence damped near interface).

In the case of the Gilliland equation for gas phase resistance to mass transfer inside long cylinders, an exponent of 0.56 on vapor phase diffusivity applies over a wide range of gas phase flow rates (133c), yet the mechanism is not unsteady-state penetration but instead a steady-state process occurring through an established turbulent boundary layer. It might be asked whether some similar condition could account for the more or less constant exponent of 0.50 on D_L in the present case.

Gilliland's gas phase transfer was characterized by a large drag of the wetted-wall on the adjacent gas, with a consequent stagnation of the gas at that point. As has been pointed out previously (Section 2.1.3), it is unlikely that at any gas rate other than very high ones the skin friction drag of the air on the liquid at the gas-liquid interface would

be large enough to cause a significant velocity gradient in the liquid. Thus, according to present concepts of fluid behavior, it would be necessary to attribute a fortuitous agreement with penetration theory to a turbulence in the liquid phase damping out in such a way near the interface as to give an effective 0.50 exponent on D_L for mass transfer. If such a fortuitous agreement with the 0.50 slope predicted by penetration theory did occur at some particular flow conditions, it is unlikely that the exponent would remain the same at other flow conditions, unless the level and intensity of the turbulence were relatively insensitive to flow rates. Whereas the presence of a solid surface affords a mode of turbulence damping that is somewhat insensitive to flow rate, it is unlikely that the damping of turbulence through surface tension alone would be so insensitive to flow rate.

It should be noted, too, that liquid phase diffusivities are so low that, for instance, for oxygen absorption by penetration, after a surface lifetime of 0.5 seconds (a relatively long value), the concentration of solute at a point 0.08 mm. away from the surface is only above the bulk concentration by 10% of the difference between the surface and bulk concentrations by Equation (2.1.23). Although turbulence might be present in the bulk of the falling liquid film, if it did not retain a significant level closer to the interface than, say, 0.08 mm. it would have no influence on the unsteady-state mass transfer process. Such a situation is not unlikely at high liquid flow rates.

Although some mode of turbulence damping near the interface resulting in an exponent of 0.50 is possible, it would be a remarkable coincidence for such behavior to occur at five very different flow conditions, and

thus, to the extent that the present results tend to indicate a constant exponent of 0.50 at each of the five flow conditions, the likelihood of any proposed mechanism other than unsteady-state penetration into no velocity gradient and a field of no turbulence is diminished.

An additional check on the applicability of simple penetration theory would be the study of a second order, irreversible, infinitely fast chemical reaction in a packed column, such as the hydrogen sulfide - caustic or ethanolamine system. As is indicated in Section 5.4.1 and Chapter 10, simple penetration and a damped turbulence system, if they coincidentally gave the same exponent of 0.50 on diffusivity for physical absorption, would show different effects in such a chemical reaction system.

5.4 Applications of Experimental Results

The most obvious consequence of the experimental results is that the individual liquid phase mass transfer coefficient in a packed absorption tower is proportional to the square root of the liquid phase diffusivity, or, in another way of speaking, that the Schmidt group, $\mu/\rho D_L$, enters to the $-1/2$ power in a correlation giving a Nusselt type group involving k_L/D_L or $k_L a/D_L$.

There are, however, several other more far-reaching consequences of the penetration mechanism indicated by the constant exponent of $1/2$ on the diffusivity. Four of these are:

- 1) The penetration mechanism presents a much different analysis of absorption with chemical reaction than does classical two film theory, and in cases of unequal diffusivities of solute

and reactant may yield significantly different results.

- 2) There are some serious questions as to the validity of the classical "additivity of resistances" concept raised by the existence of an unsteady-state penetration mechanism in the liquid phase.
- 3) It is possible, in view of this penetration mechanism and the results of the analysis of the additivity of resistances in a packed column, to form a correlating equation for k_L^* , the liquid phase transfer coefficient, that has a sounder theoretical physical basis than do such correlations as have heretofore been presented.
- 4) Because of the apparent penetration behavior of the liquid phase in the packed tower, it is possible now to accept such laboratory models as short wetted wall columns and jets, which in essence personify penetration theory, as valid models of the liquid phase mass transfer process in flow over packing.

These consequences are covered in more detail in the subsequent sections and in Chapters 8 and 9.

5.4.1 Chemical Reaction Systems

Most known solutions for penetration theory coupled with various chemical reaction mechanisms are covered in detail by Peaceman (107) and Brian (10). In the readily available literature there is no complete compilation, although there is a review article by Danckwerts (22)

summarizing several of the results. Sherwood and Pigford (133h) present the solution for a first order, backward and forward, reaction for the case of equal diffusivities of absorbing solute and reaction product. The solution presented therein for a fast, second order, irreversible reaction is, however, in error for the case of unequal diffusivities. The correct solution for this case is presented by Danckwerts (20), Carslaw and Jaeger (13d), and Crank (17). The first order irreversible reaction is also presented by Danckwerts (19), to whom credit for first publication goes. Perry and Pigford (110) present a computer solution for a second order, irreversible reaction (or with a first order reverse reaction with a finite rate) and equal diffusivities. Gilliland, Baddour, and Brian (43) give an approximate solution for the more general case of an irreversible second order reaction of finite rate and unequal diffusivities.

As a general rule, solutions for penetration theory chemical reaction processes differ very little from film theory solutions for the special case of equal diffusivities of solute and reactant, in so far as their prediction of φ , the ratio of k_L^* for the chemical reaction case (based on a driving force of physically dissolved, unreacted solute) to k_L^* for physical absorption at the same hydrodynamic conditions. For cases of unequal diffusivities it appears that a good rule of thumb may be to replace the ratio of solute and reactant diffusivities in a film theory solution by the square root of that ratio to obtain the corresponding penetration theory solution. (107a). Since this ratio is often a linear

factor in a controlling term, there may, for a diffusivity ratio of 2, be a difference of 40% between the film and penetration predictions for φ . A factor of 2 is not uncommon in industry, such being the case for H_2S or CO_2 absorbed in ethanolamines, and for H_2S or CO_2 absorbed in caustic (99).

The unique predictions of penetration theory for absorption with chemical reaction in cases of unequal diffusivities may ultimately afford an independent check of the applicability of penetration theory to packed column liquid phase behavior, in addition to the physical desorption results of this thesis. This would be so especially for a reaction system with known kinetics and diffusivities (the more unequal the better) which involve the diffusion of the chemical reactant from the bulk liquid to the reaction zone. If there were some kind of damped turbulence profile near the interface that fortuitously gave an 0.5 exponent on D_L for physical absorption, then its effect on, say, a second order, infinitely fast, irreversible reaction should certainly be otherwise than predicted by penetration theory, since the solute would be transported less rapidly and the reactant more rapidly to the reaction zone than predicted by penetration theory. Studies by Handwerk (55) and Bergholt (17) made in a stirred flask and a short wetted wall column indicate H_2S -NaOH may be an appropriate system for this.

In any instance other than a first order reaction, however, the φ factor will be a function of reactant bulk concentration and of solute interfacial concentration. This, then, requires an integration

of k_L values over tower height for a packed height of any reasonable size whatsoever, since the gas phase concentration of solute and the reactant concentration in the liquid will change throughout the column. This cannot be readily circumvented experimentally by using a pure gas phase and highly concentrated reactant solution because 1) a significant change in G would occur through the column, 2) there would be questions of hydrodynamics, effective area, and diffusivities in a highly concentrated solution, and 3) there would be large attendant heat effects. Although the problem of integration of $k_L a$ over a column for design is usually not too great when the φ factor is well known, the problem of unintegrating experimental data for a mechanism study is often more severe. Perhaps the simplest reaction system to study in this way is a second order, infinitely fast, irreversible reaction with dilute liquid and gas phases. The integration for this case over a given tower height is given in Chapter 10 of the Appendix.

It was mentioned previously that for a first order reaction the φ factor is not dependent upon solute concentrations, and hence should not vary throughout a column. φ factors for first order reactions obtained through penetration theory do, however, involve the value of k_L for physical absorption itself (133h), and thus for application of these φ values to $k_L a$ in a packed column it is necessary to have first separated k_L from $k_L a^*$. Because of this the study of such a reaction in a packed column would provide an independent check on the validity of the dead surface concept (Chapter 8) and the separation of a_e from

Fellinger's ammonia data made by Shulman, et al (137), and used in Chapter 9.

5.4.2 Additivity of Resistances

The problem of additivity of resistances in a packed tower is investigated in detail in Chapter 8 of the Appendix. The results of that chapter are summarized here.

By simple definition of individual and overall transfer coefficients the "additivity of resistances" must hold at each and every point of interface, that is

$$\frac{1}{K_L'} = \frac{1}{HK_G'} = \frac{1}{k_L'} + \frac{1}{Hk_G'} \quad (2.1.14)$$

where primed values refer to local, or point, coefficients. Two film theory extends this additivity concept to cover the whole of the interfacial area between gas and liquid, thus

$$\frac{1}{K_L a} = \frac{1}{HK_G a} = \frac{1}{k_L a^*} + \frac{1}{Hk_G a^*} , \quad (2.2.2)$$

where asterisks refer to coefficients measured for the resistance of one phase in the absence or suppression of resistance in the other phase. For this equation to hold, however, it is necessary that at each and every point of interfacial area there be a constant ratio of Hk_G' to k_L' . Such is not the case if a penetration mechanism applies in the liquid phase of a packed tower in countercurrent operation, for k_L' varies

greatly during a single liquid exposure.

An analytical solution for the case of a single liquid unsteady-state penetration coupled with a time or space constant k_G is obtained by Carslaw and Jaeger (13b), and reportedly the agreement of the absorption occurring during such a single penetration with the two film additivity equation has been discussed by Emmert (36). The maximum deviation from two film additivity comes when $Hk_G a^*/k_L a^*$ is approximately equal to 1, and corresponds to a +5% deviation in the overall coefficient.

During individual exposures in a packed tower in countercurrent operation, however, it is unrealistic to consider a constant k_G presented by the gas phase, for there is in all probability an unsteady-state laminar or turbulent boundary layer behavior in the gas phase. The extreme (and most probable) case is a complete correspondence of liquid surface "births" with gas surface "deaths" and vice versa.

Numerical solutions, made by use of the Dusenberre method (33), have been obtained for four such countercurrent cases of laminar boundary layer in contact with the liquid in a single exposure, and for three such countercurrent cases of a highly turbulent boundary layer. These solutions correspond to values of $R (= Hk_G a^*/k_L a^*)$ from 0.2 to 2.0. In obtaining the solutions it has been assumed that the gas phase boundary layer is completely insensitive transfer-wise to its "past history." This should be a relatively good assumption for

a turbulent boundary layer, but as the boundary layer becomes more laminar it is less realistic. The mathematical simplification afforded by this assumption still makes it desirable, however.

These solutions show that for the laminar boundary layer case the absolute deviation from two film additivity is apparently never greater than +6%, whereas for the turbulent boundary layer case the deviation is also apparently never greater than +6%. The conclusion, therefore, is that two film additivity is very closely satisfied during a single liquid exposure or lifetime.

The greater effect, evidently, comes from the wide distribution of liquid surface lifetimes that occurs in a packed tower. If the fraction of the total liquid surface reaching a lifetime between θ_1 and $d\theta_1$ is $\psi(\theta_1)$, then over the whole surface

$$K_L = \int_0^{\infty} \frac{\delta_i \psi(\theta_1) d\theta_1}{\frac{1}{Hk_{G1}} + 1/2 \sqrt{\frac{\pi \theta_1}{D_L}}} \quad (8.1.30)$$

where δ_i is the deviation from two film additivity occurring during a single exposure reaching a lifetime θ_1 .

A two lifetime theory is presented which, for cases showing a substantial deviation from additivity because of lifetime differences, yields

$$\frac{K_L a}{K_{LF} a} = (1 + R) \left[\frac{f}{1 + Rf} + \frac{1 - f}{1 + R \lambda f} \right] \quad (8.1.36a)$$

where K_{LF} = overall coefficient predicted by two film additivity
 f = fraction of liquid surface reaching the shorter lifetime
 R = $Hk_G a^* / k_L a^*$
 λ = square root of ratio of two lifetimes, > 1

A special case of this assumes $\lambda = \infty$ (the less active surface is completely dead):

$$\frac{K_L a}{K_{LF} a} = \frac{f + fR}{1 + fR} \quad (8.1.37)$$

Whereas there is no wide distribution of lifetimes in a stirred flask apparatus, as evidenced by the close agreement with two film additivity found therein, there does appear to be a wide distribution in a packed column. This is indicated by the fact that k_{GAF} values calculated by two film additivity from $K_G a$ values measured in gas phase influenced absorption systems are invariably lower than $k_G a$ values for vaporization, often by factors of two and three.

The only data in the literature which may be interpreted to evaluate the relative merits of the dead surface approach and of its more general case, the two lifetime approach, are those of Houston and Walker (62) for the absorption of acetone, ammonia, ethanol, and methanol into water from air on 1 inch carbon rings. From their data it is indicated that for $R > 0.1$ the dead surface approach is satisfactory and that the effective value of λ for use in the two-lifetime approach is on the order of 50.

From this it is indicated that for design purposes the ammonia data of Fellingner (38, 133g), Dwyer and Dodge (35), and Houston and Walker (62), corrected to k_{GaF} values by two film additivity, should be taken for gas phase resistance. They should be used in conjunction with the various liquid phase $k_L a^*$ data available (Table 8.9), and overall coefficients should then be computed by two film additivity. Whereas this has previously been considered conservative practice (109e, 133g), it is in reality only so for $R < 0.1$. For $R < 0.1$, it is necessary to take the finite lifetime of the less active surface into account.

The dead surface concept is entirely analogous to the effective area (a_e) concept first proposed by Shulman, et al (136), if a_e is taken equal to $f a$. A correlation proposed by Shulman, making k_{Ga} for vaporization divided by k_{Ga} for absorption (or $1/f$) equal to 0.85 times the ratio of the total hold-up to the operating hold-up was found, however, to be lacking in generality, based on available data.

5.4.3 Dimensionless Correlation

In Chapter 9 a correlating equation for k_L^* values in flow over packing is derived, based upon the penetration model of the packed column and present knowledge of the hydrodynamic and absorption properties of falling films of liquid. This equation is best presented in dimensional form:

$$\frac{k_L^*}{D_L} = \alpha \left(\frac{4L}{a_e \mu} \right)^{0.6} \left(\frac{\mu}{\rho D_L} \right)^{0.5} \left(\frac{\rho g}{\mu^2} \right)^{1/6} \quad (9.19)$$

with α having units of length $^{-1/2}$. Values of α are listed in Table 9.1 for the seven different forms of ceramic packing studied by Sherwood and Holloway (131) and by Fellingner (38).

In the above equation a_e denotes the effective area, or active portion of the interfacial area. k_L is the value of the transfer coefficient operative over that area, determined as $k_L a^*/a_e$. Values for a_e , in light of the above mentioned reliability of the dead surface concept are at present best obtained in the case of ceramic packings from the data of Fellingner (38, 133g), using an empirical correlation for k_G . Values obtained in this way are presented by Shulman, et al (137).

The utility of this equation is limited by the present knowledge of values of a_e , and can be tested for general applicability only when there is a greater knowledge of the effect of other variables on a_e , or a general correlation for a_e .

5.4.4 Mechanisms of Models

There are many instances in the recent literature where liquid phase absorption data taken in short wetted wall columns and falling jets have been found to be in almost complete agreement with the predictions of penetration theory. For example, Vivian and Peaceman (155) found the rate of desorption of carbon dioxide to vary with the height of a short wetted wall column to the $1/2$ power and, by comparison with the chlorine-hydrochloric acid system, found k_L to vary with $D_L^{0.5}$. Both these results are in agreement with penetration theory. Nijsing, et al (99)

have been able to use penetration theory to predict extremely closely the behavior of carbon dioxide absorption in short wetted wall columns and jets, and of the carbon dioxide-caustic reaction system in jets. There are also other cases where liquid phase resistance in jets has been completely predictable from penetration theory (114, 124). In light of the results of this thesis as discussed in Section 5.3 these two models therefore appear to be reliable simplifications of the liquid phase resistance to absorption in a packed tower.

It should be stressed, though, that they are truly appropriate models only for the study of pure liquid phase resistance. There is no assurance that gas phase behavior in these devices bears a close resemblance to that in a packed column. A wetted wall assembly similar to that of Vivian and Peaceman would be perhaps the most similar, especially if the gas phase velocity boundary layer were made somehow to begin or be renewed at the bottom of the column.

It is less apparent that the commonly used stirred flask is a valid model of the liquid phase process in a packed column. There is no direct evidence to support the applicability of penetration theory to a stirred flask. The problem of determining the liquid phase mechanism in a stirred flask is discussed in Chapter 11 of the Appendix, where the data of Kishinensky and Serebryansky (74) are examined.

CHAPTER 6CONCLUSIONS

From the results of this thesis, the following conclusions are made:

1. Over a range of flow rates from 26 to 91% of flooding and L/G from 1.5 to 11 the liquid phase desorption process in flow over 1.5 inch ceramic Raschig rings has been found to give a volumetric transfer coefficient always proportional to solute diffusivity to the 0.50 (+0.04) power.

2. This is in strong agreement with penetration theory which depicts an unsteady-state diffusion process into a liquid region near the interface with no turbulence and no velocity gradient. It is unlikely that any other plausible mechanism is capable of predicting a constant exponent of 1/2 on the diffusivity over such a wide range of flow conditions.

3. Short wetted wall columns and falling laminar jets, being, in essence, personifications of penetration theory, are indicated as valid models of the liquid phase absorption process in a packed tower. Thus they can be used for study of complex absorption processes.

4. The additivity of resistances as predicted by two film theory over the whole of the interfacial area in a packed column need not be valid in such an unsteady-state system. While two-film additivity seems to hold amazingly well over a single exposure of liquid to gas, even for countercurrent unsteady-state mechanisms, there is apparently

a strong effect of the wide distribution of liquid surface lifetimes in a packed column, causing marked deviations from simple two-film additivity.

5. The concept of there being a certain "dead" fraction $(1 - f)$ of the liquid surface, or conversely of there being a certain active "effective area" ($a_e = fa$) for absorption processes, and of this area obeying two-film additivity is valid for cases where $R (= Hk_G a^* / k_L a^*)$, the ratio of individual, independent phase resistances, is greater than 0.1. For $R < 0.1$ this will give conservative results for design if data for ammonia absorption in water are used as a basis.

6. A correlating equation for k_L^* (separated from $k_L a^*$ through the use of ammonia data) that is indicated by the penetration view of absorption into flow over packing is

$$k_L^* / D_L = \alpha \left(\frac{4L}{a_e \mu} \right)^{0.6} \left(\frac{\mu}{\rho D_L} \right)^{0.5} \left(\frac{\rho^2 g}{\mu^2} \right)^{1/6}, \quad (9.19)$$

where values of α for various packings are given in Table 9.1. This equation, though dimensional in form, is based on a dimensionless equation which would include only additional quantities with length dimensions.

7. On the basis of present and previous data the variation of $k_L a$ with temperature near room temperature is given by

$$k_L a \sim e^{0.020T} \quad (5.2.2.)$$

where T is Centigrade or Kelvin temperature.

CHAPTER 7
RECOMMENDATIONS

1. Short wetted wall columns and falling laminar jets should be used as reliable models of the liquid phase absorption process in a commercial packed tower.

2. The use of ammonia data and two-film additivity for design should be considered as essentially correct, rather than conservative, for cases where $Hk_G a^*/k_L a^*$, the ratio of individual, independent phase coefficients is greater than 0.1.

3. An integral study of both vaporization and gas phase influenced absorption for several solutes should be carried out in the air-water hydrodynamic system on commercial packing, using the present technique of holding flow rates and temperatures constant. Although Houston and Walker (62) have made such a study for absorption alone, it is desirable to have vaporization coefficients also measured in the same column. In this connection any method developed for measuring small humidity driving forces will be of great value.

Such a study should shed additional light on the gas phase transfer mechanism and on the validity of the additivity of resistances.

4. An investigation of a liquid phase controlled rapid, irreversible, second order reaction system with unequal diffusivities in a packed tower with dilute solutions should serve as an additional check on the applicability of penetration theory. The study of a first order

system would serve as an additional check on the dead surface and effective area concepts.

5. Greater use should be made of the technique for analyzing concentrations of nonreactive gases in solution by first separating the gas from solution in a spray-vacuum system and then utilizing gas chromatography.

A P P E N D I X

CHAPTER 8

Additivity of Resistances

8.1 Theoretical Survey of the Nature of Additivity in Penetration Systems

The additivity of the resistances of the gas and liquid phases, defined strictly, is nothing more than a definition, for at any point of interface between gas and liquid k_L and k_G are defined from the actual rate of absorption per unit area, N_A , at that point as

$$k_L = \frac{N_A}{C_i - C_L} \quad (2.1.4)$$

and

$$k_G = \frac{N_A}{P_G - P_i} \quad (2.1.3)$$

K_L and K_G are defined similarly as

$$K_L = \frac{N_A}{C_e - C_L} \quad (2.1.10)$$

and

$$K_G = \frac{N_A}{\bar{P}_G - P_e} \quad (2.1.11)$$

where C_L = solute concentration in bulk liquid (moles/volume)
 C_i = solute concentration at interface (moles/volume)
 C_e = solute concentration in equilibrium with solute
 partial pressure in bulk gas (moles/volume)

- p_G = solute partial pressure in bulk gas (atm.)
 p_i = solute partial pressure at interface (atm.)
 p_e = solute partial pressure in equilibrium with solute concentration in bulk liquid (atm.)

Accepting the Henry's Law straight line solubility relationship, $HC = p$, where H is reciprocal solubility, it is a matter of simple algebra to obtain from the foregoing equations

$$\frac{1}{K_L} = \frac{1}{k_L} + \frac{1}{Hk_G} \quad (2.1.14a)$$

and

$$\frac{1}{K_G} = \frac{H}{k_L} + \frac{1}{k_G} \quad (2.1.14b)$$

These relationships hold at any point as a matter of simple definition of k_L , k_G , K_L , and K_G . Again, solely by definition, the equations (2.1.14) need not be restricted to cases where Henry's Law is obeyed. If $p = HC +$ some constant, i.e., any straight line equilibrium curve not necessarily through the origin, the equations still hold, with H equal to the constant slope of the line. Indeed, for any curved equilibrium line (H variable), the equations (2.1.14) hold by definition alone if H for (2.1.14a) is taken as $(p_G - p_i)/(C_e - C_i)$ at the particular point and if H for (2.1.14b) is taken as $(p_i - p_e)/(C_i - C_L)$ at the particular point. In this case however K_G and K_L are functions of solute pressure and concentration even though k_G and k_L may not be.

Two film theory assumes that k_G and k_L have constant values at each and every point of gas-liquid interface. Thus the interfacial area, a , may be compounded with Equations (2.1.14) to give

$$\frac{1}{K_L a} = \frac{1}{HK_G a} = \frac{1}{k_L a} + \frac{1}{Hk_G a} \quad (2.1.15)$$

This is the common "additivity of resistances" equation, the common use of which is to predict the overall coefficients (which are based upon readily measureable concentration and pressure driving forces) from the individual phase coefficients (which are taken as functions of the hydrodynamics and solute diffusivity alone). In particular, a desirable use of this additivity equation is in the form:

$$\frac{1}{K_L a} = \frac{1}{HK_G a} = \frac{1}{k_L a^*} + \frac{1}{Hk_G a^*} \quad (2.2.2)$$

where $k_L a^*$ = $K_L a$ measured in the absence or suppression
($Hk_G a \gg k_L a$) of gas phase resistance

and $k_G a^*$ = $K_G a$ measured in the absence or suppression
($Hk_G a \ll k_L a$) of liquid phase resistance

It is most important, now, to realize that Equations (2.1.15) and (2.2.2) no longer result from pure definitions, but are based upon the two film theory assumption that k_L and k_G are constant at every point of interface. If k_G and k_L are not constants at each point of interface, however, there is no assurance that the two additivity equations will

hold. If we now adopt the convention that primed values of coefficients denote point values while unprimed coefficients designate the averaged values operative over the entire interfacial area, another way of stating this is

$$\begin{aligned}
 K_L a &= \iint_a K_L' da = \iint_a \frac{1}{\frac{1}{k_L'} + \frac{1}{Hk_G'}} da \\
 &\neq \frac{1}{\frac{\iint_a \frac{1}{k_L'} da}{a} + \frac{\iint_a \frac{1}{Hk_G'} da}{a}} = \frac{1}{\frac{1}{k_L a} + \frac{1}{Hk_G a}} \quad (8.1.1)
 \end{aligned}$$

From the inequality (8.1.1), however, it may be seen that there is a more general condition for Equations (2.1.15) and (2.2.2) to be valid, and that this condition is for Hk_G' and k_L' to bear a constant ratio to each other at each and every point, even though they both may be variant from point to point in individual magnitudes.

From the experimental results of this thesis it is strongly indicated that the mass transfer in the liquid phase in a packed absorption tower obeys penetration theory. Consequently, because of this unsteady state mechanism, there is in light of inequality (8.1.1) no assurance that the two film theory additivity of resistances equations are valid, for k_L' is most certainly not a constant from point to point of interface.

Above and beyond this, the value of $K_L a$ effective for absorption in a packed column with penetration as the liquid phase mechanism cannot

even be predicted from separately measured (in two cases where $k_L a \gg Hk_G a$ and $k_L a \ll Hk_G a$) individual phase coefficients because the k_L' at any point in a penetration system is not dependent upon hydrodynamics and solute diffusivity alone, but is also dependent upon the nature and relative magnitude of the gas phase resistance. That is, at any particular age of liquid surface the k_L' value is dependent upon the past concentration history of that surface, as is brought out readily in the derivations of the following sections. Thus k_L' for a point in a system in which gas phase resistance occurs is not at all necessarily equal to $k_L'^*$ for the same point under the same hydrodynamic conditions.

The foregoing remarks apply to the occurrence of penetration in the liquid phase, but the same reasoning can apply also to the gas phase if the gas phase mechanism is something other than a constant film resistance at all points (and it probably is something else), thus complicating the situation further.

In the following sections the deviations from two film additivity that a penetration mechanism in the liquid can cause are explored theoretically in some detail.

8.1.1 Single Lifetime - Constant Stagnant Film Gas Resistance

Perhaps the simplest combination of liquid phase penetration with a gas phase resistance to envision is the case of a constant, stagnant, no hold-up film gas resistance. For a single penetration the behavior of the system may be obtained analytically by solving the unsteady state diffusion equation

$$D_L \frac{\partial^2 C}{\partial y^2} = \frac{\partial C}{\partial t}, \quad (8.1.2)$$

coupled with the boundary conditions

$$\begin{aligned} 1) \quad C &= C_L \text{ at } y > 0, \quad t = 0 \\ 2) \quad C &= C_L \text{ as } y \rightarrow \infty, \quad t > 0 \\ 3) \text{ at } y = 0, \quad -D_L \left(\frac{\partial C}{\partial y} \right) &= k_G (p_G - p_i) \\ &= Hk_G (C_e - C_i) \end{aligned} \quad (8.1.3)$$

C_i and p_i are taken to be in equilibrium with one another, and p_G , H and k_G are taken as constant.

Comparison with Section 2.1.2 and boundary conditions (2.1.21) shows that this is the equation of penetration theory with no gas phase resistance with the exception of the last boundary condition. Condition (3) now takes k_G into account rather than requiring that C_i be constant and equal and equal to C_e , as is the case for no gas phase resistance ($k_G \rightarrow \infty$).

This equation is entirely analogous to the equation for heat transfer into a semi-infinite slab with a thin film on the surface, the solution for which is presented by Carslaw and Jaeger (13b). In terms of diffusion nomenclature, this solution is:

$$\frac{C - C_e}{C_L - C_e} = \operatorname{erf} \left(\frac{y}{2\sqrt{D_L t}} \right) + e^{\frac{Hk_G y}{D_L} + \frac{H^2 k_G^2 t}{D_L}} \operatorname{erfc} \left\{ \frac{y}{2\sqrt{D_L t}} + \frac{Hk_G \sqrt{t}}{\sqrt{D_L}} \right\} \quad (8.1.4)$$

Therefore the history of interfacial concentration is given by

$$\frac{c_i - c_e}{c_i - c_e} = e^{\frac{H^2 k_G^2 t}{D_L}} \operatorname{erfc} \left(\frac{H k_G \sqrt{t}}{\sqrt{D_L}} \right) \quad (8.1.5)$$

and the interfacial flux history is

$$\left(\frac{\partial c}{\partial y} \right)_{y=0} = \left[\frac{H k_G}{D_L} e^{\frac{H^2 k_G^2 t}{D_L}} \operatorname{erfc} \left(\frac{H k_G \sqrt{t}}{\sqrt{D_L}} \right) \right] (c_i - c_e) \quad (8.1.6)$$

The local rate of mass transfer across the interface is, from the definition of a diffusivity,

$$N_A = - D_L \left(\frac{\partial c}{\partial y} \right)_{y=0} , \quad (8.1.7)$$

and, from the definition of K_L (Equation 2.1.10), the local value of K_L in this system is

$$K_L' = H k_G e^{\frac{H^2 k_G^2 t}{D_L}} \operatorname{erfc} \left(\frac{H k_G \sqrt{t}}{\sqrt{D_L}} \right) \quad (8.1.8)$$

Emmert (36) reportedly used this solution to find the deviation of the overall mean K_L of this system from the value of K_L predicted by two film additivity. The procedure is as follows:

The mean K_L operative over the total area of the penetration (or total time, depending on whether the view of the liquid is Eulerian or Lagrangian) is given by

$$K_L = \frac{1}{\theta} \int_0^{\theta} K_L' dt \quad (8.1.9)$$

This, from Equation 8.1.8, is

$$K_L = \frac{D_L}{Hk_G \theta} \left[e^{\frac{H^2 k_G^2 \theta}{D_L}} \operatorname{erfc} \left(\frac{Hk_G \sqrt{\theta}}{\sqrt{D_L}} \right) - 1 + \frac{2 Hk_G \sqrt{\theta}}{\sqrt{\pi D_L}} \right] \quad (8.1.10)$$

Now k_L^* , for no gas phase resistance, is given by

$$k_L^* = 2 \sqrt{\frac{D_L}{\pi \theta}} \quad (2.1.26)$$

If we let R be a dimensionless group representing Hk_G^*/k_L^* , which may be rather easily determined experimentally for an absorption system, then

$$R = \frac{Hk_G}{2 \sqrt{\frac{D_L}{\pi \theta}}} \quad (8.1.11)$$

and

$$K_L = \frac{\pi}{4R^2} Hk_G \left[e^{\frac{4R^2}{\pi}} \operatorname{erfc} \frac{2R}{\sqrt{\pi}} - 1 + \frac{4R}{\pi} \right] \quad (8.1.12)$$

Denoting the K_L predicted for the system by two film theory additivity as K_{LF} , there results from Equation (2.2.2)

$$K_{LF} = \frac{Hk_G}{1 + R} \quad (8.1.13)$$

Hence K_L/K_{LF} , the ratio of the actual K_L to that predicted by two film additivity, which shall be represented by δ is

$$\delta = \frac{K_L}{K_{LF}} = \frac{\pi(1+R)}{4R^2} \left[e^{\frac{4R^2}{\pi}} \operatorname{erfc} \frac{2R}{\sqrt{\pi}} - 1 + \frac{4R}{\pi} \right] \quad (8.1.14)$$

The ratio, δ , is thus a function of R above for a given surface lifetime.

δ is plotted against R in Figure 8.1, where it may be seen that, despite the very different mechanism, the deviation of the true K_L for a single lifetime from that predicted by two film additivity is never more than 5.0%. The true K_L is always higher than that predicted by two film additivity.

Such then is the result for the case of a single lifetime if penetration theory applies to the transfer in the liquid and stagnant, no hold-up, constant thickness film theory applies to the transfer in the gas phase. It is remarkable that the two very different liquid mechanisms should give such similar results; and this is certainly a fact that could not have been anticipated a priori.

It is interesting to observe in this case how k_L' at any point differs from $k_L'^*$ for the simple penetration case. The two coefficients, K_L' and k_L' are always related by definition by the equation

$$k_L' = K_L' \frac{C_L - C_e}{C_L - C_i}$$

Therefore, using Equations (8.1.5) and (8.1.8)

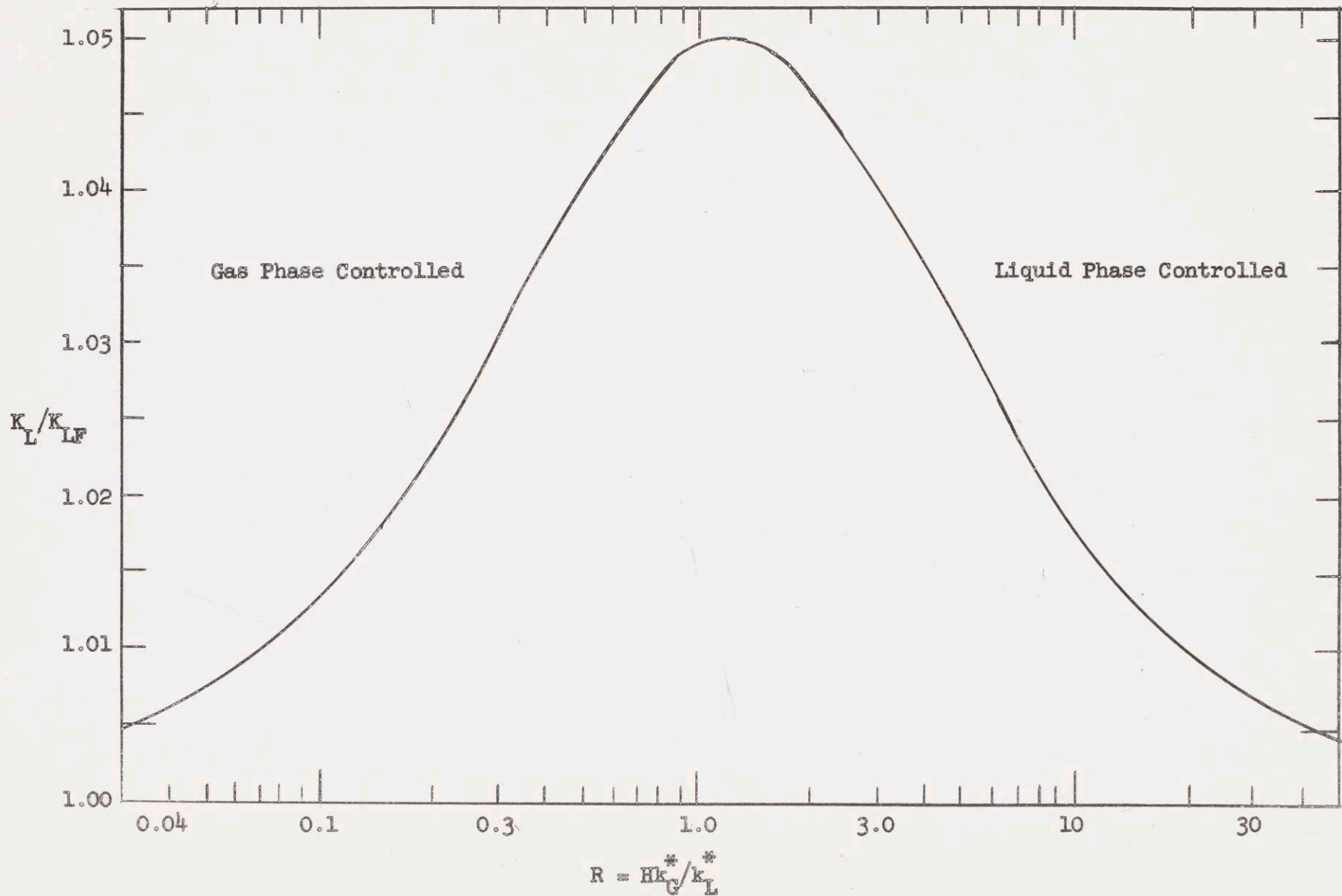


FIGURE 8.1 ADDITIVITY DEVIATION FOR LIQUID PENETRATION AND STAGNANT, NO HOLD-UP GAS FILM

$$k_L' = \frac{Hk_G e^{\frac{H^2 k_G^2 t}{D_L}} \operatorname{erfc}(Hk_G \sqrt{t/D_L})}{1 - e^{\frac{H^2 k_G^2 t}{D_L}} \operatorname{erfc}(Hk_G \sqrt{t/D_L})} \quad (8.1.15)$$

Adopting the definition of R, Equation (8.1.11), and taking k_L^* as Hk_G/R ,

$$\frac{k_L'}{k_L^*} = \frac{R e^{\frac{4R^2}{\pi} t/\theta} \operatorname{erfc}\left(\frac{2R}{\sqrt{\pi}} \sqrt{t/\theta}\right)}{1 - e^{\frac{4R^2}{\pi} t/\theta} \operatorname{erfc}\left(\frac{2R}{\sqrt{\pi}} \sqrt{t/\theta}\right)} \quad (8.1.16)$$

Figure 8.2 shows plots of k_L'/k_L^* vs. t/θ for $R = 1$ and $R = 0.2$, in comparison with the case for $R = \infty$ (simple penetration). For the constant k_G and $R = 1$ case there is some 50% increase in k_L above the simple penetration value. It is this 50% increase that causes two film additivity to hold as well as it does, however, because the $K_L a$ calculated by the left hand side of Equation (8.1.1) using k_L^* instead of k_L' would be much less than the value calculated by the right hand side (two film additivity), again using k_L^* instead of k_L' .

8.1.2 Single Lifetime - Countercurrent Problem

Because of the relatively large amount of surface drag experienced by the gas stream in a packed tower at the gas-liquid interface a stagnant film theory is more realistic for the gas phase transfer than it is for that in the liquid phase. The assumption that k_G is constant at all points under all circumstances of liquid phase behavior is probably, however, too much of a simplification.

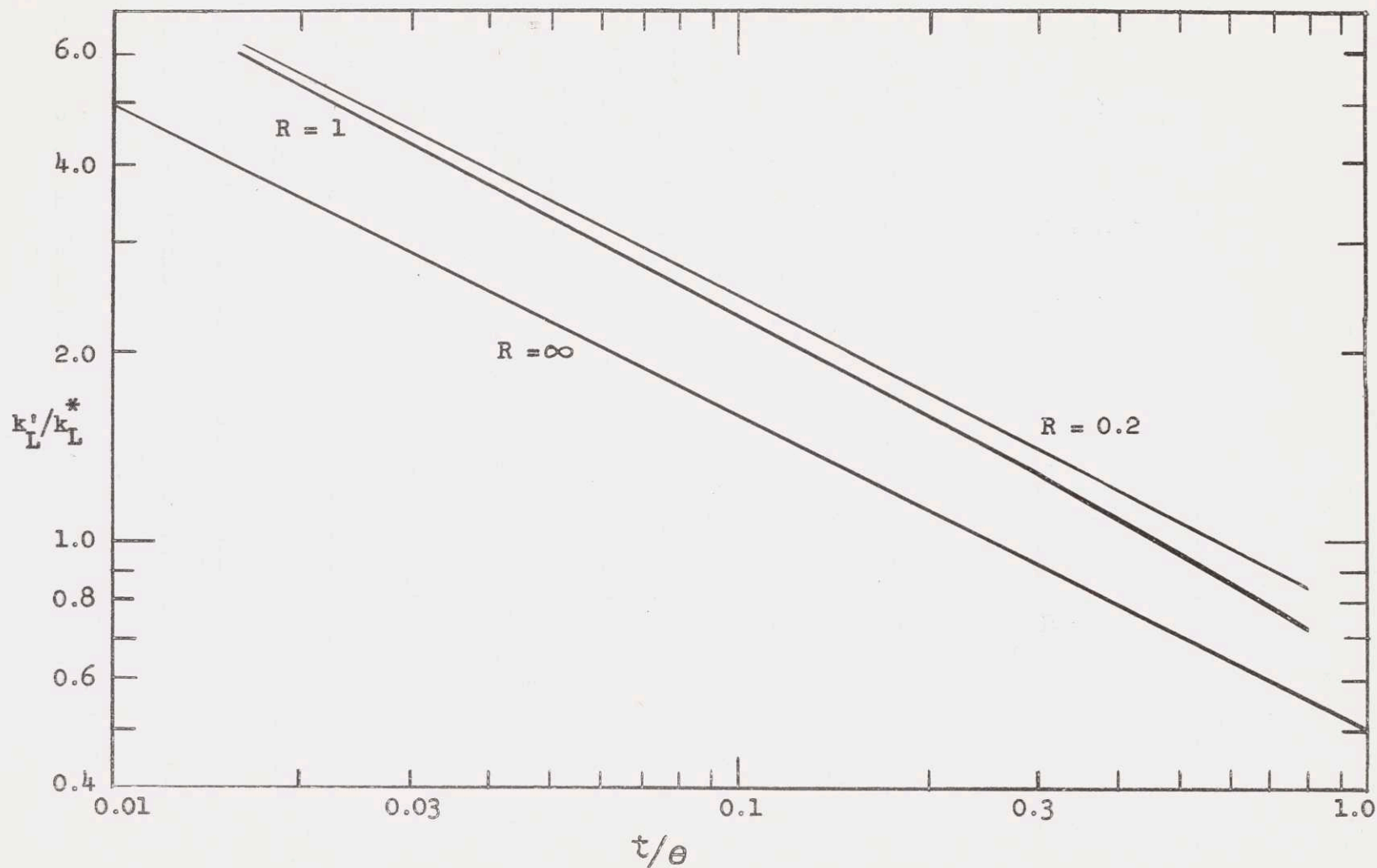


FIGURE 8.2 LOCAL VARIATION OF k'_L FOR LIQUID PENETRATION AND STAGNANT, NO HOLD-UP GAS FILM

The air forms a continuous phase in the column and undergoes a tortuous flow through the packing. Modern hydrodynamic theory (see, e.g., Knudsen and Katz (75) indicates that, whenever a conduit wall diverges suddenly by more than 7° , a new "boundary layer" is usually formed in the fluid near the conduit wall. For the purposes of a simple physical picture, the air stream could well become well mixed at points of sudden divergence in the path through the packing, and then proceed to establish a new concentration profile during the straight flow over the next piece of packing. In almost direct analogy to the penetration model for the liquid phase, the solute concentration (or partial pressure) gradient in the gas phase would initially be infinite and then become less and less in magnitude as the gas surface aged. Since the gas would probably not flow more than 3 or 4 hydraulic radii before being re-mixed, the transfer in it should remain definitely unsteady state (75). The difference between the gas and liquid models lies in the velocity gradient and possible turbulence in the gas phase near the interface.

If such is the case, and the exponent of 0.5 to 0.67 found on the gas phase diffusivity in a k_G^a correlation experimentally indicates that it is, (see Section 8.2.2) then we are faced with the problem of some sort of countercurrent, unsteady state transfer mechanism where we must take into account the resistances in both phases in a countercurrent absorption column.

The simplest and most extreme case of this would be where the

birth of a liquid surface corresponds exactly to the death of a gas surface and vice versa. In this case old liquid surface is in contact with new gas surface and new liquid surface is in contact with old gas surface. This too is probably a close approximation to the behavior in a randomly packed column, for it is at the discontinuities in packing surface that both liquid and gas streams should tend to mix, with the mass transfer process occurring in countercurrent flow along the flat surface of a piece of packing in between mixing points. Thus, to the extent that mixing points for gas and liquid tend to coincide, the births of liquid surfaces should correspond to the deaths of gas surfaces and vice versa. If there are surface areas for which births and deaths do not coincide, then the transfer process should be in some way intermediate between the constant k_G situation and this concept of a complete correlation of births with deaths between the phases.

What countercurrent unsteady state mechanism would be most realistic for the gas phase? That some sort of boundary layer theory should apply is obvious; however, boundary layer theory usually involves the assumption of a finite boundary layer thickness, or hold-up, and it is precisely the presence of such a hold-up that causes the liquid penetration model to have transfer characteristics that are dependent upon past history. Since both phases would have this behavior, a knowledge of the interfacial conditions at any point between mixings would require the knowledge of the gas phase behavior between the point of gas birth and the point under consideration and also a knowledge of the liquid phase behavior

between the point of its birth and the point under consideration. Thus the interfacial behavior over the whole of the contact interval would have to be known, or assumed, in order to obtain a solution. This presents great mathematical difficulties in so far as either an analytical or a numerical solution is concerned, and it is because of this that no solutions of countercurrent double boundary layer (liquid-liquid interface) or countercurrent boundary layer - penetration (gas-liquid interface) problems have been presented in the literature, although a solution for the general co-current double boundary layer case has been (112). The co-current case does not present this difficulty.

There is one feature of boundary layer systems that makes the problem somewhat simpler. Deissler (29) in his theoretical and experimental studies on turbulent heat and mass transfer in tubes comes to the apparently valid conclusion that "the variation across the tube or boundary layers of mass transfer per unit area has a negligible effect on the concentration distribution." He shows in Figure 12 of reference (30) that the assumption of linear variation of heat or mass flow across a well developed boundary layer gives very nearly the same temperature or concentration profile as the assumption of constant heat or mass flux. Even more to the point, he shows in Figure 9 of reference 28 that the same reasoning apparently applies for the entrance, unsteady state region.

This conclusion is equivalent to the concept that the gas phase resistance presented by a turbulent boundary layer is not significantly

dependent upon its past history, since it is not dependent on the flux profile across the boundary layer at a given time.

Deissler's solutions were made for the case of a developing concentration boundary layer and an already developed velocity boundary layer. He shows, however (29), that the solution for the case of a simultaneously developing velocity boundary layer is essentially the same, so long as the Schmidt number of the system is greater than 0.5. The case of simultaneously developing boundary layers is the important one for consideration in the present instance, in light of the picture given above of a series of complete gas phase mixings during the flow through the packing.

In a laminar boundary layer the hold-up at any given age is greater than in a turbulent boundary layer, thus response of k_G to past interfacial history should be more of a problem for a laminar boundary layer.

Knudsen and Katz (75a) show, however, that for the case of simultaneously developing laminar velocity and temperature (or concentration) boundary layers and a Prandtl (or Schmidt) number of 0.7 (a representative Schmidt number for air - light gas systems), that essentially the same variation (+10%) of local transfer coefficient with downstream distance from the point of initial boundary layer formation occurs for the three following cases:

- 1) Constant surface temperature (concentration)

- 2) Constant surface flux
- 3) Constant surface to bulk temperature (concentration) difference.

For liquid phase penetration resistance there is a distinctly greater effect of boundary conditions, as may be seen for instance in Figures 8.2 above and 8.5 below.

Thus the similar results for these three different "past histories" indicate that for the case of simultaneously developing velocity and concentration laminar boundary layers in the gas stream the assumption of a complete insensitivity of transfer behavior to past history is better than in the liquid phase penetration case, and is perhaps justified for the present purposes because of the mathematical simplicity it affords. It should also be kept in mind that the assumption is better for a turbulent gas phase than for a laminar one. The concept of complete insensitivity to past history is, interestingly enough, equivalent to that of a thin stagnant film, the thickness of which varies with location.

The question of what form of gas phase k_G variation to take now arises. It is well known that for the laminar boundary layer case the transfer coefficient varies inversely with downstream distance to the $1/2$ power as long as the boundary layer does not tend to fill the flow conduit (75a, 120a, 140). That this filling tendency should ever occur in a randomly packed tower is unlikely in view of the frequent tortuosities encountered by the gas flow. Thus for our

idealized case of a complete correlation between liquid surface births and gas surface deaths and vice versa the boundary condition that should be placed on the liquid penetration diffusional equation for the case of laminar "insensitive" boundary layer gas phase behavior is

$$\text{at } y = 0, \quad -D_L \left(\frac{\partial c}{\partial y} \right) = H \frac{k_{Gm}}{2(1 - t/\theta)^{1/2}} (C_e - C_i), \quad (8.1.17)$$

instead of #3 in (2.1.21) and (8.1.3).

Here t = age of liquid surface
 θ = lifetime of liquid surface
 and, hence, $\theta - t$ = age of gas surface.

Other nomenclature has been introduced previously (see also Chapter 20). The term $k_{Gm}/2$ appears as a constant, obtained by an integration of k_G over the contact interval.

In the case of a turbulent boundary layer behavior of the gas phase there is no simple analytical solution to indicate the proper variation of k_G with age of gas surface. Aladyev (3) measured the local variation of h_L for turbulent heat transfer to water in tubes with constant wall temperature and simultaneously developing velocity and temperature boundary layers (Prandtl number = 7, somewhat higher than the usual Schmidt number range of 0.5 - 2.5 for most absorption solutes in air) and obtained results shown in Figure 8.3. Deissler (28, 29), as has been mentioned previously, obtained semi-theoretical solutions for a

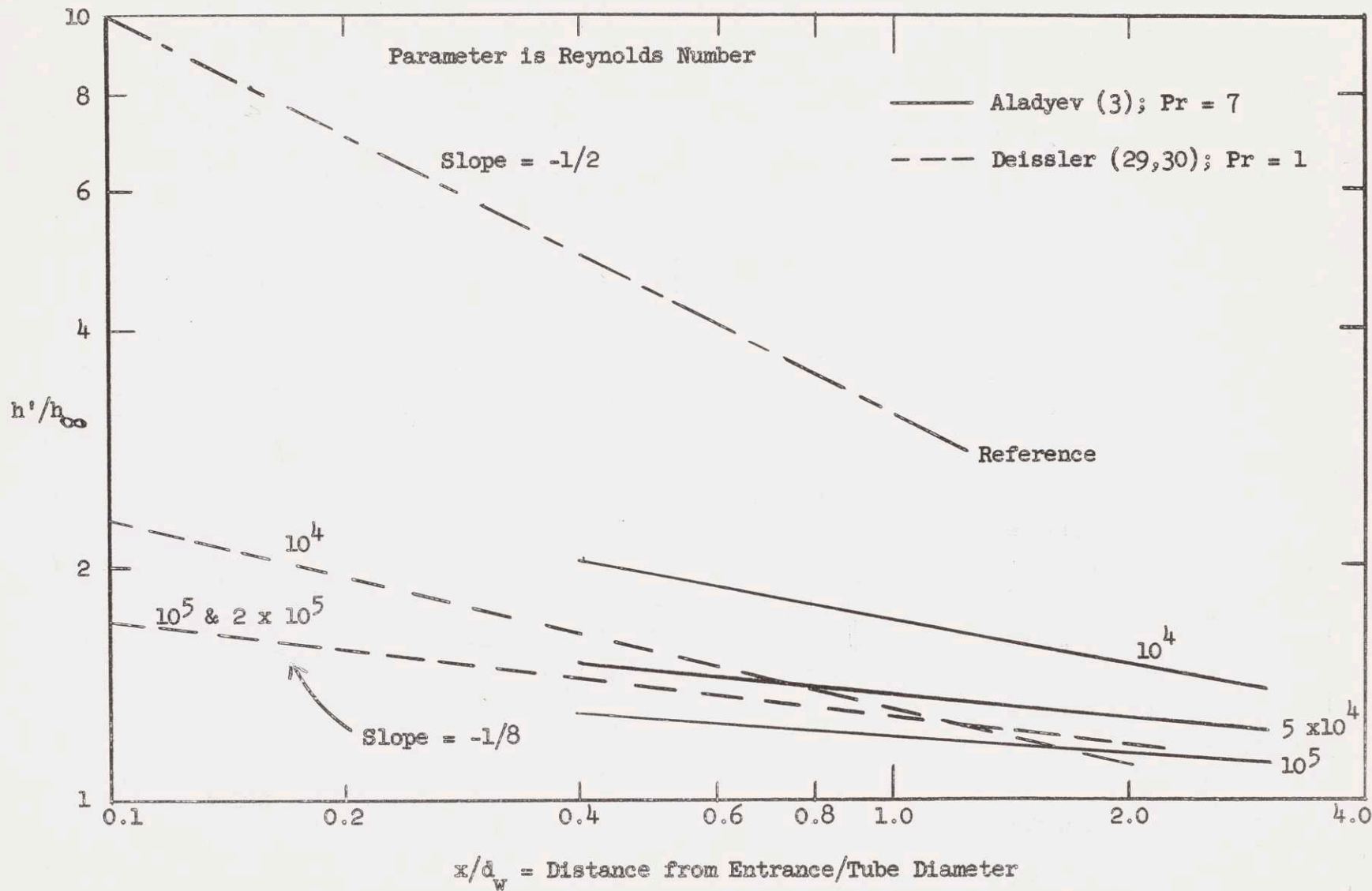


FIGURE 8.3 VARIATION OF LOCAL HEAT TRANSFER COEFFICIENT IN FLOW THROUGH TUBES

Prandtl (or Schmidt) number of 1. These are also shown in Figure 8.3. From this figure it may be seen that a good approximation for the behavior of a highly turbulent boundary layer is variation with distance or age to the $-1/8$ power. This also checks well with the -0.1 power of distance suggested empirically by Humble, Lowdermilk, and Desmon (64) from their studies of heat transfer to and from air. Therefore, the third boundary condition on the unsteady state diffusion equation for the liquid phase becomes, for the case of a highly turbulent "insensitive" gas phase developing boundary layer,

$$\text{at } x = 0, \quad -D_L \left(\frac{\partial c}{\partial y} \right) = \frac{7}{8} \frac{k_{Gm}}{(1 - t/\theta)^{1/8}} \quad (8.1.18)$$

Again the $7/8 k_{Gm}$ factor comes from an integration of the local k_G values over the contact interval.

The $-1/2$ power and $-1/8$ power variations represent extremes of behavior for laminar and for highly turbulent boundary layers. As may be seen in Figure 8.3, a lesser degree of turbulence would produce a power on distance or age intermediate between $-1/2$ and $-1/8$. It should be noticed, too, that in all cases k_G is taken to approach infinity at zero age (as does k_L in penetration theory). This is because there is initially an infinite gradient when a well mixed body of fluid is exposed suddenly to a surface concentration different from that in the fluid.

In these two countercurrent cases the third boundary condition

for the unsteady state liquid diffusion differential equation is time dependent, whereas it was not so in the cases of simple penetration (2.1.21) and penetration in contact with a constant k_G (8.1.3). This provides a nonlinear boundary condition, and the techniques of the Laplace transform or the Green's function, which are used for the cases of nontime dependent boundary conditions may no longer be used readily.

Because of this nonlinearity, it was necessary to use a numerical finite difference technique to solve the cases of penetration theory coupled with the time dependent, countercurrent k_G boundary conditions. The most common and most reliable such technique is the Dusenberre method (33, 91b). This was the method used to obtain the countercurrent solutions described in the following pages.

The unsteady state diffusion equation

$$D_L \frac{\partial^2 c}{\partial y^2} = \frac{\partial c}{\partial t} \quad (2.1.20)$$

may be transformed into the finite difference equation

$$\frac{C_{m+1, n} - 2C_{m, n} + C_{m-1, n}}{\Delta y} = \frac{1}{D_L} \frac{\Delta y}{\Delta t} (C_{m, n+1} - C_{m, n})$$

or

$$C_{m+1, n} - 2C_{m, n} + C_{m-1, n} = \frac{1}{D_L} \left(\frac{\Delta y}{\Delta t} \right)^2 (C_{m, n+1} - C_{m, n}) \quad (8.1.19)$$

Here Δy = the increment in distance normal to the surface

Δt = the increment in time

and the subscripts m and n refer to the distance, y , and the time, t , respectively. $m+1$ denotes distance $y + \Delta y$, and so forth.

Dusinberre denotes $\frac{(\Delta y)^2}{D_L \Delta t}$ as the modulus, M . Thus

$$C_{m, n+1} = \frac{C_{m-1, n} + (M-2)C_{m, n} + C_{m+1, n}}{M} \quad (8.1.20)$$

and the concentration at any point and any time is defined in terms of the concentration distribution at the next previous time. M must be chosen as a number greater than or equal to 2 in order to avoid a negative effect of $C_{m, n}$ on $C_{m, n+1}$, but otherwise the choice is somewhat arbitrary, a higher M giving more Δt intervals per Δy interval and thus usually requiring more computational effort.

This method requires some system of introducing the surface condition, boundary condition #3, into the computational process at any point of time. The most reliable method of doing this is to define N as a Biot modulus

$$N = \frac{Hk_G \Delta y}{D_L} \quad (8.1.21)$$

A material balance on the slice of liquid extending a distance Δy in from the surface gives

$$Hk_G (C_e - C_{i,n}) + \frac{D_L}{\Delta y} (C_{1,n} - C_{i,n}) = \frac{\Delta y}{2 \Delta t} (C_{i,n+1} - C_{i,n})$$

or

$$C_{i,n+1} = \frac{2NC_e + [M - (2N + 2)] C_{i,n} + 2C_{1,n}}{M} \quad (8.1.22)$$

where C_i = surface concentration

C_1 = concentration at depth Δy

and C_e = concentration in equilibrium with bulk gas

The factor of 2 in the first equation enters because there is only a half slice of liquid between the surface and the midpoint of the first Δy increment. In the present countercurrent cases k_G is time dependent, so N will have a different value after each time increment. M must be so chosen that $M > 2N + 2$ at all times.

The stability and convergence of this numerical solution are of great importance; if it is stable calculational and rounding off errors will not add upon one another as time goes on, and if it is convergent the true solution will be approached for ~~the~~ infinitesimally small increments. Mickley, et al, (91b) show that stability and convergence criteria are fulfilled by this solution for $M \geq 2$ and N positive. N , by the definition of k_G , will always be positive for these solutions.

Although the solutions are stable and convergent, nothing is said about the rate of convergence. This becomes important when solutions near the start are considered (often necessitating some sort of artificial starting condition) and when the k_G is changing rapidly with respect to time, such as occurs near the end of the liquid surface lifetime.

At the start (time-wise) of the solution for the liquid phase the k_G in the gas phase is relatively flat, that is it does not change greatly with respect to time. Thus it is a simple matter to assume a constant k_G for a short interval past the start and use the analytical, constant k_G solution, Equation (8.1.8), as a check on the starting solution.

K_L' , which is the desired result ultimately may be determined from the value of C_i at any time:

$$N_A = Hk_G' (C_e - C_i) = K_L' (C_e - C_i)$$

$$K_L' = Hk_G' \frac{(C_e - C_i)}{(C_e - C_L)} \quad (8.1.23)$$

A discussion of the difficulties encountered near the end of the liquid exposure is deferred until later.

As an initial check on the method, the constant k_G case was solved

for $R = \frac{Hk_G}{2 \sqrt{D_L / \pi \theta}} = 1$, and the result was checked with the

analytical solution. Δt was taken as 0.05 and M as 4. N was then equal to 0.504 and was constant. It was found by trial and error that the numerical solution was almost identical (deviation of $C_i < 1\%$) for an artificial starting condition which took $C_{i,1}$ as $3/4$ the value predicted by Equation (8.1.22). C_i for all time increments past the

first would then be defined normally. This particular starting condition also worked well for the various countercurrent cases investigated, as was verified by checking against an approximate analytical solution for the first few time increments.

In the following pages the solutions obtained for the various cases of laminar and highly turbulent insensitive gas phase boundary layers are presented. A detailed solution for one of the cases is given first.

a. Laminar Boundary Layer

As a detailed example of the solution technique the calculations for the $R = 1$ case of a countercurrent laminar boundary layer are now given.

It was convenient initially to take Δt equal to 0.05θ and M equal to 4, as was done in checking the constant k_G solution. Δy , then, by the definition of M , was equal to $(MD_L \Delta t)^{1/2}$, or $\sqrt{0.2 \theta D_L}$. Since the solution is for the case of $R (= Hk_G^*/k_L^*) = 1$, Hk_{Gm} may be taken as $1 \times k_L^*$, or $2 \sqrt{D_L / \pi \theta}$. From Equation (8.1.17),

$$Hk_G = \frac{\sqrt{D_L / \pi \theta}}{(1 - t/\theta)^{1/2}}$$

and

$$N = \frac{Hk_G \Delta y}{D_L} = \frac{\sqrt{0.2/\pi}}{(1 - t/\theta)^{1/2}} = \frac{0.252}{(1 - t/\theta)^{1/2}}$$

Since the modulus of 4 is used only up until $t = 0.8 \theta$, $2N + 2$ is always less than M , as is required for stability. From $t = 0.8 \theta$ on, the value of Δy is kept the same but M is increased to 8, thus making $\Delta t = 0.025 \theta$. Since Δy is the same as for the preceding time intervals, N retains the same definition. The higher M and lesser Δt serves to give more time intervals where k_G is changing faster, and keeps $M > 2N + 2$. Table 8.1 shows the complete numerical solution up until $t = 0.975 \theta$. The solution is made taking C_e arbitrarily equal to 1000 and C_L equal to zero. Fractions exactly equal to 0.50 are rounded off to the nearest even integers, to avoid cumulative errors.

From the concentration history solution it is desirable to obtain, as an end product, the local values of K_L' at the various times. This may be done by using Equation (8.1.23), which in this case becomes

$$K_L' = Hk_G' (1 - C_i/C_e) = \frac{Hk_{Gm}}{2(1 - t/\theta)^{1/2}} (1 - C_i/C_e)$$

The resultant K_L' history is most conveniently plotted as K_L'/K_{LF} , where K_{LF} is the constant value of K_L predicted at every point by two film additivity using, it should be recalled, k_L^* as the liquid phase resistance. K_{LF}/Hk_{Gm} for $R = 1$ is $1/2$; therefore

$$K' / K = \frac{(1 - C_i/C_e)}{(1 - t/\theta)^{1/2}} \quad (8.1.24)$$

for $R = 1$. This curve is plotted as Figure 8.4. It may readily be

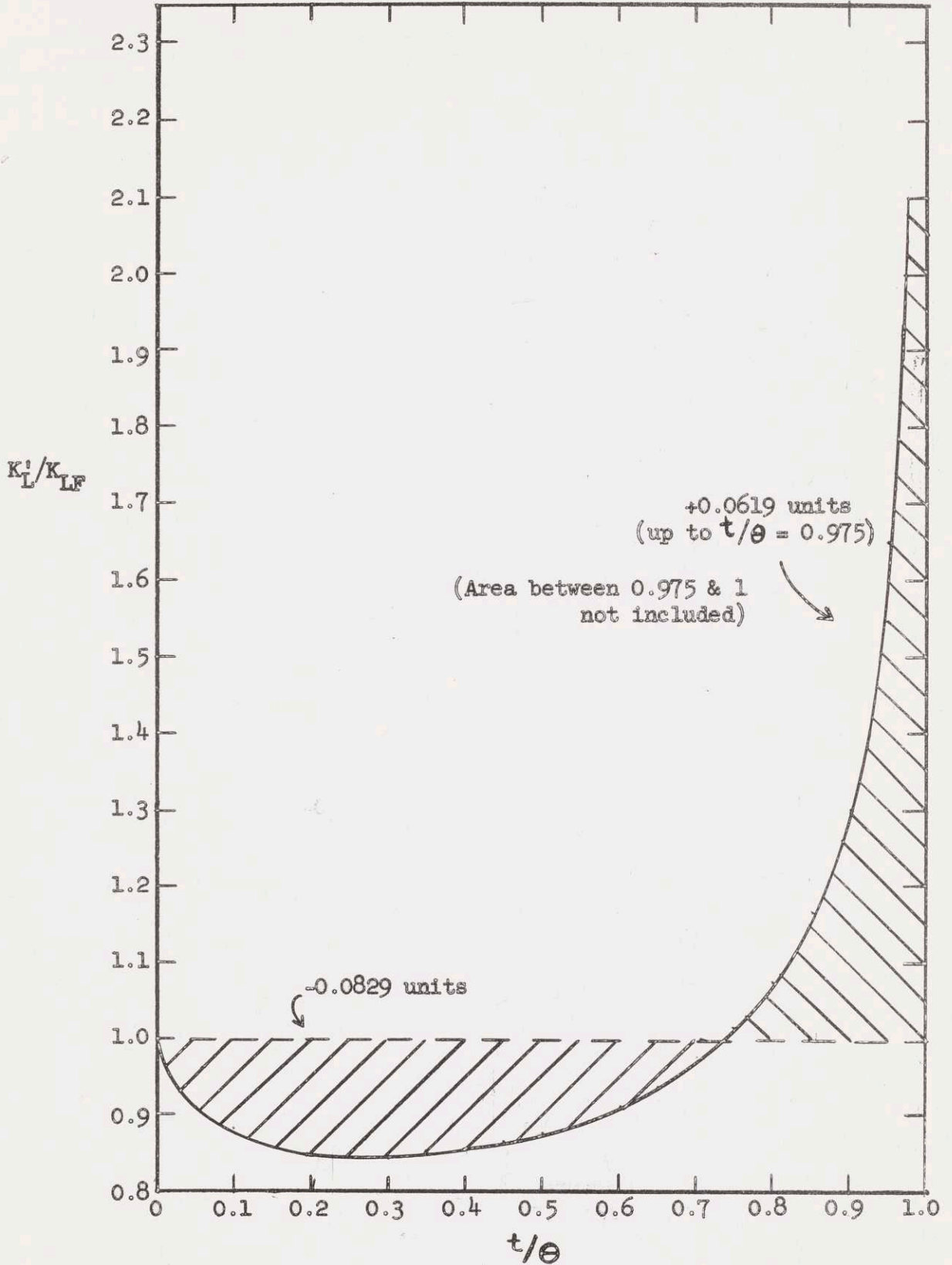


FIGURE 8.4 ADDITIVITY SOLUTION: LIQUID PENETRATION & INSENSITIVE LAMINAR GAS BOUNDARY LAYER; $R = 1$

TABLE 8.1

Numerical Solution Of Countercurrent Insensitive Laminar Boundary Layer
Penetration Case For $R = 1$

t/θ	$(1-t/\theta)^{1/2}$	N	$2NC_e$	$M-(2N+2)$	C_i	C_1	C_2	C_3	C_4	C_5	C_6	C_7	$1-C_i/C_e$	K_L'/K_{LF}
0	1.0	0.252	504	1.496	0	-	-	-	-	-	-	-	1.000	1.000
0.05	0.975	0.258	516	1.484	94*	-	-	-	-	-	-	-	0.906	0.929
0.10	0.949	0.266	532	1.468	168	24	-	-	-	-	-	-	0.832	0.877
0.15	0.922	0.273	546	1.454	207	54	6	-	-	-	-	-	0.793	0.860
0.20	0.894	0.282	564	1.436	239	80	16	2	-	-	-	-	0.761	0.851
0.25	0.866	0.291	582	1.418	267	104	28	5	-	-	-	-	0.733	0.846
0.30	0.836	0.301	602	1.398	292	126	41	10	1	-	-	-	0.708	0.847
0.35	0.806	0.313	626	1.374	316	146	54	16	3	-	-	-	0.684	0.849
0.40	0.775	0.325	650	1.350	338	166	68	22	6	1	-	-	0.662	0.854
0.45	0.742	0.340	680	1.320	360	184	81	30	9	2	-	-	0.640	0.862
0.50	0.707	0.356	712	1.288	380	202	94	38	12	3	-	-	0.620	0.877
0.55	0.671	0.376	752	1.248	401	220	107	46	16	4	1	-	0.599	0.893
0.60	0.632	0.349	798	1.202	423	237	120	54	20	6	2	-	0.577	0.913
0.65	0.592	0.426	852	1.148	445	254	133	62	25	8	3	-	0.555	0.938
0.70	0.548	0.460	920	1.080	468	272	146	70	30	11	4	1	0.532	0.971
0.75	0.500	0.504	1008	0.992	492	290	158	79	35	14	5	2	0.508	1.016
0.80	0.447	0.564	1128	4.872	519	308	171	88	41	17	6	2	0.481	1.076
0.825	0.418	0.603	1206	4.794	534	317	178	92	44	19	7	2	0.466	1.115
0.85	0.387	0.651	1302	4.698	550	326	185	97	47	21	8	2	0.450	1.163
0.875	0.354	0.712	1424	4.576	567	336	192	102	50	23	9	2	0.433	1.223
0.90	0.316	0.798	1596	4.404	586	347	199	107	53	25	10	3	0.414	1.310
0.925	0.274	0.920	1840	4.160	609	358	206	112	56	27	11	4	0.391	1.427
0.95	0.224	1.125	2250	3.750	636	370	213	117	59	29	12	4	0.364	1.625
0.975	0.158	1.595	3190	-	672	384	221	122	62	31	13	4	0.328	2.08

* = 3/4 of indicated value

seen that the deviation factor, δ , from additivity ($K_L = \delta K_{LF}$) comes from the area under the K_L'/K_{LF} vs. t/θ curve. The area between the K_L'/K_{LF} curve and $K_L'/K_{LF} = 1.0$ represents the absolute value of the deviation from additivity, i.e., $(\delta - 1)$.

As $t/\theta = 1$ is approached, K_L'/K_{LF} rises without apparent limit. It is possible, and it indeed happens in this case that much of the absolute deviation area comes under the K_L'/K_{LF} above $t/\theta = 0.975$.

In order to discuss the behavior of this curve further it is helpful to examine a plot of k_L' vs. $1 - t/\theta$. k_L' from the definitions of K_L' , k_G' , and k_L' is

$$k_L' = K_L' \frac{C_e - C_L}{C_i - C_L} = Hk_G' \frac{C_e - C_i}{C_i - C_L} \quad (8.1.25)$$

Thus k_L' may be calculated from the values in Table 8.1. Its history (presented as (k_L'/k_L^*) vs. t/θ) is shown in Figure 8.5. In Figure 8.6 it is shown plotted logarithmically against $1 - t/\theta$. Curves for K_L'/K_{LF} , k_G'/k_{Gm} , $C_i - C_L/C_E - C_L$, and k_L^{**}/k_L^* are also presented for reference. The k_L^{**}/k_L^* curve need not concern us here; it is presented merely to show the difference between k_L^{**} (for no gas phase resistance) and the k_L' actually occurring in the process.

Equation 8.1.25 shows that, as t approaches θ (and k_G' becomes infinite), either C_i must approach C_E or k_L' (and K_L') must approach infinity, or both may happen. An examination of Figure 8.5 shows that k_L' and K_L' have, since the time $t = 0$, always tended to lag behind k_G'

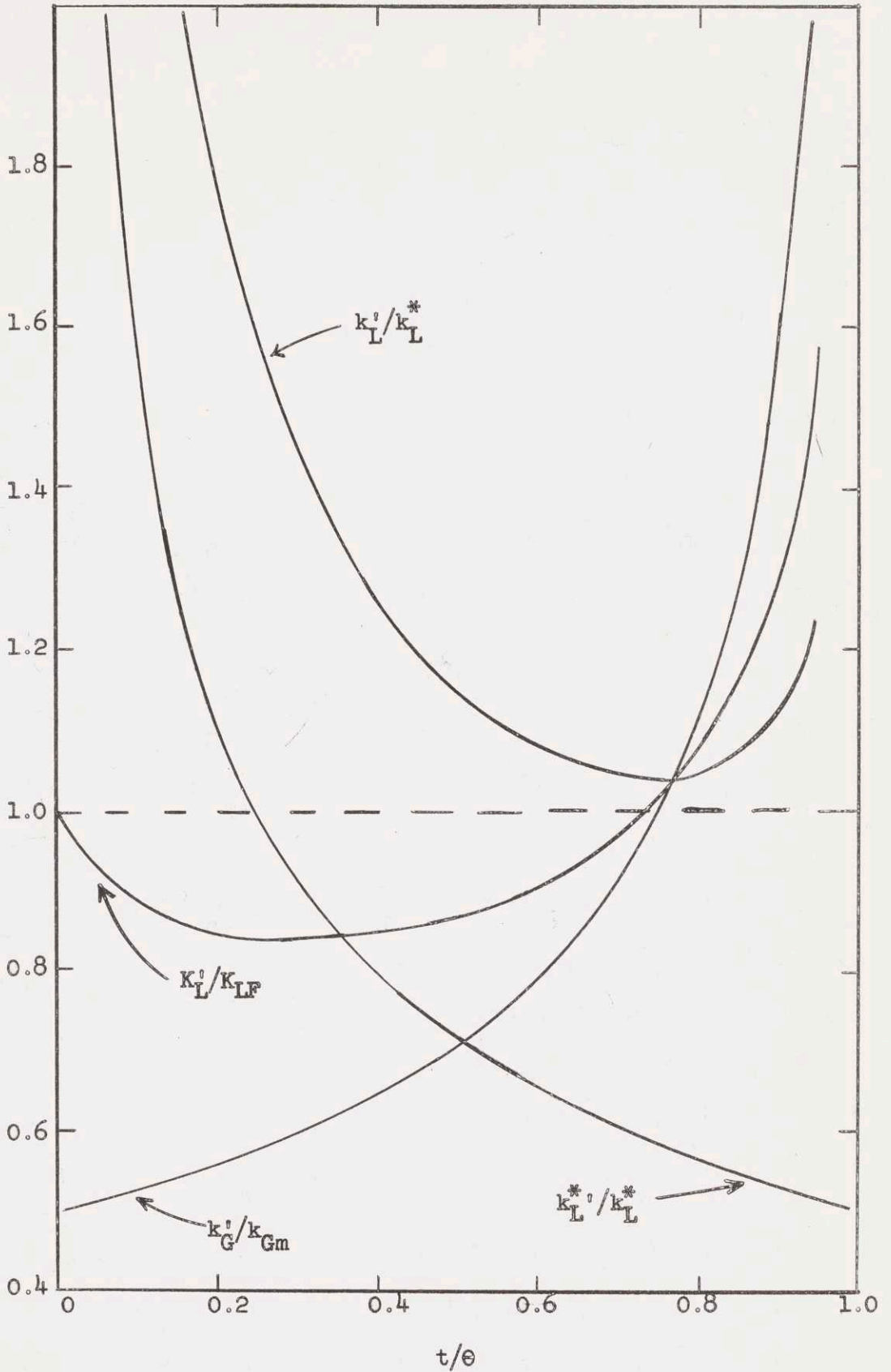


FIGURE 8.5 VARIATION OF LOCAL COEFFICIENTS: LIQUID PENETRATION & INSENSITIVE LAMINAR GAS BOUNDARY LAYER; $R = 1$

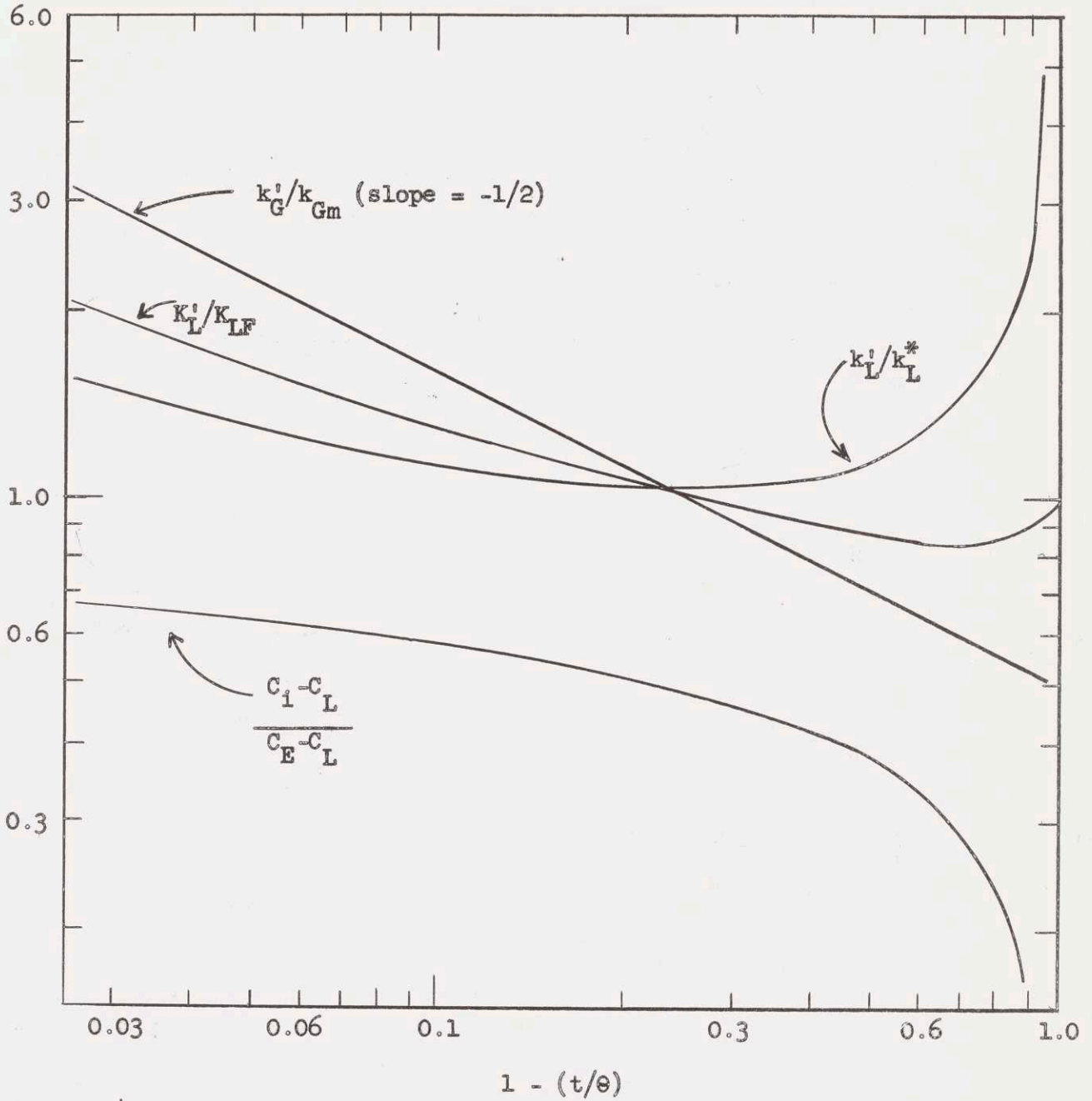


FIGURE 8.6 VARIATION OF LOCAL COEFFICIENTS: LIQUID PENETRATION & INSENSITIVE LAMINAR GAS BOUNDARY LAYER; $R = 1$

in so far as their rate of increase with respect to time is concerned. This is caused by the very nature of the penetration model k_L' itself. When in contact with a constant surface temperature, k_L' will tend to decrease with time (to the $-1/2$ power) because of the inability of the transient liquid diffusion process to remove (in the absorption case) solute rapidly enough to maintain the size of the concentration gradient at the surface at its initially high value. The layers of liquid near the surface hold up progressively more and more solute.

The only reason that k_L' eventually tends to increase again with time in the present case is because the k_G' at the surface changes faster and faster as time goes on. The surface concentration soon tends to increase more and more with time (see Table 8.1 and Figure 8.5) and the k_L' , in response to this, begins to increase again after its initial drop. The change in k_G' thus leads the change in k_L' . Since k_G' must lead k_L' in this respect, by Equation 8.1.25 C_i must eventually approach C_E as t approaches θ , that is $C_E - C_i/C_i - C_L$ must always decrease toward zero as t increases so as to make up the deficit between the change in k_G' and the change in k_L' . Thus $C_i - C_L/C_E - C_L$ becomes infinite asymptotically to $t = \theta$.

Examination of Figure 8.6 now shows that $\log(C_i - C_L/C_E - C_L)$ vs. $\log(1 - t/\theta)$ has an ever increasing (less and less negative) slope as $1 - t/\theta$ becomes less and less. This is not in conflict with the previous statement that $C_i - C_L/C_E - C_L$ increases ever faster with t as t approaches θ . In that case we were talking of $C_i - C_L/C_E - C_L$ as a function of $(1 - t/\theta)$. An examination of the surface finite difference

relationship, Equation (8.1.22), shows that this is reasonable. Although Hk_G (or N) may increase very rapidly as t approaches θ -- varying with $(1 - t/\theta)^{1/2}$ -- the interfacial concentration will not be able to do so, because of the finite amount of diffusion of solute away from the surface that does occur; thus $C_i - C_L/C_E - C_L$ varies with $(1 - t/\theta)$ to a less negative power than $-1/2$.

Apparently, then, $\log C_i - C_L/C_E - C_L$ vs. $\log (1 - t/\theta)$ approaches the asymptote of $\log (1)$, corresponding to C_i equal to C_E , as $(1 - t/\theta)$ decreases. This indicates, then that the slope, $d \log (C_i - C_L)/(C_E - C_L) / d \log (1 - t/\theta)$, always increases toward zero as $(1 - t/\theta)$ continues to decrease.

From Equation (8.1.25):

$$\frac{K_L'}{k_L'} = \frac{C_i - C_L}{C_E - C_L},$$

and therefore,

$$\frac{d \log \left(\frac{K_L'}{k_L'} \right)}{d \log (1 - t/\theta)} = \frac{d \log \left(\frac{C_i - C_L}{C_E - C_L} \right)}{d \log (1 - t/\theta)} \quad (8.1.26)$$

Thus, as $1 - t/\theta$ approaches zero, $\log (K_L'/k_L')$ must become more and more constant, since the right hand side of Equation (8.1.26) ever increases toward zero. If $\log (K_L'/k_L')$ becomes more and more constant, then the curves in Figure 8.6 for $\log (K_L'/K_{LF})$ and $\log (k_L'/k_L^*)$ must become more and more parallel.

K_L' , however, is the reciprocal average of k_L' and k_G' by definition. Thus, if $\log K_L'$ and $\log k_L'$ become parallel, they must both become parallel to $\log k_G'$, since both retain significant values in comparison to it.

As this happens both k_L' and K_L' must tend to vary with $(1 - t/\theta)$ to a power uniformly decreasing to $-1/2$, which is the constant exponent on $(1 - t/\theta)$ for k_G' .

Thus, interestingly enough, we are presented with a case where (∞) $\cdot (0)$ becomes equal to ∞ (see Equation 8.1.25), a situation that is definitely possible mathematically. K_L' and k_L' both increase to an infinite size as t approaches θ .

The fact that the transfer coefficients become infinite should not bother us, just as it should not for simple penetration theory when t approaches zero. They do so in both cases in such a way that the total amount of transfer occurring is finite; that is, the area under the K_L' vs. t curve is finite.*

The assumption that mass transfer rates can indeed become infinite

*In any real situation the flux should also become infinite near $t = 0$ as well as near $t = \theta$. It is the finite liquid hold-up that causes the infinite flux in the latter case. Since in reality there must be some small finite degree of hold-up in a gas phase the flux should also become infinite near $t = 0$. Because of the much less gas phase hold-up it is likely that this happens in such a way as to cause a minor contribution to be made to the total area.

is purely a mathematical device. In reality some phenomenon such as an interfacial resistance (the existence of an accommodation coefficient or merely the finite velocities of molecules) will limit the rate of mass transfer and never let it become infinite. As has been proven by recent studies with jets having very short contact times (see Section 2.2.6), this occurs at so high a rate that the amount of area "lost" under the K_L' vs. t curve is entirely insignificant.

Returning to the problem at hand, it is now possible, in light of the preceding discussion, to bracket the behavior of the K_L' vs. t curve in Figure 8.4 as t approaches θ . We know that K_L' will tend to vary with $(1 - t/\theta)$ to a power ever uniformly decreasing toward $-1/2$ as t approaches θ . From the last two values of C_i calculated in the numerical solution an exponent on $(1 - t/\theta)$ may be assigned as applying at the point the numerical solution calculations leave off. Thus in the present example, if the exponent on $(1 - t/\theta)$ is denoted by n , there results

$$n = \frac{-\log 2.08 - \log 1.625}{\log 0.050 - \log 0.025} = -0.389$$

From the graphical integration up to $t = 0.975 \theta$ (see Figure 8.4), the deviation from additivity is equal to

$$\delta = \frac{K_L}{K_{LF}} = 1 - 0.0829 + 0.0619 + \text{remainder above } t = 0.975 \theta$$

This remainder is bracketed by curves corresponding to exponents on $(1 - t/\theta)$ of n at 0.975 (in this case -0.389) and $-1/2$, since the

exponent between $t = 0.975 \theta$ and $t = \theta$ will vary uniformly between these two values.

The area beneath such a curve varying with $(1 - t/\theta)^n$, where n is negative and the value of K_L'/K_{LF} at the lower value of t/θ (called $(t/\theta)_L$) is denoted by α , is given by

$$\int_{(t/\theta)_L}^1 \alpha \frac{[1 - (t/\theta)_L]^n}{[1 - (t/\theta)]^n} d(t/\theta) = \frac{\alpha}{1 - n} (1 - (t/\theta)_L)$$

Thus the upper bracket is

$$\begin{aligned} \delta \text{ lying above } t = 0.975 \text{ (upper limit)} &= \\ &= \frac{1}{1-0.5} (K_L'/K_{LF})_{t=0.975 \theta} (1 - 0.975) - 0.025 \\ &= [2(2.08) - 1] (0.025) \\ &= 0.079 \end{aligned}$$

The second term above enters since the pertinent area is that between the K_L'/K_{LF} curve and the line $K_L'/K_{LF} = 1$. Similarly the lower limit is

$$\begin{aligned} \delta \text{ lying above } t = 0.975 &= \frac{1}{1-0.389} (2.08)(0.025) - 0.025 \\ &= 0.060 \end{aligned}$$

δ is therefore bracketed between 1.039 and 1.058. The deviation of the true K_L for the whole contact from the value predicted by two

additivity is between +3.9% and +5.8%.

The use of these bracketing solutions limits the absolute accuracy of the resultant deviation; however the 2% spread in δ probably corresponds to the possible error in the numerical solution, especially if it were extended further up into the region above $t = 0.975 \theta$ where K_G' varies more rapidly with t . Even though higher values of M and lower values of $\Delta \theta$ were used in this range, it would also be necessary to decrease Δy , to preserve accuracy, thus greatly increasing the computational effort. It would still be necessary to discontinue the numerical solution at some point and to adopt bracketing solutions from there on. As it stands now the bracketing solutions in the present case give as precise an estimation as could be reliably trusted in the light of the "rate of convergence" question for the numerical solution, mentioned previously. A conservative statement of the results of this and the following solutions would be: For the case of insensitive countercurrent boundary layers the deviation of K_L from K_{LF} is less than 10%, and in a positive direction.

Figures 8.7, 8.8, and 8.9 show K_L'/K_{LF} profiles obtained for the cases of laminar boundary layer with $R = 2.0$, $R = 0.5$, and $R = 0.2$. Table 8.2 summarizes the calculations of δ for all four cases.

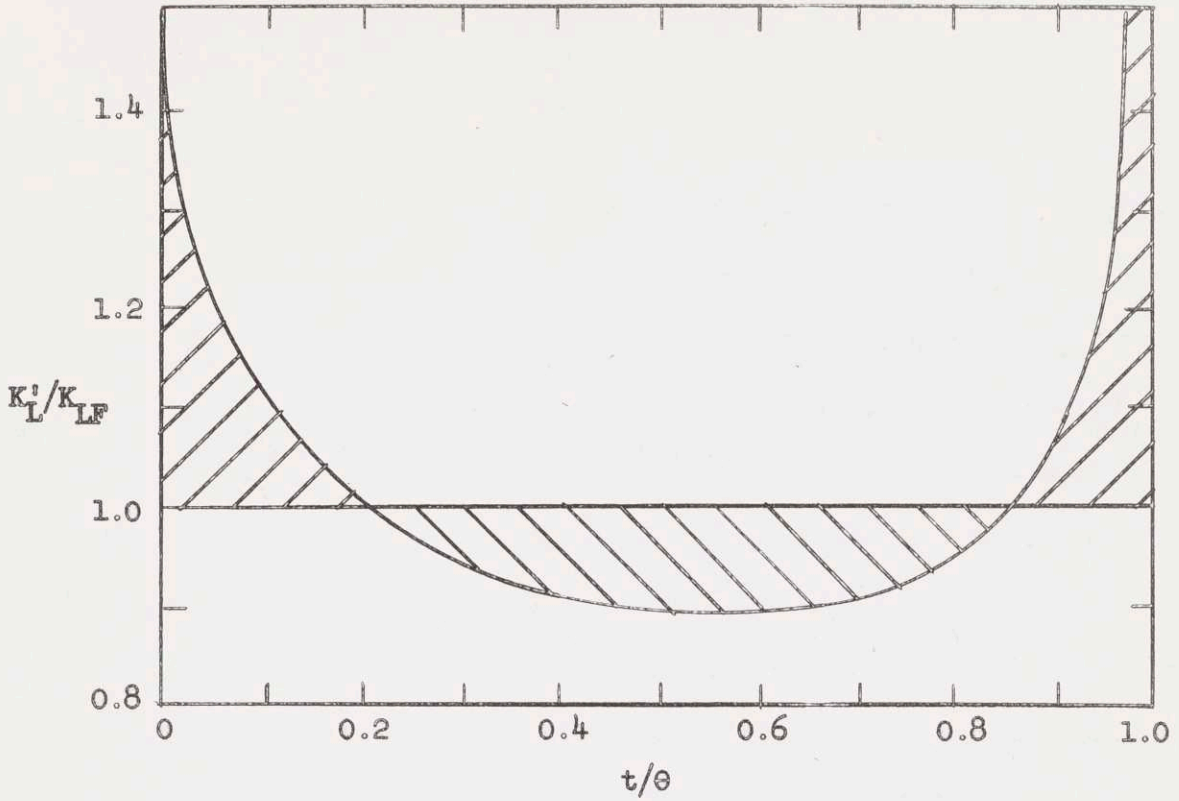


FIGURE 8.7 ADDITIVITY SOLUTION: LIQUID PENETRATION & INSENSITIVE LAMINAR GAS BOUNDARY LAYER; $R = 2$

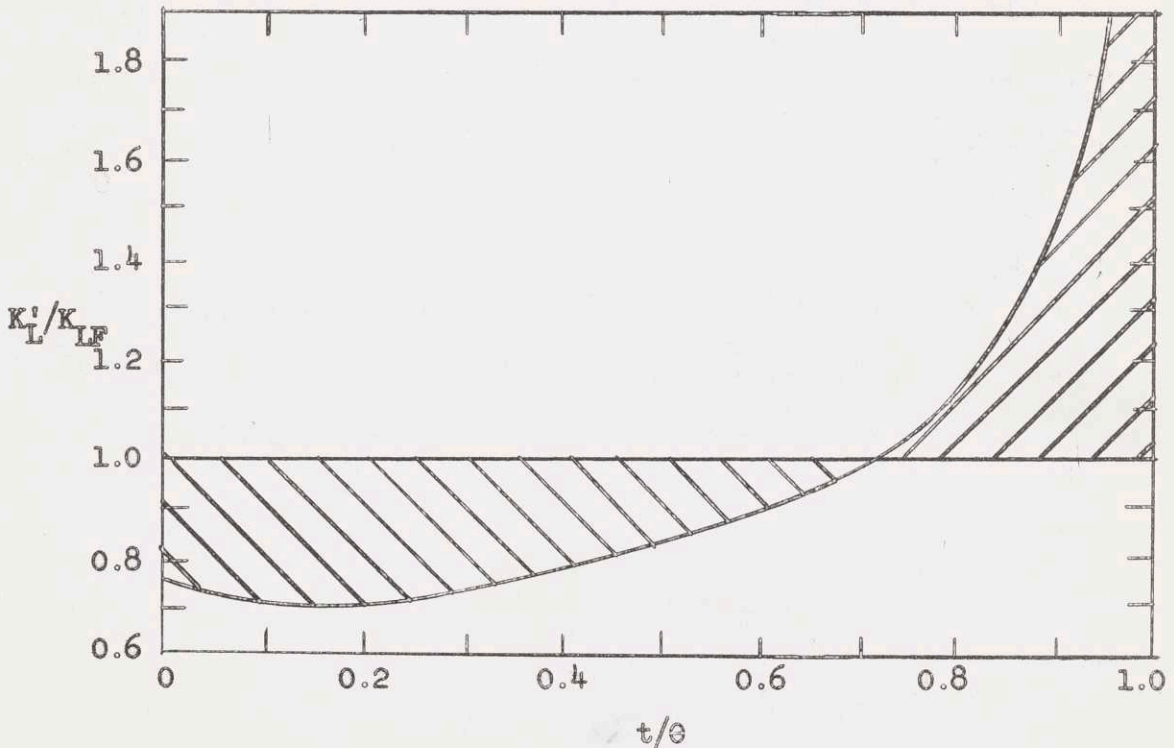


FIGURE 8.8 ADDITIVITY SOLUTION: LIQUID PENETRATION & INSENSITIVE LAMINAR GAS BOUNDARY LAYER; $R = 0.5$

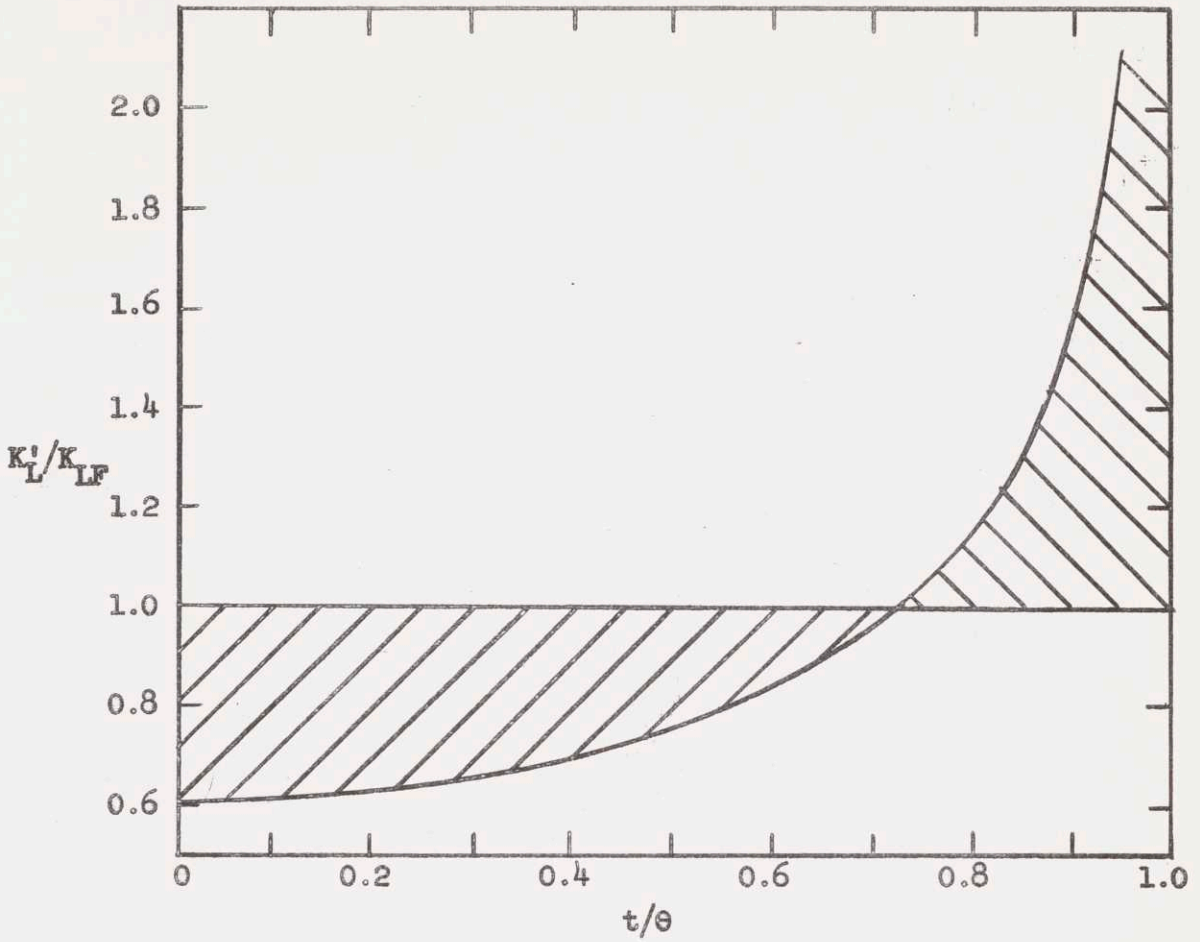


FIGURE 8.9 ADDITIVITY SOLUTION: LIQUID PENETRATION & INSENSITIVE LAMINAR GAS BOUNDARY LAYER; $R = 0.2$

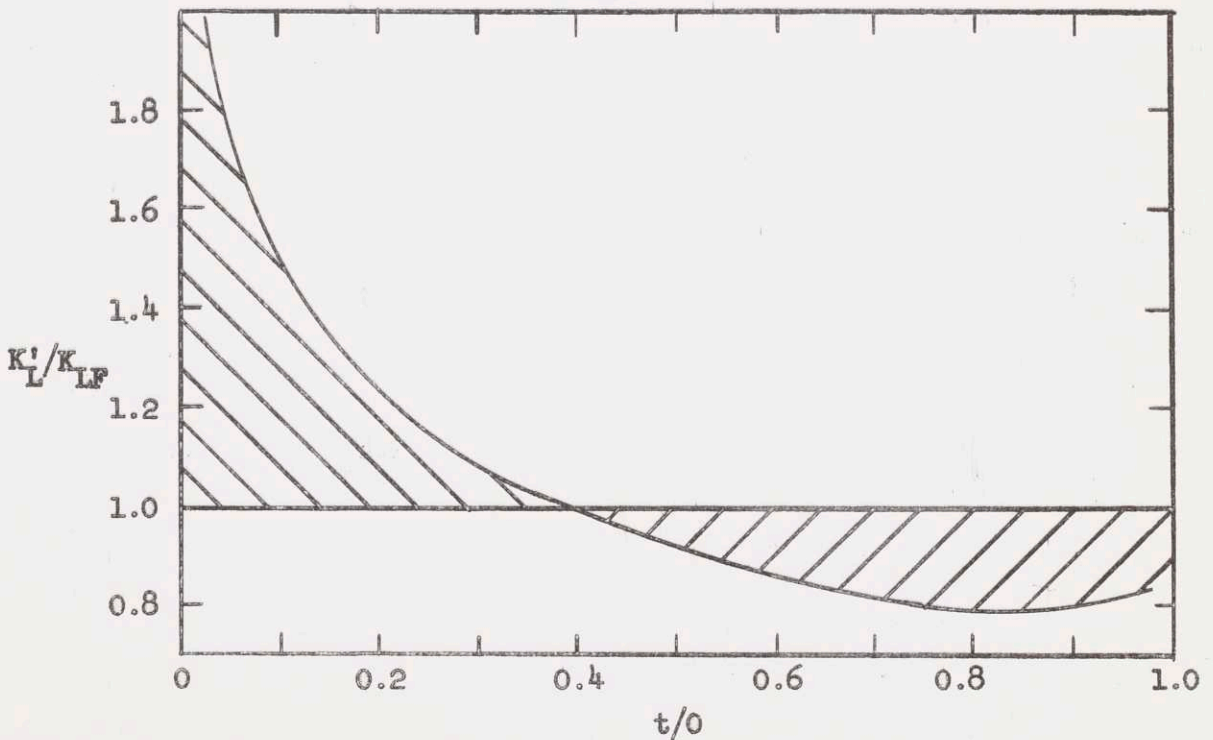


FIGURE 8.10 ADDITIVITY SOLUTION: LIQUID PENETRATION & INSENSITIVE TURBULENT GAS BOUNDARY LAYER; $R = 2$

TABLE 8.2

Summary of Calculations of δ for Cases of
Countercurrent Insensitive Laminar Boundary Layer

<u>R</u>	<u>$\delta - 1$ up to $t = 0.975 \theta$</u>	<u>($\delta - 1$) above $t = 0.975 \theta$</u>		<u>$\delta - 1$</u>	
		<u>Upper Bracket</u>	<u>Lower Bracket</u>	<u>Lower Limit</u>	<u>Upper Limit</u>
2.0	-0.005	+0.052	+0.030	+2.5%	+4.7%
1.0	-0.021	+0.079	+0.060	+3.9%	+5.8%
0.5	-0.051	+0.103	+0.085	+3.4%	+5.2%
0.2	-0.092	+0.122	+0.115	+2.3%	+3.0%

b. Highly Turbulent Boundary Layer

Three similar cases were calculated for the case of a highly turbulent boundary layer, where (from Equation (8.1.18))

$$k_G' = \frac{7/8 \quad k_{Gm}}{(1 - t/\theta)^{1/8}} \quad (8.1.27)$$

The calculational procedure was completely analogous to that for laminar boundary layer case. The solution above $t = 0.975 \theta$ in this case, though, is bracketed by curves corresponding to K_L' varying as $(1 - t/\theta)^{-1/8}$ and to K_L' varying as $(1 - t/\theta)^n$, where n is defined as in the laminar case as the exponent derived from the last two ($t = 0.95 \theta$ and $t = 0.975 \theta$) points.

This fact is derivable in precisely the same manner as was followed through for the laminar boundary layer case. The results for the three considered are shown graphically in Figures 8.10, 8.11, and 8.12. Table 8.3 summarizes the calculated deviations for these cases.

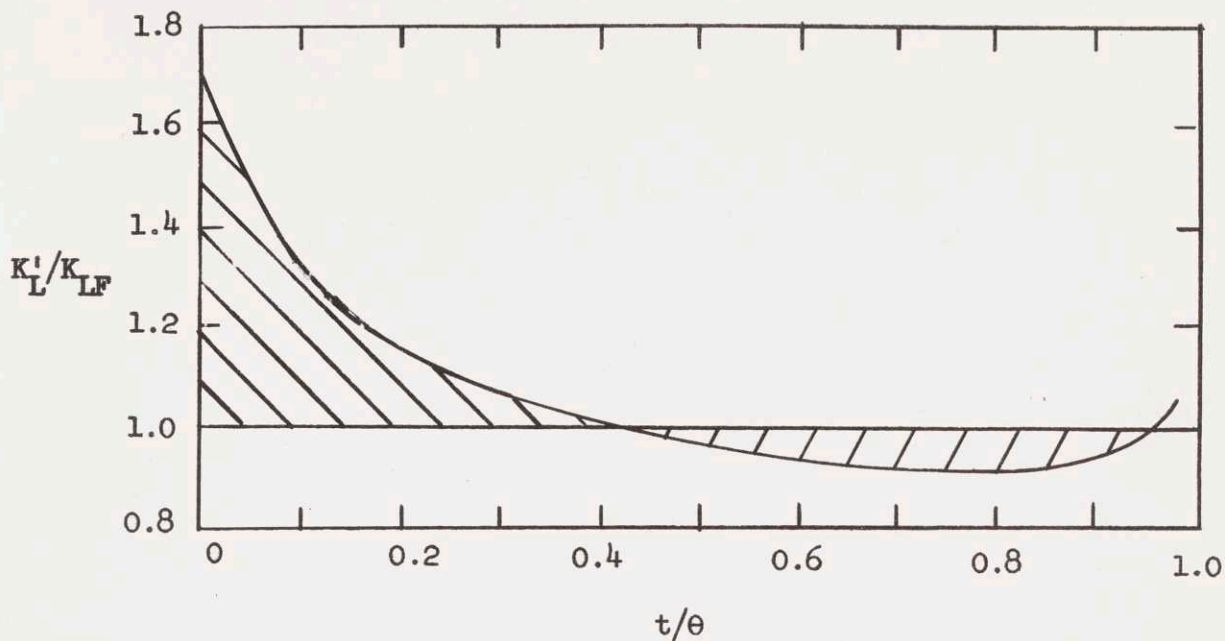


FIGURE 8.11 ADDITIVITY SOLUTION: LIQUID PENETRATION & INSENSITIVE TURBULENT GAS BOUNDARY LAYER; $R = 1$

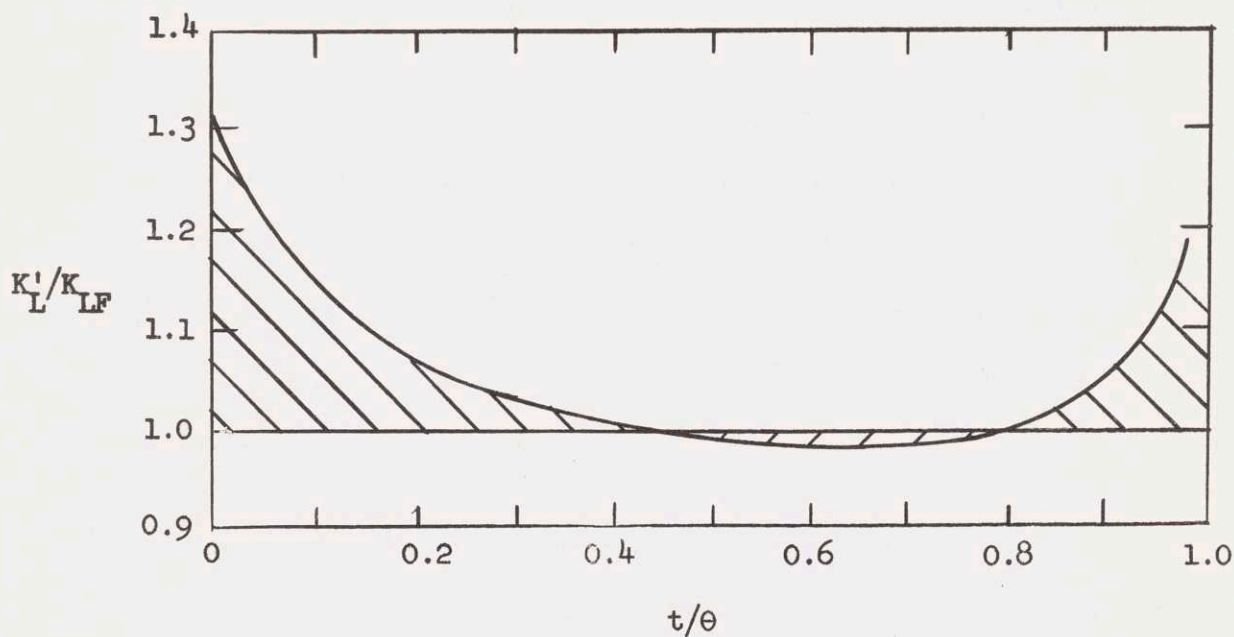


FIGURE 8.12 ADDITIVITY SOLUTION: LIQUID PENETRATION & INSENSITIVE TURBULENT GAS BOUNDARY LAYER; $R = 0.5$

TABLE 8.3

Summary of Calculations of δ for Case of
Countercurrent Insensitive Highly Turbulent Boundary Layers

R	$\delta - 1$ up to $t = 0.975 \theta$	$(\delta - 1)$ above $t = 0.975 \theta$		$\delta - 1$	
		Upper Bracket	Lower Bracket	Lower Limit	Upper Limit
2.0	0.046	-0.001	-0.003	+4.3%	+4.5%
1.0	0.052	0.005	0.003	+5.5%	+5.7%
0.5	0.042	0.009	0.008	+5.0%	+5.1%

Again, for all these cases of countercurrent unsteady state behavior, there is close (within 10%) agreement with the overall mass transfer coefficient predicted by two film theory, as was the case for unsteady state penetration behavior in the liquid and a constant k_G in the gas phase. That close agreement should result for countercurrent cases is all the more amazing. One could hardly conceive of two more different models for an absorption process than steady state two film behavior and countercurrent unsteady state penetration and boundary layer behavior, a fact pointed up by the large local variations of K_L'/K_{LF} in Figure 8.4 and Figures 8.7 - 8.12. Yet, for a single contact period the results yielded by the two approaches are essentially the same in so far as the additivity of resistances for each phase in the absence of the other is concerned.

An insight into the reason for this close agreement may be gained from an examination of the result for a hypothetical, purely academic case: That of two countercurrent laminar boundary layers that are completely insensitive to past history, or, equivalently, an insensitive laminar gas phase boundary layer in countercurrent contact with a liquid

phase showing the behavior characteristic of penetration under the condition of constant surface concentration, and for some reason being completely insensitive to past history. In such a hypothetical case, if R denotes the ratio of k_{Gm} for the phase born at $t = \theta$ to the k_{Gm} of that born at $t = 0$ (multiplied by a partition coefficient for the solute, analogous to H), then it is a simple matter to show that

$$\frac{K_L}{K_{LF}} = \int_0^1 \frac{K_L'}{K_{LF}} d(t/\theta) = \int_0^1 \frac{1+R}{2} \frac{d(t/\theta)}{R(t/\theta)^{1/2} + (1-t/\theta)^{1/2}} \quad (8.1.28)$$

For the case $R = 1$, K_L' is shown as a function of t/θ in Figure 8.13. The value of K_L/K_{LF} ($= \delta$) in this case by graphical integration is 0.75, by no means so good an agreement with two film additivity as given by the other cases above.

The reason for the close agreement with two film additivity then comes through the very fact that the liquid phase is highly sensitive transfer-wise to its past history. An examination of Figure 8.4 in comparison with Figure 8.13 shows this. The K_L'/K_{LF} curves are very similar on the lefthand, $t = 0$, side. As the right side is approached, that is as t becomes greater, the two curves become dissimilar, the actual history sensitive curve rising much more sharply and giving a substantial positive area above $K_L'/K_{LF} = 1$, which serves to offset the previous negative area and thus provide the close agreement with additivity. This occurs, as explained before, because of the rapidly

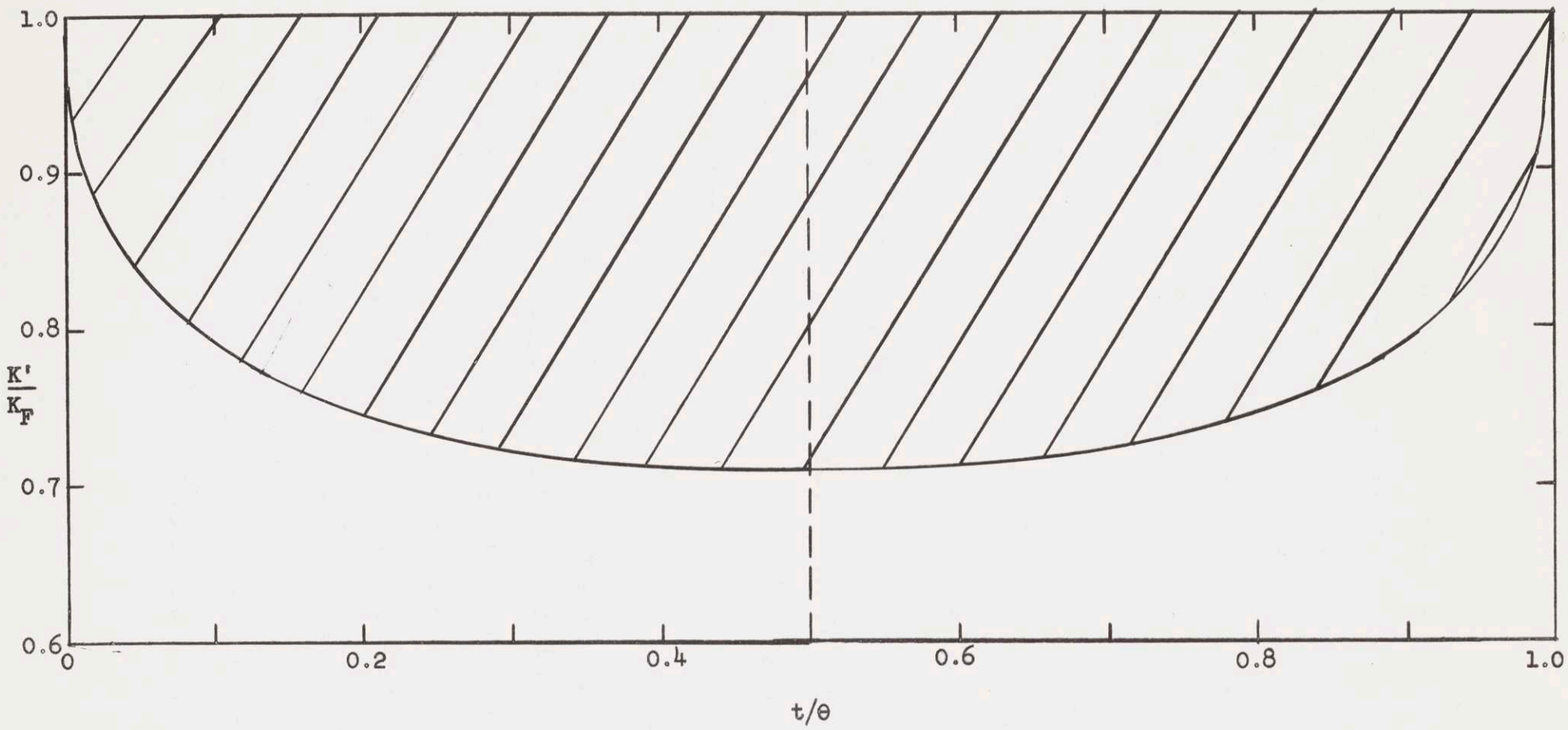


FIGURE 8.13 ADDITIVITY SOLUTION: COUNTERCURRENT INSENSITIVE LAMINAR BOUNDARY LAYERS; $R = 1$

changing surface conditions as t approaches θ which make k_L' rise to a much greater value than k_L^* (for constant surface concentration) would have (see Figures 8.5 and 8.6).

Both solutions, for the laminar boundary layer and for the highly turbulent one, show essentially the same pattern of variation of K_L/K_{LF} with respect to R , the ratio of individual, independent phase resistances. In all cases the maximum seems to occur near $R = 1$, as it does for the constant k_G case (Figure 8.1). The highly turbulent case may be considered as an intermediate between the laminar case and the constant k_G case, because the exponent of $-1/8$ on $(1 - t/\theta)$, which is intermediate between the $-1/2$ of the laminar case and the zero of the constant k_G case, denotes a less accentuated countercurrent behavior.

These solutions are for the case in which the birth of the surface in one phase corresponds to the death of the surface in the other phase, the probable behavior in flow over packing. For an instance in which this were not the case, such as when the gas surface might be renewed halfway through a liquid exposure, these solutions would not apply. Intuitively, however, it may be deduced that the behavior of such a case additivity-wise would be intermediate between the behavior for constant k_G and the behavior for a correspondence of births and deaths; one would expect, therefore, no great deviation from two film additivity.

Finally, it should be stressed that these solutions for counter-current cases are not to be taken as completely valid representations

of the physical situation of mass transfer in gas and liquid counter-current flow over a contact interval. The assumption was made prior to solution that the gas phase transfer behavior is completely insensitive to its past history. This is certainly much more true of the gas phase than of the liquid phase, (see the earlier portion of this section) and probably represents a good assumption in the case of the highly turbulent boundary layer where there is less solute hold-up than in the laminar boundary layer. The limitations of this assumption should, however, be kept in mind in applying the results of these solutions to any real physical cases in which the precision desired is greater than afforded by the assumption. The essential conclusion from these solutions -- that two film additivity holds remarkably well in such counter-current cases -- would in all probability be unaffected by the question of the rigid validity of the assumption that gas phase transfer behavior is insensitive to past history.

The discussion of this section certainly points out, though, that it is highly desirable at some time to obtain a rigid mathematical solution of the countercurrent boundary layer-penetration case.

8.1.3 Single Lifetime -- Cocurrent Cases

Although they should have little application to packed tower behavior under countercurrent operation, cases of additivity in cocurrent flow will be discussed briefly, if for no other reason than to complete the picture of additivity in different flow schemes.

Potter (125) has solved the problem of mass transfer between laminar boundary layers in cocurrent flow using the Pohlhausen quartic polynomial technique (120a). When investigated from an additivity of resistances standpoint, his results indicate perfect agreement with two film additivity in all cases of boundary layer coupled with boundary layer, or the special case of boundary layer coupled with penetration. This is not surprising upon further consideration: Under the influence of constant surface concentration, laminar boundary layer theory and its special case of penetration theory both predict a transfer coefficient that varies with the $-1/2$ power of surface age (or downstream distance from point of surface origin), no matter what the main stream velocity. Thus both phases in a cocurrent system, if subjected to constant surface concentrations, will give individual phase coefficients that bear a constant ratio ($= R$) to one another, i.e., in a gas-liquid system

$$\frac{Hk_G'}{k_L'} = \frac{Hk_{Gm}}{2(t)^{1/2}} \cdot \frac{2(t)^{1/2}}{k_{Lm}} = \frac{Hk_{Gm}}{k_{Lm}} = R$$

This constant ratio of coefficients is precisely the requirement necessary, however, to maintain the interfacial concentration constant since

$$\frac{Hk_G'}{k_L'} = \frac{(C_i - C_L)}{(C_e - C_i)}$$

If the Hk_G'/k_L' ratio is constant, then C_i is constant.

Thus cocurrent flow of two laminar boundary layers (which need not have the same main stream velocity), or cocurrent flow of a laminar gas

phase boundary layer and a liquid undergoing penetration will give perfect two film additivity of resistances, since k_L' and k_G' are everywhere equal to the values measured in the absence of resistance from the other phase. Similarly cocurrent highly turbulent boundary layers (both varying with $t^{-1/8}$) would also give perfect agreement with two film additivity.

This would not be true for a case of a highly turbulent gas boundary layer and liquid penetration in cocurrent flow, for the two processes tend to give coefficients varying with different powers of t for the case of constant surface concentration. In light of the previous discussion for constant k_G and countercurrent cases, though, it would be expected that such a situation would also give close agreement with two film additivity.

It should be kept in mind too that the concept of perfect additivity would hold strictly only for the situation in which the births of the surfaces of the two phases coincide. Were this not the case one would probably expect to find a value of δ ($= K_L/K_{LF}$) intermediate between that predicted by the coinciding births case and that predicted by the constant k_G case.

8.1.4 Distribution of Lifetimes

From investigations of instances of additivity over single lifetimes in a liquid penetration system we have come to the conclusion that there is always fairly close agreement with the additivity of resistances predicted by the two film theory. The deviation, if any, will probably be

positive (i.e., $K_L/K_{LF} > 1$) and will probably not exceed 10%. This result, however, applies for the case where there is but one liquid lifetime, whereas in a packed column or any other apparatus there must doubtless be a distribution of lifetimes.

If from single lifetime studies we are able to assign a certain deviation factor, δ_i , to the additivity of resistances over a given liquid surface lifetime, θ_i , then it is possible to express the overall coefficient effective over the whole distribution of surface lifetimes in terms of the lifetime distribution function, $\psi(\theta_i)$, defined as the fraction of the total interfacial surface that is engaged in reaching the lifetime between θ_i and $\theta_i + d\theta_i$. The units of $\psi(\theta_i)$ are reciprocal time. In order to assign the same overall coefficient to all points in the column it is necessary to assume that the same lifetime distribution, $\psi(\theta_i)$, applies at each and every horizontal level and that the amount absorbed in any given penetration may be considered infinitesimal. K_{Li} applying to any lifetime is given by

$$K_{Li} = \frac{\delta_i}{1/Hk_{Gi} + 1/2 \sqrt{\frac{\pi \theta_i}{D_L}}}, \quad (8.1.29)$$

in accordance with the penetration theory definition of k_{Li}^* for lifetime θ_i . k_{Gi} is the gas phase resistance effective in contact with the surface that is reaching the lifetime θ_i . Then, integrating over all the lifetimes,

$$K_L = \int_0^{\infty} \frac{\delta_i \psi(\theta_i) d\theta_i}{1/Hk_{Gi} + 1/2 \sqrt{\frac{\pi \theta_i}{D_L}}} \quad (8.1.30)$$

One simplification that may probably be made justifiably is to take k_{Gi} in contact with all lifetimes as a constant; that is, to say there is no tendency for a lower or higher k_G to be in contact with a surface reaching a short lifetime than with a surface reaching a long lifetime. Then

$$K_L = \int_0^{\infty} \frac{\delta_i \psi(\theta_i) d\theta_i}{1/Hk_G + 1/2 \sqrt{\frac{\pi \theta_i}{D_L}}} \quad (8.1.31)$$

The value of R (defined as Hk_G^*/k_L^*) for this situation is

$$R = \frac{Hk_G}{\int_0^{\infty} k_L'(\theta) \psi(\theta) d\theta} = \frac{Hk_G}{2 \sqrt{\frac{D_L}{\pi}} \int_0^{\infty} \frac{\psi(\theta_i)}{\sqrt{\theta_i}} d\theta_i} \quad (8.1.32)$$

R , which is conveniently obtained experimentally from $k_L a^*$ and $k_G a^*$ measurements, should be therefore considered as an independent variable.

From the two film theory for additivity:

$$K_{LF} = Hk_G \left(\frac{1}{1 + R} \right)$$

Therefore

$$\begin{aligned} \frac{K_L}{K_{LF}} &= \frac{1+R}{Hk_G} \int_0^{\infty} \frac{\delta_i \psi(\theta_i) d\theta_i}{\frac{1}{Hk_G} + 1/2 \sqrt{\frac{\pi \theta_i}{D_L}}} \\ &= (1+R) \int_0^{\infty} \frac{\delta_i \psi(\theta_i) d\theta_i}{1 + \frac{Hk_G}{2} \sqrt{\frac{\pi \theta_i}{D_L}}} \end{aligned} \quad (8.1.33)$$

Since δ_i is in theory known as a function of θ_i (actually as a function of $R_i = Hk_G/2 \sqrt{D_L/\pi \theta_i}$), K_L/K_{LF} may be considered a function (1) of the independent function, $\psi(\theta_i)$ and (2) of the independent variable R . (If $\psi(\theta_i)$ and R are known, then the second term in the denominator under the integral in Equation (8.1.33) may be determined from Equation (8.1.32).

It should also be pointed out that each and every point of the interfacial surface has been assigned a lifetime objective through use of the distribution function $\psi(\theta_i)$. Therefore the total interfacial area, a , remains a simple multiplicative factor. Thus K_L/K_{LF} in Equation (8.1.33) may as well be taken as $K_L a/K_{LF} a$ and the experimental value of R , determined as $Hk_G a^*/k_L a^*$, is equivalent to the Hk_G^*/k_L^* employed to define the R used in Equation (8.1.32).

The important fact derivable from Equations (8.1.32) and (8.1.33) is

that, if $\psi(\theta_i)$ is not such that $\theta_i = \text{constant}$ (one single lifetime), K_L/K_{LF} will not be equal to the δ value corresponding to the experimentally measured $R(= Hk_G^*/k_L^*)$ for the system.

Little additional simplification of the situation can be made without a knowledge of $\psi(\theta_i)$. One possibility, however, would be to take all values of δ_i equal to 1, in light of the preceding sections, since the probable range of δ_i from 1.00 to 1.10 is within the usual accuracy of experimental packed tower K_L measurements.

It would be difficult as well as tedious to evaluate the entire distribution function experimentally for the whole range of flow rates on various packings from additivity data; hence it is advisable to look for further simplifications to make which, although not rigidly justifiable, may seem reasonable through our knowledge of flow situations through packing.

A problem similar to the present one is encountered in the design of nuclear reactors, where there is a whole spectrum of neutron energies. The assumption that only neutrons of two different energies are present in the reactor (so called two group theory) has proven useful in the analysis of reactor behavior. Such a concept may also be helpful in evaluating the effect of the lifetime distribution in a packed tower. Indeed, such a simplification has some basis. It is likely that the

$\psi(\theta_i)$ vs. θ_i curve will show a marked peak at values on the order of magnitude of the θ_i value corresponding to the time of exposure of free

gravity fall of the liquid in active flow over a distance equal to the packing dimension. It is probable, too, that the other significant portion of the $\psi(\theta_i)$ curve will correspond to the longer lifetimes associated with liquid held in relatively stagnant pools between pieces of packing and the liquid in any other regions that do not participate in "active flow," for instance some of the inner surfaces of Raschig rings where the thickness of the falling liquid layers would be less than in the regions which have more active flow and consequent larger volumetric flow rate per unit wetted perimeter.

To simplify Equations (8.1.32) and (8.1.33) to this two group case, we define $\psi_i(\theta_i)$ as

$$\begin{aligned}\psi(\theta_i) &= f \quad \text{at } \theta_i = \theta_1 \\ &= 1 - f \quad \text{at } \theta_i = \theta_2 \\ &= 0 \quad \text{at } \theta_i \neq \theta_1 \text{ or } \theta_2\end{aligned}$$

Here f is the fraction of the interfacial surface in transit toward a lifetime θ_1 , and $1 - f$ is the fraction of the surface in transit toward a lifetime θ_2 .

Taking all δ_i equal to 1.00, Equations (8.1.32) and (8.1.33) now become, respectively

$$R = \frac{Hk_G^*a}{k_L a^*} = \frac{Hk_G}{2 \sqrt{D_L/\pi} \left(\frac{f}{\sqrt{\theta_1}} + \frac{1-f}{\sqrt{\theta_2}} \right)} \quad (8.1.34)$$

and

$$\frac{K_{L^a}}{K_{LF^a}} = (1 + R) \frac{f}{1 + \frac{Hk_G}{2} \sqrt{\frac{\pi \theta_1}{D_L}}} + \frac{1-f}{1 + \frac{Hk_G}{2} \sqrt{\frac{\pi \theta_2}{D_L}}} \quad (8.1.35)$$

It is convenient now to form another dimensionless group, λ , defined as k_{L1}/k_{L2} or $\sqrt{\theta_2/\theta_1}$. The solution for K_{L^a}/K_{LF^a} may be expressed from Equations (8.1.34) and (8.1.35) as a single equation in terms of R (measured experimentally as k_L^* and Hk_G^*), λ , and f (both parameters that may be used to fit experimental additivity data).

$$\frac{K_{L^a}}{K_{LF^a}} = (1 + R) \left[\frac{f}{1 + \left(f + \frac{1-f}{\lambda} \right) R} + \frac{1-f}{1 + (\lambda f + 1 - f) R} \right] \quad (8.1.36)$$

The nature of the deviations from two film additivity predicted by this two lifetime distribution theory (with the assumption $\delta_1 = \delta_2 = 1$) may be seen in Table 8.4, which presents values of K_{L^a}/K_{LF^a} calculated for various values of R , λ , and f . As a convention λ is always taken greater than 1; hence f is the fraction of more active surface.

TABLE 8.4

Deviations From Two Film Additivity Predicted By Two Lifetime Theory

<u>R</u>	<u>f</u>	<u>λ</u>	<u>K_L/K_{LF}</u>
1.0	0.5	2	0.97
1.0	0.5	5	0.88
1.0	0.5	10	0.80
1.0	0.5	25	0.73
1.0	0.5	∞	0.67
1.0	0.4	10	0.76
1.0	0.6	10	0.84
1.0	0.7	10	0.88
1.0	0.8	10	0.92
1.0	0.8	∞	0.89
1.0	0.9	10	0.92
2.0	0.7	10	0.92
0.5	0.7	10	0.87
0.1	0.7	10	0.91
10.0	0.7	10	0.97
10.0	0.7	∞	0.96
0.1	0.7	∞	0.72

Several interesting points are apparent from Table 8.4. In general, it is quite possible and indeed highly probable that the deviation from two film additivity emanating from there being a distribution of lifetimes of the liquid surface in a packed tower is much greater than the small deviation from two film additivity within a single lifetime. The maximum deviation (considered as a function of R) does not occur at $R = 1$, but is distorted somewhat in the direction of $R < 1$ (gas phase controlled), this distortion being more marked the greater λ is (the more dead the older surface is in comparison with the newer). Another important fact is that the deviation from two film additivity occasioned by a lifetime distribution of liquid surfaces is always negative, i.e., $K_L/K_{LF} < 1$. This is in contrast to the additivity deviations within a single lifetime, which apparently are always positive.

If λ is of a sufficient size to have a large significance, say for $\lambda > 10$, and f is greater than 0.5, then to an approximation the second terms in the brackets in either denominator of Equation (8.1.36) may be neglected, and

$$\frac{K_{L^a}}{K_{LF^a}} = (1 + R) \left[\frac{f}{1 + Rf} + \frac{1 - f}{1 + R \lambda f} \right] \quad (8.1.36a)$$

A special case of this two lifetime analysis may be considered for comparison with a recently arisen concept in the literature. If λ is taken as infinite, that is, if the $1 - f$ fraction of the surface is taken as infinitely old in comparison with the f fraction, then Equation (8.1.36) reduces to

$$\frac{K_{L^a}}{K_{LF^a}} = \frac{f + fR}{1 + fR} \quad (8.1.37)$$

This expression is entirely equivalent to the concept of Shulman, et al, (136) that the interfacial area in a packed column may be divided into two portions: Active and inactive liquid surface. Since a $k_L a$ resistance cannot affect a vaporization process, the entire interfacial area is effective for vaporization, whereas only the active fraction may be effective for an absorption or desorption process where there may be a $k_L a$ resistance (and $k_L a$ will be zero for the inactive surface). Thus if an effective area, a_e , is defined as fa in the present terminology then two film additivity applies for the a_e portion of the surface in an absorption process. Shulman's approach deals with dividing the

surface area, whereas the present approach deals with averaging K_{Li} values over the total area.

Shulman went so far as to express the total area to effective area ratio (a/a_e), which is equal to $1/f$ in the present terminology, as a linear function of the ratio of total hold-up (h_t) to the operating hold-up (h_o), obtaining

$$a/a_e = 1/f = 0.85 (h_t/h_o), \quad (8.1.38)$$

based on his hold-up data, the ammonia absorption data of Fellingner (38), and the vaporization data of Surosky and Dodge (146) and of Sherwood and Holloway (130).

For physical absorption processes the assumption of a completely dead portion of surface and the assignment of a significant transfer coefficient to the less active surface by the two lifetime theory suggest a slightly different mode of variation of $K_L a / K_{LF} a$ with R , as shown in Table 8.5.

TABLE 8.5

Values Of $\frac{K_L a}{K_{LF} a}$ From Two Lifetime Theory For $\lambda = 5, 10,$

	<u>And ∞ . (f constant at 0.7)</u>						
R:	<u>0</u>	<u>0.1</u>	<u>0.5</u>	<u>1.0</u>	<u>2.0</u>	<u>10.0</u>	<u>∞</u>
$\lambda = 5$	1.00	0.96	0.92	0.92	0.93	0.98	1.00
$\lambda = 10$	1.00	0.91	0.87	0.88	0.92	0.97	1.00
$\lambda = \infty$	0.70	0.72	0.78	0.82	0.88	0.96	1.00

Here it may be readily seen that the major effect of the $\lambda = \infty$ assumption on the variation of $K_L a / K_{LF} a$ with respect to R is to predict

a negative deviation continually increasing in magnitude with decreasing R to a limit of $K_{La}/K_{Lfa} = f$, whereas the assignment of a finite lifetime to the less active surface gives a negative deviation reaching a maximum in magnitude of deviation at some R less than one, and approaching $K_{La}/K_{Lfa} = 1$ as R approaches zero. Obviously as R becomes very small it is necessary in a real case to assign a finite lifetime to the $1 - f$ surface, so that the total a will be available for a vaporization process ($R = 0$), just as it was necessary for Shulman to distinguish in his analysis between vaporization and absorption processes.

There is also a difference in so far as the prediction for chemical reaction systems between the $\lambda = \infty$ and $\lambda = \text{finite}$ cases as will be shown in Section 8.2.2. Shulman (136) has mentioned the necessity of allowing for the area inactive in physical absorption to become significant in activity in such a case, but has not approached the problem more than qualitatively.

8.2 Re-examination of Literature Studies of Additivity

8.2.1 Stirred Flask

The work of Goodgame and Sherwood (46) studying the additivity of resistances during absorption in a stirred flask is the most recent and the most reliable from the standpoint of controlled conditions. Goodgame measured K_G and K_L for the vaporization of water into air and the absorption of carbon dioxide, ammonia, and acetone from air into water, all in dilute systems that should give the hydrodynamics of the air-water

system unaffected by the presence of the solute, and all at 25.0°C and at a constant stirrer speed of 120 rpm. Water vaporization and carbon dioxide absorption represented, respectively, cases of gas phase resistance completely controlling and liquid phase resistance completely controlling. The acetone and ammonia results then, under the assumption that both k_L and k_G vary as the diffusivity in that phase to the 0.5 power, indicated deviations from two film additivity of -2.5% and +2.4% respectively. The conclusion was that two film additivity held well.

Recourse to Goodgame's thesis (45) indicates that the solubility data were those of Sherwood (127) for ammonia and those of Othmer, Kollman, and White (103) for acetone, both the most reliable data available. Solutions were sufficiently dilute so that a Henry's Law constant held over the entire range of concentrations.

Diffusivities, however, were taken from Perry (109) for ammonia in air and water, carbon dioxide in water, and water in air, and were calculated by the Gilliland (133b) and Wilke (163, 164) correlations for acetone in air and water respectively. It is possible now to use experimental diffusivities for acetone, and somewhat more reliable values of ammonia diffusivities taken from the literature. Table 8.6 presents the "better" diffusivities selected, and their sources. Diffusivities are given for solutes that are considered at this point and also for those considered later in this chapter.

TABLE 8.6

Diffusivities of Various Solutes

<u>Solute</u>	<u>D_V in air(25°C) cm.²/sec.</u>	<u>D_L in water (25°C) cm.²/sec.</u>	<u>Source</u>
CO ₂	-	2.00 x 10 ⁻⁵	Present Work
H ₂ O	0.256	-	Gilliland (42)
NH ₃	-	2.28 x 10 ⁻⁵	Sherwood and Pigford (133); I.C.T. (66)
NH ₃	0.230	-	Wintergerst (165)
Acetone	-	1.33 x 10 ⁻⁵	Lewis (82)
Acetone	0.116	-	Deryagin, et al (31) & Goryunova, et al (49)
O ₂	-	2.41 x 10 ⁻⁵	Present Work
HCl	0.151	-	Gilliland Corr. (133b)
HCl	-	3.2 x 10 ^{-5*}	Stokes (144)
SO ₂	0.139	-	Reid & Sherwood (116b)
SO ₂	-	1.70 x 10 ^{-5**}	Peaceman (107b)
Ethanol	0.121	-	I.C.T. (66)
Ethanol	-	1.29 x 10 ⁻⁵	I.C.T. (66)
Methanol	0.144	-	Deryagin, et al (31)
Methanol	-	1.68 x 10 ⁻⁵	I.C.T. (66)
Napthalene	0.0611	-	Reid & Sherwood (116b)

* Average Value over Concentration Range

** Applies for both hydrolyzed and unhydrolyzed forms

The exponent of 0.5 on D_L is probably the most reliable in light of the Danckwerts surface renewal theory, but the best exponent to use

on D_V is open to question. For a low enough air circulation rate laminar boundary layer theory should apply and k_G should be proportional to $D_V^{2/3}$ (120a). On the other hand in a more turbulent system an exponent closer to 0.50 should apply (29, 133c). The stirring rate used by Goodgame and Sherwood was 120 rpm. with one of the two straight paddle stirrers in the air being 1/2 inch above the interface. In view of the lack of exact knowledge of the degree of turbulence in the air phase, it is of interest to calculate predicted K_L 's using both a $D_V^{0.5}$ effect and a $D_V^{2/3}$ effect.

The recalculated results of Goodgame and Sherwood are presented in Table 8.7.

TABLE 8.7

Recalculated Results of Goodgame and Sherwood (46)

Experimental Results

Water Vaporization:	$k_G = 0.203 \text{ g.mol/hr.cm.}^2\text{atm.}$
Carbon Dioxide:	$k_L = 3.62 \text{ cm./hr.}$
Ammonia:	$K_L = 1.69 \text{ cm./hr.}$
Acetone:	$K_L = 1.93 \text{ cm./hr.}$

<u>Based on $k_G \sim D_V^{1/2}$</u>	<u>R</u>	<u>K_{LF}</u>	<u>% Dev., K_L from K_{LF}</u>
Ammonia	0.82	1.75	-3.5%
Acetone	1.87	1.92	+0.5%
<u>Based on $k_G \sim D_V^{2/3}$</u>			
Ammonia	0.80	1.73	-2.3%
Acetone	1.64	1.83	+5.0%

Both phases were stirred with stirring blades attached to the same shaft; hence the process may be taken as one of cocurrent flow of both phases, for which no significant deviation from additivity in a single lifetime is to be expected (Section 8.1.3). If k_G is considered constant everywhere, then the major perceptible deviational effect should be a negative one due to any maldistribution of liquid surface lifetimes. Evidently from the results above there is no significant maldistribution of lifetimes and to the extent the diffusivity values may be trusted the exponent of $1/2$ on D_v is preferable in this instance. The overall conclusion to be made from the data remains, in the light of newer diffusivities for acetone, that there was no significant deviation from two film additivity in their stirred flask.

Goodgame and Sherwood also made two runs for absorption of ammonia in 2 to 4 M sulfuric acid, finding an asymptotic K_G reached at high sulfuric acid concentrations of 0.186 g-moles/hr. $cm.^2 atm.$ as opposed to a value of 0.195 predicted from the water vaporization data, corrected to the $1/2$ power of D_v . The "better" value of ammonia - air diffusivity gives a predicted value of 0.192, which is in better agreement and certainly within experimental error.

The only other stirred flask additivity study in which experimental conditions were under reasonable control was that of Whitman and Davis (159). Obtaining k_L values from oxygen absorption and k_G values from ammonia absorption from air into 2.3 M hydrochloric acid, they checked

two film additivity for the absorption of ammonia, hydrogen chloride, and sulfur dioxide from air into water. The work was carried out in a stirred flask with cocurrent flow of air and water, a constant stirrer speed of 60 rpm, and reported temperatures varying from 20 to 30°C. In all cases (except oxygen) the solute concentration in the gas phase was 5% or less on a mole basis. The original interpretation of their results was hampered somewhat by the lack of reliable solubility data. They also assumed that solute diffusivities within a phase could be taken equal for all solutes in order to compute their results.

Table 8.6 gives the most reliable diffusivities available for their solutes. The liquid phase coefficient should again vary with $D_L^{0.5}$. In view of the lower stirrer speed used than by Goodgame and Sherwood (46), the exponent on D_V for k_G correction may well be 0.5, 2/3, or something in between.

For three solutes (HCl, NH₃, and SO₂) pseudo-Henry's Law coefficients must be used, since the solute concentrations were above the strict Henry's Law range. It should be recalled from Section 1 of this chapter that for use in K_L evaluation H should be taken as $p_G - p_i/C_e - C_i$, whereas for K_G evaluation H should be taken as $p_i - p_E/C_i - C_L$. A value of $H = 16.5$ atm. cc./g-mol. was taken for ammonia, and a value of $H = 480$ atm. cc./g-mol. was taken for sulfur dioxide (total of molecular SO₂ and hydrolyzed forms), both from the data presented by Sherwood (127). For hydrogen chloride it is not possible to pin down a pseudo Henry's Law constant; however, it is possible from the data presented by Zeisberg (170) to show that the solubility at their concentrations is great enough to

eliminate liquid phase resistance entirely.

In recalculating the data it was necessary to allow for the effect of temperature on k_L . This was taken to be $1.6\%/^{\circ}\text{C}$ in accordance with theory for a penetration model (155). k_G was assumed to be insensitive to temperature (139).

The recalculated data of Whitman and Davis are presented in Table 8.8. Calculations based on K_G were made so that the more or less constant $p_G - p_E$ driving force could be used.

TABLE 8.8

Recalculated Results of Whitman and Davis ¹⁵⁹ (~~112~~)

<u>Experimental Results</u>				<u>T - °C</u>
Ammonia - 2.3 M. HCl	$k_G = 0.141 \text{ g.mol/hr.cm.}^2 \text{ atm.}$			28
Oxygen	$k_L = 3.3 \text{ cm./hr.}$			22
Ammonia	$K_G = 0.088$			20
Hydrogen Chloride	$K_G = 0.1092$			29
Sulfur Dioxide	$K_G = 0.0073$			20
<u>Based on $k_G \sim D_V^{1/2}$</u>				
	<u>R</u>	<u>K_{GF}</u>	<u>% Dev., from K_{GF}</u>	
Ammonia	0.75	0.081	+8%	
Hydrogen Chloride	Small	0.114	-5%	
Sulfur Dioxide	19.6	0.0053	+32%	
<u>Based on $k_G \sim D_V^{2/3}$</u>				
Ammonia	0.75	0.081	+8%	
Hydrogen Chloride	Small	0.106	+3%	
Sulfur Dioxide	18.0	0.0053	+32%	

For the cases of ammonia and hydrogen chloride agreement with additivity is as good as can be expected under the experimental conditions. For sulfur dioxide something seems awry. The difficulty cannot be attributed to the hydrolysis reaction for its effect would necessarily be to lower the K_L calculated on the basis of a "total" sulfur dioxide driving force, as is shown by Peaceman (107) and by Sherwood and Pigford (133h). Thus the sulfur dioxide results of Whitman and Davis remain a mystery. They cannot be taken as an indication of a deviation from two film additivity in a stirred flask in light of their other results and the results of Goodgame and Sherwood.

8.2.2 Packed Towers

Before further investigating the nature of additivity in packed towers it is desirable to determine the correct exponent to place on the gas phase diffusivity in an expression for $k_G a$. This will enable a comparison of data for different solute gases in the water-air hydrodynamic system.

There have been widely varying claims as to what the correct exponent should be, ranging from the 0.15 of Surosky and Dodge (146) and the 0.17 of Mehta and Parekh (130) to the $2/3$ of Houston and Walker (62). The former two values were obtained from studies of the vaporization of various liquids into air in flow over packing, and involved the assumption of an interfacial area unaffected by the nature of the liquid. Shulman, et al, (138) have shown qualitatively from their

studies of hold-ups in nonaqueous systems that the probable trend in wetted area from liquid to liquid could well necessitate a much higher exponent on D_v in both cases.

Perhaps the best approach to a determination of the exponent is that of Shulman and DeGouff (135) and later Shulman, Ullrich, Proulx, and Zimmerman (137), who studied the sublimation of naphthalene Raschig rings and Berl saddles into air and compared their data with the results of Taecker and Hougen (147) who evaporated water from completely wet porous Raschig rings and Berl saddles. In both studies the packings were made to conform to commercial specifications. There is a large factor (4.2) between the diffusivities of naphthalene and water, and Shulman found that for the two sets of data there was an apparent

correlation of $j_D = \frac{k_G M_{pBM}}{G} \left(\frac{\mu}{\rho D_v} \right)^{2/3}$ against air flow rate.

The data from the two studies are shown in Figure 8.14 for two sizes of rings; the term $D_p G / \mu (1 - \epsilon)$ comes from a correlation for flow through solids used by Shulman, but need not bother us so long as data for the same packing geometries are compared with one another.

The j_D correlation ($k_G a$ varies as $D_v^{2/3}$) certainly holds well at lower gas flow rates; however examination of Figure 8.14 and Figure 4 of the later Shulman article (146) shows that, as higher flow rates are encountered, the exponent may well drop off toward 0.50, a result in accord with the concept of transition from a laminar to a turbulent boundary layer in the gas phase, as previously mentioned (Section 8.2.1).

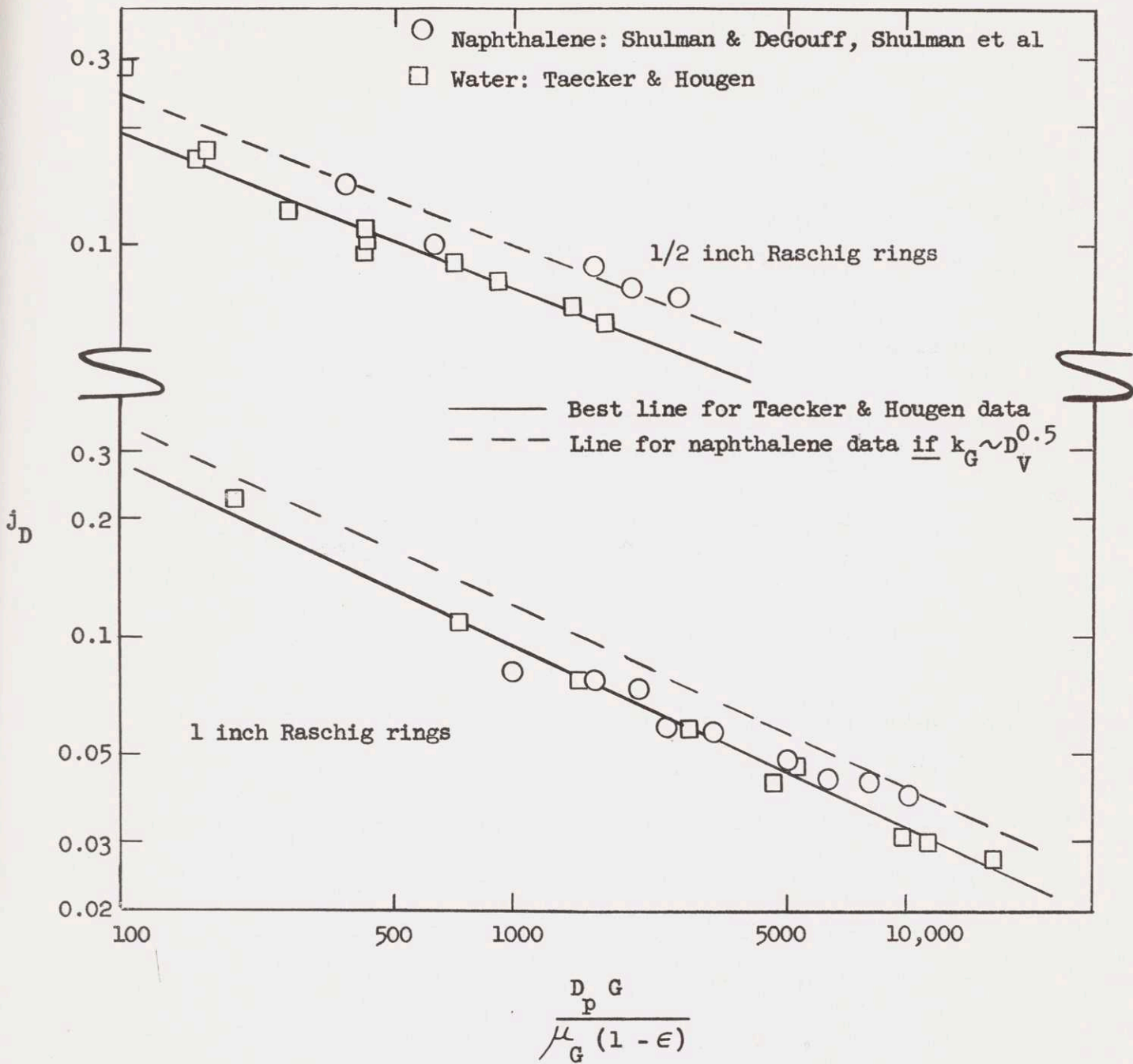


FIGURE 8.14 j_D CORRELATION FOR MASS TRANSFER FROM PACKING TO GAS PHASE

For practically all the data comparisons made in this Section $D_p G / \mu(1 - \epsilon)$ is less than 5000, so the $2/3$ power of diffusivity is indicated as the best choice.

There is truly a wealth of packed tower studies in the literature in which the aim was either to measure the $k_G a$ individual gas phase coefficient or to examine a case in which gas phase resistance was prominent. Table 8.9 provides an extensive summary of the data that are available for the water-air system and the more common commercial packings. Many of the data disagree internally (that is, for the same packing and the same solute) by 20% or more. This has often been because of questions of calculational technique. Also since k_G alone should be insensitive to temperature and has indeed been shown to be (139), there has often been a lack of close temperature control with a resultant possible effect on the interfacial area and an uncertainty of the temperature to use for liquid phase corrections. Since gas phase H.T.U. values are usually lower than liquid phase ones, extremely low packed heights have often been used, especially for vaporization data, with resultant uncertainties in height and large end transfer effects to be corrected for. Despite all this there remains a distinct general tendency for vaporization $k_G a$ values to be higher than those computed by two film additivity for absorption processes, and it appears that a liquid surface lifetime distribution effect as discussed in Section 8.1.4 may well be capable of explaining the discrepancies.

Also, once it is realized that carbon rings may well be different from ceramic Raschig rings in behavior, as evidenced by the radically different static hold-ups resulting from

TABLE 8.9

Summary of Literature Studies of the Gas Phase Resistance for Common Packings, and Sources of Liquid Phase Coefficients (Air-Water System)

Symbols: Liq. = Liquid Phase

Vap. = Vaporization of Water

Chemical symbols refer to absorption of that gas

<u>Source</u>	<u>Ceramic Raschig Rings</u>			<u>Carbon Rings</u>		<u>Berl Saddles</u>	
	<u>1/2"</u>	<u>1"</u>	<u>1-1/2"</u>	<u>1/2"</u>	<u>1"</u>	<u>1"</u>	<u>1-1/2"</u>
Sherwood and Holloway (131)	Liq.	Liq.	Liq.			Liq.	Liq.
Rennolds (61,130)				Liq. Vap.			
Shulman and DeGouff (135)					Liq.		
Mehta & Parekh (61, 130)		Vap.					
Surosky & Dodge (146) ←					Vap.		
Hensel & Treybal (58)							Vap.
Lynch & Wilke (86) ←		Vap.					
Yoshida (167)		Vap.					
Sherwood and Holloway (130) ←			Vap.				
McAdams, et al (89)					Vap.		

TABLE 8.9 (Continued)

Source	Ceramic Raschig Rings			Carbon Rings		Berl Saddles	
	<u>1/2"</u>	<u>1"</u>	<u>1-1/2"</u>	<u>1/2"</u>	<u>1"</u>	<u>1"</u>	<u>1-1/2"</u>
Doherty and Johnson (61, 130)					NH ₃ - Acid		
Borden and Squires (61, 130)					NH ₃		
Fellinger (38, 133g)	NH ₃	NH ₃	NH ₃			NH ₃ - Acid NH ₃	NH ₃
Dwyer & Dodge (35)				NH ₃	NH ₃		
Houston and Walker (62)					Acetone MeOH EtOH NH ₃		
Hutchings, et al (65)	Acetone	Acetone					
Zabban and Dodge (169)	Acetone MeOH					Acetone	
Whitney and Vivian (160, 162)		SO ₂					
Othmer and Scheibel (91)		Acetone					
Molstad, McKinney, and Abbey (93)		NH ₃				NH ₃	
Molstad and Parsley (94)		EtOH				EtOH	

the difference in surface characteristics (136), then the internal agreement of the literature data becomes almost tolerable.

In order to determine whether the "dead surface" special case of

the two lifetime concept is as effective as is the more general case in interpreting tower performance, it is desirable to estimate values of λ (the square of the ratio of surface lifetimes in the two lifetime concept) by one of the two means suggested in Section 8.1.4: Either by analysis of a chemical reaction system in which the second lifetime must eventually become important, or through an examination of the variation of K_L/K_{LF} for a given packing and given flow conditions as a function of R , the solubility-resistance ratio.

In order to estimate the λ from a chemical reaction system it is necessary only to insert the φ factor for chemical reaction (107) into Equation 8.1.36; thus

$$\frac{K_L}{K_{LF}} = \frac{(1 + R)}{\varphi} \frac{f}{1 + \frac{R}{\varphi} \left[f + \frac{1}{\lambda} (1 - f) \right]} + \frac{1-f}{1 + \frac{R}{\varphi} (\lambda f + 1 - f)} \quad (8.2.1)$$

or for moderately high values of λ

$$\frac{K_L}{K_{LF}} = \frac{(1 + R)}{\varphi} \frac{f}{1 + (R/\varphi)f} + \frac{1-f}{1 + \frac{R}{\varphi} \lambda f} \quad (8.2.1a)$$

R , it should be noticed, is still defined from the corresponding physical absorption system. In order to proceed further it is necessary to have a knowledge of φ for the system in question, either from theory or from a small scale penetration experiment. In general, except for the case of a first order (backward and forward) reaction, the value of φ will be dependent upon both the solute interfacial concentration and the bulk liquid

concentration of the chemical reactant. Thus φ will in all probability vary markedly from top to bottom of a packed tower for a reaction system other than first order, giving a variation in K_L/K_{LF} (and in K_{LF} itself) from point to point. This necessitates an integration of K_L over the tower and results in most instances in a quite cumbersome expression (see, for example, Chapter 10) which would be difficult to compare to any degree of reliability with present experimental data.

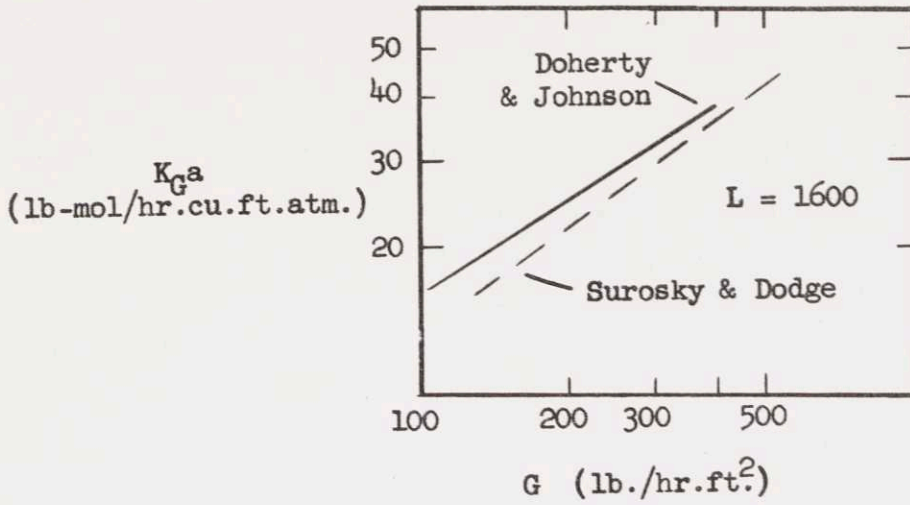
Present published data for chemical reaction systems in large packed towers are limited to the ammonia-sulfuric acid, chlorine-water, and sulfur dioxide-water systems, and various carbon dioxide-alkaline systems. In all of these cases the φ factor is dependent upon concentrations, thus introducing the problems of unintegrating the integrated data taken in the towers. In one case, the Doherty and Johnson data for ammonia and sulfuric acid (130), the data appear to cover the extremes of no influence of reaction and gas phase completely controlling; however there also appears to be insufficient knowledge of the reaction system itself to warrant an attempt to obtain an indicated value of λ from the data.

It should be stressed that the one instance, theoretically, in which the φ factor should not vary with concentrations and consequently with tower height is for a first order (backward and forward) reaction. A pseudo-first order irreversible reaction could probably also be included, since the bulk reactant concentration would probably not

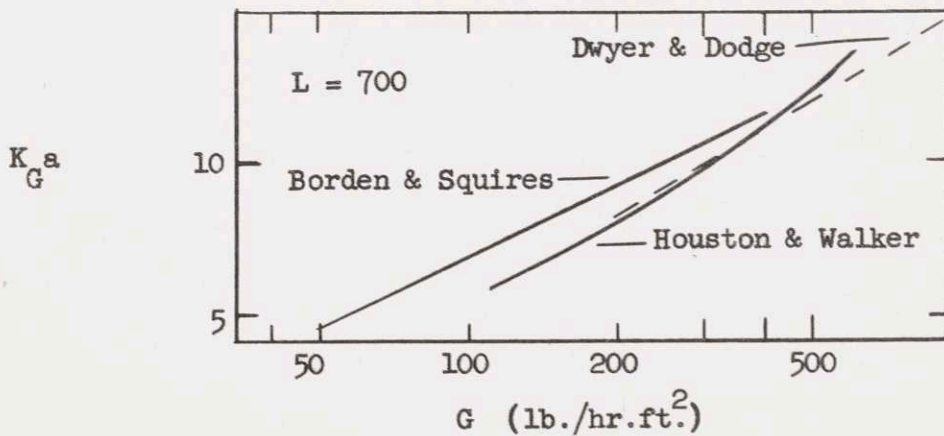
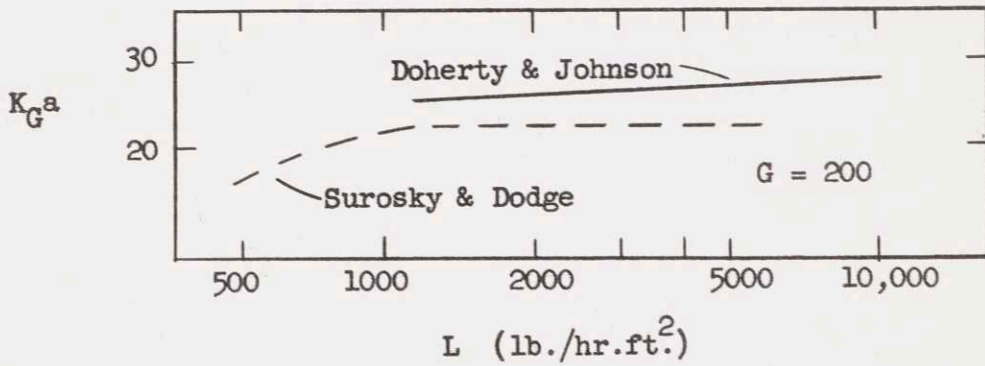
change throughout the tower. In this case φ is, however, a function of θ , the contact lifetime(s), and thus an explicit, absolute knowledge of, say, θ_1 would be necessary for an estimation of λ (i.e., the interfacial area would have to be separated).

Returning to the problem of evaluating the relative merits of the dead surface approach and the more general two lifetime approach, the remaining course is to examine the K_L/K_{LF} values as a function of R at given flow conditions on a given packing. For two packings, 1 inch ceramic rings and 1 inch carbon rings, there are data available for several solutes. Unfortunately, however, for the ceramic rings no two solutes have been studied in the same column by the same investigators. For carbon rings, though, Houston and Walker (62) have studied four solutes, and there is also vaporization data available. The Houston and Walker data should also be highly reliable, since they used dilute solute concentrations, maintained temperatures closely, and presumably eliminated end effects.

Figure 8.15 shows a comparison of data taken on 1 inch carbon rings by different investigators. The ammonia-water data of Houston and Walker are compared with the ammonia-water data of Borden and Squires (130) and Dwyer and Dodge (35). The Dwyer and Dodge data agree well with the Houston and Walker data, but the data of Borden and Squires are some 15 - 20% higher. Similarly, the data of Doherty and Johnson (130) for ammonia absorption in 3.5 N H_2SO_4 (a system in which they



a. Vaporization and Chemical Reaction



b. Ammonia - Water

FIGURE 8.15 COMPARISON OF ONE INCH CARBON RING DATA

show the liquid phase resistance has been eliminated completely) are 15-20% higher than the water vaporization data of Surosky and Dodge (146), when corrected by $D_v^{2/3}$ *. Since Borden and Squires and Doherty and Johnson used the same column and packing, it may then be concluded that the results of Surosky and Dodge are comparable in so far as packing behavior to the results of Houston and Walker.

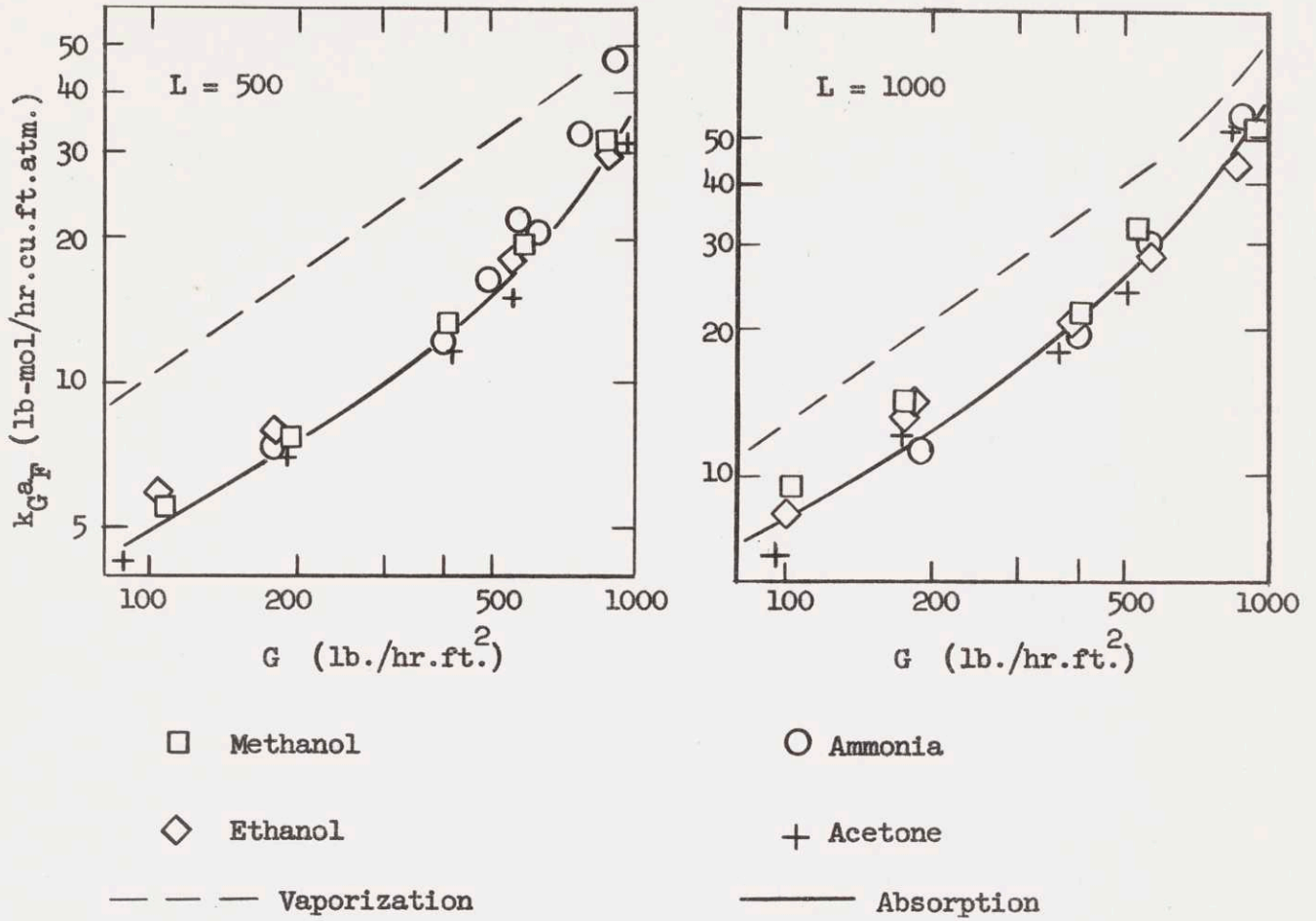
It is interesting to notice that the Surosky and Dodge and Doherty and Johnson data are two instances in which the liquid flow has little effect on the k_{Ga} . This is confirmed by McAdams, et al (89), the only others to study pure gas phase resistance on 1 inch carbon rings, who found k_{Ga} to vary as $L^{0.07}$. This is also in agreement with the small effect of L found on total hold-up for carbon rings (136).

The Surosky and Dodge data do not extend to as high flow rates as the Houston and Walker data; however it is possible to predict behavior at flow rates above loading by analogy to other vaporization data for other packings, notably those of Lynch and Wilke (86) for 1 inch ceramic rings. Loading occurs at about the same flow rates on both packings and k_{Ga} varies with the same power of G in both instances (~~the ceramic~~

*It is probable that the interfacial area is not significantly different for water and 3.5 N. H_2SO_4 . The viscosity of 3.5 N H_2SO_4 is about 1.4 times that of water, (66), and the density is also some 10% greater (109). Shulman, et al (138), indicate that the total hold-up will then be changed by less than 5% between the two cases.

(the ceramic ring data being lower). That the size of this correction is small may be seen from Figure 8.16. The original Surosky and Dodge data extend up to $G = 600$, and the Lynch and Wilke data are shown in Figure 8.18.

The Houston and Walker data, corrected by $D_V^{2/3}$ to the water-air basis using the values in Table 8.6, are plotted in Figure 8.16 as $k_{G a_F}$ vs. G , with L as a parameter. $k_{G a_F}$, a new term, is defined as the $k_G a$ value calculated from the observed $K_G a$ in a gas phase influenced system by two film additivity using an observed $k_L a^*$ value for the particular packing and flow conditions. In recalculating the data the solubilities cited by Houston and Walker were used for all four solutes, the values agreeing well with other literature data and ones employed previously in this chapter. Thus for MeOH, $H = 0.082$; for EtOH, $H = 0.0935$; for ammonia, $H = 0.314$; and for acetone $H = 0.730$, all in atm.cu.ft./lb.mole at 80°F . If the dead surface simplification of lifetime distribution theory is sufficient then $k_{G a_F}$ for all solutes should be the same at the same flow conditions, and equal to $f k_{G a^*}$, where $k_{G a^*}$ is the observed vaporization (pure gas phase) coefficient at those particular flow conditions. If, on the other hand, the two lifetimes approach with a finite λ is more appropriate, then, by Table 8.5, there should be an ordering of points for different solutes, the solutes with lower values of R (more soluble) tending to give higher values of $k_{G a_F}$ since $K_L a / K_L a_F$ would be higher. As shown also in Table 8.5 this effect should be more noticeable at lower values



Basis: Diffusivity of Water - Air System

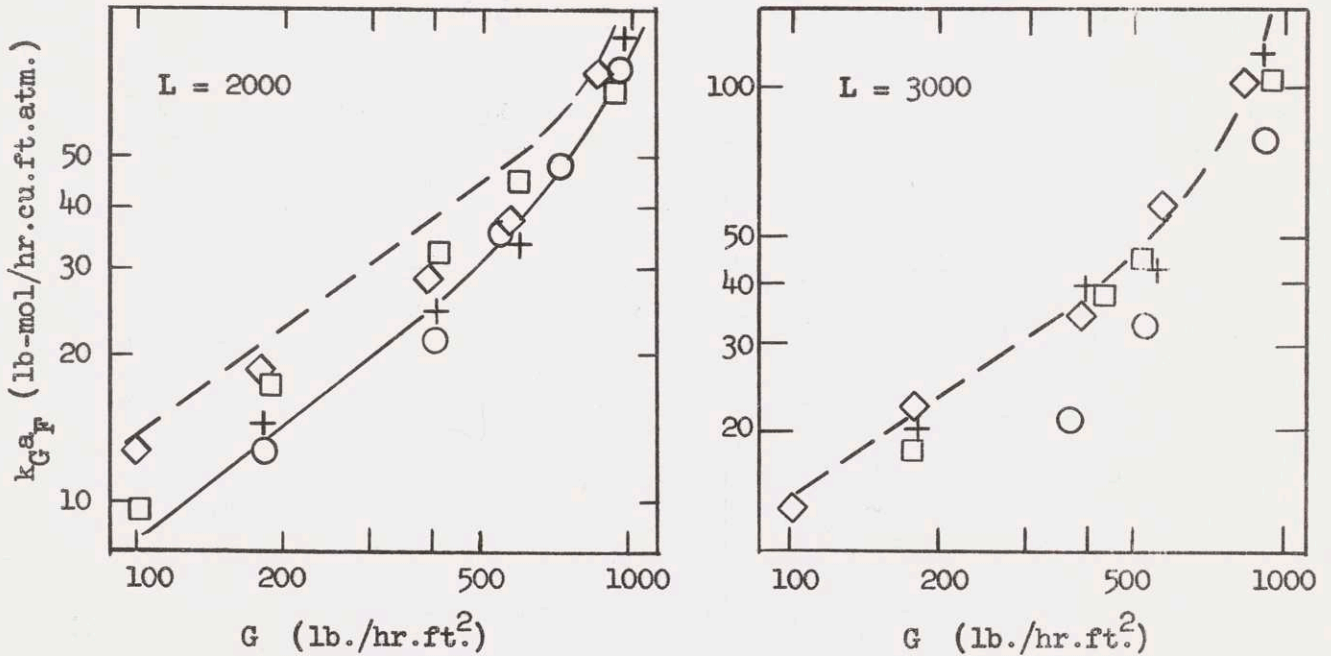


FIGURE 8.16 DATA OF HOUSTON & WALKER

of R , that is at high liquid flow rates and low gas flow rates. In the Houston and Walker data there is, at given flow conditions, an eight-fold range of R values. Between extreme flow conditions R values are encountered from 0.02 to 1.5.

From Figure 8.16 it is apparent that at low liquid rates and high gas rates there is close agreement between the k_{G^aF} values for different solutes when plotted this way, and yet the comparable $k_G a$ values for vaporization (substantiated by the NH_3 -acid data shown in Figure 8.15) are at low liquid flow rates a factor of two higher for 1 inch carbon rings. Only at the higher liquid flow rates and lower gas flow rates is there any uniform and distinct ordering of the k_{G^aF} values according to solubility. This effect becomes more apparent if one realizes, as Houston and Walker did, that the overall $K_G a$'s for acetone rise by a greater factor between $L = 2000$ and $L = 3000$ than between $L = 1000$ and $L = 2000$. This seems to indicate a sudden increase in the slope of $k_L a^*$ vs. L at these flow conditions, similar to the behavior noted at higher flow rates for ceramic rings by Sherwood and Holloway (131). This was not apparent in the data of Shulman and DeGouff (135) for carbon rings, and it was their data (in agreement with Holloway's for ceramic rings at their flow rates) that was used here for $k_L a^*$ corrections. It should, however, be kept in mind that the k_{G^aF} results shown for acetone (where liquid phase resistance is half or more of the total) at $L = 3000$ still may possibly be high for this reason.

At $L = 2000$ and $G = 185$, where the ordering is distinct, a calculation shows that the use of $\lambda = 50$ would bring the points back into close agreement. This $\lambda = 50$ corresponds for a θ_1 of 0.04 sec. (a reasonable, low value) to a θ_2 of 2500 times as long, or 100 seconds. To this we may compare a statement of Shulman, et al (136), who observed the displacement of a dye solution by water in flow over 1-1/2 inch ceramic rings in a glass column.

"It was found that a considerable portion of the water was not displaced immediately; i.e., there was no sharp line of demarcation between water and dye solution as dye was added or when dye was cut off. Instead there were pockets of what might be described as semi-stagnant liquid and splashing, and the random motion of liquid over the packing surface deposited or removed dye from these areas by means of a slow and random dilution process. Thus when dye was injected for 20 sec. some of the pockets picked up dye, which was not completely washed out by the following clear water until as much as 5 min. had passed."

Apparently, then, the λ value to be used in the two lifetime analysis is sufficiently great so that the dead surface simplification is indeed reliable for design purposes at R above 0.1 (corresponding to the ammonia case at $L/G = 10$). Thus the dead surface approximation should be reliable for usual design, since a common rule of thumb is to make HG_m/L_m (flow rates on a mole basis) approximately equal to one, corresponding to the case of parallel equilibrium and operating

lines. To the extent that a more soluble gas at a high L/G is used, then the use of the value of $k_G a_T$ predicted from ammonia absorption and two film additivity will tend to be in error and conservative. This would also apply to a chemical reaction analysis if the finite lifetime of the "dead" portion of the surface is considered infinite.

The values of f , the fraction active surface, for 1 inch carbon rings taken from Figure 8.16 are presented in Figure 8.17. (The f at $L = 3000$ may in actuality be less than one). It should be noted that f is relatively insensitive to G at gas flow rates below loading. The total interfacial area, a , is also probably relatively independent of G in this range, as is indicated by the hold-up curves of Shulman, et al (136), and by the "effective" interfacial areas found by Shulman, et al (137), who separated a_e from $k_G a_T$ values calculated from Fellingner's ammonia data (38) by means of a correlation obtained for k_G through naphthalene packing sublimation studies. Shulman's a_e would be defined in the present terminology as fa . It is necessary that f and a be insensitive to gas flow rate below loading, or at least that they bear such a relation to one another that $a_e (= fa)$ will be insensitive to gas flow rate, so that the observed lack of dependence of $k_L a^*$ on gas flow rate below loading (131) may be fulfilled. $k_L a^*$, in light of the dead surface concept, is equal to the product of the k_L for the active surface and the effective area, $a_e = fa$. Since k_L is logically independent of G below loading, any effect of gas flow rate would have to

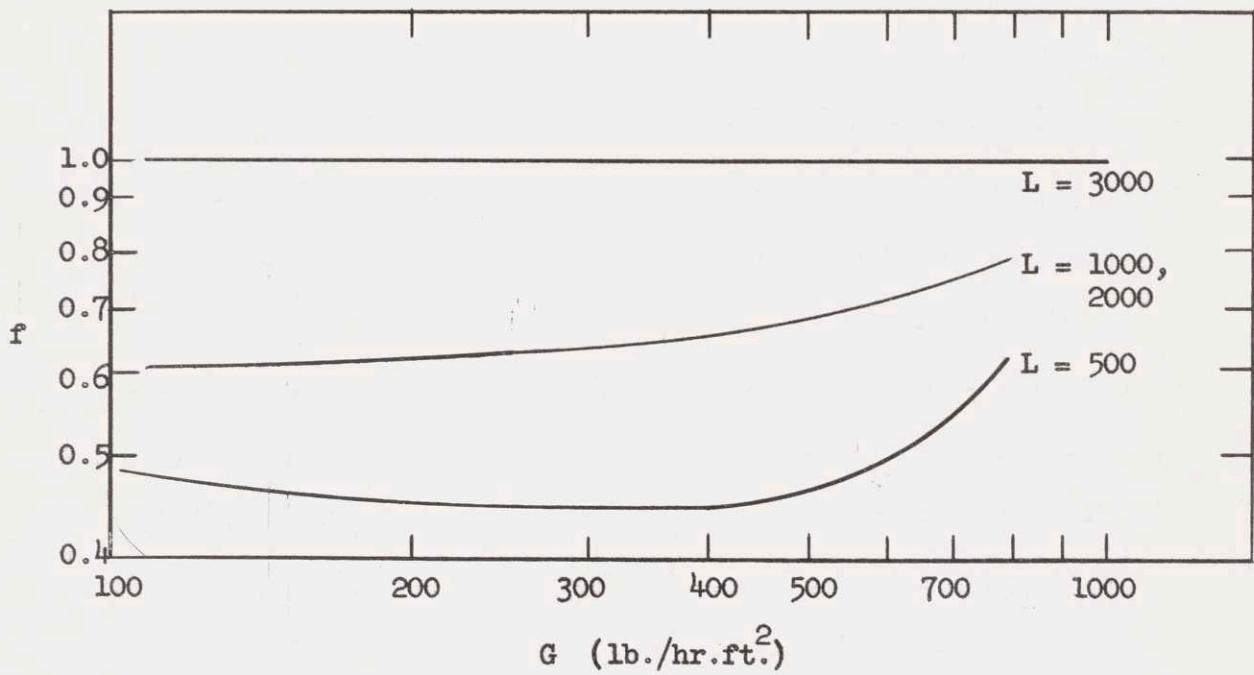
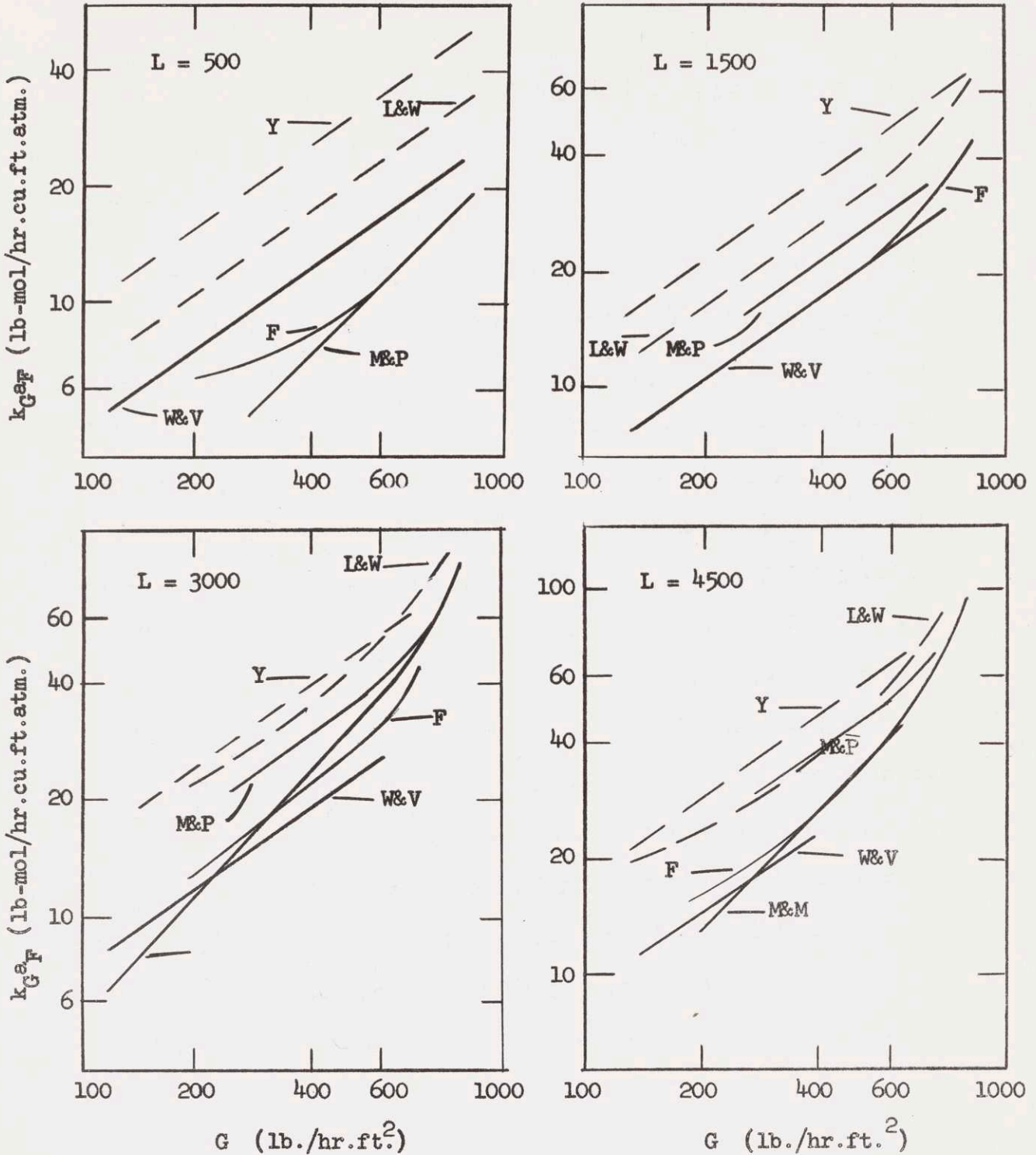


FIGURE 8.17 VALUES OF f DERIVED FROM DATA OF HOUSTON & WALKER

show up in the fa term. This insensitivity of the fa product presents an independent check on the agreement of the Houston and Walker data with the dead surface concept.

The results of this analysis of the Houston and Walker data serve to clear up a question that has heretofore existed. From Figure 8.16 (and from the results of Goodgame and Sherwood (46) covered in Section 8.2.1) it is apparent that the ammonia system is not unusual. It has been suggested (see for instance page 286 of Reference 133, page 687 of Reference 109, and the discussion following Reference 162) that ammonia $k_G a$'s may be lower than those predicted from two film additivity using vaporization data because of a slow hydrolysis in water similar to the behavior found for chlorine and sulfur dioxide (156, 162). The coefficients for ammonia in the analysis of Goodgame's and Houston's data are based on the "total" solubility of ammonia and the consequent "total" driving force. Because of the close agreement of these coefficients with data for other, physically absorbed solutes one must conclude that the ammonia hydrolysis may be considered infinitely fast and that the often large discrepancy between ammonia absorption and vaporization lies instead in the sizeable dead portion of liquid surface.

The various literature data for 1 inch ceramic Raschig rings are summarized in Figure 8.18, corrected by $D_v^{2/3}$ to the water-air basis. The data of Othmer and Scheibel (104) and Hutchings, et al (65), are omitted because they cover only small flow rate ranges and agree sub-



Key: Y Yoshida (Water vap.)
 L&W Lynch & Wilke (Water vap.)
 W&V Whitney & Vivian (SO_2 abs.)

M&P Molstad & Parsley (EtOH abs.)
 M&M Molstad, McKinney & Abbey
 (NH_3 abs.)
 F Fellinger (NH_3 abs.)

FIGURE 8.18 VAPORIZATION & ABSORPTION DATA FOR ONE INCH CERAMIC RINGS

stantially with the situation as presented. The lack of internal agreement emanating from the fact that no investigator studied more than one solute in his tower make any quantitative comparison with the dead surface theory difficult; however the qualitative agreement is very much there: Both sets of vaporization data give $k_G a$ values lying above the absorption $k_G a_F$ values for the various solutes.

The other packing for which data on several solutes are available is 1 inch Berl saddles. In this case the data for the various solutes show essentially the same agreement as do the 1 inch ceramic Raschig ring data; however there is no pure gas phase resistance data available. The ammonia-sulfuric acid data of Fellingner (38) show no region of sulfuric acid concentration over which the overall $K_G a$ values tend to level off at a constant value as the Doherty and Johnson data do. Therefore it is not possible to compare vaporization data with absorption data for 1 inch Berl saddles.

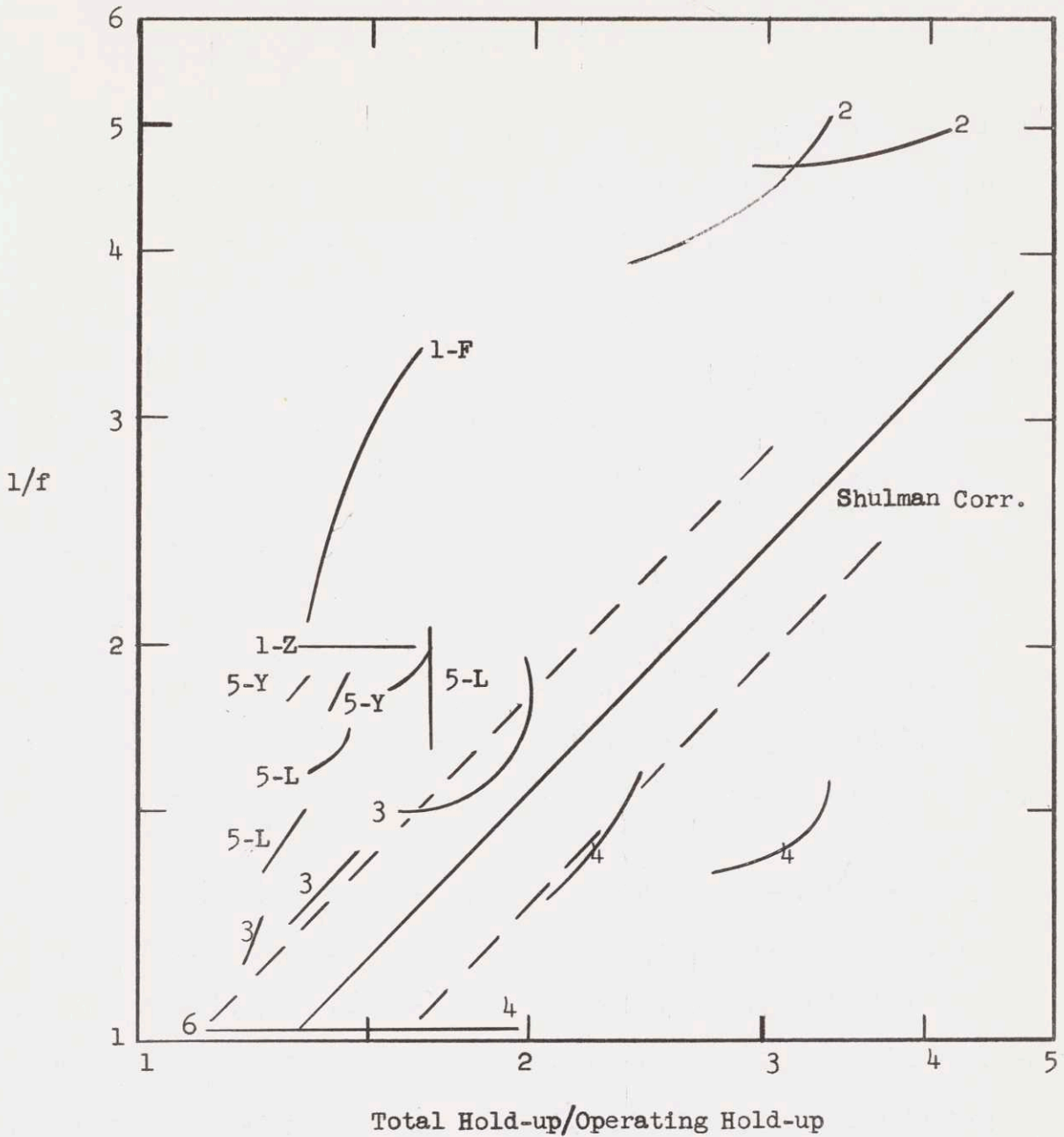
It is possible, however, to make such a comparison based on more limited data for other packings. For 1-1/2 inch ceramic rings the $k_G a$ data of Sherwood and Holloway (130) for vaporization are from 1.15 to 2 times the $k_G a_F$ values from Fellingner's data. For 1-1/2 inch Berl saddles there is close agreement between the vaporization results of Hensel and Treybal (58) and $k_G a_F$'s from Fellingner's data. For 1/2 inch carbon rings the $k_G a$ values for vaporization observed by Rennolds (61, 130) are from 4 to 5 times the $k_G a_F$ values from the ammonia absorption data of Dwyer and Dodge (35). Finally the vaporization

$k_G a$ values of Mehta and Parekh (61, 130) for 5/8 inch ceramic rings are from 2 to 3.5 times $k_{G a_F}$ values calculated from the data of Fellingner and from the data of Zabban and Dodge (169) for acetone and methanol taken on 1/2 inch ceramic rings. There is, however, very close agreement between $k_{G a_F}$ values calculated from Zabban and Dodge's acetone and methanol data. All the above comparisons are made at identical air and water flow rates and are based on corrections to the water-air D_v by $D_v^{2/3}$.

Thus the trend for pure gas resistance vaporization data to give values of $k_G a$ above the $k_{G a_F}$ values calculated from absorption data is uniform (with the exception of the Hensel and Treybal data), and lends additional qualitative confirmation to the dead surface concept.

Shulman (136) has proposed, as has been previously mentioned, that the ratio of $k_G a$ for vaporization to $k_G a$ for absorption may be correlated as 0.85 times the ratio of the total hold-up to the operating hold-up (the operating hold-up being defined as that portion which drains readily from the packing). (In the present terminology $k_G a$ for vaporization divided by $k_G a$ for absorption is $1/f$). He based this on a comparison of the Surosky and Dodge, Doherty and Johnson, and Sherwood and Holloway vaporization and chemical reaction data with the Fellingner ammonia data. Thus his comparison was not based on data taken on the same packing.

Figure 8.19 shows a plot of $1/f$ vs. the ratio of total to operating



Curve	Packing	Vaporization	Absorption
1-F	1/2 in. ceramic	Mehta-Parekh	Fellinger
1-Z	1/2 in. ceramic	Mehta-Parekh	Zabban-Dodge
2	1/2 in. carbon	Rennolds	Dwyer-Dodge
3	1 1/2 in. ceramic	Holloway	Fellinger
4	1 in. carbon	Surosky-Dodge	Houston-Walker
5-L	1 in. ceramic	Lynch-Wilke	Fellinger
5-Y	1 in. ceramic	Yoshida	Fellinger
6	1 1/2 in. Berl S.	Hensel-Treybal	Fellinger

FIGURE 8.19 SHULMAN CORRELATION OF f VS. HOLD-UP

hold-up for each of the six packings for which both vaporization and absorption data are available. The hold-up data employed are those of Shulman (136). Also shown is the line which Shulman found would correlate the data he examined to $\pm 15\%$. It should be stated that this is a critical way of presenting such data, since an error in either the absorption or the vaporization data for a given packing type will show up as the same sized error in the resultant curve for that packing. Also it should be noted that the curves for 1/2 inch rings, both of which appear to be relatively high are based on the data of Mehta and Parekh and of Rennolds, in both of which cases there is no mention of corrections having been made for end transfer effects at their low packed heights. Thus these two sets of vaporization data may well be high. Still the Shulman correlation does not appear to be a particularly reliable one on the basis of the available literature data.

If there is no significant correlation of f with respect to the hold-up ratio, there is also no confirmable quantitative correlation of f with respect to gas and liquid flow rates, as shown in Figure 8.17 for 1 inch carbon rings, although f does seem insensitive to gas rate below loading, and qualitatively increases with liquid flow rate.

The conclusions of this section may now be summarized to give recommendations for design.

Reanalysis of the data of Houston and Walker (62) indicates that the concept of an active portion of liquid surface (f_a) obeying two film additivity and an inactive, dead portion that contributes little to absorption is valid at R greater than 0.1. For more soluble gases or for operating conditions such that $R < 0.1$ this concept will tend to give conservative results when $k_G a_F$ data based on ammonia absorption are used, since in reality a finite activity, or lifetime, must be assigned to the dead portion of surface. For chemical reaction systems the finite lifetime of the inactive surface must also be considered for a true analysis, but calculations based on the dead surface concept will always be conservative (often highly so for strongly reactant solutions).

The extensive data of Fellingner (38, 109e, 133g) for ammonia absorption are representative of other absorption data for $R > 0.1$ (see Figure 8.18), and, because they were all taken in the same column by the same investigator and therefore should be uniformly reliable, should be taken for values of $k_G a_F$. These values, which have heretofore been indicated as conservative for design (109e, 133g), are probably more correct for design than conservative.

For carbon rings $k_G a_F$ values are often different from values obtained for ceramic rings. Therefore for carbon rings the data of Houston and Walker (62 and Figure 8.16) and of Dwyer and Dodge (35) should be used for $k_G a_F$ values.

In the case of vaporization, the data listed for the various packings in Table 8.9 should be used, with the realization that the

data of Mehta and Parekh and of Rennolds may be high because of no corrections for end effects. The data should also be used for chemical reaction systems in which the reactant concentration is strong enough to eliminate all liquid phase resistance (not as indicated by simple two film additivity). In such cases corrections for interfacial area changes due to changes in physical properties of the chemical solution are probably best made at present on the basis of the hold-up data for nonaqueous solutions of Shulman, et al (138).

The most reliable data indicate that k_G should be taken as proportional to $D_v^{2/3}$ (135, 137, 147) with some tendency toward a lower exponent at high gas flow rates. Vaporization data indicating an exponent of 0.15 or 0.17 (130, 146) should be discounted on the basis of probable changes in the interfacial area from liquid to liquid (138).

CHAPTER 9

DIMENSIONLESS CORRELATION

The technique of dimensional analysis is frequently used in engineering when it is desired to produce a general correlation of the variables influencing a system from data taken with only a few of the variables actually being varied independently. As an example, in the analysis of mass transfer processes data are frequently correlated in the form

$$\frac{k_L d}{D_L} = \alpha \left(\frac{dL}{\mu} \right)^m \left(\frac{\mu}{\rho D_L} \right)^n \quad (9.1)$$

or

$$N_u = \alpha (Re)^m (Sc)^n \quad (9.2)$$

where d is a characteristic length of the system and the Nusselt, Reynolds, and Schmidt numbers are defined as shown in the two above equations (see Chapter 20 for nomenclature). The three dimensionless groups represent the total number of independent dimensionless groups that may be made from the six variables taken into consideration. From experiments made measuring k_L as a function of L and D_L independently the two exponents m and n and the multiplicative constant α are determined. The resultant correlation should then give the effects of the variables μ , ρ , and d even though they were not studied directly in the experiment.

There are two facets of this sort of analysis that should be kept

in mind. First, it has been assumed that each variable may be considered to enter the correlation raised to a certain power. There may well in reality be sums of the dimensionless groups entering into the true correlation, and thus a correlation of products of groups raised to constant powers may not be adequate to describe the general behavior over a wide range. This drawback is not serious. If, for instance, the six variables composing Equation 9.1 are in truth the only ones to affect a given mass transfer process, then it still must be possible to obtain a unique correlation of Nusselt number vs. Reynolds number, with Schmidt number as a parameter. This may either be done graphically, or by making the exponents m and n themselves empirical functions of the Reynolds and Schmidt numbers.

The second drawback is more serious. If there is some variable that has not been taken into account in the analysis (whether this variable was actually varied or not), then the behavior predicted by the analysis for the other variables that were not directly varied may be incorrect. Thus, if there is another length variable (d') other than " d " in Equation 9.1, it is possible to form another dimensionless group, d'/d . If d' was not varied ever during the experimentation, then only the prediction of Equation 9.1 with respect to d will be erroneous, and the predicted behavior of μ and ρ will still be correct, even though they were not independently varied. If, however, d' was actually varied inadvertently, then the validity of the μ

and ρ predictions is not necessarily valid. Also if the neglected variable were one such as g (acceleration due to gravity) or γ (a surface tension), it would require several of the other variables to make the other dimensionless group ($\frac{\rho^2 d^3 g}{\mu^2}$ for instance) and the effect on the dimensionless correlation would be consequently more serious. In the case of $\frac{\rho^2 d^3 g}{\mu^2}$ being the missing dimensionless group the predictions with respect to d , ρ and μ would be in error even though g never varied.

These pitfalls of dimensionless analysis can, fortunately, often be foreseen or avoided through an examination of the basic differential equations of a process or through other theoretical knowledge.

Perhaps the best known equation for the prediction of $k_L a$ in a packed tower is that of Sherwood and Holloway (131):

$$\frac{k_L a}{D_L} = \alpha \left(\frac{L}{\mu} \right)^{1-n} \left(\frac{\mu}{\rho D_L} \right)^{1-s}, \quad (2.2.1)$$

where s is 0.5 and n and α are functions of packing size and shape. This is a dimensional equation of the form of Equation (9.1), which however purports to give the effects of μ and ρ under the assumptions that only length variables affect the process in addition to those included in the equation and that these length variables are maintained constant as L , D_L , μ , and ρ vary for a given type of packing.

Several subsequent investigators have proposed totally dimensionless equations to correlate the liquid phase transfer behavior for all packings. Among these are the following:

1) Van Krevelen and Hofstijzer (153):

$$k_L \frac{(\mu^2 / \rho^2 g)^{1/3}}{D_L} = 0.015 \left(\frac{L}{a_e \mu} \right)^{2/3} \left(\frac{\mu}{\rho D_L} \right)^{1/3}$$

where $a_e/a_t = 1 - e^{-0.40(L/\rho)}$ (dimensional) (9.4)

2) Shulman, et al (137):

$$\frac{k_L D_p}{D_L} = 25.1 \left(\frac{D_p L}{\mu} \right)^{0.45} \left(\frac{\mu}{\rho D_L} \right)^{0.5} \quad (9.5)$$

and a_e determined from the data of Fellingner (38) (corrected by two film additivity) and a correlation

$$j_D = \left(\frac{k_G M_{p,BM}}{G} \right) \left(\frac{\mu}{\rho D_v} \right)^{2/3} = 1.195 \left(\frac{D_p G}{\mu(1-\epsilon)} \right)^{-0.36} \quad (9.6)$$

for k_G .

3) Onda, et al (102):

$$k_L (\rho / \mu g)^{1/3} = 0.013 (L/a_t \mu)^{1/2} (\mu / \rho D_L)^{-1/2} \quad (9.7)$$

$$\text{and } a_e/a_t = 1 - 1.02 e^{-0.278 (L/a_t \mu)^{0.4}}.$$

In these correlations a_e = effective interfacial area for liquid phase transfer (area/volume).

a_t = total surface area of packing (area/volume)

M = molecular weight of gas stream

P_{BM} = logarithmic mean pressure of nonabsorbing gases (atm.)

D_p = diameter of sphere of same area as packing particle (length)

ϵ = packed bed voidage

Objections may be raised to all these correlations. It is probable that the acceleration due to gravity does need to be considered when one approaches the dimensionless problem. It was not considered by Sherwood and Holloway or by Shulman. It is probable that the effective area itself does need to be brought into an equation for k_L as a length, as will be shown later on in this chapter. Only the van Krevelen - Hoftijzer equation does this. Finally, any effective area correlations are suspect, since they have usually, with the exception of Shulman's case, been based on rather dubious data and concepts.

a. Short Wetted Wall Column

Before proceeding further with the packed tower analysis it will be

helpful to examine the liquid phase absorption situation in a short wetted wall column from the standpoint of dimensional analysis and underlying theory. (In this thesis such a column has been shown to be an effective model of the packed column transferwise because of the apparent applicability of penetration theory to both).

A solution to the unsteady state diffusion equation coupled with the hydrodynamic equation for free gravity fall yields (155) (107b)

$$\frac{k_L h^*}{D_L} = 0.725 \left(\frac{\mu}{\rho D_L} \right)^{1/2} \left(\frac{\rho^2 g h^3}{\mu^2} \right)^{1/6} \left(\frac{4 \Gamma}{\mu} \right)^{1/3} \quad (9.8)$$

Here h is the distance the "free" liquid film falls in contact with the solute laden gas phase, and Γ is the liquid flow rate per unit wetted perimeter ($4 \Gamma / \mu$ is the Reynolds number, or ratio of inertial to viscous forces, in this instance).

For application to short wetted wall columns the use of this equation would necessitate that the falling film accelerate immediately to its free fall velocity upon entering the column, that there be no effects at the take off slot that make the falling film behave hydrodynamically different from a free falling film, and that the solute not diffuse far enough into the falling film to encounter a significant velocity gradient. This last condition has been shown theoretically (69) to be valid for fall distances less than a foot.

In studies that have been made in short wetted wall columns (43, 155) it has been found that Equation (9.8) is not obeyed: k_L values are usually lower than predicted by it. This is currently thought to be caused by two effects, a finite acceleration time of liquid at the top of the column and the propagation of a stagnant liquid surface back up from the exit slot. The explanation made of the latter phenomenon up until now has been one accredited to Denbigh (18,124), which pictures a stagnating film of surfactant molecules (which are always present in water) rising upward from a region of relatively stagnant liquid at the exit slot. This surfactant film tends to rise because it has a lesser surface tension than pure water. Its height reaches an equilibrium value because of a drag force exerted on it by the downflowing liquid. This analysis was originally postulated for falling jets, but can hold equally well for a wetted wall column. The important fact to be gained from this is that the height of stagnated surface would then be a function of the difference in surface tensions of the film and pure water and of the drag force (Reynolds number) of the water.

Analysis of the acceleration effect at the top of the column is less clear, since the differential equation for an accelerating falling liquid film is nonlinear and difficult to solve. Scriven and Pigford (123) give an analysis of the problem, assuming that the surface portion of entering liquid accelerates under the influence of gravity

alone (no retardation effect of drag against the inner wall). They find the effect on the k_L^* in so far as deviation from the value predicted by Equation (9.8) to be a function of the $4 \Gamma / \mu$ Reynolds number alone. This is so even though gravity provides the impetus for acceleration, for the gravity force drops out in the final deviational equation.

The effect of acceleration is such as to give a greater deviation from the theoretical equation as Reynolds Number increases (123), whereas a stagnating exit effect gives a lesser stagnant film height and consequently a lesser deviation at higher Reynolds numbers. The results of Gilliland, Baddour, and Brian (43) show this qualitatively: At low Reynolds numbers (below 200) k_L^* for physical absorption varies with Γ to a power greater than $1/3$ (stagnation end effect), and at high Reynolds numbers (above 200) k_L^* varies with Γ to a power less than $1/3$ (acceleration). Although these investigators operated without the stagnant wave evidencing a stagnation effect, such a process -- or some effect other than acceleration -- must have been present to an extent at low Reynolds numbers. The data of Vivian and Peaceman (155) show enough scatter to occlude any such conclusions.

For the purpose of obtaining a valid dimensionless equation for the actual operation of a short wetted wall column one may write

$$\frac{k_L h^*}{D_L} = 0.725 \left(\frac{4 \Gamma}{\mu} \right)^{1/3} \left(\frac{\mu}{\rho D_L} \right)^{1/2} \left(\frac{\rho^2 g h^3}{\mu^2} \right)^{1/6} (\Delta) \quad (9.9)$$

The deviating factor, (Δ), will for a stagnation end effect be a function of Reynolds number and a group involving the difference in surface tensions between the stagnated surface and the pure liquid. For an acceleration effect it will be a function of Reynolds number alone. Thus for the acceleration case no new groups enter, and a valid dimensionless equation is

$$\frac{k_L h^*}{D_L} = \alpha \left(\frac{4 \Gamma}{\mu} \right)^n \left(\frac{\mu}{\rho D_L} \right)^{1/2} \left(\frac{\rho^2 g h^3}{\mu^2} \right)^{1/6} \quad (9.10)$$

if the acceleration effect is the only reason for deviation from free falling film theory. α and n could then be obtained from a study of k_L^* as a function of Γ .

One could as well say that the column evidenced a certain "equivalent free fall height," h' , and that this h' was defined by

$$\sqrt{\frac{h'}{h}} = \frac{1}{\Delta} = \frac{0.725}{\alpha} \left(\frac{4 \Gamma}{\mu} \right)^{1/3-n} \quad (9.11)$$

for the case of acceleration alone being responsible for the difference between h' and h . Again, if other factors contributed to the deviation,

then other dimensionless groups would need to be brought into the expression for h'/h .

This equivalent free fall height concept is even more general in application, for it may be applied to flow over surfaces other than vertical planes. As an example, in analyzing penetration into free laminar flow over a sphere, Davidson and Cullen (23) produce an equation (neglecting acceleration) analogous to Equation (9.12) in which h' would be 2.38 times the sphere radius in order to give the same absorption rate.* Thus even in this more complicated flow arrangement h' is simply a function of the sphere radius and the geometric shape, and not of the gravity group or Reynolds number. One may also consider the case of flow down a flat inclined plane (no acceleration), where h' for use in Equation (9.12) would be simply $l \sin^{1/3} \theta$, if l were the length of the plane and θ its inclination to the horizontal. (This would be so since g in Equation (9.8) would become $g \sin \theta$). Again h' is a function of plane length and geometry alone, and not of Reynolds number or gravity group.

* Davidson and Cullen give the length of a cylinder to give an equal total absorption rate as $1.68 R$; however, the valid comparison for present purposes is in terms of absorption rate per unit area; hence $z_{\text{equiv.}} = \left(\frac{4 \pi R^2}{1.68 \times 2 \pi R^2} \right)^{1/2} (1.68 R) = 2.38 R$, since the total rate varies as $z^{1/2}$ and the area varies as z .

b. Packed Tower

It is apparent by analogy to the absorption process in a short wetted wall column that the correct Reynolds number to consider for the liquid phase in a packed column is one based on Γ , the liquid flow rate per unit wetted perimeter, and not necessarily one based upon the diameter of a packing particle directly. To the extent that the wetted perimeter at a given horizontal cross section does not vary inversely with particle diameter, then a Reynolds number based on particle diameter will not be indicative of the ratio of inertial forces to viscous forces in the falling liquid layer. Another way of saying this is that it is necessary to take another length unit, the wetted perimeter, into account in a dimensionless analysis in addition to the particle diameter, provided the one is independent of the other.

This concept is not new. It has been realized by van Krevelen and Hofstijzer (153), Yoshida and Koyanagi (168), and others. The difficult part of using the wetted perimeter is to ascertain just what its value is.

From the discussion of Chapter 8 it appears that the best approach to use toward the packed tower is to speak of two portions of liquid surface: One active in which all the surface elements are engaged

in reaching the same constant lifetime, and one dead in which all elements are reaching an infinite lifetime and are therefore ineffective for mass transfer. The active portion of the liquid-gas interface may be denoted as a_e , the "effective" area per unit tower volume. In the terminology of Chapter 8, $a_e = fa$.

The effective portion of the area, as has been suggested by Shulman (136) and others, would be associated with the liquid in active flow through the tower, whereas the dead portion would be associated with stagnant pockets, insides of packing surfaces or portions wet only occasionally where there is no strong directionalized flow. Such being the case we could then identify the effective portion of the area with the perimeter wetted by the active flow. a_e is the effective interfacial area per unit tower volume or, removing the tower height dimension, the effective wetted perimeter for active flow per unit tower cross section area. Thus Γ for the active flow is simply L_{active}/a_e . If we assume that all the liquid entering the column passes through in the active flow stream, then Γ is L/a_e and the characteristic Reynolds number would be $4L/a_e \mu$. This should be a good assumption, based on the ratio of lifetimes of 50 for the two types of interfacial surface estimated in Chapter 8 and on the extremely long sweep out times required for stagnant pockets mentioned by Shulman, et al (136), and quoted in Section 8.2.2.

To proceed further it is obvious that we must have a knowledge of a_e in order to produce a satisfactory dimensionless correlation for either $k_L a^*$ or k_L^* alone. It was concluded in Chapter 8 that $K_G a$ results from ammonia absorption measurements may be reliably corrected by the two film additivity concept (dead surface theory is valid) to obtain values of $k_G a_F$ which are equal to $f k_G a$ or to $k_G a_e$. If, then, it is possible to use a known correlation to provide a value for k_G alone, then a_e may be separated from $k_G a_e$.

Based on his study of the sublimation of pre-fabricated naphthalene packings and on the study of evaporation of water from porous pre-fabricated packings of Taecker and Hougen (147), Shulman (135, 137) has presented a correlation of j_D , the mass transfer factor, against a modified Reynolds number, $\frac{D_p G}{\mu(1 - \epsilon)}$, which contains the bed voidage, ϵ . This correlation has been presented earlier as Equation (9.6). It is largely empirical, being based on a similar correlation of mass transfer in beds of irregularly shaped particles obtained by Chu, Kalil, and Wetteroth (16). Some idea of the fit of this correlation for particular packing sizes may be obtained from Figure 8.14. One note of caution should also be interjected: j factor plots vs. Reynolds numbers are often deceptive. The presence of G in the denominator of j_D and in the numerator of the Reynolds number tends to extend the scale of such a plot in the -1 logarithmic slope

direction. Since these plots have negative slopes this does not provide a critical display of the actual scatter.

It is not the purpose of this chapter to deal with a correlation for gas phase coefficients, however, and certainly the use of a k_G correlation obtained for dry packing, which should behave the same toward gas phase dynamics as does wet packing below loading, is the best approach toward the problem of unscrambling $k_G a_e$ and $k_L a_e$.* (The difference in voidage between dry and wet packings is obtained through hold-up values.)

Shulman et al (137) have taken Fellingner's ammonia data (38, 133g), the most extensive available and apparently as reliable as any, as shown in Figure 8.18 and have separated a_e in this manner. One note of caution, however, should be injected here also: Fellingner made his runs for 1 inch Berl saddles with the water in his column between 15 and 20°C. For all other packings the temperatures of the water were between 5 and 12°C. It is known both theoretically and experimentally (139) that k_G is essentially independent of temperature, but it is not known conclusively to what extent a_e is. Thus we shall have to proceed

* Such techniques as have been used for measuring the fraction of solid packing surface actually covered with liquid are unreliable, since this surface area may well be, and probably is, different from the effective interfacial area between gas and liquid. As shown by Shulman et al (137), it is only for large packing sizes that the two approach one another.

using the a_e values calculated from Fellingner's data at 5 - 12°C to compare with $k_L a^*$ data taken at 25°C with the realization that the comparison may not be valid if a_e is significantly temperature sensitive. (If, however, a_e enters into the dimensionless correlation as a multiplicative factor raised to a certain power, and a_e varies per cent-wise with T in a manner independent of packing or magnitude, then it should be possible to make a correction for the temperature difference).

It is apparent from the plots of these effective areas presented by Shulman that there is no simple, product of powers correlation for them. This is to be expected because of the extremely complex nature of the formation of effective interfacial areas. Similarly there was no simple correlation possible for the f values computed for 1 inch carbon rings in Section 8.2.2.

The most logical next step is that taken by Shulman: To leave the effective areas as tabulated or graphically presented values and to proceed to a correlation of $k_L a^*$ alone, separated from a_e . Such a correlation would not be of general utility for systems other than air and water on the packings studied by Fellingner, but it may be possible in time to obtain some sort of reliable correlation for a_e , when the effects of more variables on a_e are known experimentally. (One possible approach to this may be through hold-up data, as suggested by Shulman).

The dimensionless equation for k_L^* presented by Shulman et al, is disturbing for two reasons. First, the type of Reynolds number used is theoretically unsound, or in other words the wetted perimeter, as best expressed by the effective area itself, should have been included. Also, from a knowledge of the basic equations of falling film hydrodynamics as they result in the short wetted wall column theory, the acceleration due to gravity should have been included, else why does the liquid film fall?

Because of the applicability of penetration theory to packed tower liquid phase transfer behavior, it seems that a good starting point for a dimensionless equation for k_L^* is the theoretical result for penetration into a free falling film, Equation (9.8), which in this case would be

$$\frac{k_L^* h'}{D_L} = 0.725 \left(\frac{4L}{a_e \mu} \right)^{+1/3} \left(\frac{\mu}{\rho D_L} \right)^{1/2} \left(\frac{\rho^2 g h'^3}{\mu^2} \right)^{1/6} \quad (9.12)$$

where h' is, as for the case of the short wetted wall column, the "equivalent free fall height." h' may be assumed to be equal for all exposures in the column because of the apparent uniformity of lifetimes over the active surface (Chapter 8). It will in general be a function of several variables.

In view of the suggested penetration mechanism h' may be taken as the distance of flow between mixings of the surface liquid elements, if such factors as account for deviation from free fall between mixings are accounted for. Any stagnation effects of the sort noticed in short wetted wall columns may well be insignificant in packed towers, if for no other reason than that most of the $\frac{4\Gamma}{\mu}$ or $\frac{4L}{a_e \mu}$ Reynolds numbers of operation in packed towers are in the range where the stagnation effect becomes less important in short wetted wall columns (43) (see also Figure 9.1). Acceleration effects, however, may be important in causing the liquid films in packed towers to deviate from free fall between mixings. This effect, as mentioned previously, has been shown by Scriven and Pigford (123) to be a function of Reynolds number alone if the retarding effect of drag at the solid wall (which should be small) is neglected. Turbulent effects within the falling film (not necessarily near enough to the interface to affect mass transfer) may also cause deviations from free falling behavior, but they too should be dependent solely upon Reynolds number. It should be kept in mind, though, that the effective kinematic viscosity, μ/ρ , would now, if the turbulence is intense enough, be the sum of a molecular kinematic viscosity, $(\mu/\rho)^1$, and an eddy kinematic viscosity averaged hydrodynamically across the film, and dependent upon Reynolds number. It is this effective viscosity that would enter into the dimensionless equation.

The other factors influencing h' should be those which influence the height a film falls between mixings, or, in another way of speaking, the occurrence of mixings of the surface elements. Most obvious among these is the length of a packing particle itself: Its nominal size. Another variable it may be necessary to consider would deal with the arrangement of the packing in a dump. If the falling film did not fall all the way down one piece of packing before running into another one, or if it were fed onto a piece of packing part way along it, the whole of the surface of that piece of packing would not be available for uninterrupted film flow. Also, if the liquid could flow in an orderly fashion from one piece of packing to the next without incurring a mixing, more surface than that attributable to one piece of packing might be available for fall.

Thus we have the packing size and some function of the packing arrangement. Any remaining factors would be due to the flow itself, i.e., the hydrodynamics. In view of the penetration model of the packed column there are two conceivable ways in which the frequency of mixing could be affected by the hydrodynamics: If there is not always complete internal mixing of surface elements at packing discontinuities, then one would expect to find a kinetic energy-viscosity effect on mixing frequency similar to effects in a waterfall; or, if there is internal mixing of surface elements in the flow along a single piece of packing

due to turbulences, then the mixing frequency should be influenced by the level of turbulence, which is dependent upon Reynolds number alone.

Recourse to the work of Sherwood and Holloway (131) and comparison with Equation 9.8, which for water at 25°C reduces to

$$k_L^* \sqrt{\frac{h'}{D_L}} = 8.0 \sqrt[1/3]{} \quad (9.13)$$

(all units in grams, cm., and sec.)

shows that even at the lowest liquid flow rate used by Sherwood and Holloway, $L = 500$, the effective free fall height is always less than 0.5 times the packing diameter. This indicates that mixing of surface elements is probably complete at discontinuities in the packing and that any effect of hydrodynamics on the effective free fall height is probably due to renewals in flow over a single packing element, an effect of Reynolds number alone. If roughness of the packing surface accounted for any of this, the effects could be attributed solely to Reynolds number and "arrangement."

As has been shown previously for the cases of flow over a sphere and down an inclined surface, the only deviational effects of curvature or inclination of packing surfaces are ones of length or of packing arrangement.

The net result of this argument is that h' may be taken as a function of Reynolds number, packing size, and packing arrangement alone. If it is valid to assume that the turbulences which cause mixing of the surface elements (which may be large scale eddies) are not pronounced enough to impart a significant eddy kinematic viscosity, then Equation (9.12) may be expressed as

$$\frac{k_L^* d_p}{D_L} = 0.725 \left(\frac{4L}{a_e \mu} \right)^{1/3} \left(\frac{\mu}{\rho D_L} \right)^{1/2} \left(\frac{\rho^2 g d_p^3}{\mu^2} \right)^{1/6} \sqrt{\frac{d_p}{h'}} \quad (9.14)$$

where

$$\sqrt{\frac{d_p}{h'}} = F \left[\frac{4L}{a_e \mu}, d_p \left(\begin{array}{l} \text{through} \\ \text{packing arrangement} \end{array} \right) \right] \quad (9.15)$$

Here d_p is used as convenient length group in place of the h (height) for a short wetted wall column (any length could have been used). Thus we have maintained the $1/6$ and $1/2$ exponents on the gravity and Schmidt groups in the final k_L^* correlation. That the $1/2$ power on the Schmidt group is still valid has been proven in the experimental results of this thesis. The maintenance of the $1/6$ power on the gravity group amounts to saying that the only effect of gravitational force on the process is in determining the free fall surface velocity, and this is a theoretical consequence of the discussion on the previous pages.

If we assume for the moment that the free fall path for flow at a

given Reynolds number is determined by packing diameter alone (and that the effect of arrangement is only second order and may be neglected) then we may write:

$$\frac{k_L^* d_p}{D_L} = \alpha \left(\frac{4L}{a_e \mu} \right)^n \left(\frac{\mu}{\rho D_L} \right)^{1/2} \left(\frac{\rho^2 g d_p^3}{\mu^2} \right) \quad (9.16)$$

Since k_L^* data are available only as $K_L a^*$ or $(H.T.U.)_L$, this should be written, in order to test it against data, as

$$\frac{k_L a^* d_p}{a_e D_L} = \frac{L d_p}{a_e \rho (H.T.U.)_{OL} D_L} = \alpha \left(\frac{4L}{a_e \mu} \right)^n \left(\frac{\mu}{\rho D_L} \right)^{1/2} \left(\frac{\rho^2 d_p^3 g}{\mu^2} \right) \quad (9.17)$$

Such data of Sherwood and Holloway (61, 131) as are comparable with the a_e values obtainable from Fellingner's data (38, 137) are plotted in this manner in Figure 9.1. Since only a_e , L , and d_p are varied, the data are plotted as $\sqrt{d_p}/(H.T.U.)_L$ vs. L/a_e . This is the most critical method of plotting, since no two variables are present in both coordinates. Figure 9.2 shows the exact same data plotted in the form given by Shulman's correlation (Equation 9.5), in an equally critical manner: $1/a_e(H.T.U.)_{OL}$ vs. $d_p L$ (Shulman's D_p is directly proportional to the first power of d_p).

Both curves give the same amount of scatter (the Shulman correlation is on a less expanded scale), and, on both curves, there is a tendency for the points for a given packing size to obey the general correlating slope, although there is usually a tendency for a slight upward concavity.

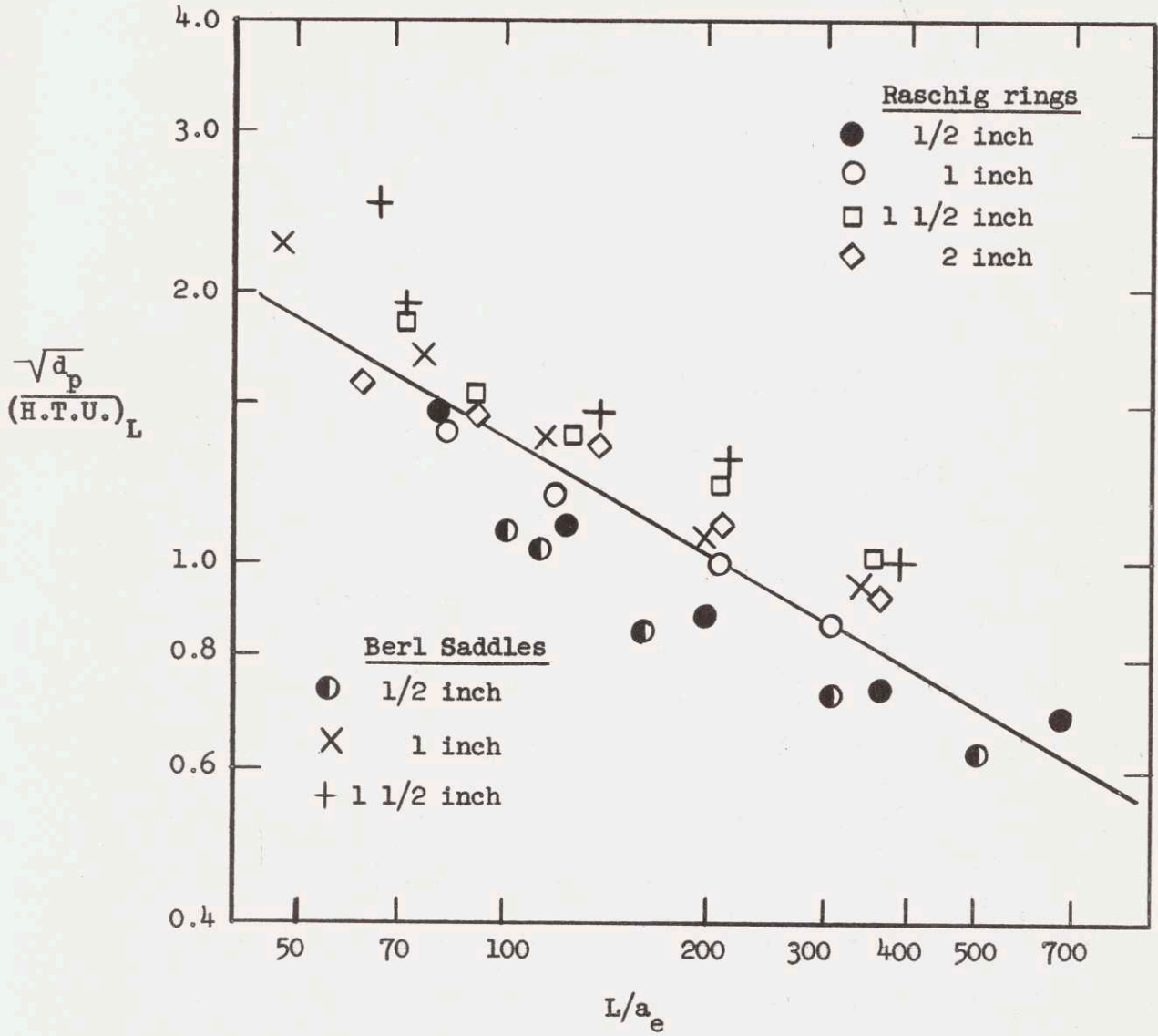


FIGURE 9.1 CORRELATION OF DATA OF HOLLOWAY

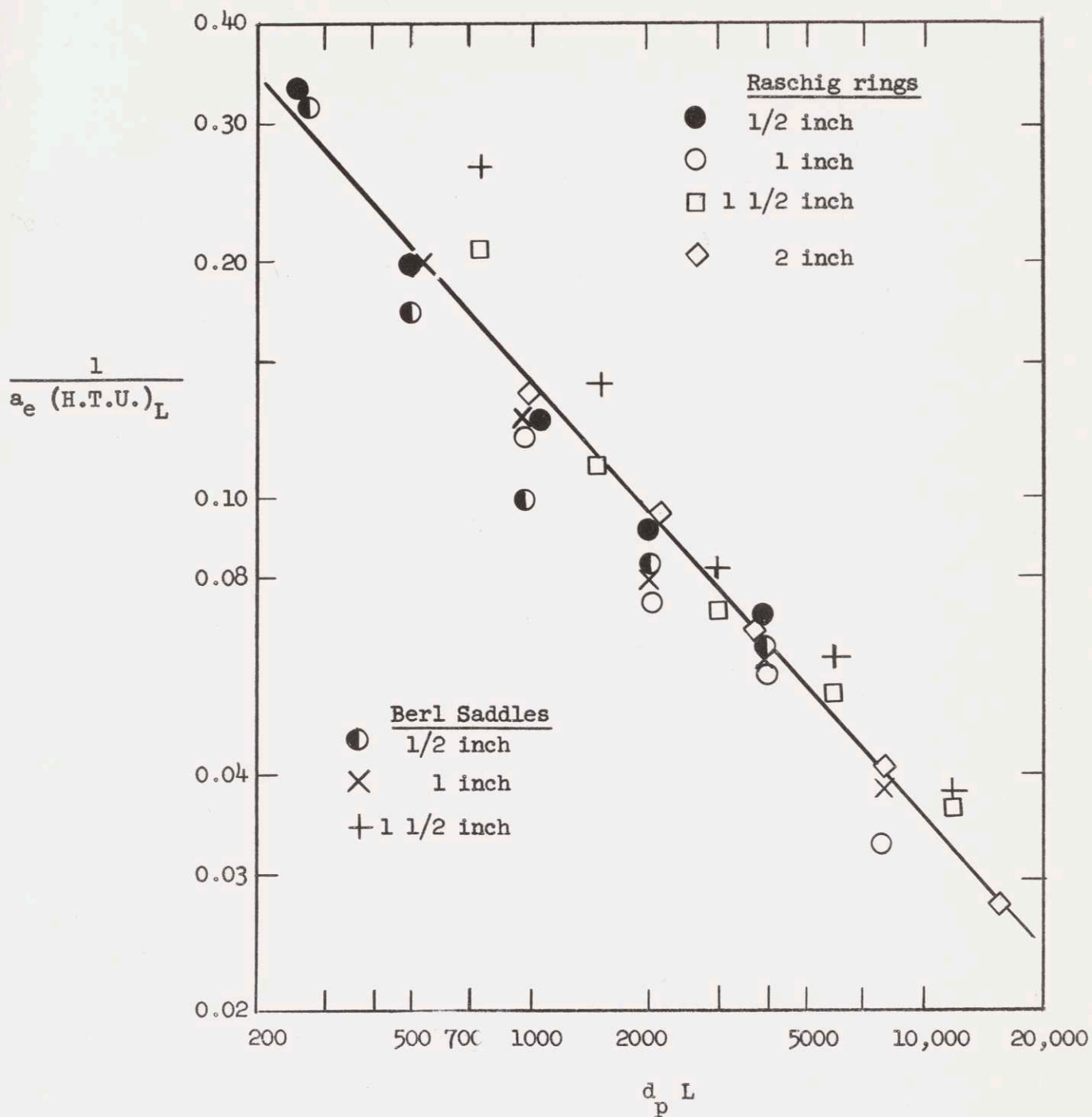


FIGURE 9.2 SHULMAN CORRELATION FOR DATA OF HOLLOWAY

The Shulman correlation, however, does not consider the effect of either wetted perimeter (effective area) or of gravitational force, and hence the present correlation is to be preferred in so far as the prediction of variables not actually studied experimentally is concerned.

The correlating line drawn in Figure 9.1 yields a variation of $\sqrt{d}/(\text{H.T.U.})$ with L/a_e to the -0.4 power. This corresponds to

$$\frac{k_L^* d_p}{D_L} = \alpha \left(\frac{4L}{a_e \mu} \right)^{0.6} \left(\frac{\mu}{\rho D_L} \right)^{1/2} \left(\frac{\rho^2 d_p^3 g}{\mu^2} \right)^{1/6} \quad (9.18)$$

The differences between this correlation and that of Shulman in predicting the effects of μ and ρ are now apparent. The shulman correlation gives, at constant a_e , $k_L^* \sim \mu^{0.05} \rho^{-0.5}$; whereas the present one gives, at constant a_e , $k_L^* \sim \mu^{-0.43} \rho^{-0.17}$, a very different prediction. Since there is no knowledge of the effect of μ and ρ on a_e , it is not possible at present to check the effects of those variables on k_L^* .

There appears to be a trend in the present correlation (Figure 9.1) with packing size, especially for Berl saddles, where $\sqrt{d_p}/(\text{H.T.U.})_L$ tends to increase with packing size at constant L/a_e . This may be attributable to the packing arrangement factor which was neglected in forming the equation.* If such is the case, then, there would be

* It may also be due to an effect of low bed heights, as discussed in Section 5.1.3. Holloway (61) used bed heights ranging from 1 to 2 feet in his Berl saddle studies.

another dimensionless group, $F^{-1/2}$, which would be called the fraction of a packing diameter available for free fall. It would be a function of packing type alone, as is d_p . Rather than including this group, however, the equation might better be written in a dimensional form:

$$\frac{k_L^*}{D_L} = \alpha \left(\frac{4L}{a_e \mu} \right)^{0.6} \left(\frac{\mu}{\rho D_L} \right)^{1/2} \left(\frac{\rho^2 g}{\mu^2} \right)^{1/6} \quad (9.19)$$

where α has units of length^{-1/2} and is unique for each packing type. The effects of μ , ρ , and g are unchanged, since F does not involve them.

This is equivalent to bringing in as many dimensionless groups as there are variables whose effects are known experimentally, thus forcing a correlation. It is, however, indicated theoretically as the best course to follow.

The best values of α for use in Equation 9.1 may be obtained from Figure 9.1, but first it is necessary to examine the effect of temperature on a_e , to ascertain whether a correction should be made for the use of the Feller data at lower temperatures.

At room temperature viscosity varies as $e^{-0.023T}$ ($^{\circ}\text{C}$ or $^{\circ}\text{K}$) (107), while the use of the Stokes-Einstein relationship indicates that D_L varies as $e^{+0.026T}$. ρ is insignificantly temperature sensitive.

Shulman's equation, then, predicts, if $k_L^* \sim e^{xT}$.

$$\begin{aligned} x &= 0.05 (-0.023) + 0.5 (.026) \\ &= 0.012 \end{aligned}$$

Adopting the variation of $k_L a^*$ with $e^{0.020T}$ found in Section 5.2.2, a_e then would vary with $e^{0.008T}$.

In Equation (9.19), however, if $a_e \sim e^{yT}$, then

$$0.020 = 0.4 (y) + 0.5 (.026) - 0.43 (-0.023)$$

or

$$y = -0.008$$

Thus the present equation, in combination with the known effect of T on $k_L a^*$, predicts $a_e \sim e^{-0.008T}$ (decreasing with increasing T) and $k_L^* \sim e^{0.028T}$ -- strongly temperature sensitive. This decrease in a_e with increasing temperature is qualitatively confirmed by the results of Dwyer and Dodge (35), Molstad, et al (92), and others who have found $k_G a_F$ to decrease with increasing temperature. The variation found by Dwyer and Dodge is in almost exact agreement with the variation for a_e predicted by Equation (9.19). To this may be added the fact that Shulman and Margolis (139) found k_G for sublimation from naphthalene packings to be totally independent of temperature. This is also indicated theoretically.

a_e at 25°C should thus be 15% less than a_e at 8°C, and 7% less than a_e at 17°C. This indicates that for 1 inch Berl saddles in Figure 9.1 the L/a_e coordinates of the points should have been 7% higher, while for all other packings the L/a_e coordinates should have been 15% higher. Values of α for the various packings for use in Equation (9.19), shown in Table 9.1, were computed using this correction. There is a small effect of packing nature for Berl saddles, and a larger effect for Raschig rings.

TABLE 9.1

Values of α for Use in Equation (9.19)

<u>Packing</u>	<u>α (ft^{-1/2})</u>
1/2 inch ceramic Raschig rings	0.91
1 inch ceramic Raschig rings	0.65
1-1/2 inch ceramic Raschig rings	0.62
2 inch ceramic Raschig rings	0.51
1/2 inch ceramic Berl saddles	0.78
1 inch ceramic Berl saddles	0.71
1-1/2 inch ceramic Berl saddles	0.68

The limitations of this equation should be stressed. It was derived solely by physical reasoning and analogy to penetration into a free falling film. To the extent that any of the assumptions made in the analysis are erroneous, then the predicted effects of those variables (μ , ρ , g) that have not been studied experimentally will be in error. It should also be pointed out that use of the equation in practical application is completely limited by the present state of knowledge of effective areas. Thus the equation can at present be used only to predict transfer

rates for packings on which it was based. Any further scope of application must await further knowledge of effective areas, and/or a correlation for effective area.

It is interesting to discuss the exponent of 0.6 found on the Reynolds number. This is much larger than $1/3$ predicted theoretically for penetration into liquid in free gravity fall. Since the effect of liquid acceleration, as discussed previously, is to lower this exponent, the raising of the exponent must be attributed to a sizeable effect of Reynolds number in increasing the frequency of surface renewal. It was shown previously, though, that to account for the magnitudes of k_L^* (or h') there must be a significant tendency for renewal to occur during the flow over a single piece of packing. This was attributed to turbulence, and so the frequency of renewal should indeed increase with Reynolds number, thus accounting for the higher exponent in the Reynolds number.

Since there is apparently a strong enough turbulence to influence the renewal rate significantly, then an important assumption involved in the derivation of the equation is the one stating that this turbulence is not of sufficient intensity to affect the effective kinematic viscosity in the falling liquid films significantly. If there is a significant eddy kinematic viscosity, then the predicted effect of μ in Equation (9.19) will be in error.

There is another important experimental result that may or may not also affect the validity of Equation (9.19). Rennolds (61, 130) studied the vaporization of water and the desorption of carbon dioxide with pure water and water containing various concentrations of several surfactants. He used both 1/2 inch carbon rings and then the same packing coated with paraffin. His results may be summarized as follows: The addition of surfactants to the water did not affect the $k_G a$ for vaporization, but did serve to lower the $k_L a^*$ for carbon dioxide desorption. The $k_L a^*$ for carbon dioxide desorption passed through a minimum as the surfactant concentration was increased. Paraffinating the packing served to decrease both the $k_G a$ for vaporization and the $k_L a^*$ for carbon dioxide desorption, but the percentage decrease in $k_G a$ tended to be greater than that in $k_L a^*$. The following conclusions from this are drawn from Sherwood and Holloway (130):

"The effect of wetting agent may be explained as due to the concentration of large organic molecules in the liquid film [referring to the "thin stagnant film" near the interface], serving to hinder the diffusion of solute. With gas film controlling, this effect is not noticed since the molecules are not large enough to effectively reduce the wetted area as in the case of evaporation of water from a glue solution. The effect of the paraffin on the packing is to reduce the interfacial area, a , since the liquid tends to flow in thick rivulets

instead of thin layers. That these rivulets are more agitated than thin layers is indicated by the fact that the coating reduced $K_L a$ for carbon dioxide desorption by a smaller amount than it did $K_G a$ for vaporization of water. With liquid film controlling, the reduction in a is partially offset by an increase in K_L ."

Little may be added to this analysis, other than to point out that the decrease in a_e caused by paraffination of the packing served to increase the Reynolds number, $4L/a_e \mu$, and thus served to increase k_L^* , in accordance with Equation (9.19). No further quantitative analysis of Rennolds' data is possible without a knowledge of f , the fraction of the total interfacial area that is "effective."

The question that arises from these results however, is whether the effect of any surface tensions have been brought into the dimensional analysis for k_L^* . The effect of the liquid-solid interfacial tension (altered by the paraffination) was solely one of changing a_e , and its only effect is thus taken care of by the Reynolds number. The liquid-gas surface tension though evidently altered k_L^* and not a_e (although it may have affected a_e by altering f and not a). The conclusion of Sherwood and Holloway was that it affected k_L^* only in so far as the large organic molecules served to hinder the diffusion of solute in the liquid near the interface. If this is so, then the effect of the surfactant was simply to make it necessary to use a corrected D_L in Equation (9.19), and

no additional surface tension group is necessary in the dimensional analysis.

If, on the other hand, there was some surface tension influenced stagnation effect akin to that mentioned previously for short wetted-wall columns,

then it would be necessary to include a surface tension group, such as

$\frac{L^2}{a_e^2 \gamma d_p}$, into account. It is unlikely, though, that any such effect

does occur in a packed column, and thus the behavior found by Rennolds may be attributed to an effect of the surfactant molecules on D_L alone.

In conclusion it should be mentioned that Equation (9.19) could have been derived by the classical methods of dimensional analysis if

1. it were assumed that the only variables affecting k_L^* other than length dimensions of the packed bed itself are the ones included in Equation (9.19),
2. it were assumed from a theoretical basis that the only influence of a_e is through its effect as the active wetted perimeter on the Reynolds number, and, conversely, that the only Reynolds number affecting the k_L^* value is the falling film Reynolds number containing the active wetted perimeter.

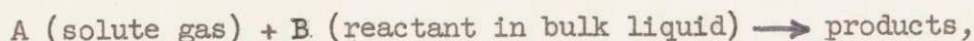
and

3. it were assumed, again on a theoretical basis, that the only influence of gravitational force is on the free fall interfacial velocity, which enters to the $1/2$ power (contact time) and is influenced by g to the $1/3$ power.

CHAPTER 10

INTEGRATION OF SECOND ORDER, INFINITELY FAST, IRREVERSIBLE
REACTION OVER PACKED TOWER HEIGHT

If the reaction is



then φ for the system is given (7c, 155) by penetration theory as

$$\varphi = \frac{k_L a^*}{k_L a^*_{\text{Phys.}}} \approx \sqrt{\frac{D_A}{D_R}} + \sqrt{\frac{D_R}{D_A}} \cdot \frac{C_R}{C_A} \quad (10.1)$$

to a close approximation for $(C_R/C_A) \sqrt{D_R/D_A} > 5$. If $(C_R/C_A) \sqrt{D_R/D_A} > 10$, then the first term may as well be taken equal to 1, provided D_A does not differ radically from D_R . The subscripts A and R here refer to the two reactants. C_A is the concentration of physically dissolved solute in equilibrium with the gas phase, while C_R is the ~~is the~~ reactant concentration in the bulk solution. $k_L a^*_{\text{Phys.}}$ is the $k_L a^*$ value measured for physical absorption at the same flow conditions. If we now assume dilute gas and liquid phases, no untoward heat effects, no change in a_e , D_A , or D_R with solution concentration, an infinitesimal absorption per penetration, and the existence of no gas phase resistance (very insoluble solute gas), a material balance when combined with the rate equation (see Section 2.1.4.) will give

$$\frac{L}{P_L} dC_R = \varphi k_L a^*_{\text{Phys.}} C_A dh = - \frac{G}{PM} d p_A \quad (10.2)$$

where p_A = partial pressure of A in gas phase (dilute).

P = total pressure

M = molecular weight of gas stream

h = tower height

C_R is taken to be greatest at the tower top, and p_A to be greatest at the tower bottom. Also it is assumed that $k_L a^*_{Phys.}$ is based on a_e , the dead surface approximation applies (see Section 8.2.2.), and φ is never so great that the less active surface comes into play.

Integration of Equation (10.2) over the total tower height now gives

$$\frac{\rho_L h k_L a^*_{Phys.}}{L} = \int_{C_{R1}}^{C_{R2}} \frac{d C_R}{\varphi C_A}, \quad (10.3)$$

the subscripts 1 and 2 referring to tower bottom and tower top respectively. Now, defining H as p_A/C_A (the reciprocal physical solubility), there results from Equation (10.2)

$$C_A = \frac{p_{A1}}{H} - (C_R - C_{R1}) \frac{LPM}{G \rho_L H} \quad (10.4)$$

Substituting this expression and the expression for φ (Equation 10.1) into Equation (10.3) yields

$$\begin{aligned} \frac{\rho_L h k_L a^*_{Phys.}}{L} &= \int_{C_{R1}}^{C_{R2}} \frac{d C_R}{\left(\frac{D_A}{D_R}\right)^{1/2} \left[\frac{p_{A1}}{H} - (C_R - C_{R1}) \frac{LPM}{G \rho_L H} \right] + \left(\frac{D_R}{D_A}\right)^{1/2} C_R} \\ &= \frac{1}{\left(\frac{D_R}{D_A}\right)^{1/2} \left[1 - \frac{LPM}{G \rho_L H} \frac{D_A}{D_R} \right]} \ln \frac{\frac{p_{A1}}{H} - \frac{LPM}{G \rho_L H} (C_{R2} - C_{R1}) + \frac{D_R}{D_A} C_{R2}}{\frac{p_{A1}}{H} + \frac{D_R}{D_A} C_{R1}} \quad (10.5) \end{aligned}$$

However, since this was considered to be a case where no gas phase

resistance enters, H must therefore be very large and, for an experimental mechanism study, it should be a simple matter to take L/G small enough so that the terms including H are negligible.

Then

$$\frac{\rho_L h k_L a^* \text{Phys.}}{L} = \left(\frac{D_A}{D_R} \right)^{1/2} \ln \left[\frac{\frac{P_{A1}}{H} + \frac{D_R}{D_A} C_{R2}}{\frac{P_{A1}}{H} + \frac{D_R}{D_A} C_{R1}} \right]$$

$$\text{for } \frac{LPM}{G \rho_L H} \ll 1; \quad \frac{HC_R}{P_A} \sqrt{\frac{D_R}{D_A}} > 5 \quad (10.6)$$

It is interesting to notice that this solution differs from that obtainable from film theory for the same conditions only in the inclusion of the $(D_A/D_R)^{1/2}$ term before the logarithm instead of D_A/D_R . Since a damped turbulence mechanism in the liquid near the interface is, in a way of speaking, an intermediate case between penetration theory and an unsteady-state view of film theory one might expect the exponent on the D_A/D_R term to be between 0.5 and 1.0 in such a case. Thus the study of a highly insoluble gas under dilute conditions being absorbed into a reactant undergoing a second order, infinitely fast, irreversible reaction would provide a means for an independent check on the applicability of penetration theory to a packed column.

CHAPTER 11

MECHANISM OF STIRRED FLASK ABSORPTION

There are many instances in the recent literature where absorption data taken in short wetted wall columns and falling jets have been found to be in almost complete agreement with the predictions of penetration theory. The suitability of these two models as representations of the liquid phase absorption process in a commercial packed tower is apparent and has been discussed in Section 5.4.4.

Absorption in a stirred flask presents other problems, however. It has been postulated by Danckwerts (21) that a penetration mechanism also applies to a stirred flask. The results of Goodgame and Sherwood (46) for acetone absorption in a stirred flask show close agreement with two film additivity if k_L is assumed to vary with $D_L^{0.5}$ (see Section 8.2.1). There is a factor of almost two in D_L between acetone and oxygen, which they used to obtain k_L^* . This lends some confirmation to the concept that the correct exponent on D_L is in the vicinity of 0.5 for a stirrer speed on the order of 120 rpm.

Despite the number of chemical reaction studies that have been made in stirred flasks (55, 68, 72, etc.) there are none that lend themselves to distinct confirmation or disproof of the applicability of the penetration solutions for absorption with chemical reaction.

The most direct study of mechanism in stirred flask absorption has been made by Kishinevsky and Serebryansky (74), who absorbed nitrogen, oxygen, and hydrogen into water in a rapidly stirred flask (1,700 rpm)

equipped with baffles to prevent large vortex formation. Amazingly enough, they found no influence of molecular diffusivity on the process although, "preliminary experiments with a stirrer speed of 1,200 revolutions/minute (when the absorption rate decreased by 4.5 times) showed that ... the value of K_L begins to depend on the value of the molecular diffusion coefficient." It is on this finding that Russian claims (70, 72) that the role of molecular diffusion in industrial equipment should be small or nonexistent are based.

It is difficult to ascertain the exact conditions of this experiment from the published article. Apparently the gas-liquid interface was by no means kept smooth (73), a necessary consequence of the high stirrer speed. It would be interesting to know just how much splashing and bubbling appeared to take place during an experiment.

Recent workers in this country and in Europe studying absorption into falling jets have obtained contact times as low as 0.001 seconds, finding close agreement with theory for penetration into a falling jet (15, 18, 99, 114, 124). There is only one instance where any sort of interfacial resistance or mechanism other than penetration is suggested by the data (15), and this is the only case where the absorption of a gas (oxygen) of lower solubility than carbon dioxide was studied. These results, presented by Chiang and Toor, are explained by the assumption of a first order (rate proportional to driving force) resistance at the surface, and an equivalent k_{LS} of 0.6 cm./sec., where S denoted surface resistance. If such a low k_{LS} were attributable to a condensation coefficient less than unity, one on the order of 10^{-6} would be required.

This is unlikely in the light of present views on such phenomena at newly formed surfaces (84, 121, 124).

Kishinevsky and Serebryansky give total absorption rates in their flask, since the interfacial area was unknown. Based upon a drawing in their article (74) and one in a previous article (73), however, the horizontal cross sectional area of their flask should have been about 80 cm.^2 , and this may be taken as a lower limit on the interfacial area so that an upper limit on k_L may be calculated. The maximum k_L calculated in this way for their 1,700 rpm runs is 0.25 cm./sec., corresponding to a minimum average lifetime of 0.001 sec. for the case of hydrogen if a renewal-penetration mechanism applied. This lifetime is equal to the lowest reached in jets, and the k_L is lower than, but comparable to, the value of k_{LS} suggested by Chiang and Toor. There is no reason at present (see, for instance, Schrage (121)) to expect a larger surface resistance for less soluble gases, though. In fact the degree of apparent surface resistance, aside from that due to a condensation coefficient less than one, should vary with the size of the absolute rate of net mass transfer (121), and should thus be less for insoluble gases that have lower transfer rates than more soluble ones over the same contact time.

The results of Kishinevsky and Serebryansky also cannot be attributed to a very rapid renewal process in which the first few molecular layers in the liquid might saturate and thereby take in a greater amount of solute than is able to diffuse inward during the contact time, because such a process, not having been observed in jets, could only occur at

a much higher transfer rate per unit area than has been studied in jets.

The gas phase in the flask did have different properties from solute to solute, since a pure gas phase was used. One could expect the primary effect of this to be a surface tension effect on the interfacial area (the amount of energy required to form new area). The surface tension of water against hydrogen, however, is not perceptibly different from that of water against air (66a).

Some absorption could have occurred through entrainment of very fine bubbles into the liquid, which would then dissolve completely before escape, giving a process independent of diffusivity. It is unlikely, however, that this was a controlling mechanism.

There is little left to explain the results other than turbulences extending near to the interface. The degree of agitation of the interface should be known before this is accepted, however, and, indeed, it might be well worthwhile to repeat the experiment.

The conclusion to be drawn from this discussion is that a penetration mechanism has not been shown definitely to apply to a stirred flask under any conditions of stirring. The stirred flask, therefore, does not at present seem to be as reliable a model of the liquid phase in a packed column as are jets and short wetted wall columns.

CHAPTER 12Effect of One Solute Gas Upon Another

At the very low concentrations of solute encountered in this work the actual rate of mass transfer in the liquid near the interface does not provide any significant effect on the hydrodynamics of the system; that is, the mass transfer itself does not contribute any significant net fluid velocity, as is found, for instance, in the case of steady state diffusion of a gas present in high concentration through a second stagnant gas, where the inclusion of the " P_{BM} " term accounts for this effect (133a). One would therefore expect that simultaneous absorptions or desorptions of these slightly soluble gases should occur independently of one another. Indeed, in all the cases studied in the present work there was an absorption of nitrogen (and oxygen, except in oxygen runs) into the water from the air accompanying the desorption of the solute gas under study.

In the case of propylene desorption, however, there was some strange behavior. During the winter, when the propylene runs at the first two flow conditions were made, the results showed a small amount of scatter and tended to correlate well with data for the other four solutes. At the third set of flow conditions ($L = 5000$, $G = 900$), however, the propylene data tended to scatter widely and to give on the average an $(H.T.U.)_{OL}$ that would require a sharp reduction in absolute value of the exponent on D_L . This sudden sharp bend in the $\log (H.T.U.)_{OL}$ vs. $\log D_L$ curve would be difficult to explain from the point of view of mechanism. Also one would expect that the bend, if the result of a turbulent mechanism, would show up at a higher D_L value at more turbulent flow conditions.

This did not happen. The scatter and the low value of HTU indicated that perhaps something was occurring which was not taken into account in the analysis of the data.

The occurrence of this phenomenon coincided with the arrival of warm weather. Titration analysis of Cambridge water indicated that the oxygen content of the water rose during this time to a value corresponding to near (above 90%) saturation with air.

If the water were nearly saturated with air, then, after the injected propylene gas was mixed with the water in flow through the line leading to the top of the tower the water would be even more nearly saturated with propylene and air. Thus while propylene might be present at the point of entrance to the tower at a concentration equal to 30% of saturation, air would also be present to nearly 70% of saturation, and the water would be nearly 100% saturated.

Then as the water passed through the column the $K_L a$ for propylene desorption would be less than the $K_L a$ for air absorption (the $K_L a$'s being in the ratio of the square roots of the diffusivities), and there would be a tendency for the water stream to supersaturate.

This effect is shown graphically in Figure 12.1. This figure is drawn for an extreme case, where D_L for air is four times the D_L for the desorbing solute, in order to show the effect. The plot shows the total amount of saturation of the water as a function of the distance from the air-water interface during a given penetration for a case in which the

water is initially 50% saturated with air and 20, 30, 40, or 50% saturated with the desorbing solute. (In actuality the oxygen and nitrogen of air have different diffusivities, but for the purpose of discussion a single diffusivity is assigned to air in water). The surface of the water is always 100% saturated (equilibrium with the air phase), and, depending upon the degree of initial saturation of the water and the relative diffusivities of the air and desorbing solute in water, the total per cent of saturation either rises above 100% as the water phase is entered or drops steadily downward from the initial value of 100%. In any event the total saturation at a large distance from the surface, of course, becomes equal to the initial degree of saturation of the water. The lower the diffusivity of the desorbing solute is below that of air, the greater the degree of supersaturation of the water corresponding to a given degree of initial saturation will be. Thus for the present experiment the degree of supersaturation would tend to be greatest for the desorption of propylene, the gas with the lower diffusivity in water. The only other case in which supersaturation could be evident would be for carbon dioxide, since all other solutes have a higher diffusivity in water than does air.

This supersaturation would probably tend to relieve itself through gas bubble formation at some time. There are two possible ways in which this could happen. First, the bubbles could tend to form during the penetration process, close to the interface in the liquid. A second possibility would be the release of gas from the supersaturated liquid

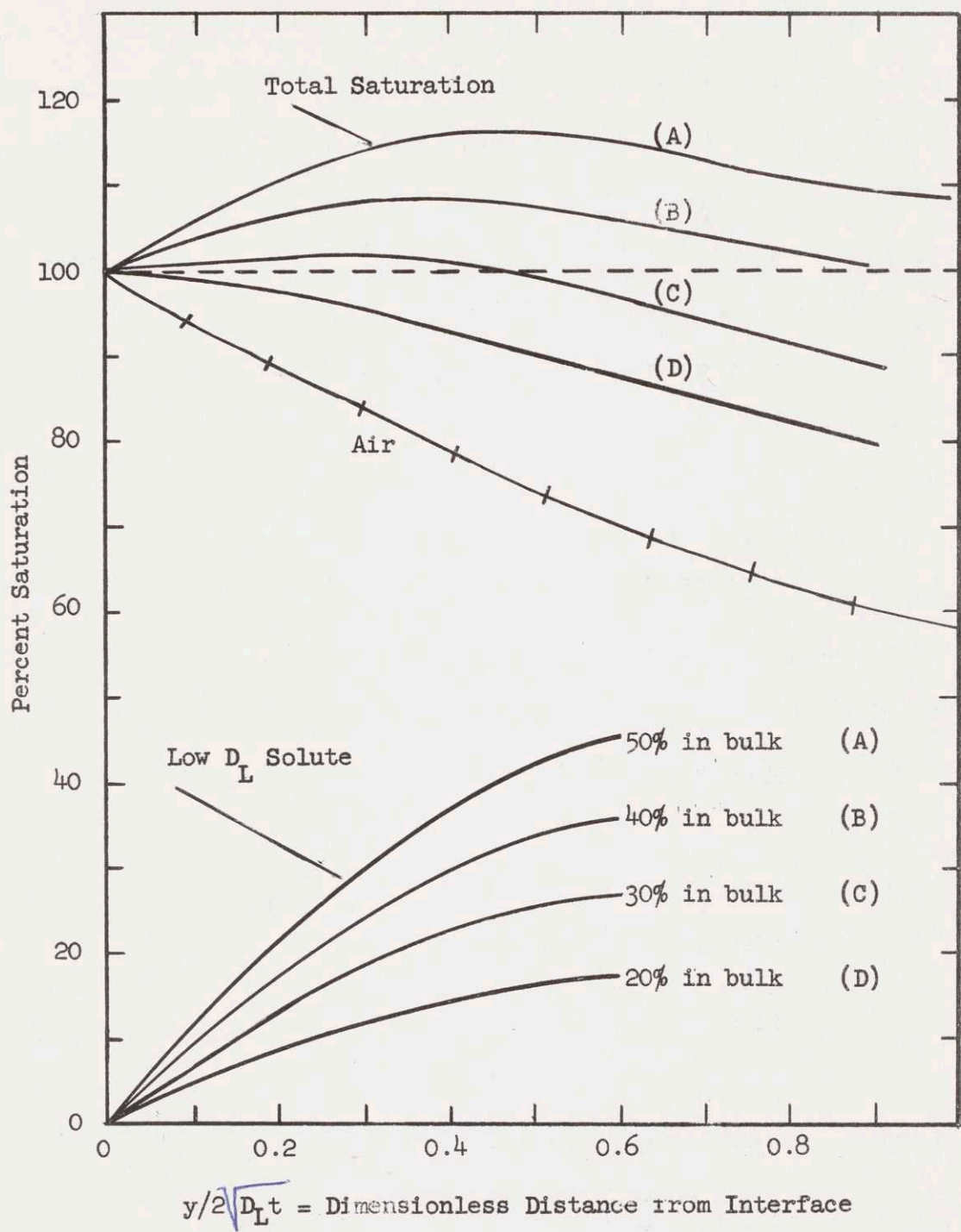


FIGURE 12.1 CONCENTRATION PROFILE NEAR INTERFACE IN CASE OF LOW DIFFUSIVITY DESORBING SOLUTE

in the turbulent mixing regions that are postulated to end a surface lifetime when the surface reaches a discontinuity in the packing array. A gas bubble would then be in equilibrium with the well mixed bulk solution, rather than with the solution at the point where supersaturation first occurred in the penetration-diffusion process. To the extent that the bulk liquid was initially saturated before a particular exposure then the mixing of the supersaturated surface layers with the bulk following the exposure would cause the bulk liquid to become supersaturated.

Since there is a curvature of the surface of a bubble, the total gas pressure within the bubble will be slightly greater than atmospheric because of surface tension. At first it might seem a violation of the Second Law of Thermodynamics that such a process could occur as the dissolution of a gas followed by its reappearance in a form of a bubble with higher total pressure in an isothermal, no outside work system. A further consideration though, verifies that at all times the system is tending toward equilibrium by transfer under a positive fugacity driving force (the partial pressure of air in a bubble must be less than the partial pressure of air in the bulk gas stream, for instance), and the entropy of a closed air-water-bubble system must increase.

The effect that the second of the above mentioned phenomena could have on the transfer rate observed in a packed column may be estimated mathematically: For the purpose of approximation the amount of transfer

occurring during a single surface exposure in flow over packing may be taken as infinitesimal in comparison with the total amount of transfer occurring through the whole of the column height. Then both $k_L a$ for the desorbing solute and that for air absorption may be taken as constant, and the requirement may be made that at all points an amount of gas in equilibrium with the bulk liquid is being released from the liquid so as to maintain the total saturation of the liquid no greater than 100%. This 100% figure neglects the finite degree of supersaturation necessary to cause bubble formation because of the higher total pressure in the bubble.

If dN denotes the molal flow of a solute entering the water in a differential element of tower volume dV ($= A_T dh$, the tower cross-section times a differential height), and dE designates the molal escaping gas flow in the same differential volume, then

$$dN_a = k_L a m_a \left[1 - (1 - f) \right] dV - (1 - f) dE \quad (12.1)$$

and

$$dN_p = \Phi k_L a m_p f dV - f dE \quad (12.2)$$

where Subscript a refers to air

Subscript p refers to propylene (desorbing solute)

N = rate of absorption (moles/time)

$k_L a$ = $k_L a$ for air absorption

Φ = $k_L a$ for desorbing solute / $k_L a$ for air

= $\sqrt{\frac{D_{Lp}}{D_{La}}}$, by penetration theory

- m = solubility at atmospheric pressure (moles/vol.)
 f = fraction bulk water is saturated with desorbing solute
 E = gas removal rate (moles/time)
 V = tower volume (vol.)

This formulation assumes that there is no propylene in the bulk gas. It also assumes that the water is initially 100% saturated, and is, therefore, the extreme case. Since the water is not permitted to become supersaturated, we have the requirement,

$$\frac{dN_a}{m_a} + \frac{dN_p}{m_p} = 0 \quad (12.3)$$

Next, adding (12.1) and (12.2), subject to (12.3)

$$(1 - \Phi) k_L a f dV - \left[\frac{(1-f)}{m_a} + \frac{f}{m_p} \right] dE = 0$$

or

$$dE = \frac{(1 - \Phi) k_L a f}{\frac{(1-f)}{m_a} + \frac{f}{m_p}} dV \quad (12.4)$$

Inserting (12.4) into (12.2), there results

$$dN_p = - \Phi k_L a f m_p dV - \frac{(1 - \Phi) k_L a f^2}{\frac{(1-f)}{m_a} + \frac{f}{m_p}} dV$$

or

$$dN_p = - k_L a m_p \left[\Phi f + \frac{m_a f^2 (1 - \Phi)}{m_p + f (m_a - m_p)} \right] dV \quad (12.5)$$

For the dilute solutions present here, the following material balance is valid:

$$dN_p = \frac{L A_T}{\rho_L} m_p df \quad (12.6)$$

where L = water flow rate (mass/area time)

ρ_L = density of water (mass/volume)

A_T = cross-section of empty tower (area).

Using (12.6) and the definition of dV as $A_T dh$, we have, from (12.5)

$$- \frac{\rho_L \Phi k_L a}{L} dh = \frac{\Phi df}{\Phi f + \frac{m_a f^2 (1 - \Phi)}{m_p + f(m_a - m_p)}} \quad (12.7)$$

The quantity on the left, when integrated from tower bottom to tower top (h positive downward) is simply the $(N.T.U.)_L$ for propylene desorption in the presence of no supersaturation when defined from the actual $k_L a$ value operative in the column. Therefore

$$(N.T.U.)_L = \int_{f_B}^{f_T} \frac{\Phi df}{\Phi f + \frac{m_a f^2 (1 - \Phi)}{m_p + f(m_a - m_p)}} \quad (12.8)$$

Since the second term in the denominator is always positive, the actual $(N.T.U.)_L$ for propylene is less than that which would be calculated by the ordinary, no-supersaturation equation (from (16.1.5)):

$$(N.T.U.)_L = \int_{f_B}^{f_T} \frac{df}{f} \quad (12.9)$$

The greater the solubility of air relative to that of the desorbing gas, the more significant the second term in the denominator will be in comparison with the first, i.e., the removal of a certain amount of gas in equilibrium with water solution containing two or more gases will have a more drastic effect on a low solubility gas than on one with a higher solubility. For the case of propylene and air, Φ is equal to about 0.81 (taking D_L of air in water at 25°C as 2.2×10^{-5} cm.²/sec.), and m_p/m_a is equal to about 12 (taking solubility data from Seidell (125)). f , in all cases, was less than 0.40. The ratio of the second denominator term to the first in the integral is

$$\Phi \left[\frac{1 - \Phi}{\frac{m_p}{m_a} \frac{(1-f)}{f} + 1} \right]$$

giving, for the present cases, a ratio always less than 1.3%. Thus the integral (12.8) is essentially equal to the integral (12.9). Had the desorbing gas been a factor of 10 or more lower in solubility this would not have been so.

The conclusion, then, is that if the supersaturating solution waits until the mixing period after the penetration to form bubbles and de-supersaturate, there will be no perceptible effect on the $(N.T.U.)_L$ for propylene or carbon dioxide, since the solubility and diffusivity of carbon dioxide are even greater than those of propylene in the present

case. This rules out the second of the two effects mentioned above.

Still remaining, however, is the first possibility: That the nucleation and bubble release comes in the supersaturated regions near the interface in the water during the actual penetration process. In this case the bubbles would be even less rich in propylene, but the actual formation of the bubbles and motion of them so near the interface could well introduce turbulences and thus markedly increase the $k_L a$ values for both desorption and absorption processes. Such an effect, although difficult to analyze quantitatively, was in all probability the reason for the low values of $(H.T.U.)_{OL}$ (and high $K_L a$ values) found for propylene desorption from ~~the~~ saturated water in the warmer weather season.

This conclusion was more or less confirmed experimentally in two runs (#47 and #48) made for propylene desorption using stock water that had previously been deaerated and hence should not tend to supersaturate so much. Laboratory steam in these runs was introduced into the water in the storage tanks in sufficient quantity to raise the water temperature to $60^\circ C$ (reducing the solubility of air). The water was then allowed to cool overnight, with a plastic film covering its open surface to prevent re-absorption of air. The two runs made with this water did indeed give higher $(H.T.U.)_{OL}$ values (and lower $K_L a$ values) than the runs made previously with non-deaerated water. The coefficient from these two runs also lines up well with the results for other solutes (see Figures 4.1, 4.3, and 4.5), and an oxygen run (#49) made using

deaerated water showed no effect of any additives present in the steam on the transfer process. Thus, apparently, supersaturation did indeed account for the H.T.U. lowering effect observed with non-deaerated water, and, probably, it was the bubbles being formed near the interface during the penetration process that served to provide turbulences and lower the H.T.U. values.

CHAPTER 13

DETAILS OF APPARATUS AND PROCEDURE

13.1 Apparatus

Diagrams of the packed tower and auxiliary apparatus have been given in Figures 3.1 and 3.2. These diagrams are reproduced again in this section to facilitate reference to them.

13.1.1 Tower and Water System

The tower consisted of four sections of standard, Schedule 30, flanged steel pipe, and was fabricated by Artizan Metals, Inc., of Waltham, Massachusetts. The flanges gave twelve bolt holes on a 14 inch circle, and were held together by $3/4$ inch steel bolts. To give a tight seal between sections, $1/4$ inch O-ring gaskets were used, except on either side of the water distributor plate where wider $1/8$ inch gaskets made of natural rubber sheet were utilized, both to prevent leaks and to prevent buckling of the distributor plate.

The bottom section was 18 inches high, and was filled with 1- $1/2$ inch ceramic Raschig rings, dry dumped in an arbitrary manner from a distance of a few inches above the packing level. During the dumping process the top level height of the packing was maintained uniform. Before being put into the column, the packing was cleaned with hydrochloric acid to remove rust and other contaminants.

The optional 12 inch section could be inserted to give an extra foot of packed height.

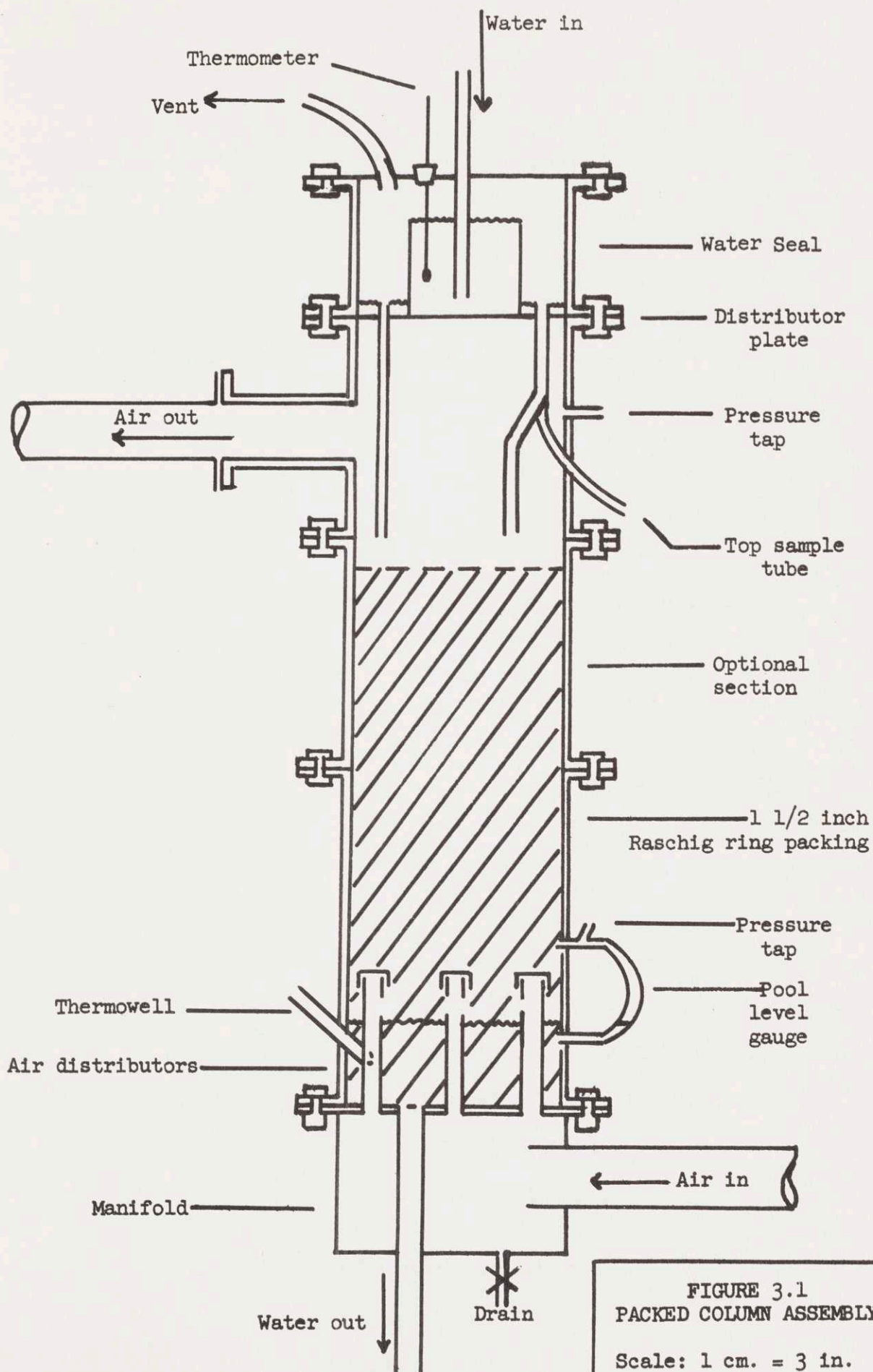


FIGURE 3.1
PACKED COLUMN ASSEMBLY

Scale: 1 cm. = 3 in.

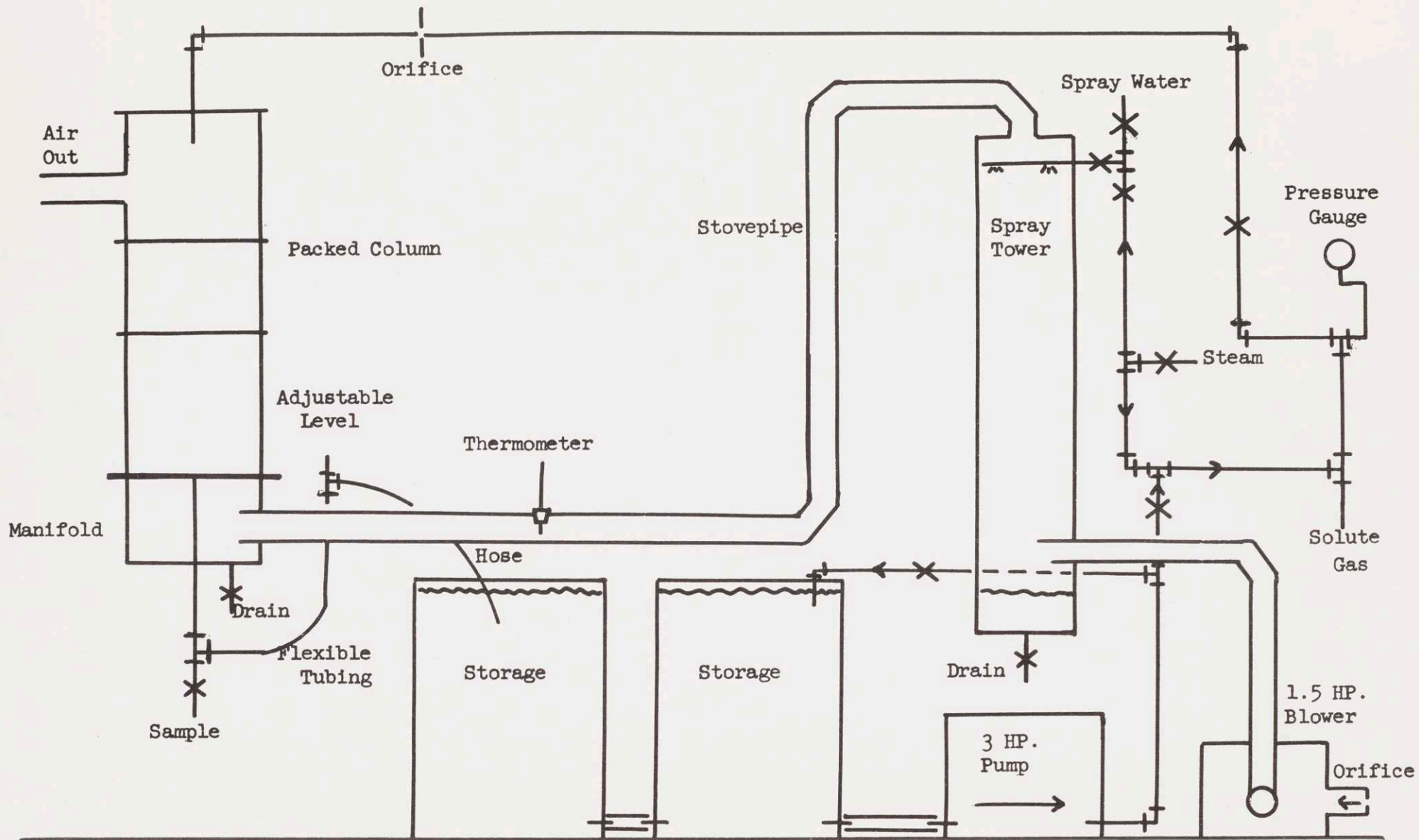


FIGURE 3.2 FLOW DIAGRAM OF APPARATUS

Below the 18 inch section was a 1/2 inch steel plate, fitted with a 2 inch brass pipe water drain and four 1-1/2 inch brass pipe air distributors. These were made from 8 inch long sections of pipe fitted with brass caps at the top, and with notches cut in them below the cap. These notches were vertical, 1/2 inch wide and 1-1/4 inch long, extending from about 6-1/4 inches above the bottom plate to about 7-1/2 inches above it. One pipe was placed in the center of the column and the others equi-angularly about it on a 4-5/8 inch radius. The central pipe had four notches and the outer ones, three.

The bottom tower section was also fitted with a well for a thermometer (outlet water temperature) and with a pool level gauge, made from Tygon tubing fitted to 3/4 inch welded nipples. A "bird cage" device, made of 3/8 inch brass strips, was placed in the packing above the drain to keep packing from occluding the flow through the drain. At the bottom of the 2 inch drain pipe was a brass tee, onto one arm of which was fitted a length of 1/2 inch copper tubing coupled with rubber tubing. Opening a pinch clamp permitted sampling of the effluent water stream through this line.

A length of 2 inch Flexaust hose led from this tee up to a leveling tee, the height of which could be adjusted to control the pool height of water in the bottom of the tower as water flow rate was altered. A length of 2 inch "Met" hose provided a return line to one of the two 55 gallon storage tanks from the leveling tee. The tower was supported

sufficiently high off the floor for there to be as much as 2 feet of head available to drive water through the exit line.

The pump, a 3 horsepower Dayton centrifugal model operating at 1750 RPM, drew water from the other storage tank. The bulk of the water was passed through a bypass line, which returned to the tank beneath the open water surface. The water to the column was drawn off this line, and came at a constant flow rate, since the high bypass flow served to absorb fluctuations arising from the pump. This water passed through two globe valves, which served to control the flow rate and adjust the pressure in the line at the steam and solute injection tees (located between the valves) to a value low enough to permit injection. The pressure was indicated by a Bourdon gauge connected to a tee upstream from the solute gas injection tee. This injection tee consisted of a length of $3/8$ inch copper tubing extending some 2 or 3 inches downstream and entering through a tee sidearm. The steam injection tee was similar, but made of $1/2$ inch copper tubing.

After passing through the second tee, the water inlet stream flowed up to a level above the top of the tower, and across to the tower in a long (10 feet) straight section of pipe. In this straight away the orifice flanges were located. Provision was made for the installation of one of three circular sharp edge orifices, $5/16$ inch, $1/2$ inch, and $11/16$ inch in diameter, held in a specific orientation by flanges with gaskets made from $1/8$ inch natural rubber sheet. The orifices were

calibrated by determining the volume of water passing through the tower for a measured time interval (see Figure 19.3).

All of the inlet water line was made from 1-1/4 inch copper and brass tubing and fittings, with soft-soldered joints. The pump was bronze-fitted.

Upon entering the top of the tower, the water flowed over a cylindrical liquid seal device, 6 inches in diameter, 5 inches high, and made of 1/32 inch rolled brass sheet. This seal was centered on the water distributor plate, described below. The top section of the column, above the distributor plate, was 8 inches high. On top of this section was a 3/32 inch brass plate, attached to the inlet water pipe, and with holes for a gas vent and a thermometer. The thermometer extended into the water seal and gave the inlet water temperature. The vent line, made of heavy wall rubber tubing, led to the inlet side of the blower driving the exit air stream into the chimney (see below). This vent was used as a safety factor when hydrogen or propylene was used as the solute.

The optional tower section could also be placed above the usual top tower section, in order to give an additional foot of head to the water distributor at high water flow rates. The inlet water line was equipped with a 1 foot optional section, attached by unions, which was used to accommodate changes in tower height.

The distributor plate was also made of brass, and was equipped with 24 compression fittings on a circle of 10 inch diameter. To these

compression fittings were attached lengths of $1/2$ inch copper tubing, which served to distribute the water over the packing. Each distributor was fitted on the bottom end with a cap containing a $1/8$ inch diameter hole. This required the distributor tubes to run full for a distance above the outlet, and thus prevented air-water contact within the distributor tubes at low water flow rates. One of the tubes led down to the center of the packing; four more led to positions on a 4 inch circle about it; six more led to points on a 7 inch circle; and 12 led to locations nearer the tower wall on a 10 inch circle. The remaining compression fitting served to feed the inlet water sample line, a length of rubber tubing, which was brought out through the side of the tower and closed with a pinch clamp.

The compression fittings by which the distributor tubes were held to the distributor plate were equipped with graphite Garlock packing rather than brass compression rings. This permitted adjustment of the height of a distributor tube above the distributor plate. Equal flow of water through each tube was assured by raising the tower section bearing the distributor plate up off the next lower section by blocks of wood, adjusting the pitch of the plate to the pitch it would have when the section was fastened in place (exactly level in this case), and measuring the flow through each tube. The sensitivity of the tube flows to slight variations in height above the plate was reduced by notching the top of each tube.

The lower ends of the distributor tubes were from $1/4$ to $1/2$ inch

above the packed surface. This tended to minimize end transfer at the top of the packing, as the more or less stagnant water pool did at the bottom. For the lowest packed height the pool surface area was only 3% of the total packing surface, and in all probability presented water surface less active for mass transfer than the water surface on the packing.

The interiors of the tower and the storage tanks were given three coats of Series K, self-priming, white Tygon paint, as a protective coating against corrosion by the water. This held up well under use, no rust pockets ever being visible on the tower lining and only a few on the storage tank lining over the five month period of actual experimental operation.

13.1.2 Air System

The air duct line was made entirely of 4 inch galvanized stovepipe. Joints in the line were made airtight by use of plastic electrical tape, secured by Glyptal where necessary.

Air was drawn into the system by a 1-1/2 horsepower, 3400 RPM (normal speed) shunt wound DC rotary blower. The blower was equipped with a field rheostat and also variable supply voltage to give speed control and thus flow rate control amounting to about 30% for a given inlet orifice size.

The inlet line to the blower could be either a 4 foot length

of 4 inch stovepipe or a 6 foot length of 6 inch stovepipe. The inlet end of the stovepipe was fitted with one of three circular sharp-edged orifices, (1 inch, 2 inch, or 4.59 inch) made in stovepipe caps. The tap for this orifice was located 4.7 inches downstream in the 4 inch pipe, and 3.2 inches downstream in the 6 inch pipe. Standard data (109e) were used for calibration, since in both cases there were 12 pipe diameters between the orifice and the blower (see Section 16.3.6).

From the blower the air passed up through the spray tower, which was made of 8 inch stovepipe and was 6 feet high. The air entered tangentially 6 inches above the bottom of the tower. Steam and water could be introduced separately or together to the tower through two Grainger spray nozzles fed with $3/8$ inch brass pipe.

In operation it was found that the spray tower, operating at about a 1 GPM water flow rate would saturate an air flow of 900 lb./hr.sq.ft. (based on the packed tower area) essentially completely, as measured by wet and dry bulb thermometry.

After leaving the top of the spray tower the air passed to a manifold at the bottom of the packed tower. At a position just before the manifold was an opening in the line, fitted with a cork holding a thermometer. This thermometer could be fitted with a wick, and thus wet and dry bulb temperatures of the air were monitored.

The manifold was made of an 8 inch length of 12 inch stovepipe,

attached to a flange and fitted with a cap. From this manifold the air passed into the packing through the four capped and notched brass pipes described previously.

After leaving the packing the air flow was drawn out from the side of the tower section between the packing and the water distributor plate. This line led to an inlet to a nearby drying tunnel, the blower of which was used to force the air into the chimney.

Pressure taps for measuring the pressure drop across the packing were located in the upper nipple leading to the Tygon level indicator and in the wall of the tower section above the packing. Low pressure drops were measured using an inclined manometer.

13.1.3 Auxiliaries

The steam line leading to the injection tee was made of 1/2 inch brass pipe, insulated with asbestos tape and equipped with a blowdown drain so as to prevent slugs of condensate from entering the water line and causing pulsations.

The solute gas passed through one of two calibrated capillary flow meters before entering the injection tee. One meter, used for lower flow rates, consisted of a 2 inch length of 1-1/4 mm. Pyrex capillary tubing, while the other meter, used for higher flow rates, was made of a 2 inch length of 2-1/2 mm. Pyrex capillary tubing.

13.2 Procedure

Before any runs were made with the apparatus, a solution of Calgon and Lakeseal laboratory detergent was pumped through the system to remove solder flux, etc. Many rinsings followed this.

Before actual absorption runs were made at a given set of flow conditions, pressure drop measurements were made by varying the air flow rate at constant water flow rate. This served to indicate the regimes of operation (i.e., below loading, at loading, or at flooding).

The first three mass transfer runs indicated that it was necessary to allow 15 minutes of preliminary operation to establish the water hold-up on the packing. The best procedure appeared to be to use a water flow 50% higher than the flow rate for the run during the preliminary operation. Then, when the flow rate was reduced to the desired value, the hold-up would quickly reach its equilibrium value. If this hold-up establishment were not allowed for, there was a tendency for mass transfer coefficient to increase with time.

When the liquid flow was returned to the operating value, the solute gas was injected into the water line. The valves in the water line were usually so set as to give a pressure of about 8 psig, while the reduction valve on the solute gas cylinder would be set to deliver an exit pressure of about 15 psig. The solute gas flow rate would be set at about 1-1/2 times the amount equivalent to the solubility of air in the water at the operating water flow rate, or at about 1-1/2 times the solubility of the solute gas in the water, whichever was higher.

The former provision was necessary in order to account for the air already in the water which had to be driven from solution, and was quite an important factor in the cases of more insoluble gases, such as helium. It was found that the passage of small amounts of undissolved gas through the water orifices did not alter their calibrations.

Steam was injected into the water stream at the rate necessary to maintain it at a temperature of 25°C. Steam and water rates into the spray tower were set so as to give wet and dry bulb temperatures of air close to 25°C. The drain valve from the spray was adjusted so as to maintain a level of water about 3 inches above the bottom, as indicated by a Tygon level gauge. The height of the leveling tee in the exit water line from the tower was adjusted to bring the pool level to the desired height, about 1/2 inch below the notches delivering the air to the tower. Barometric pressure was recorded.

From the barometric pressure and the room wet and dry bulb temperatures the pressure drop over the inlet air orifice necessary to produce the desired flow rate of air through the tower was computed (see Section 16.3.6), and the air flow rate was adjusted to this value by controlling the field rheostat in the blower motor circuit.

After ten minutes of steady operation, samples were taken of the inlet and exit water streams. At this same time the water and air temperatures and, in the case of an oxygen run, the pressure in the tower were recorded. For an oxygen run the samples were taken by placing

the opening of the sampling hose in the bottom of a 250 ml. glass-stoppered Erlenmeyer flask and allowing at least 10 flask volumes to be swept through (about 20 seconds). The flask was then immediately restoppered. Since at low water flow rates the sample stream from the top of the tower amounted to a significant portion of the total flow rate, the bottom sample was taken first, and the top sample immediately afterward. Had the sampling been done in the reverse manner, or simultaneously, the act of sampling the inlet water would have affected the solute concentration in the exit water.

For the other four solute gases, sampling was effected by flowing the sampling stream through sampling bulbs of about 90 cc. volume, equipped with stopcock arms on either end. Again at least 10 sweepout times were allowed, equivalent to about 2 minutes. In this case sampling of both streams was simultaneous since the sample flows never amounted to more than 2% of the main stream flows.

At least one more set of samples was taken at least 5 minutes after the first. Again conditions were recorded.

There was no perceptible fluctuation in the air flow rate; hence its reliability was dependent solely on the standard orifice data, and the accuracy of the temperature, humidity and pressure measurements. The absolute values reported were probably reliable to within 5%, with much less error when taken relative to one another. The error in the

water flow rate came from the orifice calibration and from long time fluctuations in flow during the run, the latter factor being probably more important. Thus the water flow rates probably tended to average out to accurate absolute values, but fluctuations from run to run or within a run of a maximum of about 5% occurred.

Runs 1 through 4 were made with an effective packed height of 2 feet. One foot of packing was then removed from the column and runs 5 through 49 were carried out. Following this the column was emptied and then repacked with the same number of packing pieces to a 1 foot effective height for runs 50 through 67. Another foot of packing was added for runs 68 through 70. In the first 5 runs the pool height was held at the bottom of the air inlet notches. For the rest of the runs it was held $1/2$ inch lower.

Runs 59, 60, 61, and 67 were made at varying temperatures; in all other runs temperatures were held constant at 25°C. Runs 47-49 were made using tap water that had been deaerated by adding steam until the temperature reached 60°C. This water was cooled overnight before use, with plastic films being floated on the open surface to prevent redissolution of air (see Chapter 12).

Calculational methods and methods of averaging the data are discussed in Chapter 16.

CHAPTER 14DIFFUSIVITY MEASUREMENTSOutline

- 14.1 Introduction
- 14.2 Methods of Measurement of Liquid Phase Diffusivities
 - 14.2.1 Techniques Used in the Past
 - 14.2.2 The Diaphragm Cell
- 14.3 Description of Apparatus
- 14.4 Experimental Procedure
 - 14.4.1 Cleansing and Loading of Cells
 - 14.4.2 Sampling and Analysis
- 14.5 Theory of the Diaphragm Cell
 - 14.5.1 Idealized Theory, Diffusivity Independent of Concentration
 - 14.5.2 Diffusivity a Function of Concentration
 - 14.5.3 Finite Hold-up in the Frit
- 14.6 Experimental Results
 - 14.6.1 Calibration of Cells
 - 14.6.2 Experimental Determinations
- 14.7 Discussion of Results
 - 14.7.1 Comparison with Literature
 - 14.7.2 Thermal Pumping
 - 14.7.3 Imperfect Mixing
 - 14.7.4 Surface Transport
 - 14.7.5 Presence of Gas Bubble
 - 14.7.6 Supersaturation
 - 14.7.7 Analytical Errors
 - 14.7.8 Data of Gertz and Loeschcke
- 14.8 Wetted Wall Data on Chlorine Diffusivity

14.1 Introduction

The analysis of the experimental desorption data presented in this thesis requires an accurate knowledge of the diffusivities in water of the various solute gases. Because of difficulties in experimental technique and a lack of theoretical knowledge of the liquid state very few reliable values of liquid diffusivities are available and only empirical or semi-empirical correlations of data for different solutes and solvents have been made.

The field in general and such correlations as have been suggested are covered by Reid and Sherwood (116b). Three main correlations are available:

1) Wilke and Chang (163, 164)

$$D_L = 7.4 \times 10^{-8} \frac{(\gamma M)^{1/2} T}{\mu V_1^{0.6}} \quad (14.1.1)$$

where D_L = liquid phase diffusivity (cm.²/sec.)

γ = an association parameter for the solvent, values of which are given for water and various organic solvents (164).

M = molecular weight of the solvent

T = absolute temperature (°K)

μ = solvent viscosity (cp.)

and V_1 = molal volume of the solute at the normal boiling point (cm.³/g-mol.). This may be obtained from the atomic volumes of LeBas (116b).

2) Scheibel (118)

$$D_L = 8.2 \times 10^{-8} \frac{[1 + (3V_2/V_1)^{2/3}] T}{\mu V_1^{1/3}} \quad (14.1.2)$$

where V_2 = molal volume of the solvent at the normal boiling point
($\text{cm.}^3/\text{g-mol.}$)

3) Othmer and Thakar (105, 116b)

$$D_L = \frac{14.0 \times 10^{-5}}{V_1^{0.6} \mu_2 \mu_w (1.1 \Delta H_{v2} / \Delta H_{vw})} \quad (14.1.3)$$

where μ_w = viscosity of water at required temperature (cp.)

μ_2 = viscosity of solvent at 20°C (cp.)

ΔH_{vw} = latent heat of vaporization of water at required temperature (cal./g-mol.)

ΔH_{v2} = latent heat of vaporization of solvent at required temperature (cal./g-mol.)

The correlations of Wilke and Chang and of Scheibel are based on the prediction of the Stokes-Einstein equation for the diffusion of large hard spheres in a viscous liquid,

$$D_L = \frac{k T}{6 \pi \mu r}, \quad (14.1.4)$$

(where k = Boltzmann's constant

and r = radius of sphere)

that the factor $\frac{D_L \mu}{T}$ should be a constant for a given solute-solvent system. The difference between the two correlations lies in Scheibel's use of the solvent molal volume in place of Wilke and Chang's solvent association parameter.

The correlation of Othmer and Thakar, on the other hand, is based on the observation that the solute diffusivity and solvent viscosity of a liquid system are similar functions of the solvent vapor pressure, and that there appears in most cases to be a constant ratio of diffusivity activation energy to viscosity activation energy. It thus is an empirical application of the activation energy concept resulting from Eyring's hole theory (95a).

For the diffusion of solutes in water all three correlations give average deviations from experimental values on the order of 10%, when considered for all solutes for which reliable data have been given. In general for smaller or lighter solute molecules (such as the gases studied in this thesis) the deviation is somewhat greater.

Actual experimental results are available for only three of the five solute gases studied (carbon dioxide, oxygen, and hydrogen), and of the three only the data for carbon dioxide and oxygen show any kind of internal consistency from investigator to investigator and method to method. These previous experimental results are covered in more detail in Section 14.7.1.

It is apparent, therefore, that an experimental study of the diffusivities of the solute gases was warranted. Experimental values for two of the gases were entirely lacking. Because of the accurate values required to obtain reliably the mode of variation of transfer coefficient with diffusivity in the packed column, such correlations for prediction as there are were inadequate. The results of such a study would also eliminate the problem of comparing and using diffusion coefficients obtained by different investigators employing different methods.

The experimental values of liquid phase diffusivities were measured before experimental work on the packed tower was begun, in order to verify that the chosen gases were ones showing as wide a variation of diffusivity from one to another as was possible to obtain at a given single temperature.

14.2 Methods of Measurement of Liquid Phase Diffusivities

14.2.1 Techniques Used in the Past

A discussion of several of the techniques used for the measurement of the diffusivities of gases in liquids prior to 1950 and their reliability has been given by Peaceman (107b). Briefly, these include:

1. Unsteady state diffusion into the solvent, which is contained in a capillary tube. The use of capillary tubes tends to eliminate convective transfer from vibration and other sources, which can

easily give transfer in addition to that from diffusion. In first using this method for measuring the diffusion of carbon dioxide, Wroblewski in 1877 (166) found that the denser solution formed by the solute entering at the top of the capillary tended to sink and thus provided a strong added tendency for convective mixing. Later Stefan (141) found that this effect could be minimized by making the diameter of the tube sufficiently small (a maximum of 1 mm.). For slightly soluble gases, however, this necessitates a very small transfer rate, and therefore for sufficient accuracy excessively long times are required for runs. There is also a question concerning the exact area presented by the liquid-gas interface at the top of the capillary tube. The only recent work using this technique for slightly soluble gases has been done by Ringbom (117).

2. The layer method. This technique was used by Carlson (11) to study dissolved gases. The method consisted of starting with separate solutions containing different concentrations of the solute gas. The density of one solution was increased by the dissolution of potassium chloride in it. The vessel containing the lighter solution was then placed on top of that containing the heavier. The vessels were so constructed that a run was started by removing a membrane that separated the solutions. The density difference would then stabilize the system. After a run was started the solutions were allowed to mix by diffusion in a constant temperature, vibration free room.

The primary difficulty in this method seems to come from the elaborate precautions necessary to prevent convection arising from vibration, as it requires very little vibration to produce a very significant effect on a measured diffusivity. There is a simultaneous diffusion of potassium chloride, which may well have affected the transfer of the solute gas, and there is the question of the effect of potassium chloride concentration on the solute gas diffusivity.

3. Diffusion into gel solutions. In an effort to control convective mixing during a diffusion measurement Hagenbach (53) and later Tammann and Jessen (148) studied the diffusion of solute gases into gel solutions. Hagenbach investigated the diffusion of oxygen and obtained an extremely high diffusion coefficient (about 7.5×10^{-5} cm.²/sec. at 25°C). The results of Tammann and Jessen for oxygen in 2% agar solution are also high in comparison to the rest of the literature (3.5×10^{-5} cm.²/sec. at 25°C). The reason for both these high results appears to lie in a reaction between the oxygen and the gel structure. The data of Tammann and Jessen for other solutes, including carbon dioxide and hydrogen, are more in line with the rest of the literature (see Section 14.7.1). The principal disadvantages of this method lie in the possibility of some sort of reaction with the gel structure and in the necessity of making an often indefinite correction for the effect of the increased viscosity of the gel on the diffusivity of the solute gas.

4. The diaphragm cell. This was the technique employed in this investigation, and is covered in detail in Section 14.2.2.

In addition to these methods two others have come into use recently, and it is claimed by their proponents that they give results that are more accurate than those obtained by older techniques:

1. Polarography. Solute gases which undergo a reaction at an electrode placed in the solution may be studied by means of a cell polarogram (current vs. voltage curve). If conditions in the cell are correctly controlled there will be a portion of the curve where the current is essentially limited by mass transfer to (or from) the electrode alone. Kolthoff and Miller (77) have studied the diffusivity of oxygen in this manner with a mercury dropping electrode, and Aikazyan and Fedorova (2) have measured the diffusivity of hydrogen in various acid and base solutions with a rotating platinum electrode.

As would be expected the limitations of the method are in obtaining a system for which the transfer process is well known and is completely limiting. There is again the problem of the effect of the concentration of other solutes in solution on the diffusivity of the solute gas. Also, obviously, the method is limited to the study of those gases which will undergo an electrode reaction in aqueous solution.

2. Penetration into laminar flow. It has long been felt that if conditions are well controlled wetted wall columns will conform to laminar penetration theory for liquid phase resistance to gas absorption. Since liquid phase resistance is entirely controlling for slightly soluble gases, such as those under investigation in this thesis, the diffusivities of such gases in water should then be predictable from wetted wall column data, provided penetration theory is obeyed by the column.

In wetted wall studies, however, it has been found for long columns that there is a tendency for surface waves and various other turbulences to arise, even at the lowest Reynolds numbers of liquid flow (9, 32, 51, 142, 149*). These turbulences and waves can evidently be eliminated to a large extent for short wetted wall columns; however for cylindrical and rectangular geometries a significant end effect due to the liquid take-off system arises (10, 87, 157), which is evidenced visually by a band of ripples 1 or 2 cm. from the bottom of the column and is believed to act as an equivalent amount of "dead" surface. This phenomenon has also been noticed in falling jets (18).

Davidson and Cullen (23), however, claim to have eliminated

* - Ref. 149 contains a bibliography of earlier studies.

these effects by employing liquid flow over a single sphere. Penetration of several slightly soluble gases into this liquid film was studied, and the diffusivities found by curve fitting. Monitoring of the closed system was done by taking the differences between inlet and outlet gas rotameter readings. The theory for penetration into flow over a sphere is presented (23), and resolves into the equation for flow over a flat surface with a suitable change of variables.

Sources of error here lie in the possibility of turbulence, end effects, or other phenomena not accounted for in the theoretical analysis, and in their effect on the curve fitting. Nijsing, et al, (99) and Kramers, et al, (78) have used a short wetted wall column for such a study, claiming to eliminate the end effect through the addition of a surface active agent to the water. A critical examination of their results and those of Davidson and Cullen (23) is made in Section 14.8.

Gertz and Loeschcke (41) have measured the rise of bubbles of several slightly soluble gases in water (and blood serum) flowing downward through a conical tube. They claim that the transfer of gas to liquid (which may be readily related to the rate of bubble rise) is proportional to the first power of the liquid phase diffusivity, and thus ratios of one diffusivity to another may be calculated from their studies. In actuality their transfer

mechanism appears to be more complex than they have assumed, and the variation with the first power of diffusivity is questionable (see Section 14.7.8).

14.2.2 The Diaphragm Cell

The diaphragm cell has been used extensively for the study of the diffusivities of electrolytes and other nonvolatile solutes. Only two previous investigators (107b, 124), however, have employed it for highly volatile solutes.

The principle of the technique is the restriction of the diffusion process to one occurring through a fritted glass disc, either side of which is in contact with a large mass of well stirred solution, the concentrations of solute in contact with either side being different from one another. If the masses of solution are much bigger in volume than the disc, a steady state diffusive transfer through the disc from the rich side to the lean side is quickly established.

The prime advantage of the diaphragm cell lies in the constrictive influence of the fritted glass on the solution in which the transfer is taking place. Convective transfer, because of the size of the pores, is almost completely absent. It might be expected that the use of the fritted disc would introduce a surface effect, but this, too appears to be absent under ordinary conditions. (See Section 14.7 for a fuller discussion of the various sources of error which may enter in using

the diaphragm cell for the study of the diffusivity of gaseous solutes).

The fritted disc method was originally devised by Northrup and Anson (100) in 1928 and was taken up shortly thereafter by several others who made extensive studies on electrolytes and other nonvolatile solutes. Their apparatus consisted usually of a vessel with a fritted glass bottom. This vessel was filled with rich solution, and placed in a larger vessel of lean solution in such a way that the fritted bottom just touched the surface of the lean solution.

Later workers have used a completely closed vessel, with the fritted disc in the center dividing the cell into two compartments in order to ensure thorough stirring of the two solutions and complete wetting of the fritted glass and to guard against solute loss through such volatility as the solute has, (41, 47, 98, 107b, 143). Some investigators have felt "density" stirring was adequate to keep the cell sides homogeneous (47, 107b); others have devised various stirring devices (often quite elaborate) for this purpose (82, 98, 143). A fuller discussion of the mixing problem is given in Section 7.3.

The diaphragm cell must be calibrated with a substance of known diffusivity, whereas other methods (Section 14.2.1) are absolute in that they do not require this. Recently, however, very reliable data for the diffusivity of potassium chloride have become available (see Section 14.5.2) and this necessity of calibration is no longer a drawback.

It has been claimed, too, that the calibration of the cell is dependent strongly on solution viscosity (47, 82) and possibly even on solute diffusivity itself if vigorous stirring is not used (82). This is thought to be caused by the existence of a laminar film or, probably more correctly, a boundary layer region on either side of the disc. The viscosity effect does not enter for a case where solution viscosity is practically invariant, such as was the case in the present study of very dilute water solutions. The other problem, possible variation with solute diffusivity, appears to be one only of mixing efficacy, and is considered in Section 14.7.3.

As was mentioned previously, all other determinations of the liquid phase diffusivity of solute gases save two (107b, 124) have been made by techniques other than the diaphragm cell. This has been primarily because use of the diaphragm cell requires that the two solutions be sampled and the concentrations of solute therein be determined analytically. With slightly soluble gases sampling without solute loss is a problem (107b), and concentrations have been difficult to measure. It was felt, however, that the present cell design (see Section 14.3), enabling the liquid sample to be enclosed by mercury at all times before the "fixation" or removal of the solute gas, eliminated the sampling problem and that the use of the solute gas removal apparatus and the vapor fractometer for analysis (Chapter 15) would facilitate the determination of such gases as helium and hydrogen for which it would otherwise be quite difficult to analyze.

14.3 Description of Apparatus

The two diaphragm cells built and used for this investigation are similar in nature and size to those originally built by Chang (14) for measuring the diffusivities of nonvolatile solutes; later used by Peaceman (107b), Goldstein (44), and Olander (101); and still in use by the M.I.T. Chemical Engineering Department. A drawing of the present cells is shown in Figure 14.1.

The primary distinction between these cells and the ones used previously lies in the inclusion of two sampling arms on each cell side, each arm enclosed by a stopcock. Chang's cells had a single arm with a stopcock on the very bottom of the cell and an open arm on the top which could be closed only by clamped rubber tubing. Sampling thus had to be effected by an elongated pipette, even for the study of solute gases (107b). This was a definite disadvantage.

The cells were constructed from Pyrex sealing tubes with a Grade F (fine) frit and Pyrex stopcocks by the glass blowing firm of Ryan, Velluto, and Anderson. The volume of each cell side was about 90 cc.

Peaceman (107b) utilized the results of Stokes (143), Hartley and Runnicles (57), and Dawson (25) to show that this grade frit allows no convection and yet apparently shows no surface effects on the transport process.

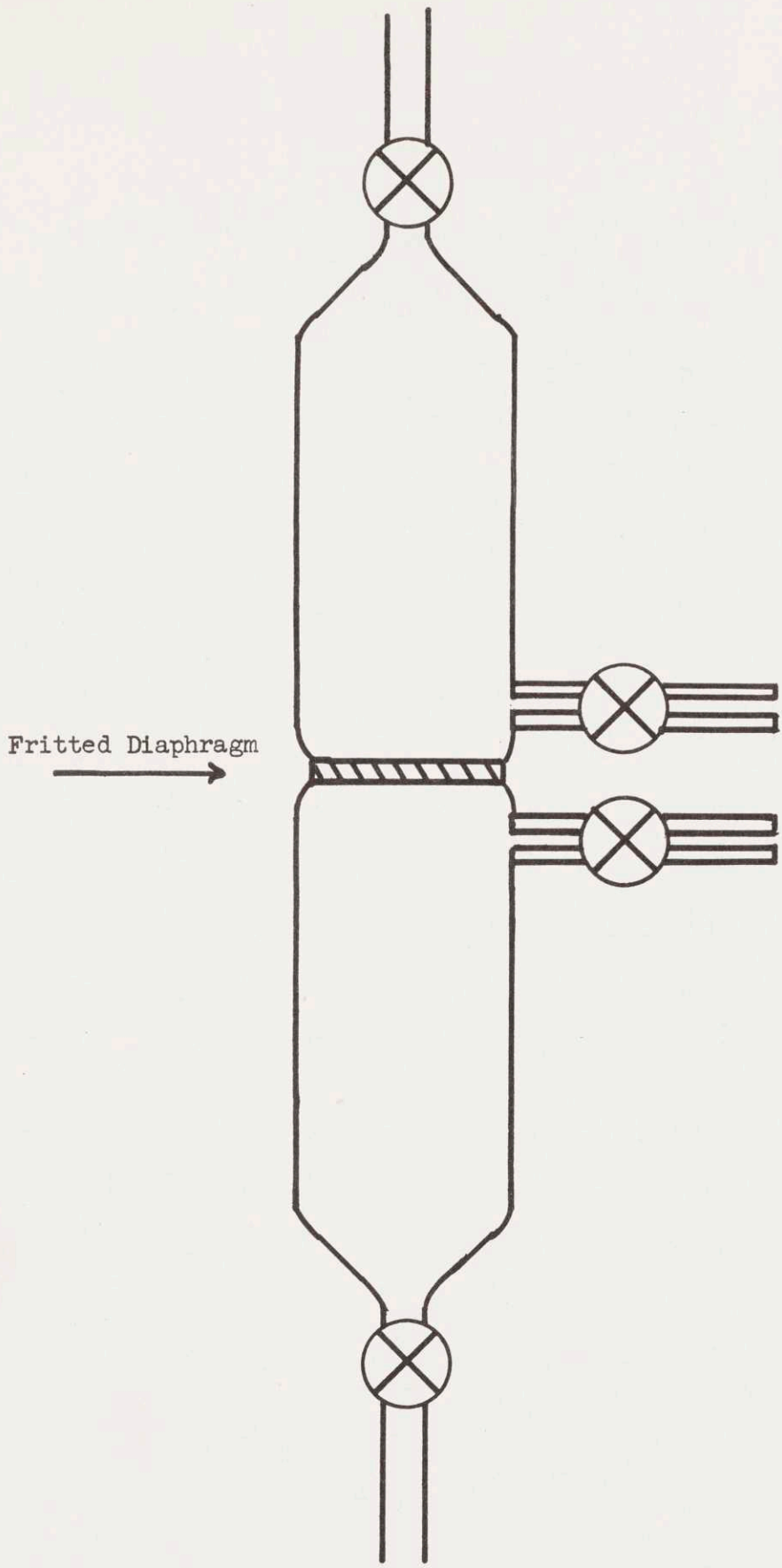


FIGURE 14.1 DIAPHRAGM CELL FOR MEASURING DIFFUSIVITIES

These cells were fitted with corks, which were placed on the top arm, and were held thereby with clamps in a 4 gallon Cenco Catalog No. 97100B constant temperature bath. Since runs were being made during the summer months, a cooling loop was made of 1/4 inch copper tubing, with about three feet of coil length immersed. Tap water was continually fed through the loop at approximately 1 to 2 liters/min. to maintain the bath temperature at 25°C. This arrangement instead of holding a temperature $\pm 0.02^\circ\text{C}$, as advertised, gave a variation of $\pm 0.1^\circ\text{C}$ during a typical 2 minute heating-cooling cycle, but this was felt to be desirable for mixing reasons (see Section 14.7.3).

14.4 Experimental Procedure

The cells were first calibrated by studying the diffusion of 0.1N KCl into pure water. Following this, runs were made for each of the solute gases, at least four being made for each, and more for those for which the results tended to scatter. At the conclusion of the experimental program the cells were recalibrated with KCl. All runs were made at 25°C, since this was the primary temperature for the packed column investigation.

The frit was thus initially solute-free in all cases. This was felt to be a much more reliable starting condition than the existence of an initial linear gradient within the frit (see Section 14.6.1).

At the conclusion of a run, the cell was removed from the bath,

and analyses were made immediately of the solute concentrations on either side.

During calibration and during most of the rest of the runs one or the other of the cells would be allowed to receive considerable vibration from the bath stirrer; this was done to detect any possible effect of vibration on the mixing and resulting apparent diffusivity in that cell. In addition, for the case of propylene, an exploratory run (not presented because a less accurate analytical technique was employed) was made with both cells inverted.

14.4.1 Cleansing and Loading of Cells

Before each run was made the cells were washed with distilled water (an organic solvent would tend to dissolve stopcock grease to an extent and might thereby foul the disc): The top side was rinsed three times, several cc. of water were pulled through the disc three times from top to bottom by vacuum, and then the lower side was rinsed three times. Following runs where analyses had been made with mercury pumping, care was taken to provide that all mercury and mercury scum was removed from the cell. Similarly, following an oxygen analysis the disc was rinsed by pulling through H_2SO_4 - KI solution to ensure removal of any iodine or manganous hydroxide accumulated; then the distilled water washing was carried out.

For potassium chloride runs, the bottom side of the cell was

completely filled with freshly distilled water. During this loading several cm.³ of water were sucked through the disc to make sure no undissolved air was left in it. The top side of the cell was then rinsed with 0.1 N potassium chloride solution, and filled with solution from a burette to a volume equal to that of the lower side.

For propylene, helium, and hydrogen runs the bottom side of the cell was filled as in the potassium chloride runs. The top side was then loaded with a concentrated solution of the gas in freshly distilled water, prepared by bubbling the gas vigorously through the water for several minutes in a two arm bulb. The cell was shaken to make sure the small gas bubble left inside the top cell (to guard against large pressure buildups which might otherwise result) was in equilibrium with the solution.

For carbon dioxide runs this same procedure was followed with degassed, distilled water being used for the bottom side, which was swept out with carbon dioxide-free air before loading. This was done since a very small amount of carbon dioxide initially present in the lean side could have a large effect on the result.

For oxygen runs, degassed distilled water was prepared, cooled under a nitrogen atmosphere, and kept covered with toluene. The bottom side of the cell was then swept with nitrogen for five minutes or more. The rubber tubing that had connected the cell to the nitrogen

cylinder was then removed and covered on the free end to exclude oxygen. This tubing was then used to siphon the degassed water into the cell. The top side was loaded as it was for the other gases.

14.4.2 Sampling and Analysis

For all runs except those for oxygen, the sample was taken by mercury pumping - allowing the mercury to come up through the end arm from a leveling bulb and force the sample out through the capillary arm either through a jet to the collection solution (carbon dioxide) or to the solute gas separation apparatus (propylene, helium, and hydrogen). Preliminary practice made it possible to eliminate any perceptible sucking or forcing of solute through the disc during the mercury pumping. Since any tendency there was for this appeared to be for forcing to the other side of the cell, the lean side was always sampled first, making the error from this effect very small.

The actual analytical techniques employed are described in Chapter 15.

14.5 Theory of the Diaphragm Cell

14.5.1 Idealized Theory, Diffusivity Independent of Concentration

The idealized theory of the diaphragm cell has been presented by Gordon (47), Peaceman (107b) and many others. In essence, the following assumptions are made:

1. Both sides of the cell are perfectly mixed (mixing times in the bulk solutions are much faster than the rate of diffusion through the disc).
2. The hold-up volume of the disc is negligibly small, so that there is no effect on the overall material balance of solute and a linear gradient is established in the disc immediately and maintained; i.e., there is always steady-state diffusion.
3. There is no bulk flow of solvent through the disc.
4. The disc may be considered as a series of parallel pores in the direction of diffusion.
5. The diffusivity of the solute is not a function of its concentration.
6. The volumes of either side of the cell are equal. Since there is a linear gradient in the disc, and concentrations are maintained uniform in either side of the cell, the rate of transfer must be

$$V \frac{dC_2}{dt} = -V \frac{dC_1}{dt} = s D_L \frac{C_1 - C_2}{l} \quad (14.5.1)$$

where V = the volume of each side of the cell

C_1 = the concentration of solute on the rich side

C_2 = the concentration of solute on the lean side

s = the effective cross-sectional area of the pores
of the disc

ℓ = the effective length of the pores of the disc
 and D_L = the liquid phase diffusivity

If C_2 is zero initially,

$$C_2 = C_{1o} - C_1 \quad (14.5.2)$$

by material balance. Equation (14.5.1) may then be solved to give

$$\ln \frac{C_{1o}}{2 C_{1f} - C_{1o}} = \frac{2s}{\ell V} D_L t_f \quad (14.5.3)$$

or

$$\ln \frac{\Delta C_o}{\Delta C_f} = \beta D_L t_f \quad (14.5.4)$$

where t_f = time elapsed before measurement of concentrations

$$\Delta C = C_1 - C_2$$

$$\beta = \text{"cell constant"} = 2s/\ell V$$

and the subscripts o and f refer to initial and final conditions respectively.

Should the volumes of the two sides of the cell not be equal to one another (assumption 6 not valid), Equation (14.5.1) is modified to become

$$V_2 \frac{dC_2}{dt} = -V_1 \frac{dC_1}{dt} = \frac{s D_L}{\ell} (C_1 - C_2) \quad (14.5.5)$$

and Equation (14.5.2), to become

$$V_2 C_2 = V_1 (C_{10} - C_1) \quad (14.5.6)$$

where V_1 and V_2 are the volumes of the rich and the lean sides respectively. The solution is now

$$\ln \frac{\Delta C_o}{\Delta C_f} = \frac{s}{\ell} \left(\frac{1}{V_1} + \frac{1}{V_2} \right) D_{L} t_f \quad (14.5.7)$$

where C_o is determined by use of Equation (14.5.6)

$$\Delta C_o = C_{1f} + \frac{V_2}{V_1} C_{2f} \quad (14.5.8)$$

Comparison of Equation (14.5.7) with Equations (14.5.3) and (14.5.4) shows the only difference to be in the factor

$\frac{1}{2} \left(\frac{1}{V_1} + \frac{1}{V_2} \right)$. Denoting this factor by γ , we have

$$\ln \frac{\Delta C_o}{\Delta C_f} = \gamma \beta D_{L} t_f, \quad (14.5.9)$$

where

$$\gamma = \frac{V_2}{2} \left(\frac{1}{V_1} + \frac{1}{V_2} \right) = \frac{1}{2} \left(\frac{V_2}{V_1} + 1 \right) \quad (14.5.10)$$

($\gamma = 1.0$ for equal volumes), assuming the β of the cell was calibrated for equal volumes, equal to V_2 , as was done in the present experimental work.

In practice it was necessary to add refinements, discussed and derived in Section 14.5.3, for interpretation of the experimental results since assumption 2 above proved to be an over-simplification.

14.5.2 Diffusivity a Function of Concentration

In cases where the diffusivity of the solute is not invariant with respect to concentration over the range of concentrations encountered in the cell an "integral" value of the diffusivity must obviously be employed rather than the "differential" value at any one concentration. The theory of the diaphragm cell for these cases has been discussed at length by Stokes (143), Gordon (47), and Peaceman (107b). In resume, their approach is as follows:

Since all the assumptions save number 5 may be retained for this case, we may say that the transfer rate is constant at any time at all points within the disc, or

$$\frac{d}{dx} \left(D_L \frac{dC}{dx} \right) = 0 \quad (14.5.11)$$

where \underline{x} is the linear distance traveled in the direction of diffusion in the disc. Two integrations with respect to \underline{x} give

$$\int_{C_1}^{C_2} D_L dC = k l \quad (14.5.12)$$

where \underline{k} is a constant with respect to \underline{x} (not with respect to \underline{t}) and

is equal to the transfer rate at time t . Since D_L is a function of C the value of k will be dependent upon time, varying as the values of C_1 and C_2 vary. This transfer rate introduced into Equation (14.5.1) gives

$$v \frac{dC_2}{dt} = -v \frac{dC_1}{dt} = s k = \frac{s}{l} \int_{C_1}^{C_2} D_L dC \quad (14.5.13)$$

Substituting in the initial-final material balance, Equation (14.5.2), yields

$$-v \frac{dC_1}{dt} = \frac{s}{l} \int_{C_1}^{C_{10} - C_1} D_L dC \quad (14.5.14)$$

or

$$\int_{C_{1f}}^{C_{10}} \frac{dC_1}{1/2 \int_{C_1}^{C_{01} - C_1} D_L dC} = \frac{2s}{lV} t_f = \beta t_f \quad (14.5.15)$$

This may be compared with a form involving an "integral" diffusivity, $D_{L \text{ int}}$, and similar to Equation (14.5.4)

$$\frac{1}{D_{L \text{ int}}} \ln \frac{\Delta C_o}{\Delta C_f} = \frac{1}{D_{L \text{ int}}} \ln \left(\frac{C_{10}}{2C_{1f} - C_{10}} \right) = \beta t_f \quad (14.5.16)$$

Comparison with Equation (14.5.15) shows that for a given value of C_{10} , the value of $D_{L \text{ int}}$ is a function of C_{1f} (or ΔC_f) alone, and may hence be determined through a graphical integration, if the variation of D_L with C is known. Such an integration was carried out by Peaceman (107b) for the diffusion of potassium chloride with an initial molarity of 0.1 into water initially free of the salt. Using the data of Harned and Nuttal (56) for the diffusivity of potassium chloride as a function of concentration at 25°C, he obtained a value of $D_{L \text{ int}}$ equal to 1.872 cm.²/sec. for ΔC_f between 0.078 M and 0.090 M, the conditions encountered in the present experiments. Later calculations made by Stokes (145) using the newer data of Gosting (50), which were obtained by means of a Gouy interference technique, verify this value.

14.5.3 Finite Hold-up in the Frit

Equation (14.5.4), developed for the relationship between diffusivity and the variation of concentrations with time, is based upon the assumption (Number 2), among others, that there is no hold-up in the disc and as a result no transient period at the beginning of a run when a linear concentration gradient has not yet been established in the disc.

The calibration results of Section 14.6.1 show, however, that the volume of liquid held in the disc is on the order of 2% of the volume of a side of the cell, and that the amount of diffusing solute held in the disc at the end of a run is from 10 to 15% of the amount that has actually reached the lean side of the cell. The effect of this finite hold-up

may then be quite significant.

If the problem is taken to be that of unsteady-state diffusion of a solute through a "slab" of length, l , with either side in contact with volumes, V , of solvent that are maintained uniform in concentration throughout at all times, the governing differential equation for solute transfer is

$$D_L \frac{\partial^2 c}{\partial x^2} = \frac{\partial c}{\partial t} \quad (14.5.17)$$

and the boundary conditions are

$$\text{at } x = 0 \text{ and } t = 0, \quad C_1 = C_{10} \quad (14.5.18)$$

$$\text{at } x = l \text{ and } t = 0, \quad C_2 = 0 \quad (14.5.19)$$

and at all x and $t > 0$,

$$V (C_1 + C_2) + s \int_0^l c \, dx = V C_{10} \quad (14.5.20)$$

where C_1 = concentration of solute in rich side at any time,

C_2 = concentration of solute in lean side at any time,

and s = effective cross-sectional area of the disc pores. The

boundary conditions state that the original lean side solute concentration

is zero, a requirement fulfilled in all the present determinations.

Barnes (6) has presented the solution of Equation (14.5.17) for these conditions as

$$c_1 = \frac{c_{10}}{2} \left[\left(1 - \frac{\lambda}{2} + \dots\right) + \left(1 - \frac{\lambda}{6} + \dots\right) \exp \left\{ - \frac{2 \lambda D_L t}{l^2} \right. \right. \\ \left. \left. \left(1 - \frac{\lambda}{6} + \dots\right) \right\} + \sum_{i=1}^{\infty} \frac{4 \lambda}{i^2 \pi^2} \left(1 - \frac{6 \lambda}{i^2 \pi^2}\right) \exp \left\{ - \frac{D_L t}{l^2} (i^2 \pi^2 + 4 \lambda) \right\} \right] \quad (14.5.21)$$

and

$$c_2 = \frac{c_{10}}{2} \left[\left(1 - \frac{\lambda}{2} + \dots\right) - \left(1 - \frac{\lambda}{6} + \dots\right) \exp \left\{ - \frac{2 \lambda D_L t}{l^2} \right. \right. \\ \left. \left. \left(1 - \frac{\lambda}{6} + \dots\right) \right\} - \sum_{i=1}^{\infty} (-1)^i \frac{4 \lambda}{i^2 \pi^2} \left(1 - \frac{6 \lambda}{i^2 \pi^2}\right) \exp \left\{ - \frac{D_L t}{l^2} (i^2 \pi^2 + 4 \lambda) \right\} \right] \quad (14.5.22)$$

where $\lambda = s l / v$.

From these equations, omitting higher order terms of series which for the low values of λ encountered in the present work are negligible,

$$\frac{\Delta C_f}{\Delta C_o} = \left(1 - \frac{\lambda}{6}\right) \exp \left\{ -\frac{2\lambda}{l^2} \frac{D_L t_f}{\pi^2} \left(1 - \frac{\lambda}{6}\right) \right\} + \sum_{\substack{i=2 \\ i \text{ even}}} \frac{4\lambda}{i^2 \pi^2} \left(1 - \frac{6\lambda}{i^2 \pi^2}\right) \exp \left\{ -\frac{D_L t_f}{l^2} (i^2 \pi^2 + 4\lambda) \right\} = \text{Term 1} + \text{Term 2}$$

(14.5.23)

where t_f is the time elapsed during the run.

For the cells utilized in this investigation the maximum values of λ and l^2 are 0.023 and 1.00 cm.², respectively. Using these values the magnitude of Term 2 in Equation (14.5.23) above may be determined relative to that of Term 1 as a function of $D_L t_f$. The results of such a calculation are shown in Table 14.1.

TABLE 14.1

<u>$D_L t_f$</u>	<u>Term 1</u>	<u>Term 2</u>
0.00 cm. ²	1.000	0.0033
0.10 cm. ²	0.997	0.000084

Since all values of $D_L t_f$ encountered in experimental runs were in the range of 4 to 8 cm.², Term 2 may in all cases be neglected.

Therefore any significant effect of finite hold-up must enter

through Term 1. Rearranging Equation (14.5.23) we have, neglecting Term

2

$$\frac{2 \lambda}{l^2} (D_L t_f) (1 - \lambda/6) = \ln \left(\frac{\Delta C_o}{\Delta C_f} \right) + \ln (1 - \lambda/6); \quad (14.5.24)$$

whereas Equation (14.5.3), which was derived for no hold-up, is

$$\frac{2s}{l^2 V} (D_L t_f) = \ln \left(\frac{\Delta C_o}{\Delta C_f} \right) \quad (14.5.3)$$

or

$$\frac{2 \lambda}{l^2} (D_L t_f) = \ln \left(\frac{\Delta C_o}{\Delta C_f} \right) \quad (14.5.25)$$

The factor $2 \lambda / l^2$ on the left hand side of these equations was used before as β , the cell constant, so the factor $(1 - \lambda/6)$ from the left hand side of Equation (14.5.24) should be included in β to account for finite hold-up. $\beta (1 - \lambda/6)$ thus becomes β^1 . Since β^1 remains the same in all calculations made for finite hold-up, both calibration and experimental, no error emanates from this -- another factor is merely added to the constant.

The remaining correction to be made depends on the magnitude of $\ln (1 - \lambda/6)$ in relation to that of $\ln (\Delta C_o / \Delta C_f)$, on the right hand side of Equation (14.5.24). The lowest value of $\ln (\Delta C_o / \Delta C_f)$ encountered in calibration or experimental runs was on the order of 0.14.

The value of $\ln(1 - \lambda/6)$ for the cells is approximately -0.003 (or $-\lambda/6$), and thus has an effect on the results. For this reason the term $\ln(1 - \lambda/6)$ was included in the calculations, and the equation employed to relate the concentrations, the elapsed time, and the diffusivity was

$$\beta^{-1} D_L t_f = \ln \left(\frac{\Delta C_o}{\Delta C_f} \right) + \ln(1 - \lambda/6) \quad (14.5.26)$$

where $\beta^{-1} = (2\lambda/l^2)(1 - \lambda/6)$ = the cell constant. ΔC_o was related to C_{1f} and C_{2f} by

$$\Delta C_o = (C_{1f} + C_{2f}) \left(1 + \frac{\lambda}{2} \right) \quad (14.5.27)$$

a material balance which allows for the solute held in the disc at the conclusion of a run.

Since the inclusion of the $\ln(1 - \lambda/6)$ term allows for the time of establishment of a gradient in the disc, it was deemed unnecessary to allow for a preliminary diffusion period of an hour or so before beginning a run. It was felt that the presence of no solute in the disc was a more reliable starting condition than the existence of a linear gradient for the study of slightly soluble gases, which are very easily stripped from solution.

For cases in which the volumes of the two sides were not made equal, the factor γ discussed in Section 14.5.1 was included with the calibrated value of β^{-1} in Equation (14.5.26)

$$\beta^{-1} D_L t_f = \ln \left(\frac{\Delta C_o}{\Delta C_f} \right) + \ln (1 - \lambda/6) \quad (14.5.28)$$

The effect of unequal volumes in the $\ln (1 - \lambda/6)$ term is second order and may be neglected. A correction for unequal volumes was also necessary, of course, in the material balance, Equation (14.5.27), which becomes

$$\Delta C_o = C_{1f} + V_2/V_1 C_{2f} + \frac{\lambda}{2} (C_{1f} + C_{2f}) \quad (14.5.29)$$

Negligible error is incurred by referring λ to the value of one of the volumes of the two cell sides for cases of unequal volumes, since volumes used in experimental work never differed by more than 3%.

14.6 Experimental Results

14.6.1 Calibration of Cells

The results of the four calibrational runs made for each cell with 0.1N potassium chloride solution are shown in Tables 14.2 and 14.3. Equal volumes of solutions were used in each side of the cells, since the solute was nonvolatile, and the presence of an air space above the solutions was not harmful. This permitted the use of Equation (14.5.26) for the calculation of values of β^{-1} . Values of λ were obtained through the use of the overall material balance, Equation (14.5.27). The value of D_L at 25°C was taken as 1.872×10^{-5} cm.²/sec. for potassium chloride, the "integral" value obtained as discussed in Section 14.5.2.

Here and elsewhere in the results of this chapter, the statistics for small numbers of observation of Dean and Dixon (26) are employed. This essentially means the median rather than the average of the data is used as the best value of a quantity (since it is less influenced by gross error in a single run). The range, multiplied by a deviation factor, K_w , related to the number of observations made, is used as a measure of the dispersion of the data, rather than the standard deviation. The range deviation is denoted by s_w . (see also Section 16.2) Values of K_w are given in Table 1 of the Dean and Dixon article. Values of s_m^2 , the variance of the median from the true value (see Section 16.2) are also given for each case.

In Table 14.2, below, values of λ , (s/l) , and $\ln(1 - \lambda/6)$ are obtained for the two cells by the material balance,

$$\Delta C_o = (C_{1f} + C_{2f}) (1 + \lambda/2) \quad (14.5.27)$$

The scatter in values obtained for λ is not a source of worry, since it is obtained as the difference between large numbers, and has only a second order effect in the calculational equations.

In Table 14.3 values of β^{-1} , the cell coefficient, s/l , s , and l are obtained for each cell through use of Equation (14.5.26).

In Table 14.4 the calibration constants obtained by recalibration at the conclusion of the experimental runs are presented.

TABLE 14.2

Determination of λ

Cell 1 $V_1 = V_2 = 90.3$ cc in all runs

<u>Run</u>	<u>C_{1o} (M)</u>	<u>C_{1f} (M)</u>	<u>C_{2f} (M)</u>	<u>λ</u>
1	0.1045	0.0955	0.00759	0.027
3	0.1043	0.0934	0.01012	0.015
5	0.1043	0.0953	0.00787	0.021
7	0.0999	0.0887	0.01003	0.024

$$\lambda = 0.023$$

$$\text{Deviation} = 26\%$$

$$s\lambda = 2.1 \text{ cc}$$

$$\ln(1 - \lambda/6) = -0.0038$$

Cell 2 $V_1 = V_2 = 87.8$ cc in all runs

<u>Run</u>	<u>C_{1o} (M)</u>	<u>C_{1f} (M)</u>	<u>C_{2f} (M)</u>	<u>λ</u>
2	0.1045	0.0959	0.00724	0.027
4	0.1043	0.0940	0.00950	0.015
6	0.1043	0.0960	0.00741	0.017
8	0.0999	0.0893	0.00951	0.022

$$\lambda = 0.019$$

$$\text{Deviation} = 32\%$$

$$s\lambda = 1.7 \text{ cc}$$

$$\ln(1 - \lambda/6) = -0.0032$$

TABLE 14.3

Calibration of Cells

Cell 1

Run	$\Delta C_o(M)$	$\Delta C_f(M)$	$\log\left(\frac{\Delta C_o}{\Delta C_f}\right)$	$\log\left(\frac{\Delta C_o}{\Delta C_f}\right) + \log(1 - \lambda/6)$	$t_f(\text{Min})$	$\beta^1(\text{cm.}^{-2})$
1	0.1045	0.08790	0.07513	0.07348	3951	0.0381
3	0.1043	0.08323	0.09800	0.09635	5392	0.0366
5	0.1043	0.08744	0.07657	0.07492	4020	0.0382
7	0.0999	0.0787	0.10360	0.10195	5527	0.0378

$$\beta^1 = 0.0380 \text{ cm.}^{-2} \quad \text{Deviation} = 2.1\%$$

$$s/l = 1.7 \text{ cm} \quad s = 1.9 \text{ cm.}^2 \quad l = 1.1 \text{ cm}$$

Cell 2

Run	$\Delta C_o(M)$	$\Delta C_f(M)$	$\log\left(\frac{\Delta C_o}{\Delta C_f}\right)$	$\log\left(\frac{\Delta C_o}{\Delta C_f}\right) + \log(1 - \lambda/6)$	$t_f(\text{Min})$	$\beta^1(\text{cm.}^{-2})$
2	0.1045	0.08862	0.07159	0.07020	4087	0.0352
4	0.1043	0.08451	0.09137	0.08998	5459	0.0338
6	0.1043	0.08861	0.07080	0.06941	4100	0.0347
8	0.0999	0.0798	0.09757	0.09618	5619	0.0351

$$\beta' = 0.0349 \text{ cm.}^{-2} \quad \text{Deviation} = 2.0\%$$

$$s/l = 1.6 \text{ cm} \quad s = 1.7 \text{ cm.}^2 \quad l = 1.1 \text{ cm}$$

TABLE 14.4

Recalibration of Cells

Cell 1

Run	$\Delta C_o(M)$	$\Delta C_f(M)$	$\log\left(\frac{\Delta C_o}{\Delta C_f}\right)$	$\log\left(\frac{\Delta C_o}{\Delta C_f}\right) + \log(1 - \lambda/6)$	$t_f(\text{Min})$	$\beta^1(\text{cm.}^{-2})$
1	0.1013	0.08506	0.07569	0.07404	3955	0.0383
3	0.1009	0.07919	0.10534	0.10369	5575	0.0381

Cell 2

2	0.1008	0.08563	0.07063	0.06924	4014	0.0354
4	0.1005	0.08011	0.09836	0.09697	5655	0.0352

14.6.2 Experimental Determinations

Table 14.5 gives the results obtained for the five solute gases studied. Calculations were made using Equations (14.5.28) and (14.5.29). Table 14.6 summarizes these results.

Some runs were also made with ethylene as solute, using the erroneous bromine water analytical technique originally employed for propylene runs (see Chapter 15). Since these runs indicated a diffusivity value approximately equal to that for carbon dioxide, and therefore showed ethylene not to be as useful for the study of effect of diffusivity in a packed column, it was not studied again using the more reliable gas

chromatography technique. The results reported for propylene were obtained by the latter technique.

TABLE 14.5

Experimental Determinations*

A. Carbon Dioxide

Cell	$C_{1f}(\text{MM})$	$C_{2f}(\text{MM})$	$\Delta C_o \text{ MM}$	$\log\left(\frac{\Delta C_o}{\Delta C_f}\right) + \log(1 - \lambda/6)$	$t_f(\text{Min})$	$D_L(10^5)\text{cm}^2/\text{sec}$
1	18.90	1.685	20.81	0.08072	4153	1.97
2	22.25	1.193	24.37	0.07759	4248	2.03
1	23.09	2.212	25.58	0.08656	4306	2.04
2	23.50	1.995	25.66	0.07533	4404	1.90

B. Oxygen

2	0.891	0.1024	1.000	0.1018	4060	2.79
1	0.797	0.1129	0.919	0.1266	5451	2.35
1	0.819	0.0677	0.896	0.0750	4028	1.89**
2	0.839	0.0820	0.928	0.0870	4165	2.32
1	0.766	0.0848	0.860	0.0997	4055	2.49
2	0.789	0.0842	0.880	0.0948	4235	2.49
1	0.604	0.0935	0.705	0.1385	5717	2.46
2	0.752	0.1025	0.860	0.1206	5840	2.30

** Rejected statistically (90% confidence).

* In all runs: Cell 1 $V_1 = 90.9 \text{ cc}$ $V_2 = 90.3 \text{ cc}$ $\bar{v} = 0.9967$
 Cell 2 $V_1 = 89.9 \text{ cc}$ $V_2 = 87.8 \text{ cc}$ $\bar{v} = 0.9883$

C. Helium

Cell	$C_{1f}(\text{MM})$	$C_{2f}(\text{MM})$	$\Delta C_o \text{ MM}$	$\log\left(\frac{\Delta C_o}{\Delta C_f}\right) + \log(1 - \lambda/6)$	$t_f(\text{Min})$	$D_L(10^5)\text{cm}^2/\text{sec}$
1	0.153	0.0602	0.216	0.3628	3880	9.48**
2	0.287	0.0653	0.354	0.2022	3951	5.70
1	0.282	0.0506	0.336	0.1605	2578	6.31
2	0.269	0.0470	0.318	0.1555	2641	6.55
1	0.241	0.0435	0.288	0.1614	2602	6.28
2	0.283	0.0416	0.327	0.1300	2718	5.32
1	0.259	0.0460	0.308	0.1588	2826	5.69
2	0.273	0.0508	0.326	0.1647	2580	7.10
1	0.232	0.0417	0.277	0.1608	2437	6.69
2	0.218	0.0375	0.257	0.1522	2490	6.80

D. Hydrogen

1	0.504	0.0741	0.584	0.1317	2794	4.79
2	0.342	0.0848	0.429	0.2207	2880	8.53**
1	0.510	0.0627	0.579	0.1104	2325	4.81
2	0.564	0.0612	0.630	0.0963	2428	4.41
2	0.626	0.0589	0.690	0.0838	2599	3.67**
1	0.588	0.0437	0.639	0.0678	1439	4.77
2	0.429	0.0393	0.472	0.0817	1498	6.07**

E. Propylene

1	3.40	0.136	3.58	0.03800	2916	1.30
1	3.13	0.278	3.45	0.08204	5768	1.44
2	3.20	0.263	3.49	0.07493	5945	1.40
1	3.60	0.164	3.81	0.04442	3054	1.47
2	3.67	0.222	3.92	0.05616	4337	1.44

** Rejected statistically (90% confidence).

TABLE 14.6

Summary of Experimental Determinations

<u>Solute Gas</u>	<u>$10^5 (D_L) \text{ cm.}^2/\text{sec.}$</u>	<u>Deviation - %</u>
Propylene	1.44	5.0
Carbon Dioxide	2.00	3.5
Oxygen	2.41	3.0
Hydrogen	4.8	4.0
Helium	6.3	10.0

14.7 Discussion of Results

The magnitude of the deviations from the average in the results obtained is about what would be expected. For the two solute gases with the more precise analytical techniques (oxygen and carbon dioxide) the deviation is least, and the deviation in general tends to increase as the solubility of the gas in water tends to decrease.

The values of s (effective cross-sectional area of pores) and l (effective pore length) seem reasonable physically for the two frits employed. The geometrical cross-sectional area of the frits are about 6 cm.^2 and the widths of the frits are about 0.3 cm. Thus the s and l values indicate a void fraction of about 30% and a path length through the pores about three times the straight line distance.

14.7.1 Comparison with Literature

Table 14.7 gives the values that various investigators in the past have obtained for the five solute gases studied in the present work. Since the correlations of Scheibel (118) and of Othmer and Thakar (105) give essentially the same values as those predicted by the correlation of Wilke and Chang (163, 164), only the values predicted by the latter correlation are presented. As it is to be expected for these light solutes, there are sizeable deviations between experimental values and values predicted by the correlation. The experimental values of Gertz and Loeschcke (41) are not presented for reasons given in Section 14.7.8.

In cases where a literature investigation was not made at 25°C the value obtained at the temperature closest to 25°C has been extrapolated to 25°C by use of the Stokes-Einstein relationship:

$$D_L \propto T/\mu \quad (14.1.4)$$

The agreement between the present data and the literature is quite good in the cases of carbon dioxide and oxygen. For the other gas for which previous experimental data are available, hydrogen, there is no value other than that of Aikazyan and Federova (2) with which the present value tends to agree. There is, however, little internal agreement within the literature, and, for what little it is worth, the present value lies near the center of the range of literature values.

TABLE 14.7

Gas	Investigator	Year	$D_L(10^5)$ at 25°C	
			cm. ² /sec.	Method
Propylene	Present	1960	1.44 \pm 5%	Diaphragm Cell Correlation
	Wilke and Chang(163,164)		1.32	
Carbon Dioxide	Present	1960	2.00 \pm 3.5%	Diaphragm Cell Correlation Capillary Capillary Layer Gel Capillary Diaphragm Cell Wetted Sphere Diaphragm Cell Wetted Wall
	Wilke and Chang(163,164)		2.3	
	Stefan (141)	1878	2.01	
	Hufner (63)	1897	2.02	
	Carlson (11)	1911	2.08	
	Tammann and Jessen (148)	1929	1.75	
	Ringbom (117)	1938	1.81	
	Peaceman (107b)	1951	2.03	
	Davidson and Cullen (23)	1957	1.92	
	Scriven and Pigford (124)	1958	1.9	
Nijsing, et al (99)	1959	1.95		
Oxygen	Present	1960	2.41 \pm 3%	Diaphragm Cell Correlation Capillary Layer Gel Polarography - Layer Polarography Wetted Sphere
	Wilke and Chang(163,164)		2.3	
	Hufner (63)	1897	2.02	
	Carlson (11)	1911	2.38	
	Tammann and Jessen (148)	1929	3.55	
	Kolthoff and Miller (77)	1941	2.6	
	Semerano, et al (126)	1949	1.85	
	Kreuzer (79)	1950	1.9	
	Pircher (111)	1952	2.3	
	Davidson and Cullen (23)	1957	2.43	
Hydrogen	Present	1960	4.8 \pm 4%	Diaphragm Cell Correlation Capillary Gel Layer Polarography Wetted Sphere
	Wilke and Chang(163,164)		3.4	
	Hufner (63)	1897	5.8	
	Tammann and Jessen (148)	1929	3.2	
	Ipatieff and Teodorovich (67)	1937	3.0	
	Aikazyan and Federova(2)	1952	4.1 - 4.8	
	Davidson and Cullen (23)	1957	7.0	
Helium	Present	1960	6.3 \pm 10%	Diaphragm Cell Correlation
	Wilke and Chang(163,164)		2.1	

14.7.2 Thermal Pumping

If there is much variation in temperature in the diaphragm cell during the course of a run, the thermal coefficient of expansion of the solvent may cause a significant amount of pumping of solution (and thereby solute) from the rich side through the disc and into the lean side. This fact was recognized by Goldstein (44) and has been a reason for the extremely accurate control of temperature (as close as $\pm 0.01^\circ\text{C}$) used by most other recent investigators.

In the present work the control allowed the temperature to fluctuate by about 0.2°C at all times, and also allowed as much as 0.5°C downward drift of the time-mean temperature in a 15 hour period (overnight). The former behavior was a function of the lag (hysteresis) in the response of the relay to the mercury thermoregulator, while the latter appeared to be the result of a mechanical deficiency in the thermoregulator.

An estimation of the amount of thermal pumping occurring relative to the volume of the disc may readily be obtained. At 25°C the coefficient of cubical expansion of water is $0.2 \times 10^{-3} \text{ }^\circ\text{C}^{-1}$ (109e), whereas for Pyrex glass the value is $0.01 \times 10^{-3} \text{ }^\circ\text{C}^{-1}$, a value negligibly small for the purpose of approximation.

In the two cells the ratios, λ , of disc volume to the volume of

one side are 0.023 and 0.019 (Section 14.6.1). Hence in 0.3°C the ratio, r , of expansion in the lower compartment to disc volume is

$$\begin{aligned} r &= (0.2 \times 10^{-3} \text{ } ^\circ\text{C}^{-1}) (1/\lambda) (0.3^\circ\text{C}) \\ &= (6 \times 10^{-5})/\lambda \\ &= 0.26\% \text{ for Cell 1} \\ &= 0.32\% \text{ for Cell 2} \end{aligned}$$

or roughly 0.1% of the disc volume is purged per 0.1°C temperature change. Thus even for the overnight drops of 0.5°C the disc volume was not appreciably "swept through."

14.7.3 Imperfect Mixing

The degree of mixing completeness attained in the sides of a diaphragm cell has been the source of much controversy and worry. As was mentioned previously Stokes (143), Lewis (82) and others have published data showing the calibration constant, β , of their cells to vary markedly with rate of stirring in either side; whereas Gordon (47) suggested that for electrolyte solutions density stirring is usually adequate, and Peaceman (107b) obtained what appear to be reliable data using only "density" stirring in his cells.

That there was any density stirring in Peaceman's study of carbon dioxide and chlorine diffusion is questionable. Both are relatively

insoluble gases, and therefore low concentrations were present in the cell, thereby reducing the driving force for density mixing in either side. Indeed, for propylene, a gas of only slightly less solubility, the two runs made in the present study and mentioned above showed no difference in indicated solute diffusivity depending on whether the cells were placed in the bath with the lean or the rich side on top. This suggests there was no influence of density mixing at all.

As a test for mixing perfection during the present study, one of the cells was kept in contact with the motor driven bath stirrer by means of a connecting piece of metal rod, linking the stirrer motor and the clamp holding the cell in place. This imparted a substantial vibration to this cell; whereas there was no vibration in the other cell sufficient to be detected by hand. The cell receiving the vibration was not always the same one, but instead alternately one, then the other. No trend toward a higher diffusivity or calibration constant was noticed for the cell receiving the vibration. It was possible, too, to observe with a beam of light small particles in the water in random motion within the cells when they were in the bath. Finally there appeared to be no trend for a lower or higher diffusivity value or calibration constant to result from a run made for a longer time.

Apparently, then, there was some factor or group of factors which caused efficient mixing within the cells. The chief factor was in

all probability the establishment of local natural convection currents within the cell; a secondary factor is probably the entrance of stray vibrations from the room into the system.

A heat transfer analysis shows that the controlling resistance to heat flow from the bath to a cell is the natural convection transfer of heat from the cell wall to the water within the cell. The temperature fluctuations resulting in the water from a varying wall temperature may now be examined mathematically, taking the temperature of the water immediately adjacent to the cell wall as equal to the bath temperature at any time.

For a problem analogous to this, that of an infinitely long solid cylinder with surface temperature varying sinusoidally with time, Carslaw and Jaeger (13c) give the temperature as

$$T = \frac{T_0 M_0 (\omega^1 r)}{M_0 (\omega^1 a)} \sin \left\{ \omega t + \epsilon + \theta_0 (\omega^1 r) - \theta_0 (\omega^1 a) \right\} + \text{a transient term} \quad (14.7.1)$$

where T = temperature
 T_s = surface temperature
 $= T_0 \sin (\omega t + \epsilon)$
 a = cylinder radius
 r = radius of point in question
 t = time
 $\omega^1 = (\omega / \kappa)^{1/2}$

k = thermal diffusivity of the solid

M_0, θ_0 = cylindrical Bessel functions of zero order, defined and tabulated by McLachlan (90)

For our purposes the transient term is of no importance since it soon dies out during a run.

An indication of the mixing in the bulk of solution may be obtained from an application of the coefficient of expansion of water to give a density as a function of time and position and then solving the Navier-Stokes equations for the resulting fluid velocities as has been done for predicting laminar natural coefficients from a flat plate by Lorenz (85) and others. The velocity variation with time would then be used to obtain a "mixing length" effective diffusivity for mixing.

Such a solution is, however, difficult to obtain and would hold only for an infinitely long diffusion cell. It is simpler to present the temperature distribution and then speak of the resultant mixing qualitatively.

The amplitude of temperature variation at any point is, from Equation (14.7.1), given by

$$\Delta T_{\max.} = T_0 \frac{M_0(\omega^1 r)}{M_0(\omega^1 a)} \quad (14.7.3)$$

Taking the typical on-off period in the bath to be three minutes

and the temperature oscillation in the bath to be 0.2°C the values in Table 14.8 are obtained for the value of ΔT_{max} at various radii. There is also a progressive lag encountered in the temperature fluctuation as distance from the cell wall toward the cell axis increases. This lag is computed from the sine term in Equation (14.7.1) as

$$\text{Lag} = \theta_0 (\omega^1 a) - \theta_0 (\omega^1 r) \quad (14.7.3)$$

and is also shown in Table 14.8. A lag of 180° indicates a temperature completely out of phase with the surface temperature.

TABLE 14.8

ΔT_{max} And Lag As a Function Of Radius In An
Infinitely Long Cell

<u>r (cm.)</u>	<u>$\omega^1 r$</u>	<u>$\Delta T_{\text{max}} - ^{\circ}\text{C}$</u>	<u>Lag - $^{\circ}$</u>
1.5	7.4	0.20	0
1.4	6.9	0.14	20
1.2	5.9	0.08	58
1.0	4.9	0.04	98
0.7	3.4	0.018	163
0.4	2.0	0.009	224
0.0	0.0	0.007	276

Although the temperature oscillations within the cell tend to become very much less near the center than at the wall, they still retain a value that, when coupled with the lag of some 20° per 0.1 cm of radius and integrated over the cell cross-section (the amount of solution present

at a given radius varies directly with the radius), may well be adequate to promote efficient mixing in the bulk of the water.

Lewis (82) claims that the major effect of inadequate stirring or mixing within a diaphragm cell lies in a boundary layer near the fritted disc, most probably a boundary layer resulting from a damping of the natural convection process in the present instance. Such a boundary layer would probably present a transfer rate proportional to the $2/3$ power of the solute diffusivity, as occurs in laminar boundary layer theory for forced convection (120a). Thus to the extent a boundary layer is present on either side of the frit a certain portion of the diffusive process varies as the $2/3$ power of solute diffusivity rather than the first power. Such an effect is not as great per unit "resistance thickness" as would be the effect from a series resistance independent of diffusivity or varying with a lower power of diffusivity. Thus the change in calibration coefficient evidenced by stirring or by more rapid stirring would ^{NOT} by any means correspond to as great an effect on the diffusivity value obtained for a solute in the calibrated cell.

A stronger effect on the transfer coefficient through a laminar boundary layer is that of a solvent viscosity (120a), which would appear if the viscosity of the solvent in the experimental system were different from the viscosity of the calibrational solvent. The

viscosity of 0.1 N potassium chloride is, however, equal to that of water within 0.1% (66b), so this is not a worry in the present study.

The resistance of such a boundary layer to solute transport should be diminished for a cell receiving appreciable vibration from the bath stirrer and consequently the cell should give a lower value of β^{-1} (or a higher value of D_L in an experimental run) than for a cell not receiving this vibration. Since there was no effect of this kind noticeable during the present runs, it may be concluded that the boundary layers on either side of the frit contributed a negligible portion of the overall frit resistance to transfer.

Another observation which could support this conclusion is the constancy of transfer coefficient (or apparent diffusivity) with respect to the time of the run. One would in general expect a higher transfer coefficient for a shorter run, since there is the necessity of initially establishing a concentration profile within the boundary layer. It should be stated, though, that the scatter of the data, in the propylene runs for instance where the run time was varied most, is probably sufficient to occlude any effect of this kind. The motion of particles noticed in the water also says nothing about a boundary layer effect, but instead indicates only mixing in the main body of solution.

In summary, because of the lack of effect of vibration effect on

the cell transfer process and because of the motion of particles noticed within the bulk of solutions, it appears that the mixing process was efficient enough to warrant the use of Assumption 1 of Section 14.5.1. This mixing probably came from the temperature variations of the bath.

14.7.4 Surface Transport

About 3 m.^2 of surface area is present within such a fritted disc as used here (98), and this brings forth the question of possible surface effects on the transport process through the disc.

Nielson, et al (98) have noticed some anomalies in electrolyte diffusivity values obtained in diaphragm cells with the rich side concentration below 0.01 N and have attributed the phenomenon to double layer transport, with anions being primarily adsorbed to the glass surface. Such a double layer effect is, however, limited to electrolyte solutions, and the potassium chloride concentrations in the present work were well above the region where Nielson found this effect.

It is improbable that any of the nonionic solute gases would be so preferentially adsorbed with respect to the polar water molecule to give an added transfer due to surface flow. Therefore, for lack of experimental information to the contrary, it is probably safe to assume there were no significant surface effects on the transfer process.

14.7.5 Presence of Gas Bubble

In order to avoid breakage of the cells because of the expansion

and contraction of the solutions due to temperature fluctuations of the bath, it was necessary to leave a small gas bubble - about 0.1 cc in volume - above the rich solution in the top side of the cell. For such dilute solute gas solutions as are encountered here the amount of gas contained in the bubble may be quite significant in comparison to that present in solution. As the rich solution is depleted by the diffusion process, gas may enter solution from the bubble in an effort to maintain equilibrium. This behavior is most marked in the case of helium, the least soluble gas.

For a rich side volume of 90 cc, an 0.1 cc gas bubble, and a solution initially in equilibrium with 0.75 atmosphere of helium,

$$\begin{aligned} \text{He in solution} &= (90 \text{ cc}) (3.9 \times 10^{-4} \text{ mmol/cc atm.}) (0.75 \text{ atm}) \\ &\quad (25 \text{ cc/mmol}) \\ &= 0.66 \text{ cc (RTP)} \end{aligned}$$

$$\begin{aligned} \text{He in bubble} &= (0.75)(0.1 \text{ cc}) \\ &= 0.075 \text{ cc (RTP)} \end{aligned}$$

At the conclusion of a typical run the rich side concentration is diminished to about 63% saturation (diminished by 12%). The gas bubble, if it remained at one atmosphere pressure, would lose some 0.012 cc of helium to the solution if it remained in equilibrium with the solution at all times - the worst case error-wise.

An indication of the error introduced by this is obtained by re-solving for the idealized equal-volume cell:

$$V \frac{dC_2}{dt} = \frac{sD_L}{l} (C_1 - C_2) \quad (14.5.1)$$

subject to the new material balance:

$$\begin{aligned} C_2 &= C_{10} - C_1 + (C_{10} - C_1)(V_B) \\ &= (1 + V_B) (C_{10} - C_1) \end{aligned} \quad (14.7.4)$$

where V_B = bubble volume, cc.

and C is expressed as cc of solute (RTP) per cell side volume of solution. The term including V_B allows for the equilibrium entrance of solute to the solution from the bubble.

Rearranging Equation (14.7.4):

$$C_1 = C_{10} - \frac{1}{1 + V_B} C_2 \quad (14.7.5)$$

$$C_1 - C_2 = C_{10} - \frac{2 + V_B}{1 + V_B} C_2 \quad (14.7.6)$$

$$d(C_1 - C_2) = -\frac{2 + V_B}{1 + V_B} dC_2 \quad (14.7.7)$$

Integrating Equation (14.5.1) subject to this material balance, there results

$$\ln \frac{\Delta C_o}{\Delta C_f} = \frac{2s}{V} \left(\frac{2 + V_B}{1 + V_B} \right) D_L t_f \quad (14.7.8)$$

$$\text{or } \ln \frac{\Delta C_o}{\Delta C_f} = \beta \left(\frac{2 + V_B}{2 + 2 V_B} \right) D_L t_f \quad (14.7.9)$$

where $\beta = 2s/l V$, as defined in Section 14.5.1.

The corresponding material balance is

$$\Delta C_o = C_{1f} + \frac{1}{1 + V_B} C_{2f} \quad (14.7.10)$$

For a typical case where $C_{1f} = 0.58$ cc RTP/cell side volume and $C_{2f} = 0.08$ cc RTP/cell side volume, the idealized equations, (14.5.2) and (14.5.4), give

$$\Delta C_f = 0.50$$

$$\Delta C_o = 0.66$$

and

$$\beta D_L t_f = \ln \left(\frac{0.66}{0.50} \right) = 0.278,$$

whereas, for a bubble volume of 0.1 cc, equations (14.7.9) and (14.7.10) give

$$\Delta C_f = 0.50$$

$$\Delta c_o = 0.58 + (0.909)(0.08) = 0.653$$

and

$$\beta D_{L^t f} = \left(\frac{2.2}{2.1}\right) \ln \left(\frac{0.653}{0.50}\right) = 0.280$$

The value of diffusivity calculated neglecting the presence of the bubble is, then, less than 1% lower than the value calculated assuming the bubble to remain in equilibrium with the solution at all times. The existence of this bubble thus appears not to be a prime source of error.

14.7.6 Supersaturation

If there were enough air (or nitrogen in the case of oxygen runs) dissolved in either side of the cell to bring the solution close to one atmosphere equilibrium pressure, then the difference between the diffusivities of the two solutes might tend to build the equilibrium pressure up to one atmosphere and then cause supersaturation with a possible consequent formation of bubbles and loss of solute from solution. Bubbles forming in the frit could also increase its resistance to diffusion and distort the transfer process through it.

In the present work distilled water (which by analysis, is at worst 50% saturated with air) or degassed water was used as the lean side solvent. The rich side solution was also prepared by bubbling the gas in question through distilled water. Because of this, and because no bubble formation was ever noticed in the cells, supersaturation

tendencies should not have been a source of error.

14.7.7 Analytical Errors

The amount of effect of analytical error obviously varies with the duration of a run. For an absolute error introduced by the analytical technique used to determine the values of C_{1f} and C_{2f} , an optimum run time may be derived for minimization of the resultant error in D_L . An absolute analytical error corresponds to a percentage error inversely proportional to concentration level and corresponds, for instance, to the error usually encountered in titrations.

Taking Equations (14.5.2) and (14.5.4) for the idealized cell behavior

$$D_L = \frac{1}{\beta t_f} \ln \frac{C_{1f} + C_{2f}}{C_{1f} - C_{2f}} \quad (14.7.11)$$

The total differential of D_L , with C_{1f} and C_{2f} as independent variables, is

$$d D_L = \frac{1}{\beta t_f} \frac{(-2 C_{2f} d C_{1f}) + (2 C_{1f} d C_{2f})}{(C_{1f} + C_{2f})(C_{1f} - C_{2f})} \quad (14.7.12)$$

Since errors may be cumulative, $d C_{1f}$ and $d C_{2f}$ may be taken of opposite sign ($= \Delta C$) for purposes of a determination of ΔD_L , the error in D_L .

$$\Delta D_L = \frac{4 \Delta C}{C_{1f} - C_{2f}} \quad (14.7.13)$$

Combining this with Equation (14.7.11), there results for the relative error in D_L

$$\frac{\Delta D_L}{D_L} = \frac{4 \Delta C}{(C_{1f} - C_{2f}) \ln \left[\frac{C_{1f} + C_{2f}}{C_{1f} - C_{2f}} \right]} \quad (14.7.14)$$

or

$$\frac{\Delta D_L}{D_L} = \frac{4 \Delta C}{(2 C_{1f} - C_{10}) \ln \left[\frac{C_{1f}}{C_{1f} - C_{10}} \right]} \quad (14.7.15)$$

To obtain the optimum run time, the denominator of (14.7.15) is maximized by setting its derivative with respect to C_{1f} equal to zero and holding C_{10} constant. There results

$$C_{1f} = \frac{C_{10}}{2} \left(1 + \frac{1}{C} \right) = 0.684 C_{10} \quad (14.7.16)$$

This occurs for $D_L t_f = 1/\beta$, and for the present cells requires a run on the order of 24 days for potassium chloride diffusion. This would be inconvenient.

For the optimum run length, the resultant error in D_L is

$$\frac{\Delta D_L}{D_L} = 11 \frac{\Delta C}{C_{10}} ; \quad (14.7.17)$$

whereas for a run of 4 days, or 1/6 the optimum time

$$\frac{\Delta D_L}{D_L} = 24 \frac{\Delta c}{c_{10}} \quad (14.7.18)$$

Thus, for the much shorter runs used in the present study only twice the error of the optimum, 24 day run results.

Stokes (144) has given a similar analysis for the case of a constant relative (or percentage) error in concentration determinations. He finds the minimum error in D_L to occur for the shortest possible run. The relative error in D_L is very flat rising slowly with run time and never exceeding twice the relative error in concentrations for the run times encountered in the present work.

For runs made with solutes requiring chromatographic analysis, a relative error of this latter type is encountered, and is on the order of some 4 or 5 per cent. Thus a maximum error of 10% may result in the diffusivity values.

For the oxygen titrations there is an error resulting from burette inconsistencies of some 0.05 cc, which corresponds to an error of 0.1% in a concentration of the size of ΔC_0 , or a possible 2.5% error in D_L , assuming concentration errors to be absolute. For the carbon dioxide runs there is more uncertainty to the titration endpoint and a larger possible error in D_L , probably on the order of 7 to 10%.

Thus analytical errors may have contributed largely to the experimental scatter, but it is also likely that some scatter resulted also from run conditions alone.

14.7.8 Data of Gertz and Loeschcke

Gertz and Loeschcke (99) have claimed to measure diffusivity values in a somewhat questionable manner. In their apparatus they flowed water at a very slow rate (1.5 cc/min) downward through a downwardly divergent 2.4 - 2.8 mm cylinder 30 cm long. They introduced a bubble of the gas whose diffusivity they wished to measure at the bottom of the cylinder and monitored its rate of rise. From this ascension rate they computed a mass transfer coefficient (akin to the commonly used K_L) and then assumed this coefficient to be proportional to the first power of diffusivity.

Garner (39, 54) and others have shown that laminar flow about a bubble of this size behaves the same as flow about a solid sphere, i.e., the liquid adjacent to the bubble surface is stagnated. For laminar flow about the solid sphere in an infinite region, boundary layer theory (120) and experimental results (40) indicate a variation of transfer coefficient with the $2/3$ power of diffusivity. There is a question as to whether Gertz and Loeschcke's apparatus corresponds to an infinite fluid medium about the bubble; however, the mass transfer situation near the liquid-bubble interface should be the same in both cases.

Figure 14.2 shows the K_L values of Gertz and Loeschcke plotted versus the present diffusivity values for helium, hydrogen, carbon dioxide and oxygen. Diffusivities at 37°C were obtained through use of the Stokes-Einstein relationship.

The data of Gertz and Loeschcke correlate well with the $2/3$ power of diffusivity. This affords an explanation of their data and also provides a confirmation of the present diffusivity data.

14.8 Wetted Wall Data on Chlorine Diffusivity

It is interesting to notice that recently (23, 78, 99) diffusivity data has been obtained through wetted wall studies. If such techniques prove reliable, a considerable saving of data taking time will be possible.

Davidson and Cullen (23) report a diffusivity for carbon dioxide in water measured by absorption into water flowing over a sphere that is in substantial agreement with the diffusivity reported by Nijsing, et al, (99) for absorption both into a laminar jet and into water flowing down a wetted wall column (with the stagnant wave end effect eliminated through use of a surface active agent). The values agree over a 10° to 30°C temperature range, and agree closely at 25°C with the results of the present work (see Table 14.7).

Davidson and Cullen (23) and Kramers, et al, (78), using Nijsing's apparatus, have studied the diffusion of chlorine into water, and have

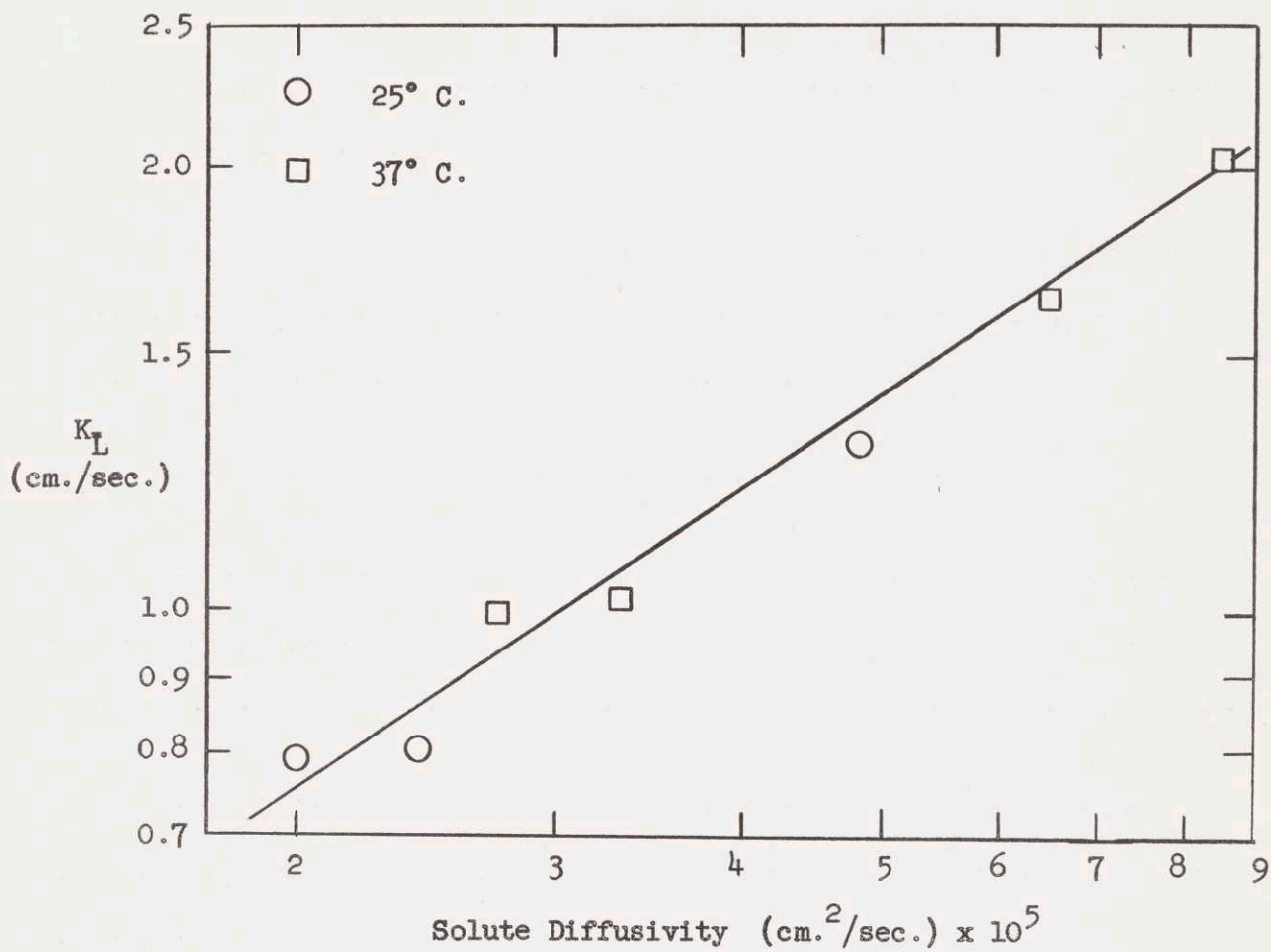


FIGURE 14.2 DATA OF GERTZ AND LOESCHCKE PLOTTED VS. PRESENT
DIFFUSIVITY VALUES

obtained mass transfer rates at variance with one another, both as to the magnitude of indicated "diffusivity" and to the effect of temperature. For the contact times encountered in a packed column (1 inch rings) Vivian and Whitney (154, 156) have shown that the chlorine-water system is one in which there is a chemical reaction rate (for hydrolysis) comparable to the diffusion rate. Kramers, et al (78) claim that the reaction has been shown by Shilov and Solodushenkov (134) and by Morris (96) to be substantially complete for contact times greater than 0.1 sec. For their experiments they report having used a contact time varying from 0.3 to 1.0 second.

For the studies of Davidson and Cullen (23) of flow over a sphere contact times were not reported; however they may be calculated from the water flow rates as follows:

From Equations (2) and (3) of the Davidson and Cullen article, and in the nomenclature of this thesis,

$$u_i = \frac{3Q}{4\pi R} \left(\frac{2\pi Rg}{3\nu Q} \right)^{1/3} \sin^{-1/3} \varphi \quad (14.8.1)$$

- where u_i = interfacial velocity
 Q = volumetric flow rate
 R = radius of sphere
 ν = kinematic viscosity
 g = acceleration due to gravity

and φ = co-latitude of position on the sphere, measured from the upward vertical.

Now

$$d\theta = \frac{R d\varphi}{u_1} \quad (14.8.2)$$

where θ = contact time

and

$$\theta = \frac{4\pi R^2}{3Q} \left(\frac{3\nu Q}{2\pi R g} \right)^{1/3} \int_0^\pi (\sin \varphi)^{1/3} d\varphi \quad (14.8.3)$$

$$\theta = (2.59) \frac{4\pi R^2}{3Q} \left(\frac{3\nu Q}{2\pi R g} \right)^{1/3} \quad (14.8.4)$$

$$\theta = 8.47 \left(\frac{R^5 \nu}{Q^2 g} \right)^{1/3} \quad (14.8.5)$$

Taking a water temperature equal to 25°C, the radius of their sphere equal to 1.89 cm, and a value of Q varying from 0.5 to 2.5 cc/sec, the resulting range of contact times is

$$0.3 \text{ sec.} < \theta < 0.8 \text{ sec.} \quad (14.8.6)$$

These should be equivalent to contact times for flow down a planar wall for small depths of penetration.

The range of contact times encountered in the packed column of Vivian and Whitney may be estimated by separating the wetted area from k_L using the a_e values obtained by Shulman, et al, (137) from the data of Fellingner (see Chapter 9).

Vivian and Whitney found $K_L a = 15 \text{ hr}^{-1}$ at $L = 1000$ (where their data indicate the $K_L a$ based on total chlorine driving force is the most correct to consider, i.e., relatively fast reaction compared to mass transfer rate), and $K_L a = 95 \text{ hr}^{-1}$ at $L = 10,000$ (where their data indicate the $K_L a$ based on molecular driving force is most correct, i.e., relatively slow reaction rate compared to mass transfer rate). These correspond to $K_L = 1.25 \text{ ft/hr}$ and 3.2 ft/hr respectively (since a_e has respective values of 12 and 30 sq.ft./cu.ft. (137)).

An average contact time may now be obtained from the penetration theory solution:

$$k_L = 2 \sqrt{\frac{D_L}{\pi \theta}} \quad (2.1.26)$$

Using $D_L = 1.5 \times 10^{-5} \text{ cm}^2/\text{sec}$ as an approximation for both total and molecular chlorine, the extreme flow conditions of Vivian and Whitney correspond to average contact times of 0.17 sec and 0.03 seconds.

The contact times encountered in the three investigations are summarized in Table 14.9.

TABLE 14.9

<u>Authors</u>	<u>Contact Times - Seconds</u>
Vivian and Whitney (156)	0.03 - 0.17
Davidson and Cullen (23)	0.3 - 0.8
Kramers, et al (78)	0.3 - 1.0

For a relatively fast rate of mass transfer into liquid (or a relatively short contact time) most of the chlorine will diffuse as unreacted, molecular chlorine for a certain distance into the liquid; on the other hand, for a relatively slow rate of mass transfer (or long contact time) the chlorine will hydrolyze essentially instantaneously upon coming into solution at the interface. Vivian and Whitney (156) have indicated that their two extreme flow rates (or contact times) correspond closely to those two cases. This is in qualitative agreement with the reaction rate studies of Morris (96) and Shilov and Solodushenkov (134) (see also Quincy (113), who obtained predicted absorption coefficients from these data), and substantiates the claim of Kramers, et al (78) that for contact times on the order of theirs and of Davidson and Cullen's the chlorine should diffuse as "total" or completely hydrolyzed chlorine.*

*It should be pointed out that this whole analysis could be carried out using a k_L pseudo - coefficient, which for an infinitely rapid hydrolysis becomes equal to H/H' times the physical absorption k_L , giving the same rate as the k_L based on the "total" driving force. H/H' is the ratio of the "total" solubility of chlorine to that of molecular chlorine alone.

Habib (52) studied the absorption of chlorine in a short wetted wall column at contact times varying from 0.1 to 0.7 sec. He presents coefficients based on the molecular (unhydrolyzed) chlorine driving force. A recalculation of his data, however, gives an interesting result if a "total" chlorine driving force (based on the solubility data of Whitney and Vivian (161) is used and Peaceman's measured diffusivities (107b) are employed. Such a calculation shows that for a pure chlorine gas phase the absorption process occurred as if the hydrolysis were instantaneous, that is, as the diffusion of "total" chlorine over the whole range of contact times. At lower partial pressures of chlorine (below 0.3 atm) in the gas phase a finite hydrolysis rate must be taken into account, especially at the lower contact times. This behavior can be accounted for theoretically, as is shown by Habib himself and by Peaceman (107), but need not really concern us here. Since Davidson and Cullen and Kramers, et al, used a pure chlorine gas phase, the results of Habib lend additional support to the tenet that in analysis of their cases the hydrolysis may be considered infinitely rapid. Vivian and Whitney used a chlorine partial pressure of about 0.2 atm in their packed tower. This analysis of Habib's data also verifies qualitatively that at their longer contact times they were approaching the infinitely rapid hydrolysis case.

The diffusivity of "total" chlorine measured by Kramers, et al, at 25°C is 1.42×10^{-5} cm/sec, based on the "total" chlorine solubility

data of Adams and Edmonds (1). Peaceman (107b), using the diaphragm cell technique, reports a "total" chlorine diffusivity of $1.51 \pm 0.01 \times 10^{-5}$ cm^2/sec at 25°C , a value some 6% higher. This result, of course, did not require a knowledge of solubility in order to be calculated. If the solubility data of Whitney and Vivian (161) are applied to the results of Kramers, et al, the resultant value of diffusivity from their data at 25°C becomes 5% higher, or 1.49×10^{-5} cm^2/sec , a value in close agreement with that of Peaceman.* Kramers, et al, report a close agreement with the Stokes-Einstein equation for the effect of temperature on the "total" chlorine diffusivity in water from 10° to 35°C . Peaceman, too, reports good agreement with the Stokes-Einstein equation over the range from 10° to 30°C . Thus there appears to be excellent agreement between Kramers, et al (78), Peaceman (107b), and the solubility data of Vivian and Whitney (156).

Davidson and Cullen (23), however, report values that give a diffusivity of total chlorine at 25°C equal to 1.83×10^{-5} cm^2/sec . They also found a much more radical variation with temperature than predicted by the Stokes-Einstein relation. If, for some reason, they had actually had short enough contact times to make the rapid hydrolysis assumption invalid, their reported values should lie below those of

*Strictly speaking, the use of the "total" driving force is valid only for a reaction in which the diffusivities of the reacting solute and the reaction product(s) are equal (107d). Coincidentally, this is the case for physically dissolved chlorine and total chlorine, as found by Peaceman (107b).

Peaceman and of Kramers, et al, for the molecular chlorine driving force is lower than the total chlorine one, and thus produces a lower transfer rate, as shown and found by Vivian and Whitney (156). Peaceman (107) and Sherwood and Pigford (133h) also show this.

A possible explanation for the high value reported by Davidson and Cullen lies in the solubility data they used. They cite Seidell (125) for all their solubilities. Two different sets of chlorine solubility data are given by Seidell. One is that of Winkler (1912), which gives a Bunsen coefficient (volumes of chlorine gas reduced to 760 mm pressure and 0°C dissolved per volume of water) of 1.985 at 25°C, whereas the data of Goodwin (1882) give a solubility coefficient (volumes of chlorine gas per volume of water at the given temperature and 760 mm pressure) of 2.06, corresponding to a Bunsen coefficient of 1.89. The solubility decreases with increasing temperature.

The mass transfer data given for chlorine by Davidson and Cullen may be taken from their Figure 9 and inserted into their equations (16) and (17) to find the values of C^* they used. Such an analysis, utilizing also their reported diffusivity of 1.90×10^{-5} cm²/sec at 26.0°C indicates that the value of the Bunsen coefficient they used was 2.06 at 26°C. This evidently came from the data of Goodwin, the solubility coefficient having been taken erroneously as equal to the Bunsen coefficient.

An interpolation of the Whitney and Vivian solubility data gives a Bunsen coefficient of 2.00 at 25°C. The solubility used by Davidson and

Cullen is therefore probably too high if anything. This would tend to make the diffusivity calculated from their data too low and thus the discrepancy between their result and those of Peaceman (107b) and Kramers, et al (78) would be accentuated if anything.

The fact that Davidson and Cullen tend to be high in their chlorine data takes some of the sting out of the fact that their hydrogen diffusivity value at 25°C (7.0×10^{-5} cm²/sec) is so much higher than that found in the present work (4.8×10^{-5} cm²/sec).

The above discussion also points up a drawback of the "absorption" techniques for measurement of solute gas diffusivities. Knowledge of the gas solubility is required, and since the calculated diffusivity is inversely proportional to the square of the solubility, any error in the solubility value is magnified in the calculated value of diffusivity.

CHAPTER 15

ANALYTICAL TECHNIQUES

15.1 Difficulties in Analyzing Solutions of Sparingly Soluble Gases in Water

A deterrent to the use of the diaphragm cell for the measurement of diffusivities of sparingly soluble gases in water has been the difficulty of performing analyses. For this same reason no really extensive measurements of helium or hydrogen absorption or desorption in a packed tower have heretofore been carried out.

The two prime difficulties in analysis are the danger of losing the highly volatile gases from solution during analysis or sampling and the necessity of analyzing very dilute solutions of these gases.

These disadvantages are largely overcome by the standard Winkler oxygen technique (Section 15.2) and the standard barium hydroxide method for carbon dioxide (Section 15.3). Hydrogen has heretofore been analyzed by the tedious combustion pipette technique (61e, 102, 152b). This has required a very large solution sample volume.

The analytical technique developed for helium, hydrogen, and propylene in this work (Section 15.4) depends on the use of mercury pumping to confine the sample solution prior to the separation of the dissolved gases from it (to avoid loss through volatility), and utilizes gas chromatography to analyze the extremely small amounts of gas present in solution.

None of the solute gases interfered with one another in analysis, except for helium and hydrogen (Section 15.4.2).

15.2 Oxygen

The method used for the analysis of oxygen in water was the standard Winkler technique, as modified by Holloway (61e). Holloway's modification differs from the standard technique (122d) in that a large excess of potassium iodide is added to hold the iodine (liberated in equivalence to oxygen) in solution. This is necessitated because of the relatively high range of oxygen concentrations encountered.

The analysis involves the oxidation of manganous hydroxide to a higher state in basic solution. Addition of potassium iodide and then acidification yield an amount of iodine equivalent to the oxygen originally present in solution. This iodine is titrated against standard thiosulfate solution to a starch endpoint (106b, 122b). The thiosulfate is standardized against weighed, dry potassium iodate samples (106b, 122b). This method gave reproducibility of $\pm 0.02\%$ between duplicate standardizations.

The overall analysis is, then,



The thiosulfate is oxidized to the tetrathionate. The standardization

reaction is



Four stock reagent solutions are necessary:

- 1) 4 N manganous sulfate solution
- 2) A solution of 0.4 g sodium hydroxide and 0.1 g potassium iodide per cc.
- 3) A solution of 1 g potassium iodide per cc.
- 4) 18 N sulfuric acid.

The strong iodide solution tends to undergo a photochemical decomposition. Hydrogen iodide, present to an extent in solution, reacts with oxygen in the air to produce free iodine. This may be avoided by adding a sodium hydroxide pellet to make the solution slightly basic and by keeping the solution in a brown-glass bottle under a layer of toluene.

The bacteriological decomposition of the starch indicator solution is suppressed by adding a trace of mercuric cyanide and keeping the solution under toluene.

The photochemical decomposition of hydrogen iodide can also affect the final titration against thiosulfate. This can be eliminated to all intents by making the iodine solution only slightly acid and by performing the titration quickly.

For packed tower runs, the samples were received in 250 cc glass stoppered Erlenmeyer flasks of known volume by introducing the sample through a rubber tubing outlet at the bottom of the flask, sweeping out some ten or fifteen flask volumes (about 30 seconds), and stoppering quickly.

One cc of the sodium hydroxide - weak potassium iodide solution was added through a pipette to the bottom of the flask, followed by 1 cc of the manganous sulfate solution. The flask was restoppered and shaken. A fluffy brown precipitate of oxidized manganous hydroxide formed, and was allowed to settle. The flask was then shaken again, and the precipitate allowed to settle again. Three cc of the strong potassium iodide solution were then added to the bottom of the flask through a pipette, followed by 1 cc of the sulfuric acid. This liberated the iodine. Part of the solution was then transferred to another flask so that the titration could be carried out. Two endpoints thus had to be attained per analysis.

For determination of concentrations the oxygen solution volume was taken to be that of the flask, less the 2 cc of the first two reagents added. Since the oxygen was tied up in the precipitate, no oxygen was displaced by the latter two reagents.

The thiosulfate solution was on the order of 0.005 normal to oxygen. This gave an endpoint easily determinate to within 0.05 cc.

After much previous investigation of various sampling methods, the oxygen analyses for diffusivity cell studies were carried out within the individual cell sides themselves. By this technique possible contamination from the air in the analytical process, a serious problem especially for the lean solution, was minimized. The reagents were introduced by an elongated pipette through the end stopcock bore of either cell side. There was sufficient clearance between the pipette stem and the bore wall to allow the displaced solution to escape. A cotton swab was used to remove displaced solution from the stopcock arm. In the final calculation, as in the packed tower analysis, a correction was made for the volume of solution displaced by the first two reagents. The quantities of reagents used were about one third of those used in the packed tower analyses. This was the ratio of solution volumes between the two cases.

After liberation of iodine the solution from a cell side was drained into a flask. The cell side was then rinsed with a small amount of distilled water, and the rinse solution added to the flask. The titration was then carried out. The thiosulfate solution employed was about 0.001 normal to oxygen.

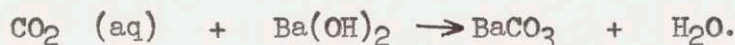
There was a possibility of some oxygen being held in precipitate that became trapped in the fritted disc of the cell, with consequent plugging of the cell and loss of oxygen from the analysis. When the cells were washed following an oxygen run a small quantity of potassium iodide and sulfuric acid reagents was first sucked through the disc.

In no case was discoloration due to iodine noticed in this solution. The fact that the same cell constants were obtained upon recalibration after the oxygen runs as were obtained by the original calibrations (see Section 14.6.1) indicates there was no perceptible permanent plugging of the frit by the precipitate or erosion of the frit by the caustic solution used in the first part of the analysis.

This was undoubtedly the most accurate of the analyses used. The close agreement of check samples taken during the packed tower runs attest its accuracy as better than 1%.

15.3 Carbon Dioxide

The carbon dioxide analysis used was the standard technique of fixation through reaction with barium hydroxide (61a, 152a). The principle of the analysis is as follows: Barium hydroxide is prepared freshly in solution (since it tends to absorb carbon dioxide from the atmosphere upon standing). The carbon dioxide bearing solution is received beneath the surface of the barium hydroxide solution and reacts to form insoluble barium carbonate, thus



The excess hydroxide is then back titrated with standard hydrochloric acid.

In the packed tower runs the samples were taken in two stopcock-arm sample bulbs of about 100 cc volume, flushing them out some ten or more

times (2 minutes). A glass delivery jet was fitted to the top arm and the sample delivered beneath the surface of the hydroxide solution by mercury pumping. A mercury leveling bulb was attached to the lower arm by strong rubber tubing for this purpose. The first 10 or 20 cc of solution pumped through the jet assembly were discarded to ensure that the sample would be truly representative.

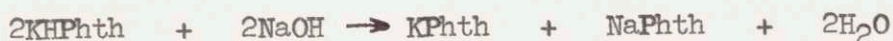
The barium hydroxide solution was prepared by adding about 40 cc of 0.015 normal (to carbon dioxide) sodium hydroxide solution and some three or four times the stoichiometric amount of barium chloride solution to a glass-stoppered, 250 cc Erlenmeyer flask. Distilled water was added to provide adequate volume. All work in the analysis was done under a nitrogen atmosphere to preclude absorption of carbon dioxide from the air.

The flask was weighed on an analytical balance before and after receipt of the sample. From the weight of sample added the volume was determined from standard density data (109a). The sample volume taken was on the order of 30 cc for strong carbon dioxide solutions and 60 cc for weak ones. Duplicate analyses were performed where possible.

The excess hydroxide was then titrated against standard hydrochloric acid (about 0.009 normal to oxygen) to a phenolphthalein endpoint, corresponding to a pH of 9.0 at which barium carbonate is negligibly soluble. The endpoint was determinate to within 3 or 4

drops (± 0.15 cc). This gave an analytical error no greater than 2%.

The standard solutions were standardized against weighed, dry potassium acid phthalate samples. Because of the very small back driving force exerted by the low percentage of carbon dioxide in the air the standardization was by no means so important as in the case of oxygen analyses; however, standardizations were reproducible to $\pm 0.05\%$ for duplicate phthalate samples. The standardization reaction is



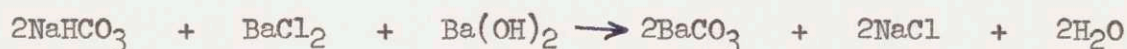
The use of this analytical technique affords a strong acid-strong base titration rather than a strong base - weak acid one, and gives consequent better accuracy.

In the case of diffusivity cell analyses an entirely analogous procedure was carried out, with the tubing to the mercury leveling bulb attached to the lower end arm of the diaphragm cell and solution being pumped out through the capillary side arm.

As has been shown by Holloway (61f), there is a significant amount of bicarbonate ion in Cambridge water. This amount is a fixed quantity in fresh Cambridge city water and occurs because of the treatment of this water with lime. The equilibrium relationships of the carbonate ions, bicarbonate ions, free carbonic acid, and dissolved carbon dioxide is such as to make bicarbonate ion the only substance present significantly aside from dissolved carbon dioxide, and the bicarbonate ion concentration remains essentially constant over the entire range of carbon

dioxide concentrations encountered in a packed column, i.e., equilibrium with carbon dioxide pressures ranging from one atmosphere down to the partial pressure in air (61f). Thus the presence of the bicarbonate suppresses a significant hydrolysis which would tend to occur for equilibrium with low partial pressures of carbon dioxide, and assures the occurrence of physical desorption alone. The concentration of bicarbonate was measured by Holloway in 1939 to be 4.4×10^{-4} molar. Check measurements made in the present study using Holloway's technique of titration against hydrochloric acid to a methyl red endpoint at pH = 5.7 gave concentrations of 4.3×10^{-4} , 4.5×10^{-4} , and 4.4×10^{-4} molar.

Half the bicarbonate appears as carbon dioxide in the carbon dioxide analysis in the following way:



Thus a correction of 2.2×10^{-4} moles per liter is necessary on the carbon dioxide concentration obtained from the analysis.

When water is recirculated there can be a build-up of bicarbonate ion in solution, as concentrations of counter ions, etc., change through corrosion. In this study the hold-up volume of the storage tanks was such that the sweep out time of the packed tower system was

more than ten minutes at the highest water flow rate. Also the number of transfer units occurring through the packing was always low enough to make the bicarbonate correction a very secondary one. Hence the effect of any build-up of bicarbonate was probably negligible.

A similar problem of carbonate ion presence and build-up has been shown by Holloway (61g) to account for the low transfer rates and relative independence of $(N.T.U.)_L$ on liquid rate found by Sherwood, Draemel, and Ruckman (128) who desorbed carbon dioxide from recirculated water in a 4-1/2 foot high column, with a consequent very low driving force at the tower bottom. They used the standard analysis involving titration against sodium carbonate solution to a phenolphthalein endpoint (122c), a method which is sensitive to carbonate ion concentration as well as carbon dioxide.

Failure to allow for the effect of bicarbonate (if there is any in Chicago water) may also account for the results of Koch, et al (76) who absorbed carbon dioxide into water on 3/8 inch, 1/2 inch, 3/4 inch, and 1-1/4 inch rings in 4 foot high towers, finding low rates on the order of those of Sherwood, Draemel, and Ruckman, and an N.T.U. substantially independent of liquid flow rate and packing size. They used both city water and recirculated "distilled" water. Analyses were performed by the barium hydroxide technique.

In the diffusivity cell studies of the present thesis, degassed,

distilled water was used, and hence no bicarbonate correction was necessary. Concentrations were high enough to suppress any significant hydrolysis (61f).

15.4 Helium, Hydrogen, and Propylene

Analyses of inert gases in liquid solution are difficult to perform, especially when they are present in extremely low concentration. Helium in water presents such a problem and yet was desirable as a solute gas because of its relatively very high diffusivity in water. Evidently, therefore, the helium had to be removed from solution and analyzed in the gaseous form.

The simplest method of quantitative analysis of small gas sample volumes is gas chromatography, an apparatus for which is owned by the M.I.T. Chemical Engineering Department. For separation of the gas from solution the simplest and shortest technique appeared to be that described below (Section 15.4.1).

Although hydrogen in water solution is usually analyzed by means of boiling it out and igniting it in a combustion pipette (61e, 102, 152b), the gas separation - gas chromatography approach was used because of the greater simplicity and the lesser sample volume required.

Originally it was felt that propylene and ethylene would be

desirable solute gases because they would lend themselves to chemical analysis with bromine water, in a technique analagous to that utilized ordinarily for measuring unsaturate components of hydrocarbon gas mixtures,(152c).

The analytical system originally devised was to receive the ethylene (or propylene) solution into a standard bromine water solution (made freshly from potassium bromate and potassium bromide, the bromine being liberated by acidification). The sample would be delivered through a jet in the same manner as in carbon dioxide analyses. Addition of excess potassium iodide would then convert the remaining free bromine into iodine, which was back titrated against thiosulfate to a starch endpoint.

In practice, it resulted that for any usable sample vessel volume there was a significant loss of bromine from solution during the analysis because of its high volatility. This was confirmed by experiment and by calculation.

When the chromatography technique proved suitable for propylene, all analyses for it were made in that way. The use of ethylene as a solute gas was discontinued when it became apparent from diffusivity runs made using the bromine analysis that ethylene has essentially the same diffusivity as carbon dioxide.

15.4.1 The Separation Apparatus

The apparatus used for the separation of gases from water solution was an adaptation of that used by Rakestraw and Emmel (115) to measure the oxygen, nitrogen, and noble gases dissolved in sea water. A schematic diagram of the apparatus is shown in Figure 151. The principle of the apparatus is the desorption of solute gases from water solution through repeated spraying into a vacuum.

In the apparatus leveling bulbs A and E contain mercury, about 150 cc each. Flasks C and D are round bottom with 24/40 and 19/38 standard taper necks, respectively. The volumes of the flasks are 100 cc and 50 cc, respectively. The standard taper joints are held by rubber gasketed ball joint clamps. Bulb F is for the extracted gas sample, and has a volume of 10 cc. There are several Tygon bound joints in the apparatus; these and the standard taper joints make it possible to take the apparatus apart for cleaning. All the glass used in construction of the apparatus is Pyrex.

Before a sample is taken, the line from leveling bulb A to the sampling bulb (or diaphragm cell) B is filled with mercury and the mercury from bulb E is forced through flask D up above stopcock G. Solution is then forced from sample bulb B through stopcock G and into flask D by raising bulb A and lowering bulb E. About 10 cc are

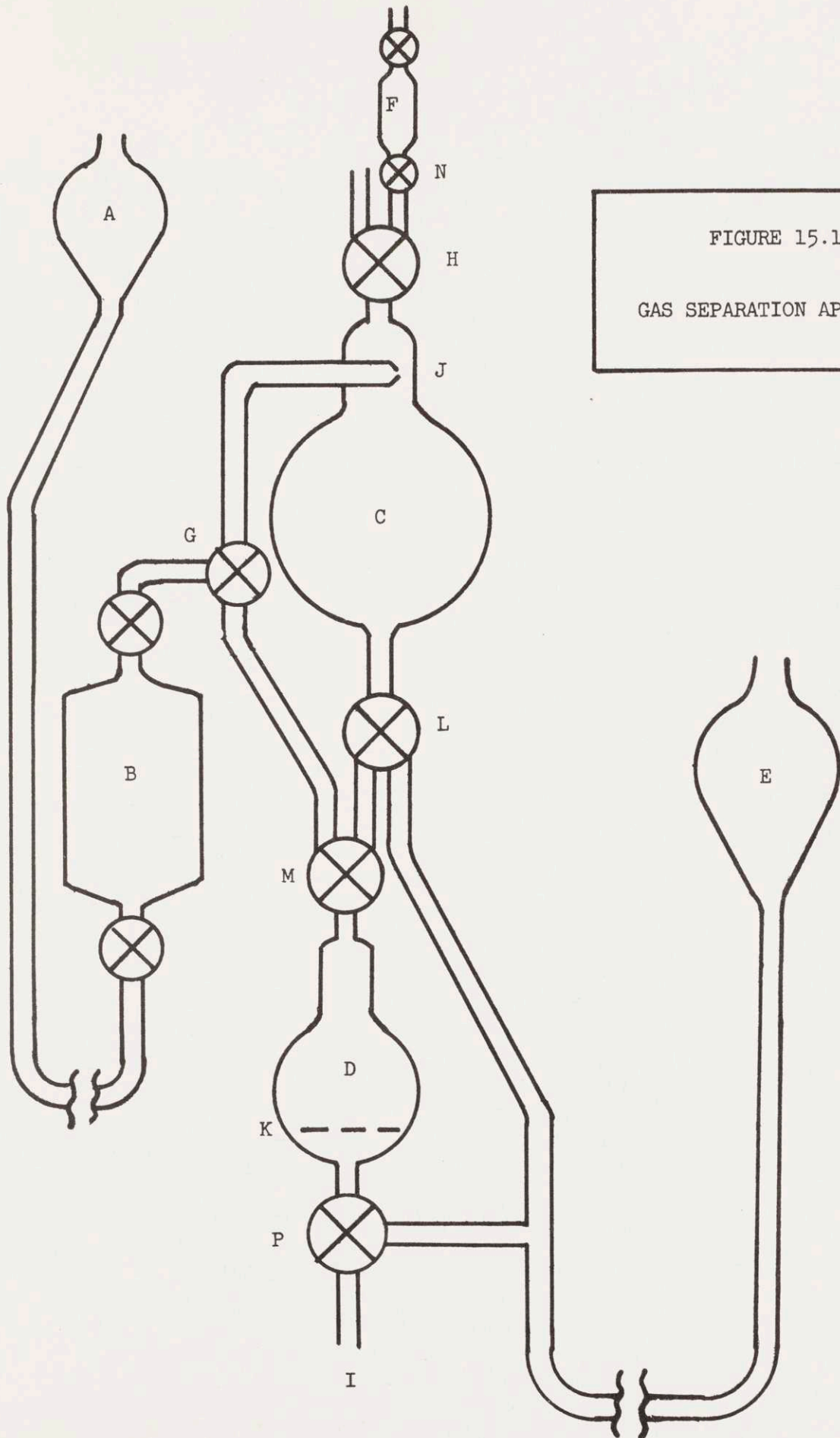


FIGURE 15.1

GAS SEPARATION APPARATUS

taken this way to ensure that the sample actually taken for analysis will be truly representative. The mercury is then drained back into bulb E by opening stopcocks G and H to the atmosphere. The solution taken in is next drained out through I.

Flask D and the line up to the jet J are then refilled with mercury from bulb E. Sample is again taken from the sample bulb B, this time until the water - mercury interface has dropped to the mark K on flask D. This sample is closed off by stopcocks G and P. The volume between mark K and stopcock G is 54 cc.

Mercury from bulb E is then brought up through stopcock L, flask C, and gas sample bulb F to stopcock O. Stopcock O is then closed, and bulb E is lowered so as to bring the mercury level back below stopcock L and thereby evacuate bulb F and flask C.

Bulb E is raised and stopcocks G, M, and P are opened so as to force the water sample to squirt through jet J under mercury pressure and vacuum. A fine spray occurs through J, impinging with considerable velocity against the other wall of the flask neck, since J has a diameter on the order of 0.5 mm. When the mercury reaches the jet J, stopcocks G and P are closed, and stopcocks L and M are opened. Stopcock P is then reopened and bulb E lowered still more to drain the water from flask C to flask D. Then stopcock P is closed and stopcock L is reversed. Bulb E is raised and the extracted gas is

forced into gas sample bulb F, the mercury being brought up to stopcock N, which is then closed to enclose the gas sample.

Following this, flask C is re-evacuated and the stripping operation is repeated twice more, the total extracted gas sample being collected in bulb F. For propylene an additional pass is necessary.

If the spray operation were completely efficient, equilibrium would be attained between the gas remaining in solution and that extracted from it in flask C. For the most soluble gas, propylene, the fraction, f , extracted per pass would be determined from

$$p = H c \quad (\text{Henry's Law}) \quad (15.4.1)$$

$$p = \frac{f c_0 V_s RT}{V_c - V_s} \quad (\text{Perfect Gas Law}) \quad (15.4.2)$$

$$c = (1 - f) c_0 \quad (\text{Definition}) \quad (15.4.3)$$

where p = partial pressure of propylene in the gas space

H = Henry's Law constant (reciprocal solubility)

c = concentration left in solution

V_s = water sample volume

V_c = volume of flask C

R = gas constant

c_0 = concentration originally in solution

combined, these three equations give

$$f = \frac{H}{H + \frac{V_s}{V_c - V_s} RT} \quad (15.4.4)$$

In this case $V_s = 54$ cc, and $V_c = 100$ cc, H for propylene = 5.8×10^3 atm/mole fraction at 20°C (109d), or 1.04×10^2 atm/mol/liter.

Thus

$$\begin{aligned} f &= \frac{104}{104 + \frac{54}{46} (.082) (293)} \\ &= 0.79 \end{aligned}$$

For hydrogen $f = 0.98$ and for helium $f = 0.99$. It was found experimentally that these figures were very closely approached for a pass through the jet. Hence the three passes for helium and hydrogen and the four for propylene were more than sufficient.

The total time required for a separation was about 30 to 45 minutes.

A feature of this separation technique is that the extracted gas sample and the water solution are at all times under vacuum with respect to the atmosphere, since the volume of the gas sample bulb is larger than the one atmosphere volume of the extracted gas in all cases.

This means that, if there is any leak in the system, it will be a leak of oxygen and nitrogen in from the atmosphere. There would be no interference with the chromatographic analysis from these gases.

In carrying out the separation, it was always necessary to add to the gas sample a few drops of water which remained on the surface of the mercury. This came from the reduction in volume of a gas mass already saturated with water vapor and also from water clinging to various portions of the system. This water did not interfere with the chromatographic analysis.

15.4.2 Chromatographic Analysis

For quantitative analysis of the extracted gas samples a model 154 Perkin - Elmer Vapor Fractometer was utilized. This unit provides for isothermal operation from room temperature to 180°C, a wide range of carrier gas flow rates, interchangeable columns of various adsorbents and absorbent supporters, and a detection unit consisting of matched thermistors in a bridge circuit. The output signal from the thermistor bridge is proportional to the difference in thermal conductivity between the gas passing through the detector thermistor and the carrier gas passing by the reference thermistor, and is recorded by a 6 volt Brown recorder. The signal is, therefore, also proportional to the particular gas concentration in the carrier stream at that point for dilute concentrations (116a). Each gas in a sample produces a voltage "peak" upon passing through the detector thermistor, dependent in size and spread upon concentration of the gas, upon the amount of effective

axial diffusion it has undergone in the adsorption - desorption process in the column and in the flow through the lines, and upon the difference in thermal conductivity between the gas and the carrier gas.

A six foot column (about 1/8 inch inside diameter) of silica gel was used as adsorbent in all analyses. A highly adsorbent material such as this gives the highest resolution for light gases, and readily separates the components of air from nonadsorbed gases such as helium and hydrogen. A system was set up whereby the gas samples could be injected in one of two ways, as is shown in Figure 15.2.

The sampling valve supplied with the column (and intended for constant volume gas samplings) was equipped with fittings and rubber tubing so that the 10 cc gas sample bulbs from the separation apparatus could be inserted there and injected into the carrier line between the reference thermistor and the column. The carrier gas line to the column was also fitted with a sampling device, which provided for injection prior to the reference thermistor.

The former injection method was used normally; the latter was used when it was desired to spread a peak out more since the sample would travel farther before reaching the detector cell. Different calibrations (see below) were, of course, encountered for the two methods. The second injection method caused the sample to pass through the reference thermistor; hence a "reverse" peak was obtained from it. However,

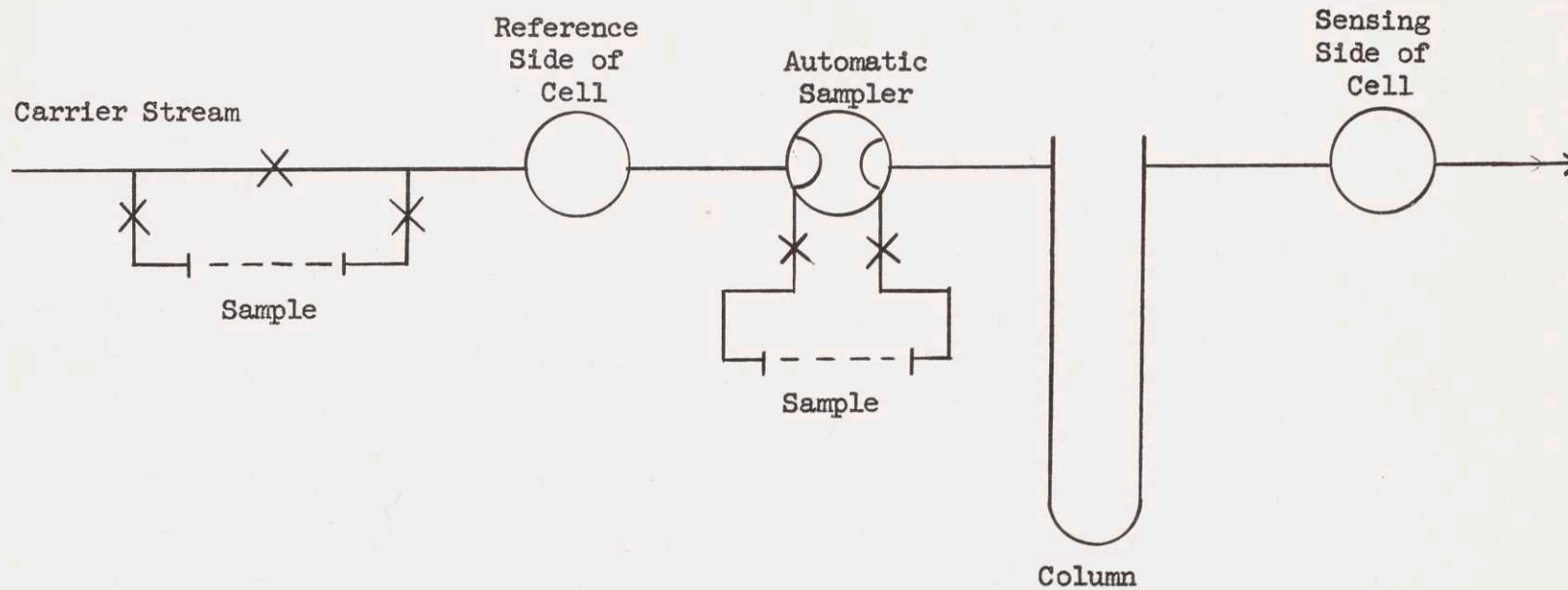


FIGURE 15.2 SAMPLING FACILITIES FOR CHROMATOGRAPH

since the carrier flow passes directly through the detector thermistor and only diffuses into the reference one from the main stream, this was a very wide and low peak and did not interfere with measurement of the sharper output peak from the detector.

Higher temperature tends to reduce the retention time of the column for a particular gas, in general, since the gas is less strongly adsorbed. For this reason higher temperature also tends to reduce the resolution of one gas from another. Peak height tends to increase with increasing temperature and peak width tends to decrease. Peak height and degree of resolution are relatively insensitive to carrier gas flow rate. Peak spread decreases with increasing flow rate, and retention time, of course, decreases with increasing flow rate. In general, therefore, it is preferable to use the highest possible carrier flow rate.

For helium and hydrogen analyses, oil-pumped nitrogen was used as the carrier in order to maximize the thermal conductivity difference. Since it was necessary to resolve the other component of air, oxygen, from the helium or hydrogen, the temperature of operation was 30°C, a relatively low temperature. A carrier flow of 50 cc/min was employed.

Since the amount of hydrogen or helium to be measured in a sample ranged from about 0.05 cc (RTP) to 1.0 cc or more, three calibrational gas holding vials with volumes in this range were prepared by blowing three-arm stopcocks together so as to enclose the desired volume within the joined arms. The two smallest volumes (0.08 cc and 0.16 cc) were

prepared from 2 mm capillary arm stopcocks, the larger (0.8 cc) was made from 5 mm arm stopcocks. A vial would be filled with the gas at room conditions, the arms and bores would be swept out with air, and then the known volume would be sucked into an evacuated 10 cc sample bulb and injected from there into the column. This was done so that the initial dispersion of the gas in the carrier gas would be the same as that of the experimental samples.

Hydrogen and helium showed linear variations of peak height with respect to quantity injected. This was to be expected, for both are essentially nonadsorbed gases, and peak spread is therefore determined by axial diffusion alone, a process independent of concentration. Combining the peak height per unit amount of gas with the quantity of a water solution taken into the separation apparatus (54 cc) the calibration for normal injection of helium was 4.25×10^{-6} moles per liter per millivolt of peak height, and for normal injection of hydrogen was 2.50×10^{-6} moles per liter per millivolt of peak height. The full scale deflection of the Brown recorder is 10 millivolts. The peak height is also controlled in a directly proportional manner by the voltage placed across the thermistor bridge, which is readable on a voltmeter to ± 0.1 volt. In this instance the voltage supplied to the bridge was 4.0 volts so a sensitivity of about 0.2 millivolts was attainable in the output signal. Thus a concentration in a water solution equal to 4% of

saturation for helium and 1% of saturation for hydrogen could be determined to +5%.

Output voltages greater than 10 mv. are read on the 10 mv scale by a set of scaling resistors; therefore the percentage of error in analysis tended to be essentially independent of concentration level.

It is interesting to notice, too, that the values obtained for N.T.U. in the packed tower measurements and for $\ln \left(\frac{\Delta C_0}{\Delta C_f} \right)$ in the diaphragm cell measurements are actually independent of the calibration, so long as it is linear. Thus the error influencing factors are only the degree of linearity of the calibration and the amount of wandering of the voltage across the bridge between the time of the rich sample analysis and that of the lean sample.

For propylene a carrier gas of helium was chosen, again for maximum difference in thermal conductivities. The carrier flow rate was 50 cc/min and the temperature was, in this case, 150°C, since there was no nearby peak to interfere with the propylene peak. In the case of propylene, a strongly adsorbed gas, the peak was nonsymmetrical because of the nonlinearity of the adsorption isotherm. As a consequence, the peak height was distinctly nonlinear with respect to the quantity of propylene in the sample. It was found upon calibration, however, that the area under a peak did tend to be linear (indicating thermal

conductivity directly proportional to concentration of propylene in the carrier at these concentrations). Injection and flow conditions were chosen to give a peak as high as it was wide at the operating recorder speed. For propylene the calibration was 2.5×10^{-4} moles per liter per minute-millivolt. Areas were measured with a planimeter. Assuming a possible error due to bridge voltage variation and background variation on the order of 5% of an area, a propylene concentration equal to 2% of saturation could be measured with +5% error. The above remarks concerning independence of mass transfer results of calibration and concerning constancy of relative error with respect to concentration level also apply for propylene.

Typical peaks for hydrogen and helium and for propylene are shown in Figures 15.3 and 15.4. The detector bridge circuit is so set up that a negative deviation from carrier gas thermal conductivity gives a positive peak and vice versa. Hydrogen and helium, therefore, give negative peaks with a nitrogen carrier; whereas propylene gives a positive peak with a helium carrier.

15.5 Potassium Chloride

In the calibration runs for the diffusivity cells the chloride concentrations were analyzed by the standard Mohr technique (106a, 122a). This involves a titration against silver nitrate using potassium chromate as an indicator. The chromate ion is adsorbed by the colloidal

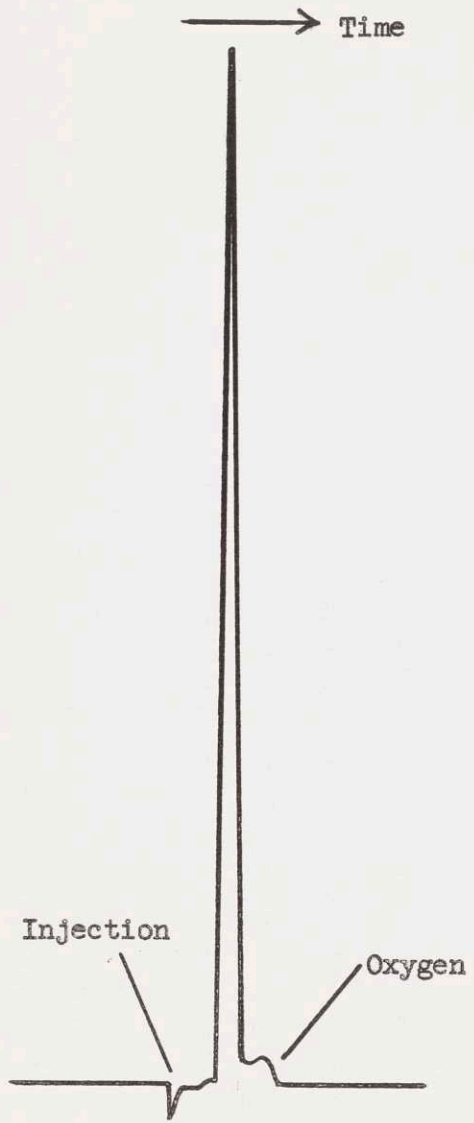


FIGURE 15.3 TYPICAL PEAK FOR HELIUM & HYDROGEN

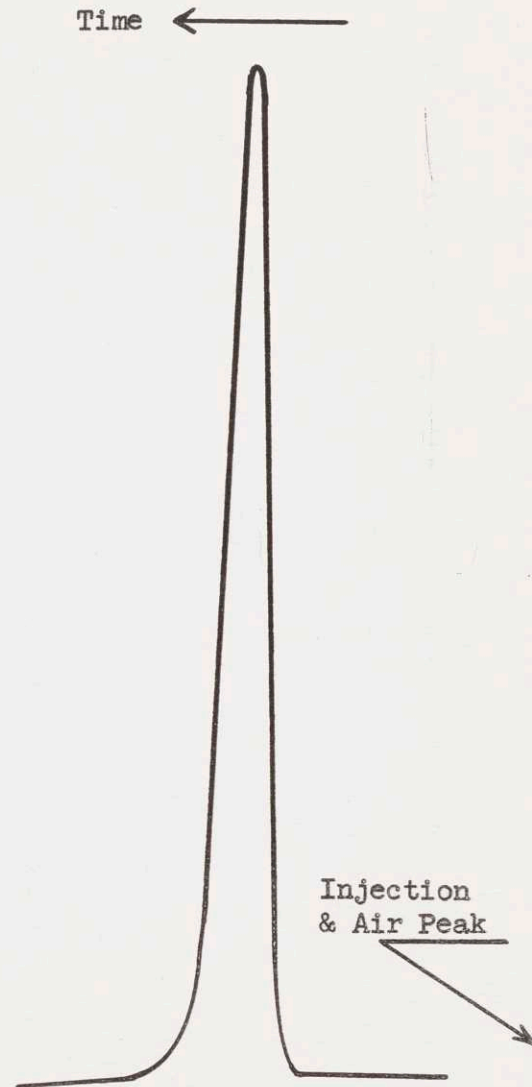


FIGURE 15.4 TYPICAL PEAK FOR PROPYLENE

silver chloride precipitate, giving a light yellow color when chloride ion is in excess over silver ion in solution, and a reddish-brown color when silver ion is in excess. At the concentrations used in this study (0.1 N and 0.01 N chloride) the endpoint is determinate within a drop or so (0.05 cc). An experimentally determined correction on the order of 0.05 cc is necessary to account for the amount of silver nitrate needed to initiate the color change.

Two samples were taken by draining solution into flasks from the rich side of a cell, and one sample was taken from the lean side. The quantity of sample taken was computed from the difference in flask weights before and after receiving the sample, determined on an analytical balance. The weight thus found was corrected by standard density data (109b) to obtain the sample volume taken.

CHAPTER 16

Method of Treatment of Data

16.1 Method of Calculating Transfer Coefficients

For the purpose of obtaining coefficients of absorption plug flow of gas and liquid through the packing was assumed, and the $K_L a$ coefficient was taken to be independent of concentration and tower height. The latter assumption is predicted by two-film theory and also by penetration theory if the tower height is large compared to the distance a liquid surface falls during an exposure (see also Section 5.1.3). The independence of concentration level effect on $k_L a$ is a basic tenet of mass transfer theory for dilute solutions in which the physical nature of the solution is constant throughout the tower. As shown in Section 5.1.1, it is valid to assume that $K_L a$ is for all intents and purposes equal to $k_L a$ for the gases under study. For dilute solutions where L and ρ_L do not vary throughout the tower, then, the following equations apply (see Section 2.1.4)

$$K_L a = \frac{L}{\rho_L (\text{H.T.U.})_{OL}} = \frac{L}{\rho_L h} (\text{N.T.U.})_{OL} \quad (16.1.1)$$

$$(\text{N.T.U.})_{OL} = \int_{C_B}^{C_t} \frac{d C_L}{C_L - C_e} \quad (16.1.2)$$

- where $K_L a = \frac{N_A}{C_L - C_e}$ (see Section 2.1.4) (length/time)
- N_A = Mass transfer rate per unit area of interface
(moles/time area)
- C_L = Solute concentration in water (moles/volume)
- C_e = Solute concentration in equilibrium with gas
phase concentration at a point (moles/volume)
- ρ_L = Liquid density (= water density) mass/volume)
- L = Liquid flow rate (= water flow rate) (mass/time area)
- h = Tower height (length)
- (H.T.U.)_{OL} = Height of a liquid phase transfer unit based
on overall driving force (length)
- (N.T.U.)_{OL} = Number of transfer units based on overall driving
force
- C_T = Solute concentration in water entering at top of
column
- C_B = Solute concentration in water leaving at bottom
of column

The evaluation of the integral representing N.T.U. may be performed analytically if the driving force ($C_L - C_e$) at any point is a linear function of the solute concentration in the water at that point. In that case

$$\frac{d(C_L - C_e)}{d C_L} = \frac{(C_L - C_e)_T - (C_L - C_e)_B}{C_T - C_B} \quad (16.1.3)$$

at every point. Equation (16.1.2) then becomes, upon integration,

$$(N.T.U.)_{OL} = \frac{C_T - C_B}{(C_L - C_e)_T - (C_L - C_e)_B} \ln \frac{(C_L - C_e)_T}{(C_L - C_e)_B} \quad (16.1.4)$$

16.1.1 Helium, Hydrogen, and Propylene

For the desorption of helium, hydrogen, and propylene there is no solute present in the incoming air stream entering the bottom of the column. Also there is such a low rate of transfer (because of the low solubilities and consequent very small amounts of solute in the incoming water stream) that in no case does the gas phase concentration of solute build up to such a degree that C_e becomes significant in comparison with C_L before the air stream leaves the top of the packing. C_e is always less than 0.3% of C_L . Hence C_e may be taken as constant and equal to zero in Equation (16.1.2). The driving force is then equal to C_L at all points, and is, obviously, linear in C_L . Equation (16.1.4) is then applicable in the form

$$N.T.U. = \ln \frac{C_T}{C_B} \quad (16.1.5)$$

This, coupled with Equation (16.1.1), enabled calculation of $(N.T.U.)_{OL}$, $(H.T.U.)_{OL}$, and $K_L a$ for helium, hydrogen, and propylene runs. Values

of C_T and C_B were obtained from solution analyses.

16.1.2 Oxygen

For oxygen runs the total rate of mass transfer is again so small in all cases that there is no perceptible build-up of oxygen in the air stream above the concentration present in laboratory air. Oxygen, however, composes some 21% of air, and the concentration of oxygen in the inlet water stream was never greater than that in equilibrium with one atmosphere of oxygen gas phase partial pressure, and usually was a quantity in equilibrium with something like 0.5 atmosphere partial pressure. The C_e term in the driving force was therefore quite significant in comparison with C_L at every point of tower height.

If the value of C_e were the same at tower top and tower bottom, and at all points of height in between, then $C_L - C_e$ would again be linear in C_L , and Equation (16.1.4), would reduce to

$$(N.T.U.) = \ln \frac{(C_L - C_e)_T}{(C_L - C_e)_B} \quad (16.1.6)$$

This was the relationship utilized by Holloway (61i) for calculation of his results for oxygen desorption.

In actual operation, however, C_e did not retain a constant value throughout the tower. C_e at any point is defined by

$$C_e = Y_{O_2} (P - p_w) / H \quad (16.1.7)$$

where Y_{O_2} = mole fraction of oxygen in dry air

P = total pressure (atm)

p_w = vapor pressure of water (atm)

H = Henry's Law constant (atm/(moles/vol))

p_w is used and is valid because the air is saturated at every point. Were it not, the partial pressure of water would be substituted for the vapor pressure. Since there was no oxygen build-up, Y_{O_2} is a constant, equal to 0.210.

C_e varied throughout the column for two reasons:

- 1) The water temperature would change slightly from tower top to tower bottom (about 0.5°C).
- 2) There was a pressure drop through the packing (a secondary effect).

The pressure drop served to alter the size of P in Equation (16.1.7), whereas the temperature change affected both H and p_w . Both are temperature sensitive terms, H changing by 2% per °C, and p_w changing so as to make $(P - p_w)$ change by 0.2% per °C.

It is important to notice that these effects serve to make C_e a linear function of tower height, rather than of C_L . P , because of pressure drop, is a linear function of height and if the temperature change occurs through heat loss to the surrounding atmosphere alone

H and p_w are linear in height. If any of the temperature effect is due to humidification or heat transfer to the air stream, it occurs at a greater rate near the tower bottom than near the top, whereas C_L changes more rapidly with height near the tower top. Humidification and heat transfer to air stream temperature effects therefore serve to accentuate the nonlinearity of C_e in C_L .

The evaluation of the N.T.U. integral may now be discussed, with reference to Figures 16.1 and 16.2. Figure 16.1 depicts the value of the driving force ($C_L - C_e$) as a function of C_L , and Figure 16.2 depicts the curve $1/C_L - C_e$ as a function of C_L , the area under which would give the value of the N.T.U. integral. Both figures are exaggerated to point out the significant effects but apply to typical desorption runs at 1 ft. packed height.

For the case in which C_{eB} is less than C_{eT} , the difference in equilibrium concentrations, $C_{eT} - C_{eB}$, may be denoted by ϵ . If C_e were a linear function of C_L (rather than of tower height) the history of ($C_L - C_e$) would be given by curve A in Figure 16.1, and the N.T.U. integral would be given by the area under curve A in Figure 16.2. Since ($C_L - C_e$) would be linear in C_L in this case, the value of this integral would be given by Equation (16.1.4) as

$$(N.T.U.)_{OL} = \frac{C_T - C_B}{C_T - C_B - \epsilon} \ln \frac{(C - C_e)_T}{(C - C_e)_B} \quad (16.1.8)$$

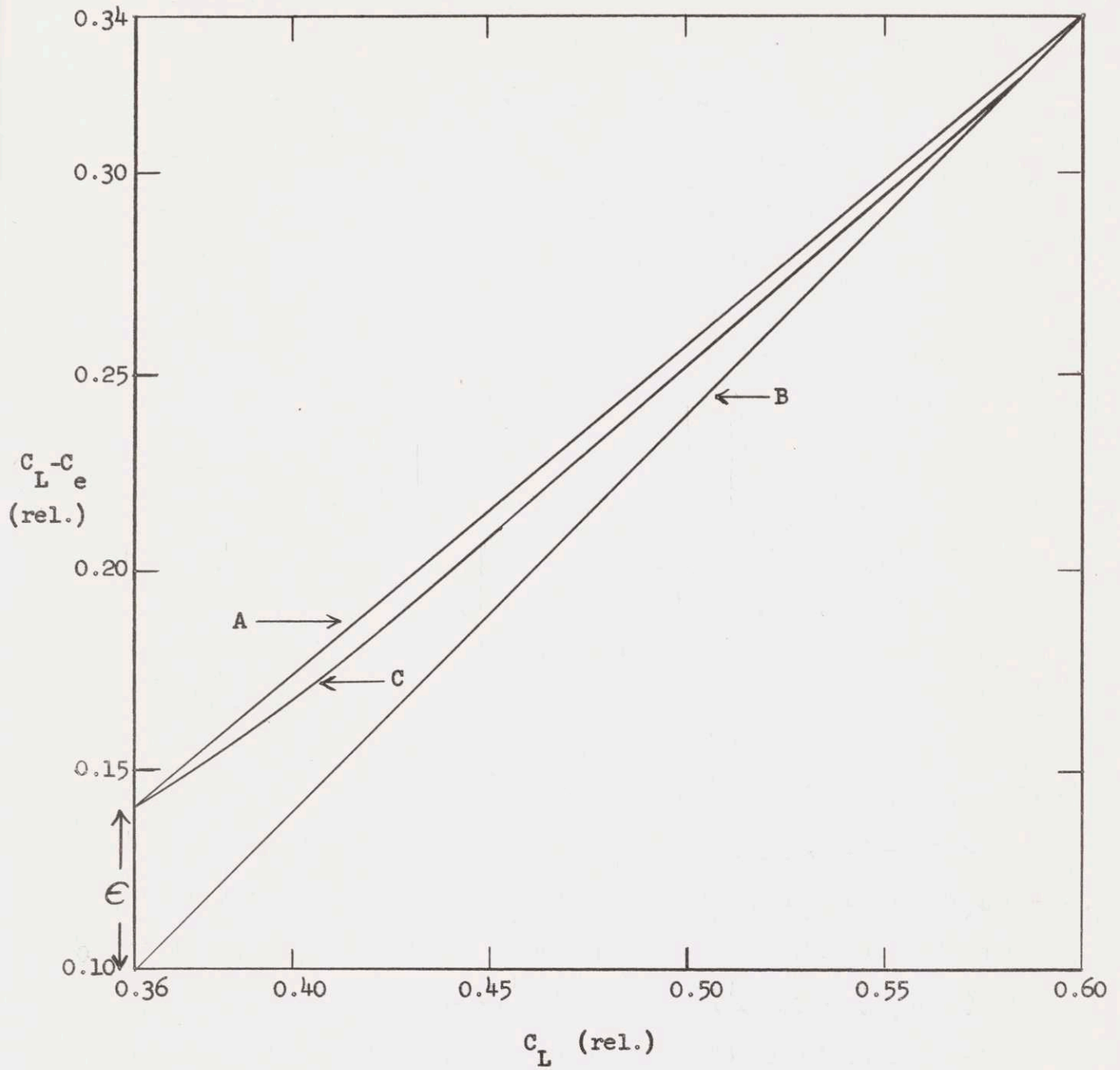


FIGURE 16.1 DRIVING FORCE PROFILE FOR OXYGEN RUN

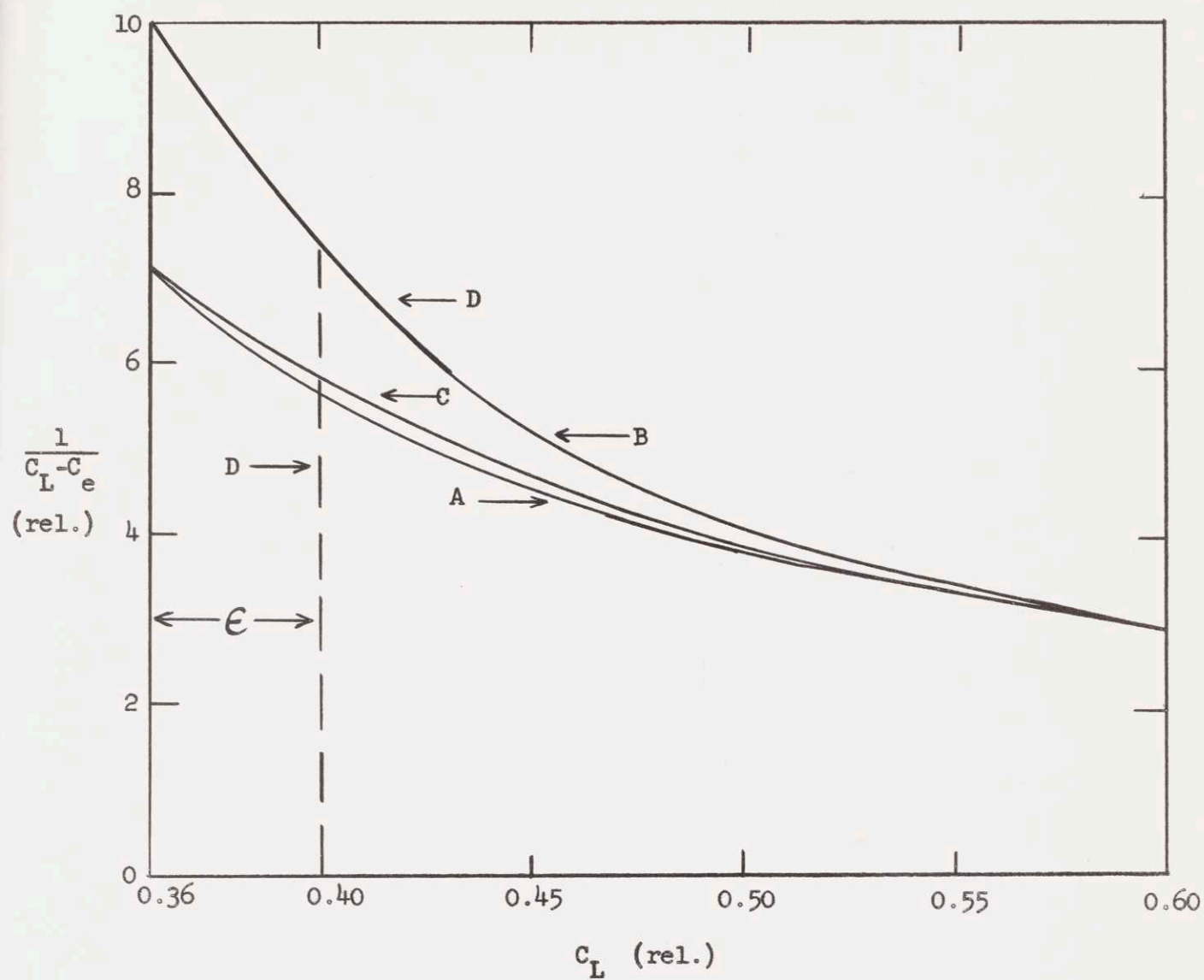


FIGURE 16.2 N.T.U. INTEGRAL FOR OXYGEN RUN

A second helpful case to consider is the fictional one in which C_e retains a constant value equal to C_{eT} throughout the column. C_e at the bottom then differs from C_{eB} above by ϵ , and $(C_L - C_e)_B$ Case II = $(C_L - C_e)_B$ Case I - ϵ . Curves corresponding to this second case are denoted by B in Figures 16.1 and 16.2. Here again $(C_L - C_e)$ is linear in C_L , and the value of the integral is given by Equation (16.1.4) as

$$(\text{N.T.U.})_{OL} = \ln \frac{(C - C_e)_T}{(C - C_e)_B - \epsilon} \quad (16.1.9)$$

where the two driving forces, $(C - C_e)_T$ and $(C - C_e)_B$, are those actually computed from the data, and $(C - C_e)_B - \epsilon = (C_T - C_{eT})$ is the fictional driving force assumed to apply at the tower bottom in this second case.

In the present runs the controlling heat effect was loss of heat from the tower to the atmosphere surrounding it, since the entering air was saturated with water vapor and a significant change in air temperature after passage through the tower could not be detected. Therefore the water temperature change and consequently C_e may be taken linear in tower height.

The history of $C_L - C_e$ as a function of C_L when C_e is linear in height may be estimated by use of the following approximate equation which applies to the case of $\epsilon = 0$ (curve B):

$$\ln \frac{(C_L - C_e)_h}{(C_L - C_e)_B} = \frac{h}{h'} \ln \frac{(C_L - C_e)_T}{(C_L - C_e)_B} \quad (16.1.10)$$

which is an integration of Equation (16.1.2). h is the height of a level above the bottom, and h' is the total height. From this equation, the approximate tower level corresponding to a given value of C_L may be determined, and then the value of C_e corresponding to that level and C_L can be computed from the assumed linearity in height. Curves C in Figures 16.1 and 16.2 were computed in this manner for the case at hand. The "true" $C_L - C_e$ curve follows curve B near the tower top, where C_L changes rapidly with height, and then approaches curve A near the tower bottom, with ever decreasing slope, since C_L changes less and less rapidly with height as the tower bottom is approached.

In this case, the area under curve C, the "true" curve, is nearly that under curve A, being about 15% away in the direction of the area under curve B. Although this calculation was for a desorption case at 1 foot packed height, similar calculations and plots for absorption cases and for desorption at 2 feet packed height show this behavior to apply there, also.

For oxygen runs, therefore, the true N.T.U. was taken as

$$\text{N.T.U.} = (\text{N.T.U.})_1 + 0.15 \left[(\text{N.T.U.})_2 - (\text{N.T.U.})_1 \right] \quad (16.1.11)$$

where $(N.T.U.)_1$ was computed by Equation (16.1.8) and $(N.T.U.)_2$ was computed by Equation (16.1.9).

An entirely analogous situation applies when C_{eB} is greater than C_{eT} , with Equation (16.1.11) again being the best to use for calculation. The same relationship also applies to the case of a desorption run. To use Equation (16.1.11) for these various cases, ϵ must always be taken as $C_{eT} - C_{eB}$ (and will be a positive or negative number, depending on the case at hand), and the driving forces must always be taken as $C_L - C_e$. They would therefore be negative numbers for an absorption case.

In most of the runs the N.T.U. calculated from Equation (16.1.8) differs by no more than a per cent from that calculated by Equation (16.1.9), so the problem of the "best" approximation to use becomes a moot question. What is important though, is that the N.T.U. predicted by either of these integrals is in many cases several per cent different from that calculated by Equation (16.1.6), which was the equation used by Holloway and is the one that would normally be employed when one neglects pressure drop and temperature change effects.

The curves marked D in Figures 16.1 and 16.2 correspond to the use of Equation (16.1.6). In order to fit this equation to an analytical integration of the form (16.1.4) for $(C_L - C_e)$ linear in C_L it is necessary to integrate only from $C_L = C_B - \epsilon$ to $C_L = C_T$ so that the

multiplicative term before the logarithmic term in (16.1.4) becomes equal to one. This requirement is the primary reason for the lesser area under curve D and corresponding erroneous result predicted by Equation (16.1.6).

An error of three or four per cent in N.T.U., H.T.U., and $K_L a$ would not have a serious effect on the variation of $K_L a$ with liquid flow rates found by Holloway in most cases (see Chapter 18). In the current study, however, a small error in $K_L a$ and H.T.U. can have an appreciable effect on the slope of the plots of H.T.U. and $K_L a$ versus diffusivity. This is so because of the small range of diffusivities and transfer coefficients (a factor of 4.5 in diffusivities), because the correction would apply only to the oxygen point, and also especially because of the great weight given to oxygen data in determining the slopes of log H.T.U. versus log D_L (see Section 16.2).

Since the values of C_e carry such weight there is also a problem of which literature values of oxygen solubilities to use. Seidell (125) gives several sets of oxygen solubility data. At room temperature these various sets of data have a range of about 3%, which means that the choice of data can definitely affect the N.T.U. computed from packed tower runs, especially in instances where the rate or tower height was great enough to bring the oxygen in the water close to equilibrium with the air at the tower bottom. Seidell (125) gives

several sets of solubility data. Winkler's data cited therein lie between the two most recent literature values; also they were checked to an extent by some preliminary experiments made by Holloway (61h). For these somewhat arbitrary reasons the Winkler data were adopted for calculations in the present work. A plot of the Winkler data is given in Figure 19.2. A comparison of the absorption data for oxygen for Runs 63, 64, and 66 with the desorption data of Run 65 throws the exact accuracy of the Winkler oxygen data into question (see Section 5.1.2).

16.1.3 Carbon Dioxide

Contrary to the situations for the other four solute gases there was, in the carbon dioxide runs, often a concentration of carbon dioxide in the inlet water sufficient to give a significant build-up of solute in the air stream, and a consequent increase in C_e in the air as it passed up through the tower. This was a result of the higher solubility of carbon dioxide in water.

For the dilute streams encountered in this work the air and water solution flow rates may still be treated as constant throughout the tower, and the carbon dioxide partial pressure in the air at any point is given by the following simple material balance, which says that the amount of carbon dioxide leaving the water between any point and the tower bottom equals the amount entering the air stream between

the bottom and that point.

$$\frac{L}{\rho_L} (C_L - C_B) = \frac{G}{\rho_A RT} (p - p_B) \quad (16.1.12)$$

where G = air flow rate (mass/time area)

ρ_A = air density (mass/volume)

R = gas constant (atm. volume/mole degree)

p = solute partial pressure at any height (atm.)

p_B = solute partial pressure at tower bottom (atm.),

and other terms have been introduced previously.

Combining this material balance with a Henry's Law relationship for carbon dioxide ($p = Hc_L$), there results

$$c_e = 1/H \left[\frac{L}{G} \frac{\rho_A RT}{\rho_L} (C_L - C_B) + p_B \right] \quad (16.1.13)$$

In this case, as in the oxygen case, H , ρ_A , and T may all vary somewhat from tower top to tower bottom; however in all instances for carbon dioxide runs the percentage variation in $C_L - C_B$ was such as to overshadow the effects of variations in H , T , and ρ_A . For carbon dioxide runs the first term in parentheses is much greater than the second (p_B) term; whereas for oxygen runs the second term is much greater than the first (no significant solute build-up in the air stream). The result is

that for carbon dioxide C_e may be taken as a linear function of C_L , while for oxygen C_e has to be taken as a linear function of h , the tower height.

Because of the linearity of C_e , and thus $C_L - C_e$, in C_L , Equation (16.1.4) (or its alternate form (16.1.8)) applies for the calculation of N.T.U. for carbon dioxide.

$$(N.T.U.)_{OL} = \frac{C_T - C_B}{C_T - C_B - \epsilon} \ln \frac{(C_L - C_e)_T}{(C_L - C_e)_B} \quad (16.1.8)$$

Here C_{eT} is calculated from Equation (16.1.13), and p_B may be taken as 6×10^{-4} atm, a value found by Holloway in preliminary work (61b) and about twice the normal value cited for the average concentration of carbon dioxide in air. The actual magnitude of this number has practically no effect on the N.T.U. calculated; the important effect is the build-up of carbon dioxide in the air stream because of the relatively large rate of mass transfer.

The magnitude of C_e in carbon dioxide runs is never so great relative to C_L as in oxygen runs; therefore the reliability of the solubility data employed is by no means as important. Seidell (125) gives the data of Bohr (1899), which are representative of other literature data, and were measured at sufficiently high pressures (1 atmosphere) to suppress the hydrolysis reaction which would occur in pure water (see Section 15.3 and Reference 61f for a discussion of the possible hydrolysis of

carbon dioxide in distilled water and Cambridge city water). The data of Bohr were used for the present calculations.

16.1.4 Temperature Corrections

Sherwood and Holloway (131) found a variation of k_{La} with $e^{+0.023T}$ (T in degrees Centigrade or Kelvin); however the results discussed in Section 5.2.2 indicate that a better relationship is for k_{La} to vary as $e^{+0.020T}$. This corresponds to a change of 2.0% per degree in H.T.U. All H.T.U. and K_{La} ($= k_{La}$) values were corrected to 25°C in this manner, using a plot shown as Figure 19.1. In no case, other than when the effect of temperature was being studied, did this correction exceed 2.0%.

16.2 Method of Averaging and Plotting Results

16.2.1 Plots of $(H.T.U.)_{OL}$ versus D_L

The methods of statistics applied to small numbers of observations as presented by Dean and Dixon (26) were used to obtain "best" values of the H.T.U. at each flow condition for each solute. In essence the procedure involves taking the median rather than the mean of the various values measured for individual sets of samples in individual runs. The median is more efficient for a number of observations less than eight, primarily because it is less influenced by a gross error in a single

observation. In only three cases was the median not taken as the best value. In these cases the data tended to cluster in groups of relatively equal size at either end of the range, and the mean was taken instead as the best value.

The best measure of the population (true, for an infinity of measurements) standard deviation for eight or less observations is given by s_w , a factor obtained as the product of the range, w and a factor K_w , which is tabulated by Dean and Dixon and is a function only of the number of observations. Similarly the best estimate of the population-variance is s_w^2 .*

As is shown by Mickley, et al, (91a), the best estimation of the variance of the best value of a set of observations from the true value is the sample estimate of the variance from the true mean, defined as

$$s_m^2 = \frac{s_w^2}{n_i} \quad (16.2.1)$$

*If the usual statistics of large numbers of observations applied, the best estimate of the population standard deviation would be the sample estimate of the standard deviation, defined as

$$s = \sqrt{\frac{\sum_{i=1}^{n_i} (x_i - \bar{x})^2}{n_i - 1}}$$

where n_i is the number of observations and $x_i - \bar{x}$ is the difference between an individual observation and the mean value.

where n_i is the number of observations and s_w^2 is the variance computed from the sample. s_w^2 is used here rather than s^2 because of its greater efficiency. A summary of the best values of the experimental data is given in Table 17.2, along with the values of s_m^2 and s_w in each case.

Since there is a wide range of values of s_m^2 for the various solute gases at the various flow conditions, it is desirable to use a weighted least squares technique to derive the best plot of $\log(\text{H.T.U.})$ vs. $\log D_L$ for each flow condition.

The ordinary least squares method of fitting a straight line to a plot of two variables is the linear regression of one variable, y , upon the other, x . Such a technique involves minimizing the sum of the squares of the differences between the reported values of y and the values given by the straight line at the corresponding x . The procedure however assumes that, if the straight line is a true functional relationship, only the measurements of the y variable may be in error.

Such is not the case here, for both the H.T.U. values and D_L values were measured experimentally, and an examination of the s_m^2 values for each indicates that the error in one is certainly not negligible in comparison to that in the other; in fact the relative errors in H.T.U. and D_L are roughly equal for a given solute gas.

Davies (24) presents a method for fitting a straight line functional

relationship to data by least squares for a case in which both variables may be in error. Use of the method requires that σ_y^2 (population variance) be the same for all points and that σ_x^2 also have a certain constant value, not necessarily equal to σ_y^2 . The line is required to go through the mean - \bar{x} , \bar{y} - of the observed data, and has a slope, b , determined by

$$b = m + \sqrt{m^2 + k^2} \quad (16.2.2)$$

$$\text{where } k^2 = \sigma_y^2 / \sigma_x^2 \quad (16.2.3)$$

$$\text{and } m = \frac{\left\{ \sum_{n_1} (y_i - \bar{y})^2 - k^2 \sum_{n_1} (x_i - \bar{x})^2 \right\}}{2 \sum_{n_1} (x_i - \bar{x})(y_i - \bar{y})} \quad (16.2.4)$$

In the present instance some points (i.e., oxygen) have very small variances (s_m^2) with respect to both H.T.U. and D_L , and others (i.e., helium) have relatively larger variances. There is also not too marked a tendency for the H.T.U. variances and the D_L variances to bear the same ratio one to another for all five solute gases at the same flow condition. There is, however, a strong tendency for the solute gases to line up in the same order for H.T.U. variances as for D_L variances.

Since by visual inspection there was only a choice of a few per cent to be made in the establishment of the slope of a log H.T.U. vs. log D_L plot, the absolute reliability and validity of the least squares technique

could be sacrificed to the simplicity of using an analytical method rather than employing a more tedious trial and error method.

In applying the analytical method, a weighting factor, W_i , was applied to each point. W_i was defined thus:

$$W_i = \left[\frac{(H.T.U.)_{OL}^2 (D_L)^2}{(s_m^2)_{H.T.U.} (s_m^2)_{D_L}} \right]^{1/2} \quad (16.2.5)$$

That the reciprocal variance is indeed the proper weighting factor⁶ is shown by Mickley, et al, (91a). The geometrical mean was employed somewhat arbitrarily in order to retain an equal influence of both values of s_m^2 on the resulting W_i values. Relative dimensionless variances ($s_m^2 \div (\text{measured value})^2$) rather than the absolute, dimensional s_m^2 values are employed because we are here dealing with log-log plots, rather than simple rectilinear ones.

The weighting factors are introduced into Equation (16.2.4) so as to "count" each point a number of times proportionate to the weighting factor. Thus (16.2.4) becomes

$$m = \frac{\sum_{n_i} W_i (y_i - \bar{y}_w) - k^2 \sum_{n_i} W_i (x_i - \bar{x}_w)^2}{2 \sum_{n_i} W_i (x_i - \bar{x}_w) (y_i - \bar{y}_w)} \quad (16.2.6)$$

where \bar{y}_w and \bar{x}_w are now weighted averages of the points.

$$\bar{y}_w = \frac{\sum_{i=1}^{n_i} W_i y_i}{\sum_{i=1}^{n_i} W_i} \quad (16.2.7)$$

The line now must pass through \bar{y}_w , \bar{x}_w , and will have a slope, b , defined by Equation (16.2.2).

It remains to define a value of k^2 for use in Equations (16.2.2) and (16.2.6). If we let $\log (\text{H.T.U.})_{OL}$ correspond to y and let $\log D_L$ correspond to x , then k^2 equals an average value of $\left[(s_m^2)_{\text{H.T.U.}} (D_L)^2 / (s_m^2)_{D_L} (\text{H.T.U.})^2 \right]$. The simplest obvious way of doing this is to define k^2 thus:

$$k^2 = \text{antilog} \left(\frac{\sum_{i=1}^{n_i} W_i \log k_i^2}{\sum_{i=1}^{n_i} W_i} \right) \quad (16.2.8)$$

where $k_i^2 = \left[(s_m^2)_{\text{H.T.U.}} (D_L)^2 / (s_m^2)_{D_L} (\text{H.T.U.})_{OL}^2 \right]_i$

The logarithmic averaging method is necessary so a k_i^2 of 0.5 will carry the same weight as a k_i^2 of 2.0. In one case ($L = 2100$, $G = 1400$) the individual variances were such that k_i^2 for the three points measured were much different from one another, and the weighted means required

the line to pass essentially through the oxygen point. In that case k^2 was taken as 1.0. The data were such in all cases that a change of a factor of two in k^2 would have an almost negligible effect on the resulting slope.

Thus the analytical least squares technique that was employed treated the points in the set for the five solute gases at a given flow condition as if $(s_m^2)_{H.T.U.}/(H.T.U.)_{OL}^2$ was in the same ratio to $(s_m^2)_{DL}/(D_L)^2$ at all points, and as if $(s_m^2)_{H.T.U.}$ at one point bore the ratio to $(s_m^2)_{H.T.U.}$ at another point that $\sqrt{\frac{(s_m^2)_{H.T.U.}}{(H.T.U.)_{OL}} \frac{(s_m^2)_{DL}}{D_L}}$ bore between the points (and, of course, that $(s_m^2)_{DL}/(D_L)$ bore between the points). Such a technique, although certainly not rigidly valid, represents in most cases a close approach to the true situation, and certainly an accurate enough technique to give the desired 2% accuracy in the resulting slope of the line.

For his case Davies (24) gives the variance in the resultant slope as

$$s(b) = \frac{\sigma_x^2 (k^2 + b^2)^2}{k^2 \sum_{n_i} (x - \bar{x})^2 + b \sum_{n_i} (x - \bar{x})(y - \bar{y})} \tag{16.2.9}$$

Applying the weighting factors as defined by Equation (16.2.5) to this, there results

$$s^2 (b) = \frac{0.18 (k^2 + b^2)^2}{k^3 \sum_{n_i} W_i (x - \bar{x}_w)^2 + b k \sum_{n_i} (x - \bar{x}_w)(y - \bar{y}_w)} \quad (16.2.10)$$

The best estimate of the standard deviation of the slope is then $\sqrt{s^2 (b)}$. The factor of 0.18 is equal to $(1/2.303)^2$, and results from the fact that the weighting factors were based on fractional variances defined as $s_m^2 / (\text{best value})^2$, whereas the absolute variance in the \log_{10} of the quantity is $[\log e]^2$, or $(1/2.303)^2$, times the fractional variance in the quantity itself.

16.2.2 Plots of $\log (H.T.U.)_{OL}$ vs. T.

The problems encountered in the fitting of a line in the $\log (H.T.U.)$ vs $\log (D_L)$ plots do not enter in the case of plotting $\log (H.T.U.)$ against temperature. This is so because the temperature values may be considered error free in measurement compared to the H.T.U. values.

With such being the case, a simple regression of $\log (H.T.U.)_{OL}$ upon T gives the best straight line fit of the data. No weighting is necessary either, since all H.T.U.s presumably have the same precision. The line must pass through $\overline{\log (H.T.U.)}$ and \bar{T} , and the slope is given

(24) by

$$b = \frac{\sum_{n_i} (\bar{x}_i - \bar{x})(y_i - \bar{y})}{\sum_{n_i} (x_i - \bar{x})^2} \quad (16.2.11)$$

where y denotes $\log (\text{H.T.U.})_{\text{OL}}$ and x denotes T . The variance of the slope is given (24) by

$$s^2 (b) = \frac{\sum_{n_1} (y_i - Y_i)^2}{(n - 2) \sum_{n_1} (x - \bar{x})^2} \quad (16.2.12)$$

where Y_i is the value of y predicted by the line at x_i .

16.3 Sample Calculations

16.3.1 Diffusivity: Carbon Dioxide (Run 2)

NaOH = 0.0314 M

HCl = 0.0420 M

	<u>Lean Sample</u>	<u>Rich Samples</u>	
		<u>1</u>	<u>2</u>
ml. NaOH	16.48	42.75	43.21
Weight of Sample - g.	50.35	9.37	9.99
Vol. Sample			
= $\frac{\text{weight}}{\rho_{\text{H}_2\text{O}}}$ - ml.	50.45	9.39	10.01
ml. HCl	7.68	21.99	21.72
mmoles. NaOH (=0.0314 x ml.)	0.5175	1.342	1.357
mmoles. HCl (=0.0420 x ml.)	<u>0.3226</u>	<u>0.924</u>	<u>0.912</u>

	<u>Lean Sample</u>	<u>Rich Samples</u>	
		<u>1</u>	<u>2</u>
mmoles. CO ₂ (=1/2(mm. NaOH - mm. HCl))	0.0975	0.209	0.222
Conc. CO ₂ = $\frac{\text{mmoles. CO}_2}{\text{ml. sample}}$	C _{2f} = 0.001932 M	0.0223 M	0.0222 M
		C _{1f} = ave. = 0.02225 M	

$$\begin{aligned}\Delta C_f &= C_{1f} - C_{2f} \\ &= 0.02225 - 0.00193 \text{ M} \\ &= 0.02032 \text{ M}\end{aligned}$$

For Cell 2: $V_2/V_1 = 0.9766;$ $\lambda = 0.019$

$$\begin{aligned}V_2/V_1 C_{2f} &= (0.9766)(0.001932) \\ &= 0.001887 \text{ M}\end{aligned}$$

$$\begin{aligned}\lambda/2 (C_{1f} + C_{2f}) &= \frac{0.019}{2} (0.02225 + 0.00193) \\ &= 0.000230 \text{ M}\end{aligned}$$

$$\begin{aligned}\Delta C_o &= C_{1f} + V_2/V_1 C_{2f} + \lambda/2 (C_{1f} + C_{2f}) \quad (\text{Eq. (14.5.29)}) \\ &= 0.02225 + 0.001887 + 0.000230 \\ &= 0.02437 \text{ M}\end{aligned}$$

$$\begin{aligned}\log_{10} \left(\frac{\Delta C_o}{\Delta C_f} \right) &= \log \left(\frac{0.02437}{0.02032} \right) \\ &= 0.07898\end{aligned}$$

$$\begin{aligned}\log_{10} (1 - \lambda / 6) &= \log \left(1 - \frac{0.019}{6} \right) \\ &= -0.00139\end{aligned}$$

$$t_f = 4248 \text{ minutes}$$

$$\beta' = 0.0349 \text{ cm.}^{-2}$$

$$\nu = 0.9883$$

$$\begin{aligned}D_L &= \frac{2.303}{\nu \beta' t_f} \left[\log_{10} \left(\frac{\Delta C_o}{\Delta C_f} \right) + \log_{10} (1 - \lambda / 6) \right] \text{ Eq. (14.5.28)} \\ &= \frac{2.303}{(0.9883)(0.0349)(60)} \cdot \frac{1}{t_f \text{ (min.)}} \cdot \left[\log \left(\frac{\Delta C_o}{\Delta C_f} \right) + \right. \\ &\quad \left. \log (1 - \lambda / 6) \right] \frac{\text{cm}^2}{\text{sec.}} \\ &= 1.1130 \frac{\left[\log \left(\frac{\Delta C_o}{\Delta C_f} \right) + \log (1 - \lambda / 6) \right] \text{cm}^2}{t_f \text{ (min.)}} \text{ sec. for Cell 2} \\ &= 1.1130 \frac{[0.07898 - 0.00139]}{4248} \\ &= 2.03 \frac{\text{cm}^2}{\text{sec.}}\end{aligned}$$

16.3.2 Helium (H.T.U.)_{OL}: Run 63, Sample Set #1.

Fractometer Calibration: 0.00425 millimolar/millivolt

Peak Heights: Lean $3.12 \times 1 = 3.12$ mv

Rich $4.79 \times 8 = 38.3$ mv

$$C_T/C_B = \frac{0.163}{0.0133} = 12.26$$

$$(N.T.U.)_{OL} = \ln \left(\frac{C_T}{C_B} \right) \quad \text{Equation (16.1.5)}$$

$$= \ln (12.26)$$

$$= 2.51$$

Packed Height = 1.17 feet = h

$$(H.T.U.)_{OL} = \frac{h}{(N.T.U.)_{OL}}$$

$$= \frac{1.17}{2.51}$$

$$= 0.467 \text{ ft.}$$

Water Temperature: Top = 24.7°C

Bottom = 24.7°C

Average = 24.7°C

Temperature correction to $(H.T.U.)_{OL}$ (see Figure 19.3)

$$= 0.7\%$$

$$(H.T.U.)_{OL} \text{ at } 25^\circ\text{C} = (0.993)(0.467)$$

$$= 0.46 \text{ feet}$$

16.3.3 Oxygen (H.T.U.)_{OL}: Run 69, Sample Set #1

Room Pressure = 762.0 mm. Hg

Room Temperature = 28.0°C

Na₂S₂O₃ = 6.134 MN to O₂

	<u>Bottom</u>	<u>Top</u>
ml. Na ₂ S ₂ O ₃	13.25	26.75
Corrected flask volume	252.9 ml.	243.1 ml.
$C \left(= \frac{\text{ml. S}_2\text{O}_3 \times 6.134}{\text{flask volume}} \right)$	0.3214 MM = C _B	0.6750 MM = C _T
Water Temperature	24.2°C	25.0°C
Vapor Pressure of Water (p _w)	22.6 mm Hg	23.8 mm Hg

Pressure at low tower top = 1.7 mm Hg gauge

Pressure at drop through packing = 2.0 mm Hg

∴ Pressure at tower bottom = 762.0 + 1.7 + 0.3 mm
= 764.0 mm Hg = π_B

Pressure at tower top = 762.0 + 1.7 - 1.7 mm
= 762.0 mm Hg = π_T

Solubility of oxygen at 24.2°C = 1.279 millimoles/l.-atm

Solubility of oxygen at 25.0°C = 1.261 millimoles/l.-atm

$$C_e = 0.21 (\pi - p_w)/H \quad \text{Equation (16.1.7)}$$

$$\begin{aligned} C_{eB} &= 0.21 \frac{(764.0 - 22.6)}{760.0} (1.279) \\ &= 0.2620 \text{ MM.} \end{aligned}$$

Similarly,

$$\begin{aligned} C_{eT} &= 0.2572 \\ \epsilon &= C_{eT} - C_{eB} = 0.2572 - 0.2620 = -0.0048 \text{ MM.} \end{aligned}$$

Now

$$\begin{aligned} (\text{N.T.U.})_{OL1} &= \frac{C_T - C_B}{C_T - C_B - \epsilon} \ln \frac{(C - C_e)_T}{(C - C_e)_B} \quad \text{Eq. (16.1.8)} \\ &= \frac{0.6750 - 0.3214}{0.6750 - 0.3214 + 0.0048} \ln \frac{(0.6750 - 0.2572)}{(0.3214 - 0.2620)} \\ &= 0.987 \ln (7.03) \\ &= 1.92 \end{aligned}$$

$$\begin{aligned} (\text{N.T.U.})_{OL2} &= \ln \frac{(C - C_e)_T}{(C - C_e)_B - \epsilon} \quad \text{Eq. (16.1.9)} \\ &= \ln \frac{(0.6750 - 0.2572)}{(0.3214 - 0.2620) + 0.0048} \\ &= 1.87 \end{aligned}$$

$$\begin{aligned} (\text{N.T.U.})_{OL} &= 1.92 - 0.15 (0.05) \\ &= 1.91 \end{aligned}$$

$h = \text{packed height} = 2.13 \text{ feet}$

$$(\text{H.T.U.})_{OL} \frac{h}{(\text{N.T.U.})_{OL}} = \frac{2.13}{1.91} = 1.12 \text{ ft.}$$

Average water T = 24.6°C
 Temperature correction (see Figure 19.3) = -0.9%
 (H.T.U.)_{OL} at 25°C = (0.991)(1.12)
 = 1.11 feet

16.3.4 Carbon Dioxide (H.T.U.)_{OL}: Run 40, Sample Set #1

NaOH = 16.50 MN to CO₂

HCl = 8.92 MN to CO₂

	<u>Bottom</u>		<u>Top</u>	
	<u>I</u>	<u>II</u>	<u>I</u>	<u>II</u>
ml. NaOH Added	20.00	20.00	40.00	40.00
Sample Weight	51.9 g	16.8 g	29.6 g	25.1 g
Sample Volume	52.0 ml.	16.8 ml.	29.7 ml.	25.2 ml.
(= $\frac{\text{weight}}{\rho_{\text{H}_2\text{O}}}$)				
ml. HCl	2.69	26.03	18.14	26.75
meq. NaOH (= $\frac{\text{ml} \times \text{MN}}{10^3}$)	0.330	0.330	0.660	0.660
meq. HCl = (= $\frac{\text{ml} \times \text{MN}}{10^3}$)	0.024	0.232	0.162	0.239
meq. CO ₂ (= NaOH-HCL)	0.306	0.098	0.498	0.421

	<u>Bottom</u>		<u>Top</u>	
	<u>I</u>	<u>II</u>	<u>I</u>	<u>II</u>
Conc. total $\text{CO}_2 + \text{HCO}_3^-$ ($\frac{\text{eq. CO}_2}{\text{ml. sample}}$)	5.90 MM	5.83 MM	16.82 MM	16.77 MM
Conc. CO_2 (= Conc. total - 0.22 MM)	5.68 MM	5.61 MM	16.60 MM	16.55 MM

$$\text{Accept } C_T = 16.60 \text{ MM}$$

$$C_B = 5.68 \text{ MM}$$

To compute C_{eB} and C_{eT} :

$$\begin{aligned} P_{\text{CO}_2} \text{ in inlet air (assumed)} &= 6 \times 10^{-4} \text{ atm} \\ \text{solubility at } 25^\circ\text{C} &= 0.145 \text{ g/100 g H}_2\text{O atm} \\ &= \frac{0.145}{44} \times 10^4 = 33.0 \text{ MM.} \end{aligned}$$

$$\therefore C_{eB} = (33.0)(6 \times 10^{-4}) = 0.02 \text{ MM}$$

$$\begin{aligned} C_T - C_B &= 16.60 - 5.68 \\ &= 10.92 \text{ MM.} \end{aligned}$$

$$\begin{aligned} \text{Amount of CO}_2 \text{ desorbed} &= (0.01092 \text{ g mol/l.})(2100 \text{ lb/hr.ft}^2)(0.454 \text{ l./lb}) \\ &= 10.4 \text{ g mol/hr.ft}^2 \end{aligned}$$

$$\text{Air flow rate} = (285 \text{ lb/hr.ft}^2) \left(\frac{1 \text{ ft}^3}{0.075 \text{ lb}} \right) (28.3 \text{ l/ft}^3) \left(\frac{1 \text{ g mol}}{24.5 \text{ l.}} \right)$$

$$= 4390 \text{ g mol/hr.ft}^2$$

$$P_{\text{CO}_2} \text{ at top} = \frac{10.4}{4390} + 6 \times 10^{-4}$$

$$= 0.0030 \text{ atm}$$

$$C_{eT} = (0.0030)(33.0) = 0.10 \text{ MM}$$

$$\epsilon = C_{eT} - C_{eB} = 0.10 - 0.02 = 0.08 \text{ MM}$$

$$(\text{N.T.U.})_{\text{OL}} = \frac{C_T - C_B}{C_T - C_B - \epsilon} \ln \frac{(C - C_e)_T}{(C - C_e)_B} \quad \text{Equation (16.1.8)}$$

$$= \frac{10.92}{10.92 - 0.08} \ln \frac{16.60 - 0.10}{5.68 - 0.02}$$

$$= 1.08$$

$$\text{Packed height} = 1.17 \text{ ft} = h$$

$$(\text{H.T.U.})_{\text{OL}} = h / (\text{N.T.U.})_{\text{OL}}$$

$$= \frac{1.17}{1.08}$$

$$= 1.09 \text{ ft.}$$

$$\text{Average water } T = 25.4^\circ\text{C}$$

$$\text{Temperature correction} = +0.9\%$$

$$(\text{H.T.U.})_{\text{OL}} \text{ at } 25^\circ\text{C} = (1.009)(1.09)$$

$$= 1.10 \text{ ft.}$$

16.3.5 Least Squares Fit of Log (H.T.U.) vs log D_L plot:

$$L = 2100, \quad G = 900$$

Solute	Median H.T.U. (ft)	Range (ft)	No. Obs. n	Ref. (39) K_w	$s_w/H.T.U.$	$s_m^2/(H.T.U.)^2 =$
						$s_w^2/(H.T.U.)^2_n$
C_3H_6	1.20	0.12	4	0.49	0.0490	0.00060
CO_2	1.05	0.13	7	0.37	0.0458	0.00030
O_2	0.93	0.06	10	0.33	0.0258	0.000062
H_2	0.66	0.07	5	0.43	0.0456	0.00042
He	0.62	0.13	7	0.37	0.0776	0.00086

Solute	$\log_{10} x$ (H.T.U.) _{OL}	$\frac{s_m^2}{(H.T.U.)^2}$	(see Table 14.6.5) $\log D_L$	$\frac{s_m^2 D_L}{D_L^2}$	$= \frac{(H.T.U.)^2 (D_L)^2}{s_m^2 H.T.U. s_m^2 D_L}$
					w_i
C_3H_6	1.079	6.0×10^{-4}	0.158	5.0×10^{-4}	0.18×10^4
CO_2	1.021	3.0	0.301	3.1	0.33
O_2	0.968	0.62	0.382	1.3	1.11
H_2	0.820	4.2	0.681	4.0	0.24
He	0.792	8.6	0.799	11.1	<u>0.10</u>
					$1.96 \times 10^{+4}$

$$= \frac{s_m^2 \text{H.T.U.} (D_L)^2}{s_m^2 D_L (\text{H.T.U.})^2}$$

Solute	k_i^2	$\log(10 \times k_i^2)$	$W_i \log(10 \times k_i^2)$
C ₃ H ₆	1.20	1.079	0.194 x 10 ⁴
CO ₂	0.97	0.986	0.325
O ₂	0.48	0.682	0.757
H ₂	1.05	1.022	0.245
He	0.77	0.886	<u>0.089</u>
			1.610 x 10 ⁴

$$k^2 = 0.1 \text{ antilog } \frac{\sum_{n_i} W_i \log(10 \times k_i^2)}{\sum_{n_i} W_i} \quad \text{Equation (16.2.8)}$$

$$= 0.1 \text{ antilog } \left(\frac{1.610 \times 10^4}{1.96 \times 10^4} \right)$$

$$= 0.66$$

$$k = \sqrt{0.66}$$

$$= 0.81$$

Letting $y_i = \log(10 \times \text{H.T.U.})_{OL i}$, and $x_i = \log(D_L)_i$

Solute	$W_i y_i$	$W_i x_i$
C ₃ H ₆	0.194 x 10 ⁴	0.028 x 10 ⁴
CO ₂	0.337	0.099
O ₂	1.074	0.424
H ₂	0.197	0.163
He	<u>0.079</u>	<u>0.080</u>
	1.881 x 10 ⁴	0.794 x 10 ⁴

$$\bar{y}_W = \frac{\sum_{n_i} W_i y_i}{\sum_{n_i} W_i} = \frac{1.881 \times 10^4}{1.96 \times 10^4} = 0.960$$

$$\bar{x}_W = \frac{\sum_{n_i} W_i x_i}{\sum_{n_i} W_i} = \frac{0.794 \times 10^4}{1.96 \times 10^4} = 0.405$$

Solute	$y_i - \bar{y}_i$	$x_i - \bar{x}_i$	$W_i(y_i - \bar{y}_W)^2$	$W_i(x_i - \bar{x}_W)^2$	$W_i(x_i - \bar{x}_W)(y_i - \bar{y}_W)$
C ₃ H ₆	0.119	-0.247	25.4	109.8	-52.9
CO ₂	0.061	-0.104	12.3	35.7	-20.9
O ₂	0.008	-0.023	0.7	5.9	-2.0
H ₂	-0.140	0.276	47.0	182.8	-92.7
He	-0.168	0.394	<u>28.2</u>	<u>155.2</u>	<u>-86.2</u>
			113.6	489.4	-254.7

$$m = \frac{\sum_{n_i} W_i (y_i - \bar{y}_W)^2 - k^2 \sum_{n_i} W_i (x_i - \bar{x}_W)^2}{2 \sum_{n_i} W_i (y_i - \bar{y}_W)(x_i - \bar{x}_W)} \quad \text{Equation (16.2.4)}$$

$$= \frac{113.6 - (0.66)(489.4)}{(2)(-254.7)}$$

$$= 0.411$$

$$b = m + \sqrt{m^2 + k^2} \quad \text{Equation (16.2.2)}$$

$$= 0.411 + \sqrt{0.169 + 0.66}$$

$$= 0.411 - 0.911 \quad (\text{taking negative root for negative slope})$$

$$= 0.50$$

To compute $s^2(b)$:

$$s^2(b) = \frac{0.18 (k^2 + b^2)^2}{k^3 \sum_{n_i} W_i (x_i - \bar{x}_W)^2 + bk \sum_{n_i} W_i (x_i - \bar{x}_W)(y_i - \bar{y}_W)} \quad \text{Eq. (16.2.10)}$$

$$= \frac{(0.18) ((0.66)^2 + (0.50)^2)^2}{(0.66)^{3/2} (489.4) + (-0.50)(0.81)(+264.7)}$$

$$= 0.000407$$

$$\sqrt{s^2(b)} = (0.000407)^{1/2}$$

$$= 0.021$$

$$\sqrt{s^2(b)} / b = \frac{0.021}{0.50} = 4\%$$

16.3.6 Air flow rates

a. General formulae

From ref. 109, p. 404:

$$q_i = 45.5 \text{ KYD}_{2i}^2 \sqrt{\frac{H_m (\rho_m - \rho_A)}{\rho_1}}$$

where q_i = air flow (ft³/hr)

$$K = C(1 - \beta^4)^{-1/2}$$

C = orifice coefficient of discharge

$$\beta = D_{2i}/D_i$$

D_{2i} = orifice diameter (in.)

D_i = upstream pipe diameter (in.)

$\rightarrow \infty$ for butt-end orifice

ρ_m = density of manometer fluid

ρ_l = density of air, upstream

ρ_A = density of air in manometer leads

H_m = manometer reading (in.)

Y = expansion factor

To convert q_i to G (based on empty tower cross-section):

$$G = \alpha \rho_{25} \cdot 1/A_T \cdot q_i$$

if α = density of air at room T and pressure/density of air at 25°C and 1 atmosphere.

ρ_{25} = density of air at 25°C and 1 atmosphere (lb/ft³)

A_T = tower cross section (ft²) = 0.797 ft²

G = air flow in tower (lb/hr.ft²)

Since red gauge oil ($\rho = 0.826$ gm/cc) was the manometer fluid:

$$G = \frac{45.5 \rho_{25} C Y \alpha}{A_T} D_{2i}^2 \left(\frac{\rho_m - \rho_A}{\alpha \rho_{25}} \cdot H_m \right)^{1/2}$$

$$\begin{aligned}
 &= \frac{(45.5)(0.001186 \times 62.4) \alpha^{1/2} \text{CY}}{0.797} D_{2i}^2 \left(\frac{0.826 - 0.001}{0.001186} H_m \right)^{1/2} \\
 &= 111.3 \text{ CY } \alpha^{1/2} D_{2i}^2 (H_m)^{1/2}
 \end{aligned}$$

Since H_m is actually measured in cm: $H_{cm} = 2.54 H_m$

$$\begin{aligned}
 G &= \frac{111.3}{\sqrt{2.54}} \text{ CY } \alpha^{1/2} D_{2i}^2 (H_{cm})^{1/2} \\
 &= 69.9 \text{ CY } \alpha^{1/2} D_{2i}^2 (H_{cm})
 \end{aligned}$$

Y, the expansion factor, is given by Figure 47, p. 403, in reference 109 as a function of the relative pressure drop across the orifice. In all cases encountered in the present work it differed from 1.00 by less than 1 per cent. Thus

$$G = 69.9 C \alpha^{1/2} D_{2i}^2 (H_{cm}) \quad (16.3.1)$$

b. Calculation of Desired Air Manometer Pressure Drop for

a Specific Run: Run #2

In this case $D_{2i} = 2$ inches
 Pressure tap = 4.75 inches downstream
 Stovepipe diameter = 4.08 inches

From Figure 51, page 403, ref. 109, since for any G above 210 lb/hr.ft²

the Reynolds number through the orifice will be greater than 30,000:

$$C = 0.635$$

Hence

$$\begin{aligned} G &= 69.9 \alpha^{1/2} (0.635)(2)^2 (H_{cm})^{1/2} \\ &= 178 \alpha^{1/2} (H_{cm})^{1/2} \end{aligned}$$

Since the air flowing through the tower is saturated with water vapor, whereas that flowing through the orifice contains only the room content of water vapor, another correction must be made to this expression to account for the gain in water vapor content.

$$G = 178 \alpha^{1/2} (1 + h_{25} - h)(H_{cm})^{1/2}$$

where h_{25} = absolute humidity of saturated air at 25°C (lb.H₂O/lb.air)

h = absolute humidity of room air (lb.H₂O/lb.air)

Room Pressure = 776.5 mm Hg

Room Dry Bulb T = 18.9°C

Room Wet Bulb T = 7.8°C

h = 0.0022 lb.H₂O/lb.air

h_{25} = 0.0209 lb.H₂O/lb.air

$$1 + h_{25} - h = 1.0000 + 0.0209 - 0.0022$$

$$= 1.0187$$

$$\alpha = \frac{776.5}{760} \times \frac{298}{291.9}$$

$$= 1.04$$

$$\alpha^{1/2} = 1.02$$

$$\text{Desired } G = 900 \text{ lb/hr.ft}^2$$

$$\therefore 900 = (178)(1.02)(1.0187)(H_{\text{cm}})^{1/2}$$

$$H_{\text{cm}} = (4.87)^2$$

$$= 23.7 \text{ cm of red gauge oil.}$$

CHAPTER 17

Summarized Data and Calculated Results

Table 17.1 lists the original data and the values of H.T.U. calculated therefrom.

Table 17.2 presents the "best" value of H.T.U. for each solute gas at each flow condition, together with the estimated variances and range standard deviations of these values from the true value. "Best" values are also given for runs at 2 ft. packed height and deaerated water.

Table 17.3 summarizes the least squares slopes of the log H.T.U. vs. $\log D_L$ and log H.T.U. vs T plots, and the estimated standard deviations in these slopes.

In Figure 17.1 are presented the original pressure drop vs. air flow rate data.

TABLE 17.1

Summary of Packed Column Description Data & Calculated Results

Run	Solute	L (lb/hr ft ²)	G (lb/hr ft ²)	Atmos. P (MM. Hg)	$\frac{h}{\text{lb. air}}$ $\left(\frac{\text{lb. H}_2\text{O}}{\text{lb. air}}\right)$	Air T (°C)	Water Top (°C)	T Bottom (°C)	C_T (MM/l)	C_B (MM/l)	C_{eT} (MM/l)	C_{eB} (MM/l)	$(C-C_e)_T$ (MM/l)	$(C-C_e)_B$ (MM/l)	(N.T.U.) _{OL}	(H.T.U.) _{OL} (Ft)	T _{ave} (°C)	(H.T.U.) ₂₅ (Ft)	
-----Effective Packed Height = 2.04 Ft.-----																			
1*	O ₂	2000	900	Preliminary															
2*	O	2000	900	776.5	0.0022	24.4	24.9	24.4	0.502	0.293	0.263	0.266	0.239	0.0340	1.91	1.07	24.6	1.06	
						24.6	24.8	24.8	0.513	0.297	0.264	0.264	0.249	0.0333	2.01	1.01	24.8	1.00	
						24.6	25.5	24.3	0.518	0.295	0.260	0.266	0.258	0.0291	2.06	0.99	24.9	0.99	
3*	O ₂	2100	900	778.4	0.0030	25.1	26.3	25.3	0.624	0.310	0.259	0.263	0.365	0.0478	2.00	1.02	25.8	1.04	
						25.2	26.7	25.7	0.610	0.305	0.255	0.260	0.354	0.0426	2.06	0.99	26.2	1.02	
						25.2	26.8	25.8	0.634	0.303	0.255	0.260	0.379	0.0430	2.11	0.97	26.3	1.00	
4*	O ₂	2100	900	754.2	0.0065	24.9	25.0	24.8	0.632	0.302	0.255	0.256	0.378	0.0468	2.08	0.98	24.9	0.98	
						25.1	25.6	25.1	0.627	0.303	0.252	0.255	0.376	0.0486	2.01	1.02	25.4	1.02	
						25.1	25.6	25.2	0.631	0.301	0.252	0.254	0.379	0.0469	2.06	0.99	25.4	1.00	
						25.1	25.6	25.1	0.625	0.305	0.252	0.255	0.373	0.0508	1.96	1.04	25.3	1.05	
-----Effective Packed Height = 1.07 Ft.-----																			
5*	O ₂	2100	900	782.2	0.0035	24.0	26.6	25.1	0.783	0.421	0.257	0.265	0.526	0.156	1.18	0.91	25.9	0.93	
						23.9	25.4	24.7	0.790	0.434	0.262	0.266	0.528	0.168	1.13	0.95	25.1	0.95	
						24.0	25.9	24.8	0.803	0.433	0.261	0.266	0.542	0.167	1.15	0.93	25.4	0.93	
						24.1	25.8	24.9	0.820	0.433	0.262	0.266	0.558	0.168	1.18	0.91	25.4	0.92	
-----Effective Packed Height = 1.17 Ft.-----																			
6	O ₂	2100	900	769.3	0.0050	25.0	25.7	25.1	0.769	0.407	0.257	0.260	0.513	0.147	1.23	0.95	25.4	0.96	
						25.1	25.5	25.1	0.778	0.409	0.258	0.260	0.520	0.149	1.24	0.94	25.3	0.94	
						25.2	26.4	25.5	0.765	0.405	0.254	0.258	0.511	0.146	1.23	0.95	26.0	0.97	
						25.2	27.1	25.9	0.767	0.397	0.250	0.256	0.517	0.141	1.27	0.92	26.5	0.95	
7	CO ₂	2100	900	749.6	0.0025	23.0	25.9	24.8	3.02	1.07	0.02	0.02	3.00	1.05	1.05	1.12	25.4	1.13	
						25.0	26.6	25.7	3.24	0.98	0.02	0.02	3.14	0.96	1.19	0.98	26.2	1.01	
8	CO ₂	2100	900	768.0	0.0038	24.3	25.0	24.4	23.7	7.46	0.08	0.02	23.6	7.44	1.16	1.01	24.7	1.00	
						24.4	26.1	25.1	23.9	7.48	0.08	0.02	23.8	7.46	1.16	1.01	25.6	1.02	
						24.5	25.8	24.9	22.5	7.96	0.06	0.02	22.4	7.93	1.04	1.13	25.4	1.13	

* Pool height at bottom of air notches. (Pool height 3/4" lower in all other runs).

Run	Solute	L (lb/hr ft ²)	G (lb/hr ft ²)	Atmos. P (MM. Hg)	$\frac{h}{\text{lb. air}}$ ($\frac{\text{lb. H}_2\text{O}}{\text{lb. air}}$)	Air T (°C)	Water Top (°C)	T Bottom (°C)	C _T (MM/l)	C _B (MM/l)	C _{eT} (MM/l)	C _{eB} (MM/l)	(C-C _e) _T (MM/l)	(C-C _e) _B (MM/l)	(N.T.U.) _{OL}	(H.T.U.) _{OL} (Ft)	T _{ave} (°C)	(H.T.U.) ₂₅ (Ft)
9	CO ₂	2100	900	757.7	0.0060	25.5 25.4	24.2 25.0	24.0 24.6	21.3 24.2	7.41 7.55	0.06 0.08	0.02 0.02	21.2 24.1	7.39 7.53	1.06 1.17	1.10 1.00	24.1 24.8	1.08 1.00
10	He	2100	900	766.7	0.0049	24.3 24.2	24.9 26.0	24.3 25.2	0.216 0.262	0.0385 0.0426	- -	- -	0.216 0.262	0.0385 0.0426	1.73 1.82	0.68 0.64	24.6 25.6	0.67 0.65
11	He	2100	900	757.0	0.0068	24.6 25.0	25.4 26.1	24.8 25.5	0.257 0.245	0.0388 0.0393	- -	- -	0.257 0.245	0.0388 0.0388	1.89 1.83	0.62 0.64	25.1 25.8	0.62 0.65
12	He	2100	900	758.0		25.4	24.1	24.5	0.285	0.0412	-	-	0.285	0.0412	1.94	0.61	24.3	0.60
13	H ₂	2100	900	760.5	0.0055	24.3	25.5	25.0	0.465	0.0785	-	-	0.465	0.0785	1.78	0.66	25.3	0.66
14	H ₂	2100	900	752.4	0.0058	24.7	25.0	24.6	0.478	0.0752	-	-	0.478	0.0752	1.85	0.63	24.8	0.63
15	H ₂	2100	900			24.5 24.5	25.2 26.2	24.6 25.1	0.471 0.510	0.0880 0.0931	- -	- -	0.471 0.510	0.0880 0.0931	1.68 1.70	0.70 0.69	24.9 25.7	0.68 0.70
16	C ₃ H ₆	2100	900	773.3	0.0040	25.8 25.8	25.2 26.0	25.0 25.7	1.23 1.34	0.465 0.457	- -	- -	1.23 1.34	0.465 0.457	0.98 1.07	1.20 1.09	25.1 25.9	1.20 1.11
17	C ₃ H ₆	2100	900	759.0	0.0058	24.6 24.7	25.1 25.5	24.7 24.9	1.29 1.28	0.488 0.495	- -	- -	1.29 1.28	0.488 0.495	0.98 0.96	1.20 1.23	24.9 25.2	1.20 1.23
18	He	2100	900	766.5	0.0036	25.3 25.3	24.1 25.5	24.1 25.1	0.247 0.244	0.0290 0.0274	- -	- -	0.247 0.244	0.0290 0.0274	2.14 2.18	0.55 0.54	24.1 25.3	0.54 0.54
19	O ₂	2100	900	756.3	0.0050	25.2 25.3 25.3	23.8 24.7 25.4	24.0 24.6 25.0	0.714 0.722 0.721	0.390 0.385 0.380	0.262 0.257 0.254	0.261 0.258 0.256	0.452 0.465 0.467	0.129 0.127 0.125	1.26 1.30 1.31	0.93 0.90 0.90	23.9 24.7 25.2	0.91 0.90 0.90
20	O ₂	2100	285	742.2	0.0045	25.5 25.9	25.4 24.2	24.2 24.2	0.706 0.711	0.405 0.424	0.249 0.254	0.255 0.255	0.458 0.456	0.150 0.169	1.09 0.99	1.08 1.18	24.8 24.2	1.08 1.16
21	O ₂	2100	285	765.3	0.0046	25.5 25.6	23.9 24.8	23.5 24.5	0.719 0.718	0.414 0.418	0.264 0.258	0.266 0.261	0.456 0.459	0.148 0.157	1.12 1.06	1.05 1.10	23.7 24.8	1.02 1.09
22	O ₂	2100	285	767.7	0.0045	24.8 25.3 25.3 25.3	24.4 25.1 25.8 26.5	24.0 24.5 25.1 25.8	0.726 0.737 0.735 0.731	0.420 0.417 0.413 0.405	0.262 0.259 0.255 0.252	0.264 0.262 0.259 0.255	0.464 0.478 0.480 0.479	0.156 0.155 0.154 0.149	1.08 1.11 1.12 1.15	1.08 1.05 1.05 1.01	24.2 24.8 25.5 26.2	1.06 1.04 1.06 1.04
23	He	2100	285	771.4	0.0055	23.4 24.2	24.4 25.5	23.9 24.8	0.263 0.270	0.0379 0.0364	- -	- -	0.263 0.270	0.0379 0.0364	1.94 2.01	0.60 0.58	24.2 25.2	0.59 0.58

Run	Solute	L (lb/hr ft ²)	G (lb/hr ft ²)	Atmos. P (MM. Hg)	$\frac{h}{\text{lb. air}}$ ($\frac{\text{lb. H}_2\text{O}}{\text{lb. air}}$)	Air T (°C)	Water Top (°C)	T Bottom (°C)	C _T (MM/l)	C _B (MM/l)	C _{eT} (MM/l)	C _{eB} (MM/l)	(C-C _e) _T (MM/l)	(C-C _e) _B (MM/l)	(N.T.U.) _{OL}	(H.T.U.) _{OL} (Ft)	T _{ave} (°C)	(H.T.U.) ₂₅ (Ft)
24	He	2100	285	763.7	0.0032	25.3	23.9	23.7	0.240	0.0415	-	-	0.240	0.0415	1.75	0.67	23.8	0.65
25	C ₃ H ₆	2100	285	763.5		24.6 25.6	24.7 25.8	24.1 25.4	1.28 1.18	0.449 0.479	-	-	1.28 1.18	0.449 0.479	1.05 0.90	1.12 1.30	24.4 25.6	1.10 1.31
26	C ₃ H ₆	2100	285	763.4		25.4 25.3	25.2 26.3	25.3 25.8	1.38 1.37	0.532 0.523	-	-	1.38 1.37	0.532 0.523	0.95 0.97	1.23 1.20	25.3 26.0	1.24 1.23
27	H ₂	2100	285	771.3		25.2	25.5	24.9	0.153	0.0304	-	-	0.153	0.0304	1.61	0.73	25.2	0.73
28	H ₂	2100	285	765.5		23.3 25.4	26.1 26.2	25.1 25.6	0.280 0.298	0.0445 0.0505	-	-	0.280 0.298	0.0445 0.0505	1.84 1.77	0.63 0.66	25.6 25.9	0.65 0.67
29	H ₂	5000	900	758.5	0.0070	24.5 24.5	24.5 25.6	24.3 25.0	0.311 0.286	0.0640 0.0708	-	-	0.311 0.286	0.0640 0.0708	1.58 1.40	0.74 0.84	24.4 25.3	0.73 0.84
30	H ₂	5000	900	755.4	0.0095	24.5 25.6	25.2 26.6	24.7 26.1	0.237 0.242	0.0548 0.0543	-	-	0.237 0.242	0.0548 0.0543	1.47 1.50	0.80 0.78	25.0 26.4	0.80 0.81
31	C ₃ H ₆	5000	900	750.2	0.0055	25.0 24.9	25.6 25.6	25.1 25.2	2.15 2.22	0.968 0.954	-	-	2.15 2.22	0.968 0.954	0.80 0.85	1.47 1.38	25.4 25.4	1.47 1.40
32	C ₃ H ₆	5000	900	753.2	0.0048	24.9 24.8	24.6 25.8	24.2 25.3	2.68 3.18	1.08 1.10	-	-	2.68 3.18	1.08 1.10	0.91 1.06	1.28 1.11	24.4 25.6	1.27 1.12
33	C ₃ H ₆	5000	900	764.2	0.0045	24.7 24.8	24.7 25.4	24.3 25.0	2.75 2.76	1.14 1.12	-	-	2.75 2.76	1.14 1.12	0.88 0.91	1.33 1.29	24.5 25.2	1.32 1.30
34	He	5000	900	757.7	0.0068	24.4 25.2	25.3 25.9	24.8 25.5	0.131 0.136	0.0256 0.0226	-	-	0.131 0.136	0.0256 0.0226	1.63 1.80	0.72 0.65	25.1 25.7	0.72 0.66
35	He	5000	900	764.9	0.0075	25.4 25.4	24.9 25.7	24.7 25.3	0.131 0.130	0.0261 0.0220	-	-	0.121 0.130	0.0261 0.0220	1.53 1.78	0.76 0.66	24.8 25.5	0.76 0.67
36	O ₂	5000	900	761.4	0.0050	24.4 24.9	25.4 26.3	24.8 25.7	0.730 0.748	0.431 0.439	0.256 0.251	0.259 0.255	0.474 0.497	0.172 0.184	1.00 0.98	1.17 1.20	25.1 26.0	1.17 1.22
37	O ₂	5000	900	759.5	0.0085	24.2 24.6 24.9	25.4 25.5 25.3	24.8 25.0 24.8	0.761 0.774 0.780	0.442 0.453 0.457	0.255 0.255 0.256	0.258 0.257 0.258	0.506 0.519 0.524	0.184 0.196 0.199	1.00 0.96 0.95	1.17 1.21 1.23	25.1 25.3 25.1	1.17 1.22 1.23
38	O ₂	2100	900	764.6	0.0062	24.7 25.3 25.9	24.4 25.1 25.4	23.8 24.3 24.6	0.786 0.781 0.795	0.416 0.411 0.409	0.262 0.258 0.257	0.264 0.262 0.261	0.524 0.523 0.538	0.152 0.149 0.148	1.23 1.24 1.27	0.95 0.95 0.92	24.1 24.7 25.0	0.93 0.94 0.92

Run	Solute	L (lb/hr ft ²)	G (lb/hr ft ²)	Atmos. P (MM. Hg)	$\frac{h}{\text{lb. air}}$ ($\frac{\text{lb. H}_2\text{O}}{\text{lb. air}}$)	Air T (°C)	Water Top (°C)	T Bottom (°C)	C _T (MM/L)	C _B (MM/L)	C _{eT} (MM/L)	C _{eB} (MM/L)	(C-C _e) _T (MM/L)	(C-C _e) _B (MM/L)	(N.T.U.) _{OL}	(H.T.U.) _{OL} (Ft)	T _{ave} (°C)	(H.T.U.) ₂₅ (Ft)
39	O ₂	2100	285	768.6	0.0088	24.6	24.5	23.7	0.798	0.438	0.262	0.266	0.536	0.172	1.12	1.05	24.1	1.03
						24.5	25.0	24.3	0.796	0.430	0.260	0.263	0.536	0.167	1.16	1.01	24.7	1.02
						25.3	25.6	24.8	0.792	0.427	0.257	0.261	0.535	0.166	1.15	1.01	25.2	1.01
40	CO ₂	2100	285	759.4	0.0075	24.7	25.8	25.0	16.60	5.68	0.10	0.02	16.50	5.66	1.08	1.09	25.4	1.10
						25.4	24.8	24.5	17.52	5.98	0.12	0.02	17.40	5.96	1.08	1.08	24.7	1.07
41	CO ₂	2100	285			25.2	26.1	25.2	17.65	5.75	0.12	0.02	17.53	5.73	1.13	1.04	25.7	1.05
						25.1	25.1	24.9	18.24	6.01	0.12	0.02	18.12	5.99	1.12	1.05	25.0	1.05
42	CO ₂	5000	900	762.4	0.0039	24.9	24.5	24.1	16.84	6.51	0.10	0.02	16.74	6.49	0.96	1.23	24.3	1.21
						24.7	25.6	25.1	18.44	7.20	0.11	0.02	18.33	7.18	0.95	1.26	25.4	1.27
43	CO ₂	5000	900	766.3	0.0035	25.1	24.4	23.2	12.38	5.20	0.07	0.02	12.31	5.18	0.87	1.35	23.8	1.31
						25.3	24.9	23.7	13.86	5.40	0.08	0.02	13.76	5.38	0.95	1.24	24.3	1.22
44	C ₃ H ₆	5000	900	763.4	0.0039	24.5	24.4	24.0	1.59	0.575	-	-	1.59	0.575	1.02	1.15	24.2	1.13
						24.8	25.5	24.9	1.37	0.564	-	-	1.37	0.564	0.89	1.32	25.2	1.32
45	C ₃ H ₆	5000	900	769.4	0.0080	24.5	25.5	24.8	0.698	0.275	-	-	0.698	0.275	0.93	1.26	25.2	1.26
						25.2	25.8	25.3	0.728	0.304	-	-	0.728	0.304	0.87	1.34	25.6	1.36
46	C ₃ H ₆	5000	900	766.3	0.0063	24.5	24.6	24.2	0.580	0.318	-	-	0.580	0.318	0.60	1.94	24.4	1.92
						24.5	25.2	24.7	0.580	0.242	-	-	0.580	0.242	0.87	1.34	25.0	1.34
47**	C ₃ H ₆	5000	900	760.2	0.0074	24.4	25.3	24.8	0.446	0.181	-	-	0.446	0.181	0.90	1.30	25.1	1.30
						25.5	26.3	25.8	0.455	0.202	-	-	0.455	0.202	0.82	1.44	25.4	1.45
48**	C ₃ H ₆	5000	900	764.6	0.0061	25.8	25.7	25.4	0.509	0.214	-	-	0.509	0.214	0.87	1.35	25.6	1.37
						25.8	26.3	25.9	0.514	0.231	-	-	0.514	0.231	0.80	1.46	26.1	1.50
49**	O ₂	5000	900	769.1	0.0065	24.9	25.5	25.0	0.711	0.429	0.258	0.260	0.453	0.169	0.97	1.20	25.3	1.20
						25.0	25.4	24.9	0.728	0.437	0.258	0.261	0.470	0.176	0.97	1.21	25.2	1.21
						25.1	25.9	25.3	0.751	0.440	0.255	0.259	0.496	0.181	0.99	1.18	25.6	1.20
-----Repack Column-----																		
50	O ₂	5000	900	763.1	0.0059	24.5	25.7	25.0	0.592	0.378	0.254	0.258	0.338	0.120	1.01	1.16	25.4	1.17
						25.0	25.8	25.2	0.597	0.380	0.254	0.257	0.343	0.123	1.01	1.16	25.5	1.17
						25.3	25.7	25.3	0.596	0.379	0.254	0.257	0.342	0.123	1.01	1.16	25.5	1.17

**Steam deaerated water (cooled with plastic films over tanks).

Run	Solute	L (lb/hr ft ²)	G (lb/hr ft ²)	Atmos. P (MM. Hg)	^h lb. H ₂ O (lb. air)	Air T (°C)	Water Top (°C)	T Bottom (°C)	C _T (MM/l)	C _B (MM/l)	C _{eT} (MM/l)	C _{eB} (MM/l)	(C-C _e) _T (MM/l)	(C-C _e) _B (MM/l)	(N.T.U.) _{OL}	(H.T.U.) _{OL} (Ft)	T _{ave} (°C)	(H.T.U.) ₂₅ (Ft)
51	O ₂	10,000	900	770.3	0.0047	25.4 25.4 25.1	25.1 25.0 24.8	24.5 24.7 24.7	0.862 0.869 0.878	0.497 0.502 0.510	0.259 0.260 0.261	0.264 0.263 0.263	0.603 0.609 0.617	0.233 0.239 0.247	0.93 0.92 0.91	1.25 1.27 1.29	24.8 24.9 24.8	1.24 1.27 1.28
52	H ₂	10,000	900	768.3	0.0037	25.2 25.1	25.1 25.3	24.6 25.0	0.286 0.302	0.097 0.082	- -	- -	0.286 0.302	0.097 0.082	1.08 1.30	1.08 0.90	24.9 25.2	1.08 0.90
53	H ₂	10,000	900	769.1	0.0110	25.4 25.3	25.4 25.5	25.1 25.2	0.343 0.346	0.090 0.101	- -	- -	0.343 0.346	0.090 0.101	1.34 1.23	0.88 0.95	25.3 25.4	0.88 0.96
54	He	10,000	900	765.6	0.0133	24.9 24.9	24.6 25.1	24.2 24.8	0.122 0.140	0.0272 0.0302	- -	- -	0.122 0.140	0.0272 0.0302	1.50 1.53	0.78 0.76	24.4 25.0	0.77 0.76
55	He	10,000	900	764.8	0.0149	25.1 24.8	25.3 25.3	24.8 24.9	0.129 0.142	0.0255 0.0306	- -	- -	0.129 0.142	0.0255 0.0306	1.62 1.54	0.72 0.76	25.1 25.1	0.72 0.76
56	CO ₂	10,000	900	762.7	0.0104	24.9	25.5	25.1	9.70	4.20	0.08	0.02	9.62	4.18	0.84	1.40	25.4	1.41
57	CO ₂	10,000	900	761.4	0.0083	25.4	25.3	25.2	5.11	2.19	0.06	0.02	5.05	2.17	0.85	1.38	25.3	1.39
58	C ₃ H ₆	10,000	900	752.5	0.0102	25.2 25.0	25.2 24.8	25.2 24.8	0.665 0.746	0.305 0.320	- -	- -	0.665 0.746	0.305 0.320	0.78 0.85	1.50 1.38	25.2 24.8	1.51 1.38
59	H ₂	2,100	900	755.8	0.0062	20.2 21.8	19.4 21.1	19.0 21.0	0.330 0.334	0.0605 0.0633	- -	- -	0.330 0.334	0.0605 0.0633	1.70 1.66	0.69 0.70	19.2 21.1	
60	H ₂	2,100	900	760.0	0.0050	24.6 26.8	25.0 27.4	24.4 26.5	0.296 0.329	0.0450 0.0455	- -	- -	0.296 0.329	0.0450 0.0455	1.88 1.98	0.62 0.59	24.7 27.0	
61	H ₂	2,100	900	759.5	0.0037	32.4 33.6	32.5 35.6	31.8 33.8	0.294 0.329	0.0448 0.0333	- -	- -	0.294 0.329	0.0448 0.0333	1.88 2.29	0.62 0.51	32.2 34.7	
62	H ₂	2,100	1,400	768.7	0.0078	26.6 26.2	25.8 26.1	25.8 26.0	0.289 0.259	0.0396 0.0376	- -	- -	0.289 0.259	0.0396 0.0376	1.99 1.93	0.59 0.61	25.8 26.1	0.60 0.62
63	He	2,100	1,400	768.8	0.0105	25.5 25.1	24.7 25.6	24.7 25.1	0.163 0.186	0.0133 0.0162	- -	- -	0.163 0.186	0.0133 0.0162	2.51 2.44	0.47 0.48	24.7 25.4	0.46 0.48
***	O ₂					25.6 25.2	25.2 26.2	24.9 25.3	0.1572 0.1502	0.2403 0.2395	0.2594 0.2545	0.2621 0.2602	-0.1022 -0.1043	-0.0218 -0.0207	1.60 1.76	0.73 0.67	25.1 25.8	0.73 0.68

***Absorption

Run	Solute	L (lb/hr ft ²)	G (lb/hr ft ²)	Atmos. P (MM. Hg)	$\frac{h}{\text{lb. air}}$ ($\frac{\text{lb. H}_2\text{O}}{\text{lb. air}}$)	Air T (°C)	Water Top (°C)	T Bottom (°C)	C _T (MM/l)	C _B (MM/l)	C _{eT} (MM/l)	C _{eB} (MM/l)	(C-C _e) _T (MM/l)	(C-C _e) _B (MM/l)	(N.T.U.) _{OL}	(H.T.U.) _{OL} (Ft)	T _{ave} (°C)	(H.T.U.) ₂₅ (Ft)
64	O ₂	2100	1400	766.5	0.0137	25.2	25.0	25.0	0.6324	0.3367	0.2595	0.2608	0.3729	0.0759	1.58	0.74	25.0	0.74
						25.0	25.6	25.1	0.6237	0.3331	0.2565	0.2604	0.3672	0.0727	1.58	0.74	25.4	0.75
						25.0	25.3	25.1	0.6259	0.3349	0.2581	0.2604	0.3678	0.0745	1.58	0.74	25.2	0.75
						25.1	25.7	25.2	0.6218	0.3320	0.2560	0.2599	0.3658	0.0721	1.58	0.74	25.5	0.75
65	H ₂	2100	1400	767.6	0.0087	25.6	25.7	25.0	0.346	0.0365	-	-	0.346	0.0365	2.25	0.52	25.4	0.52
						26.3	25.6	25.2	0.332	0.0405	-	-	0.332	0.0405	2.10	0.56	25.4	0.56
***	O ₂					25.8	26.2	25.3	0.1595	0.2391	0.2541	0.2598	-0.0946	-0.0207	1.67	0.70	25.8	0.71
						26.7	26.1	25.3	0.1562	0.2379	0.2546	0.2598	-0.0984	-0.0219	1.62	0.72	25.7	0.73
66	H ₂	2100	1400	767.1	0.0087	24.7	25.6	25.0	0.333	0.0405	-	-	0.333	0.0405	2.11	0.56	25.3	0.56
						24.9	25.2	24.3	0.335	0.0349	-	-	0.335	0.0349	2.56	0.46	24.7	0.45
***	O ₂					24.8	25.3	25.0	0.1568	0.2409	0.2583	0.2610	-0.1015	-0.0201	1.68	0.70	25.2	0.70
						25.0	25.6	24.4	0.1571	0.2434	0.2569	0.2640	-0.0998	-0.0206	1.70	0.67	25.0	0.67
67	O ₂	5000	900	762.4	0.0110	27.2	27.1	26.8	0.6761	0.3960	0.2474	0.2492	0.4287	0.1468	1.06	1.10	27.0	-
						29.3	29.4	29.0	0.6611	0.3799	0.2377	0.2395	0.4234	0.1404	1.10	1.07	29.2	-
						31.2	32.3	31.3	0.7473	0.3886	0.2268	0.2306	0.5205	0.1580	1.17	1.00	31.8	-
						21.3	20.7	21.3	0.8017	0.4781	0.2804	0.2804	0.5213	0.2005	0.96	1.22	21.0	-
-----Effective Packed Height = 2.13 Ft.-----																		
68	O ₂	5000	900	766.6	0.0125	24.9	24.6	24.2	0.8410	0.3711	0.2611	0.2639	0.5799	0.1072	1.67	1.28	24.4	1.26
						25.0	25.1	24.6	0.8380	0.3640	0.2586	0.2619	0.5794	0.1021	1.71	1.25	24.9	1.24
						25.2	24.8	24.7	0.8477	0.3658	0.2600	0.2612	0.5877	0.1046	1.72	1.24	24.8	1.24
69	O ₂	2100	900	762.0	0.0141	24.9	25.0	24.2	0.6750	0.3214	0.2572	0.2620	0.4178	0.0594	1.91	1.12	24.6	1.11
						24.4	26.1	24.7	0.6641	0.3150	0.2520	0.2593	0.4121	0.0557	1.94	1.10	25.4	1.11
						24.4	25.9	25.1	0.6729	0.3169	0.2529	0.2575	0.4200	0.0594	1.92	1.11	25.5	1.12
70	H ₂	2100	900	770.5	0.0094	25.5	24.9	25.2	0.551	0.0318	-	-	0.551	0.0318	2.85	0.75	25.1	0.75
						25.4	25.1	25.1	0.570	0.0334	-	-	0.570	0.0334	2.84	0.75	25.1	0.75

*** Absorption

TABLE 17.2

"Best" Values Of Data

L (lb/hr ft ²)	G (lb/hr ft ²)	Solute	(H.T.U.) _{OL} (Ft)(at 25°C)	(S _w /H.T.U.)	(S _m ² /H.T.U. ²) (x 10 ⁴)
-----2.04 Ft. Height - High Pool-----					
2,100	900	O ₂	1.02	3%	
-----1.07 Ft. Height - High Pool-----					
2,100	900	O ₂	0.93	2%	
-----1.17 Ft. Height - Low Pool-----					
2,100	900	O ₂	0.93	2%	0.62
2,100	900	CO ₂	1.05	5%	3.0
2,100	900	He	0.62	8%	8.6
2,100	900	H ₂	0.66	5%	4.2
2,100	900	C ₃ H ₆	1.20	5%	6.0
2,100	285	O ₂	1.06	2%	0.85
2,100	285	He	0.59	5%	6.2
2,100	285	H ₂	0.67	7%	16.5
2,100	285	CO ₂	1.06	2%	1.3
2,100	285	C ₃ H ₆	1.24	8%	17.2
5,000	900	O ₂	1.20	2%	0.92
5,000	900	H ₂	0.80	7%	11.6
5,000	900	He	0.70	7%	12.3
5,000	900	CO ₂	1.25	4%	3.8
5,000	900	C ₃ H ₆	1.30	10%	
5,000*	900	C ₃ H ₆	1.41	7%	
5,000*	900	O ₂	1.20	1%	
-----Repacked Tower, 1.17 Ft. Height - Low Pool-----					
5,000	900	O ₂	1.17	-	
10,000	900	O ₂	1.27	2%	1.15
10,000	900	H ₂	0.93	11%	28.0
10,000	900	He	0.76	3%	2.6
10,000	900	CO ₂	1.40	1%	0.81
2,100	1,400	H ₂	0.56	12%	24.0

*Deaerated water

L (lb/hr ft ²)	G (lb/hr ft ²)	Solute	(H.T.U.) _{OL} (Ft)(at 25°C)	(S _w /H.T.U.)	(S _m ² /H.T.U. ²) (x 10 ⁴)
2,100	1,400	He	0.47	4%	7.2
2,100	1,400	O ₂	0.75	1%	0.11
2,100	1,400	O ₂ **	0.70	3%	

-----2.13 Ft. Height - Low Pool-----

5,000	900	O ₂	1.24	1%
2,100	900	O ₂	1.11	1%
2,100	900	H ₂	0.75	-

**Absorption

TABLE 17.3

Least Squares Slopes of Plots

A. Log (H.T.U.)_{OL} vs. log (D_L)

-----1.17 Ft. Packed Height, Low Pool-----

L	G	b	S ² (b)	S ² (b)/b	\bar{y}_w	\bar{x}_w
2,100	900	-0.50	0.02	4%	.960	.405
2,100	285	-0.53	0.02	5%	.999	.393
5,000	900	-0.54	0.03	6%	1.049	.423
10,000	900	-0.53	0.03	5%	1.087	.414
2,100	1,400	-0.48	0.03	6%	.863	.408

B. Log (H.T.U.)_{OL} vs. T

-----1.17 Ft. Packed Height, Low Pool-----

L	G	Solute	b	2.3b	S ² (b)	S ² (b)/b
5,000*	900	O ₂	-0.0083°C ⁻¹	-0.019°C ⁻¹	0.0008°C ⁻¹	10%
2,100*	900	H ₂	-0.0072°C ⁻¹	-0.016°C ⁻¹	0.0021°C ⁻¹	29%

*Repacked Column

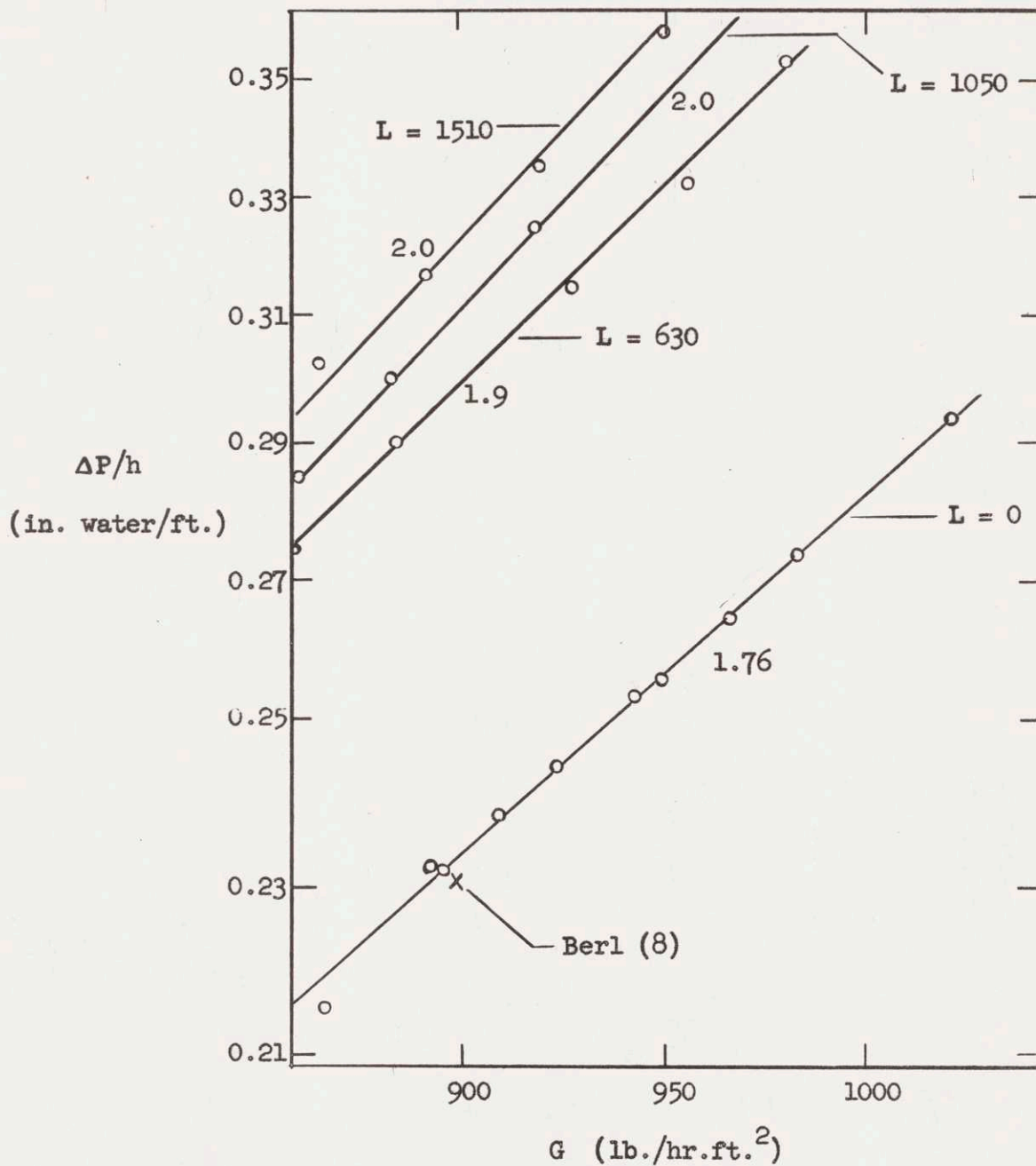


FIGURE 17.1 LOGARITHMIC PLOT OF TOWER PRESSURE DROP VS. AIR RATE

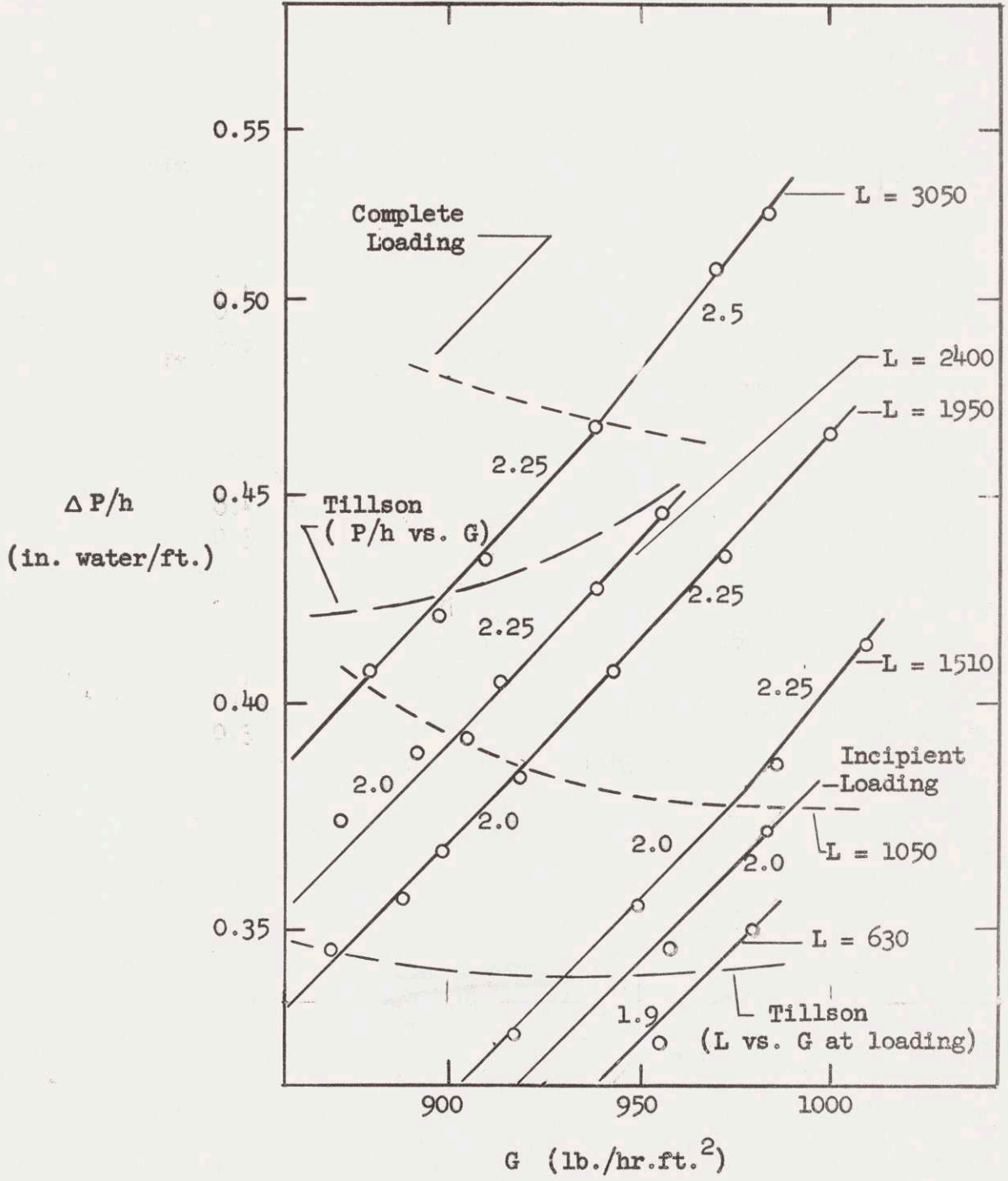


FIGURE 17.1 (CONT.)

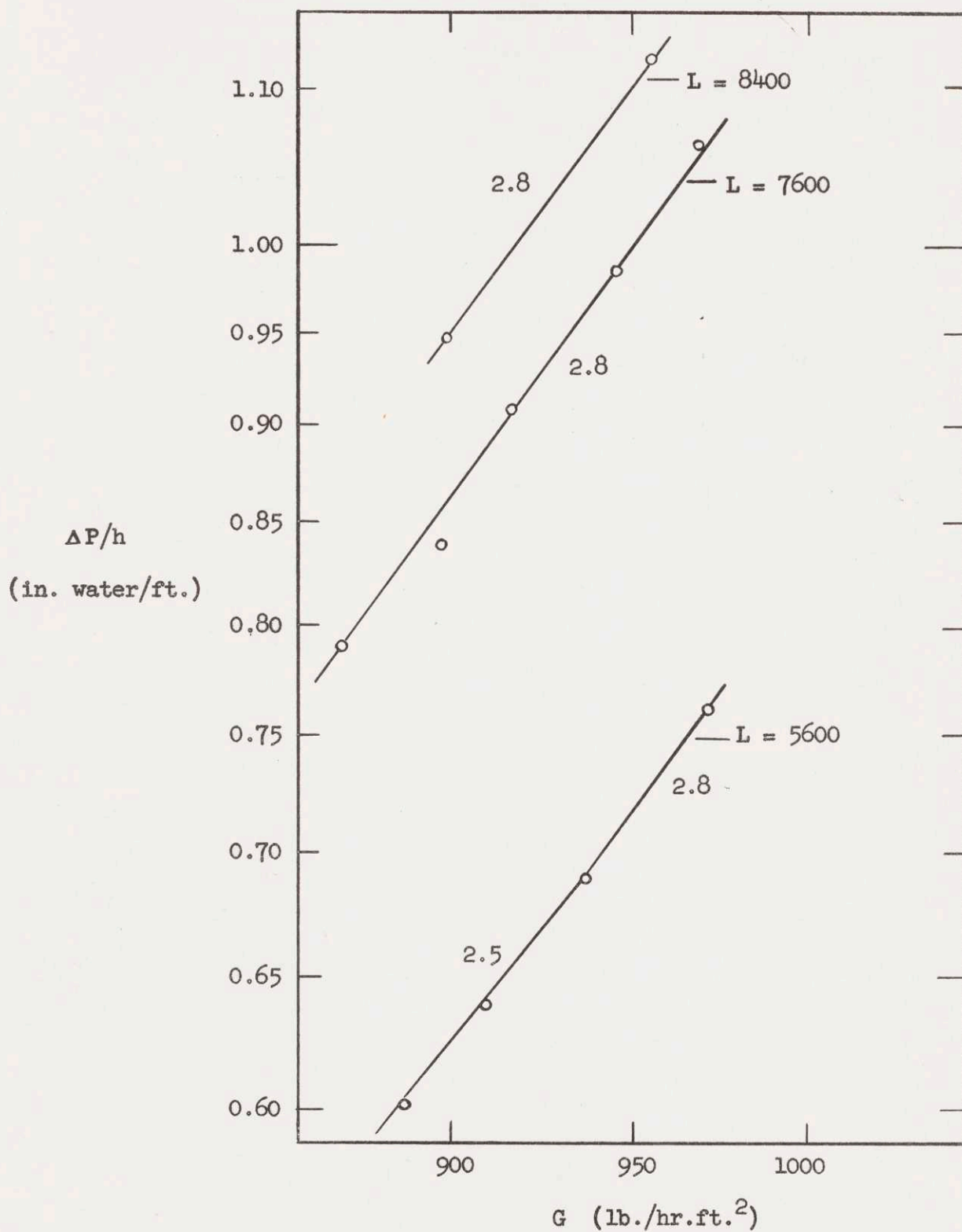


FIGURE 17.1 (CONT.)

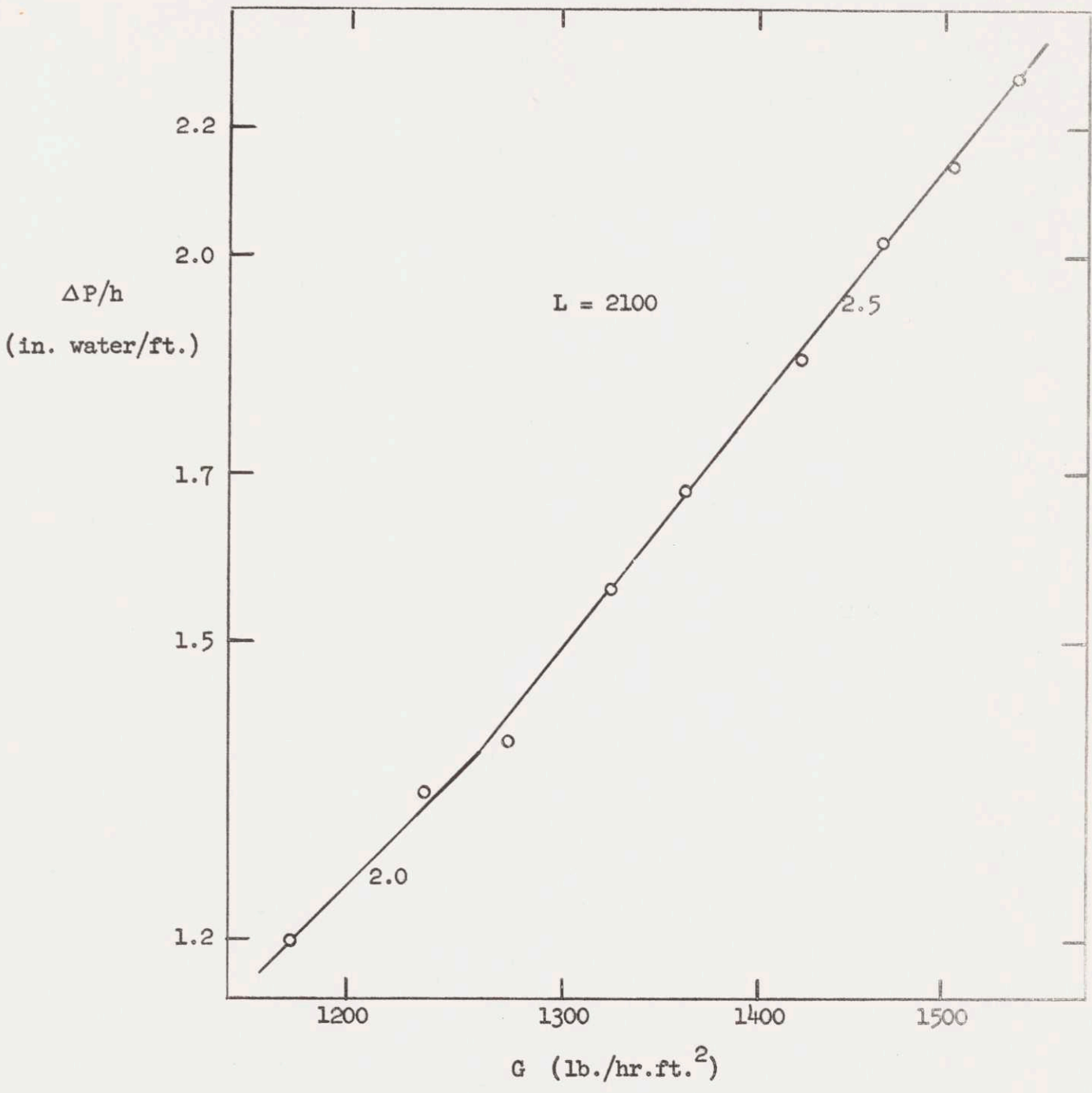


FIGURE 17.1 (CONT.)

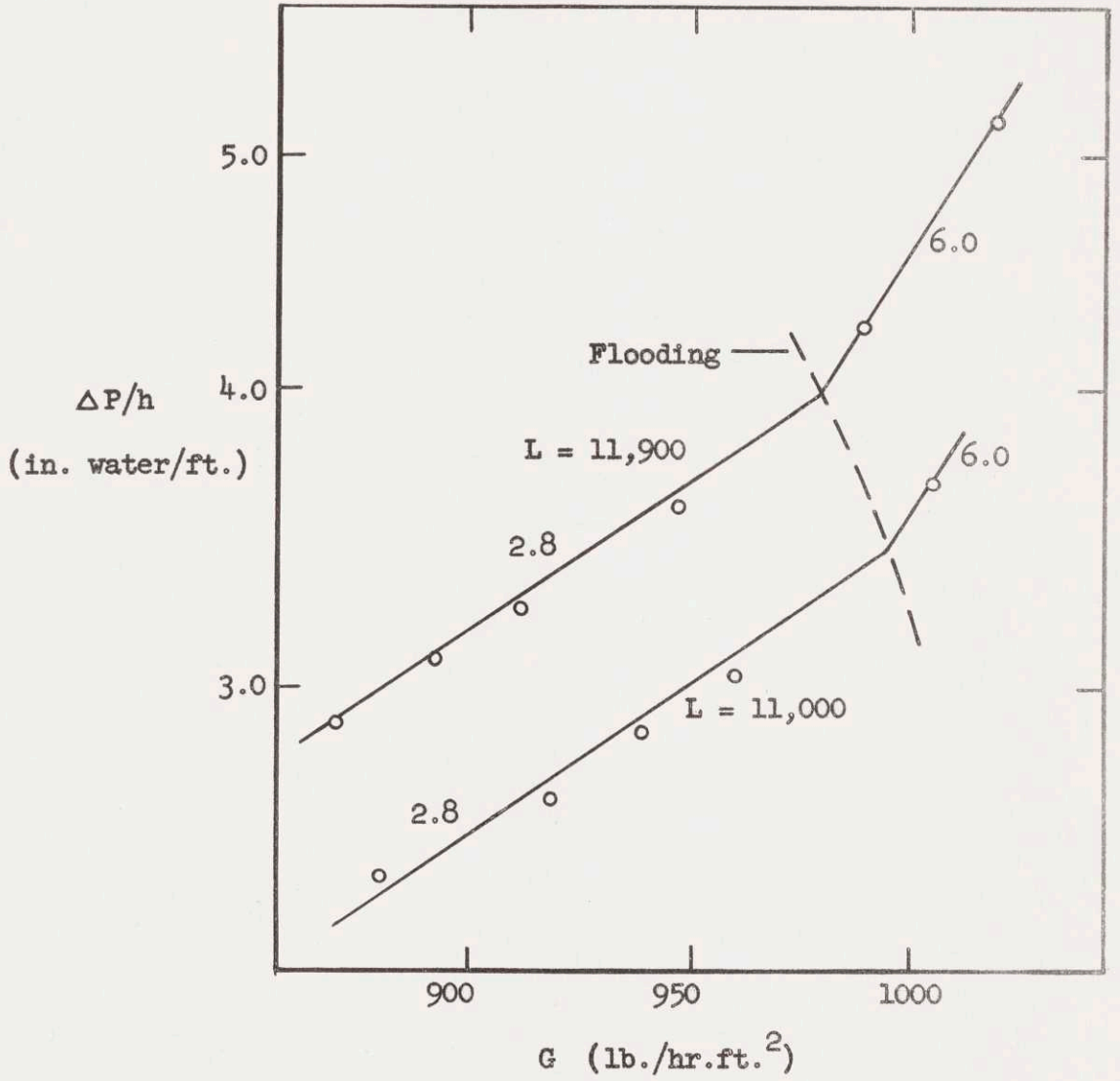


FIGURE 17.1 (CONT.)

CHAPTER 18RE-EXAMINATION OF THE OXYGEN DATA OF HOLLOWAY

The accuracy of Holloway's calculated oxygen transfer rates (61) has been thrown open to question for two reasons:

- 1) An equation (16.1.6) which was derived for the case of no change in interfacial equilibrium solute concentration was applied to cases where there was a significant change.
- 2) In instances when, either because of a small H.T.U. or because of a large packed height, the concentration driving force at the bottom of the tower becomes very small, there is a question of the reliability of the Winkler oxygen solubility data, upon which the calculated H.T.U.'s are based.

Holloway's liquid phase results are divided into two parts. In the first a single dump was studied (containing an equivalent six inches of end effect in eight inches of packed height) with primary attention being paid to the effects of temperature and different solute gases. In the second part many different packings were studied, with oxygen as the solute and the temperature being maintained constant at essentially 25°C.

The Part I results are of interest for comparison with the present data for the effects of temperature and of solute diffusivity.

All of Holloway's data were originally calculated using

$$(\text{N.T.U.})_{\text{OL}} = \ln \frac{(C_L - C_e)_T}{(C_L - C_e)_B}, \quad (16.1.6)$$

whereas the discussion of Section 16.1.2 shows that the correct value of $(\text{N.T.U.})_{\text{OL}}$ lies between the two bracketing values of

$$(\text{N.T.U.})_{\text{OL}} = \frac{C_T - C_B}{C_T - C_B - \epsilon} \ln \frac{(C_L - C_e)_T}{(C_L - C_e)_B} \quad (16.1.8)$$

and

$$(\text{N.T.U.})_{\text{OL}} = \ln \frac{(C_L - C_e)_T}{(C_L - C_e)_B - \epsilon} \quad (16.1.9)$$

where $\epsilon = C_{eT} - C_{eB}$.

In the case of Holloway's data, ϵ , when it has a significant value, usually does so primarily because of heat transfer to the air stream from the water and because of humidification (see Section 16.1.2). In the case of the present data most of the change in C_e through the tower comes from heat loss through the tower walls, an effect essentially linear in tower height and not linear in C_L . Heat transfer to the air stream and humidification occur primarily at the bottom of the tower and serve to accentuate the nonlinearity of C_e in C_L . This serves to make the correct value of $(\text{N.T.U.})_{\text{OL}}$ calculated from the raw data lie further away from Equation (16.1.8) in the direction of Equation (16.1.9). The magnitude

of this effect is derived in the following calculation for Holloway's Run 47, Part I:

Data for the run were as follows:

$$p_w: \text{ Top } = 22 \text{ mm}$$

$$\text{ Bottom } = 9 \text{ mm}$$

$$\text{ Water Temperature: Top } = 36.8^\circ\text{C}$$

$$\text{ Bottom } = 30.6^\circ\text{C}$$

$$X_T = 1.48 \times 10^{-5} \text{ lb O}_2/\text{lb H}_2\text{O}$$

$$X_{eT} = 0.70 \times 10^{-5} \text{ lb O}_2/\text{lb H}_2\text{O}$$

$$X_B = 0.830 \times 10^{-5} \text{ lb O}_2/\text{lb H}_2\text{O}$$

$$X_{eB} = 0.776 \times 10^{-5} \text{ lb O}_2/\text{lb H}_2\text{O}$$

$$\epsilon = -0.076 \times 10^{-5} \text{ lb O}_2/\text{lb H}_2\text{O}$$

$$L = 400 \text{ lb/hr ft}^2$$

$$G = 230 \text{ lb/hr ft}^2$$

Here ϵ is definitely significant, being of the same magnitude as the bottom driving force. The N.T.U. calculated by Holloway's equation (16.1.6) is 2.66; whereas those calculated by the bracketing equations, (16.1.8) and (16.1.9) are 2.38 and 1.79. Thus the 2.66 value is in error by at least 11%, an amount which can be important in the determination of the effect of temperature on the $(\text{H.T.U.})_{OL}$.

The total heat loss by the water may readily be calculated as

$$\text{Total heat loss} = (400 \text{ lb/hr ft}^2) \left(1 \frac{\text{Btu}}{\text{lb } ^\circ\text{F}}\right) (6.2 \times 1.8^\circ\text{F})$$

$$= 4500 \text{ Btu/hr ft}^2$$

The amount of this due to vaporization of water is also readily calculated.

$$\begin{aligned} \text{Vap. Loss} &= (230 \text{ lb/hr ft}^2) \left(\frac{1 \text{ lb-mol}}{29 \text{ lb}} \right) \left(\frac{22.9 \text{ m.f.}}{760} \right) \left(\frac{18 \text{ lb}}{\text{lb mol}} \right) \left(\frac{1042 \text{ Btu}}{\text{lb}} \right) \\ &= 2500 \text{ Btu/hr ft}^2 \end{aligned}$$

The amount of heat transfer occurring from the water stream may be estimated as follows: From the results of McAdams, Pohlentz, and St. John (89) the value of h_{Ga} for 1 inch carbon rings at these flow conditions is $150 \text{ Btu/hr ft}^3 \text{ } ^\circ\text{F}$. The value of h_{La} is 1200 in the same units, so h_{Ga} controls. Assuming that the effect of packing dimension on h_{Ga} is small (see e.g., (133f) by analogy to k_{Ga}), a combination rate expression and heat balance may be set up.

$$\begin{aligned} (150 \text{ Btu/hr ft}^3 \text{ } ^\circ\text{F})(1 \text{ ft height}) \Delta T_{lm} &= \\ &= (230 \text{ lb/hr ft}^2)(0.24 \text{ Btu/lb } ^\circ\text{F})(T_T - T_B) \end{aligned}$$

One foot is taken as the effective packed height, since Holloway found a lesser end effect on the same dump for gas phase transfer behavior than for liquid phase behavior. Since this run was apparently made in the winter, T_B may be taken as 18°C . Water temperature, for purposes of approximation, may be taken constant at 33°C . Then

$$\ln \frac{33 - T_B}{33 - T_T} = \frac{150}{(230)(0.24)} = 2.7$$

or

$$\frac{33 - 18}{33 - T_T} = 15$$

and $T_T = 32^\circ\text{C}$, corresponding to close equilibrium of air and water temperatures at the top.

The heat loss through transfer to the air stream is then

$$\begin{aligned} \text{Heat Transfer} &= (230 \text{ lb/hr ft}) (0.24 \text{ Btu/lb } ^\circ\text{F}) (14 \times 1.8^\circ\text{F}) \\ &= 1400 \text{ Btu/hr ft}^2 \end{aligned}$$

The heat loss from the column to the surrounding atmosphere was then, by difference

$$\begin{aligned} \text{Heat loss to atmosphere} &= 4500 - (2500 + 1400) \\ &= 600 \text{ Btu/hr ft}^2 \end{aligned}$$

Most (87%) of the heat effect on C_e therefore occurred through heat transfer to the air stream and vaporization, effects concentrated at the bottom rather than linear in height.

The true history of the $C_L - C_e$ curve through the column may now be approximated, assuming C_e linear in water temperature, in a manner analogous to that used in Section 16.1.2 for temperature linear in height.

The temperature effects due to vaporization and heat transfer are represented approximately in Figure 18.1 as functions of tower height as "decay" functions, characterized by the (H.T.U.) of either process. Thus, since to a first approximation, the water temperature drop due to heat transfer follows:

Per cent of total water temperature drop due to heat transfer \sim
 $\%$ of total heat transfer accomplished \sim increase in air temperature,
 the water temperature change due to heat transfer is denoted by a straight
 line semi-logarithmic plot of a pseudo-water temperature against tower
 height, with such a slope that $\Delta T_{\text{Bottom}} / \Delta T_{\text{Top}} = 15$, since

$$\frac{(T_{\text{air}} - T_w)_B}{(T_{\text{air}} - T_w)_T} = 15 \text{ (see previous page).}$$

Similarly, from Holloway's water vaporization results, the water ΔT due to vaporization is characterized by a semi-logarithmic plot vs. height such that $\Delta T_{\text{Bottom}} / \Delta T_{\text{Top}} = 3$ (since $(\text{H.T.U.})_G = 1.0$ ft and $e^{h/\text{H.T.U.}} = 3$). These two curves are shown in Figure 18.1.

If the small heat loss to the atmosphere is neglected, these two curves may be compounded in the proportion of the heat effect due to each to give an approximation of the temperature (and C_e) profile in the water stream. This profile and also the one for a linear variation of C_e in height are plotted in Figure 18.1.

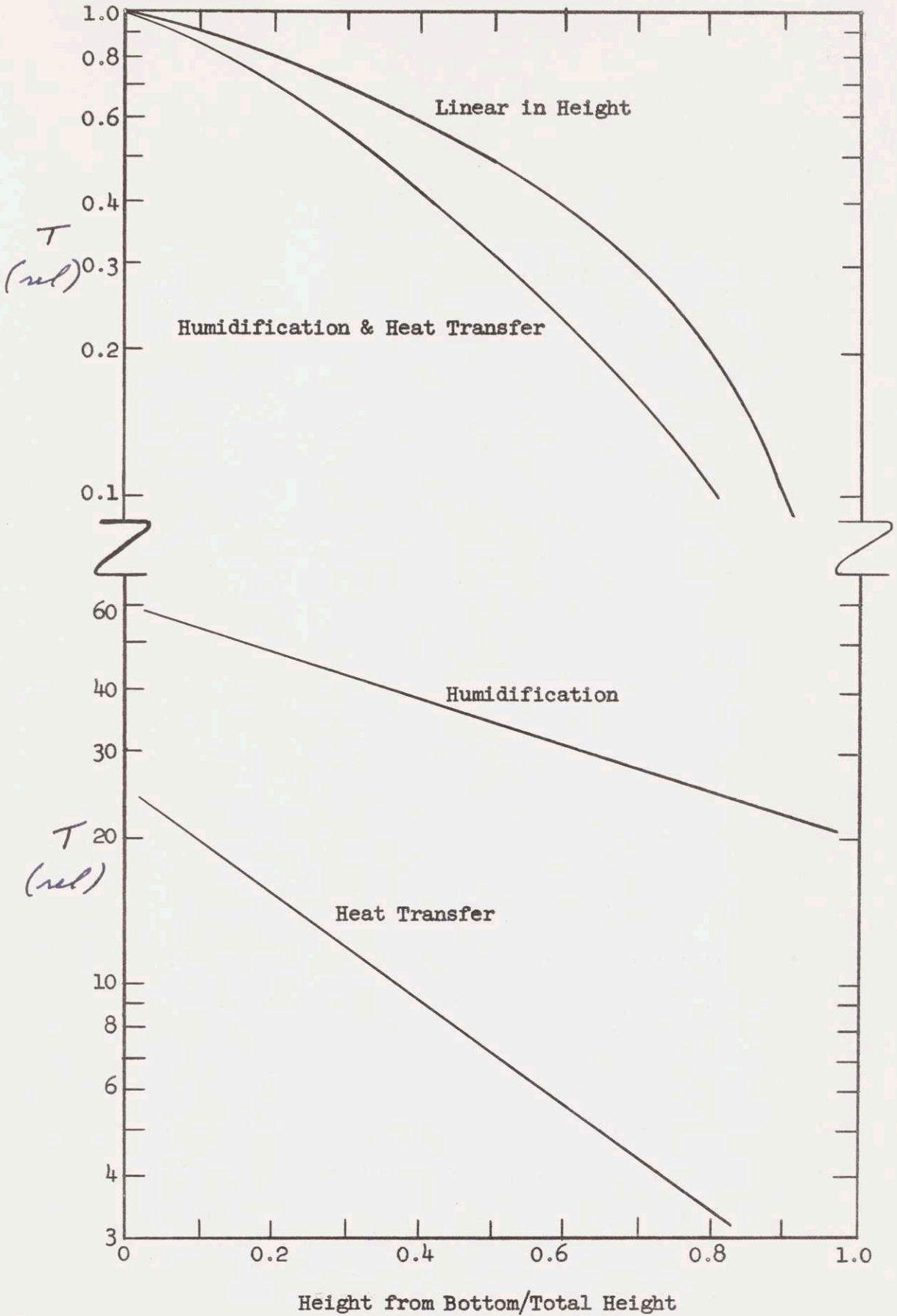


FIGURE 18.1 HEAT EFFECTS FROM HUMIDIFICATION & HEAT TRANSFER

In the exact same manner that was employed in Section 16.1.2, this C_e profile in height may be used to obtain plots of $C_L - C_e$ and $1/(C_L - C_e)$ vs. C_L . Figures 18.2 and 18.3 show this for Holloway's Run 47. Whereas a heat effect linear in height in this case gives an $(N.T.U.)_{OL}$ only about 15% between the two brackets, the effect of vaporization and heat transfer serves to make the $(N.T.U.)_{OL}$ lie about 25% of the distance, area-wise, between Equation (16.1.8) and Equation (16.1.9).

The 25% figure applies in general to Holloway's Part I data, as may be verified in this same manner for other runs. Table 18.1 presents Holloway's Part I temperature variation data recalculated by this criterion.

For the Holloway's Part II data, a correction of this sort rarely exceeds 1 or 2%, with some few exceptions, because the water temperature was held essentially constant and hence C_e did not vary so markedly as in Part I. Also, these corrections would affect all data more or less equally, with the slope of the $\log(H.T.U.)$ vs. $\log L$ plots for the various packings being unaffected. With a probable 10% variation of H.T.U. between various packed columns, such a correction in the absolute values of Holloway's H.T.U.'s would have little meaning.

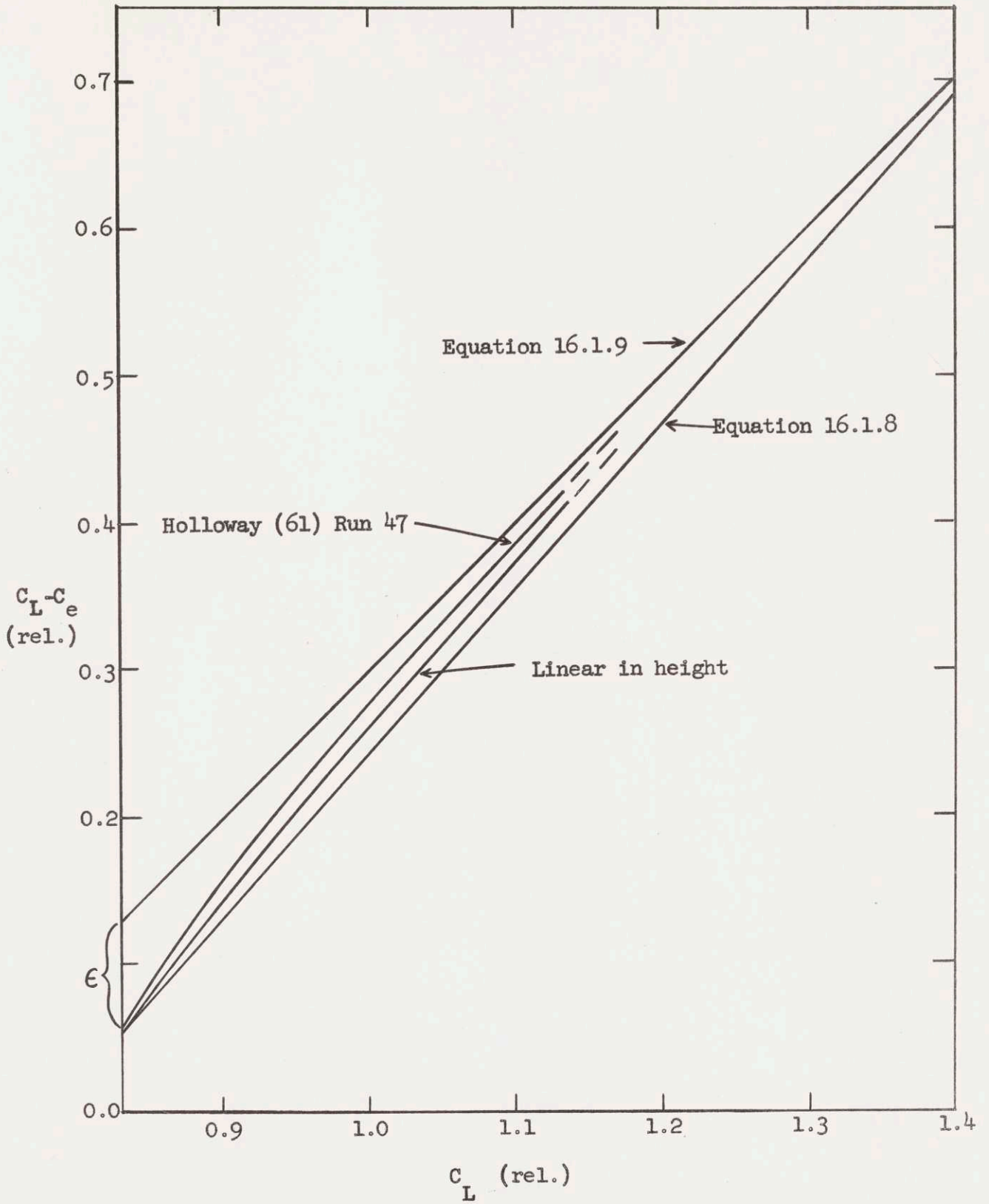


FIGURE 18.2 DRIVING FORCE PROFILE FOR HOLLOWAY RUN NO. 47

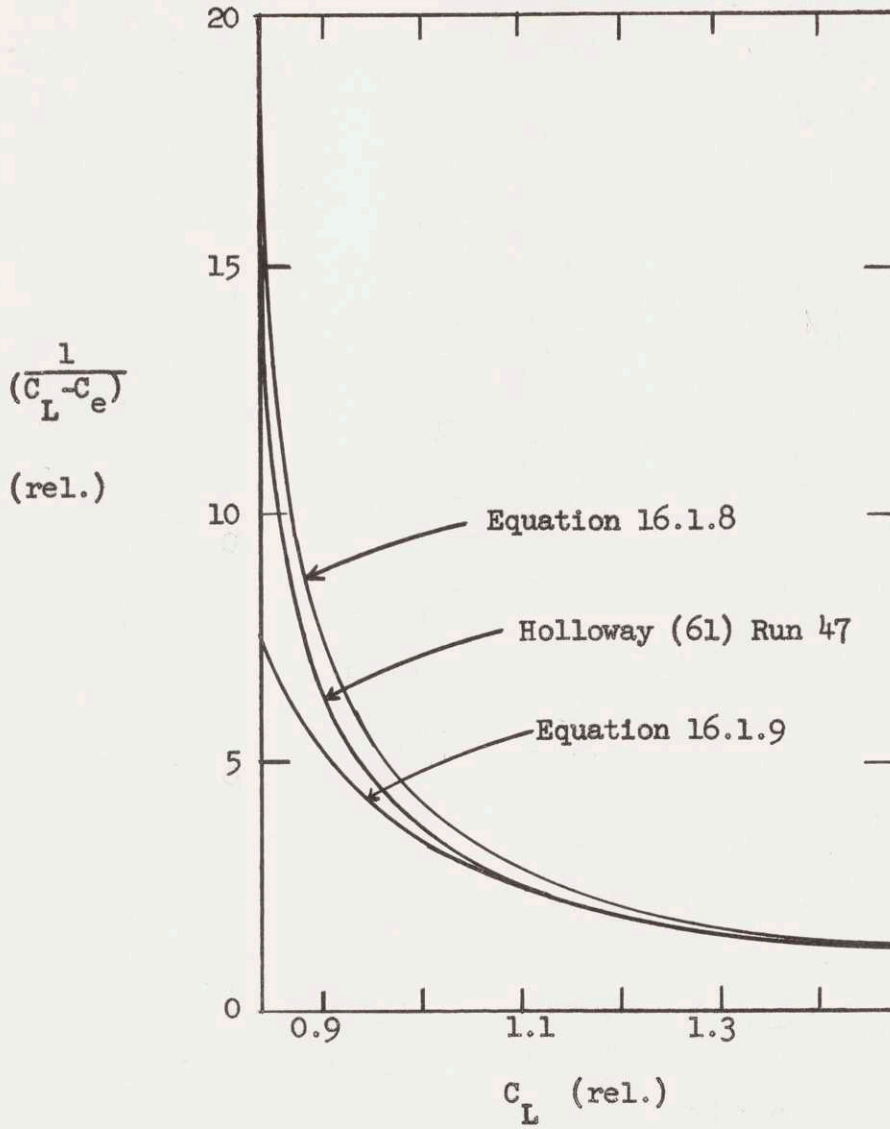


FIGURE 18.3 N.T.U. INTEGRAL FOR HOLLOWAY RUN NO. 47

TABLE 18.1

Re-calculation of Holloway's Part I Oxygen Data

(Values only Relative because of End Effect).

G = 230 in all runs

Run	L	Ave. T°C	(H.T.U.) _{Holloway} ft.	(H.T.U.) _{corr.} ft.	% corr.
22	440	10.0	0.47	0.46*	- 2
46	400	13.0	0.46	0.44	- 4
47	400	34.0	0.24	0.28	+16
48	400	25.5	0.32	0.34	+ 6
21	2,200	6.1	0.80	0.80**	-
32	2,000	37.0	0.39	0.43	+10
33	2,000	25.5	0.51	0.53	+ 4
34	2,000	32.5	0.44	0.46	+ 4
35	2,000	44.0	0.28	0.32	+12
36	2,000	19.3	0.57	0.57	-
41	10,000	8.8	1.11	1.10	- 1
43	10,000	37.4	0.59	0.64	+ 8
44	10,000	30.0	0.72	0.76	+ 5
45	10,000	17.0	0.94	0.94	-

* Corrected to L = 400

** Corrected to L = 2000

As was mentioned at the beginning of this chapter, another source of inaccuracy in Holloway's calculated results is the possible 1% error in the Winkler oxygen solubility data (see Section 5.1.2), which was used for calculations by Holloway and in the present study. To the extent that the $(C_L - C_e)$ driving force at the bottom of the tower is small in comparison with the absolute value of C_e , a small error in the solubility data can have a large effect on the resultant (N.T.U.) and (H.T.U.). In Holloway's work such a condition was approached in cases of comparatively

low values of H.T.U., and in instances of high packed heights. The percentage error in (H.T.U.) resulting from a 1% error in C_e may be estimated using Equation (5.1.2)

$$\frac{\Delta(\text{H.T.U.})_{\text{OL}}}{(\text{H.T.U.})_{\text{OL}}} = \frac{\Delta(\text{N.T.U.})_{\text{OL}}}{(\text{N.T.U.})_{\text{OL}}} = - \frac{(C_T - C_B)(C_e)}{(C_L - C_e)_T(C_L - C_e)_B(\text{N.T.U.})_{\text{OL}}} \cdot \frac{\Delta C_e}{C_e} \quad (5.1.2)$$

Since the error in C_e is expected to be about -1% (Section 5.1.2), the error in an H.T.U. for desorption calculated with a Winkler C_e is such as to give too high a value of H.T.U. For absorption an opposite effect occurs.

Table 18.2 summarizes the possible corrections in some of Holloway's typical H.T.U. values. The main variables affecting the correction are the magnitudes of the $(\text{H.T.U.})_{\text{OL}}$ and of packed height.

TABLE 18.2

Possible Corrections Of Holloway's Oxygen Data
for -1.0% Error Present in Winkler Data

Part I (Six inches of end effect)

<u>Run</u>	<u>Packed Height Inches</u>	<u>L</u>	<u>Packing in. R.R.</u>	<u>Calc. (H.T.U.)_{OL}</u>	<u>% Possible Correction</u>
47	8	400	1-1/2	0.28	-6
46	8	400	1-1/2	0.44	-1
43	8	10,000	1-1/2	0.64	-1
32	8	2,000	1-1/2	0.43	-3

TABLE 18.2

Part II

Run	Packed Height Inches	L	Packing in. R.R.	Calc.(H.T.U.) _{OL}	% Possible Correction
106	19.0	400	1-1/2	0.64	-3
112	19.0	8,000	1-1/2	1.22	-2.5
134	6.5	500	1-1/2	0.55	-2
80	49.0	4,000	1	0.96	-9
83	49.0	32,000	1	3.4	-1
90	17.0	4,000	1	0.96	-2
98	6.5	4,000	1	0.86	-1

In the Part I data the effect of the solubility error is small in all cases except for the lowest flow rate ($L = 400$) at high temperatures. Even in this case the effect on the best slope of the log H.T.U. vs. T curve (see Figure 5.6) would be for all intents and purposes insignificant.

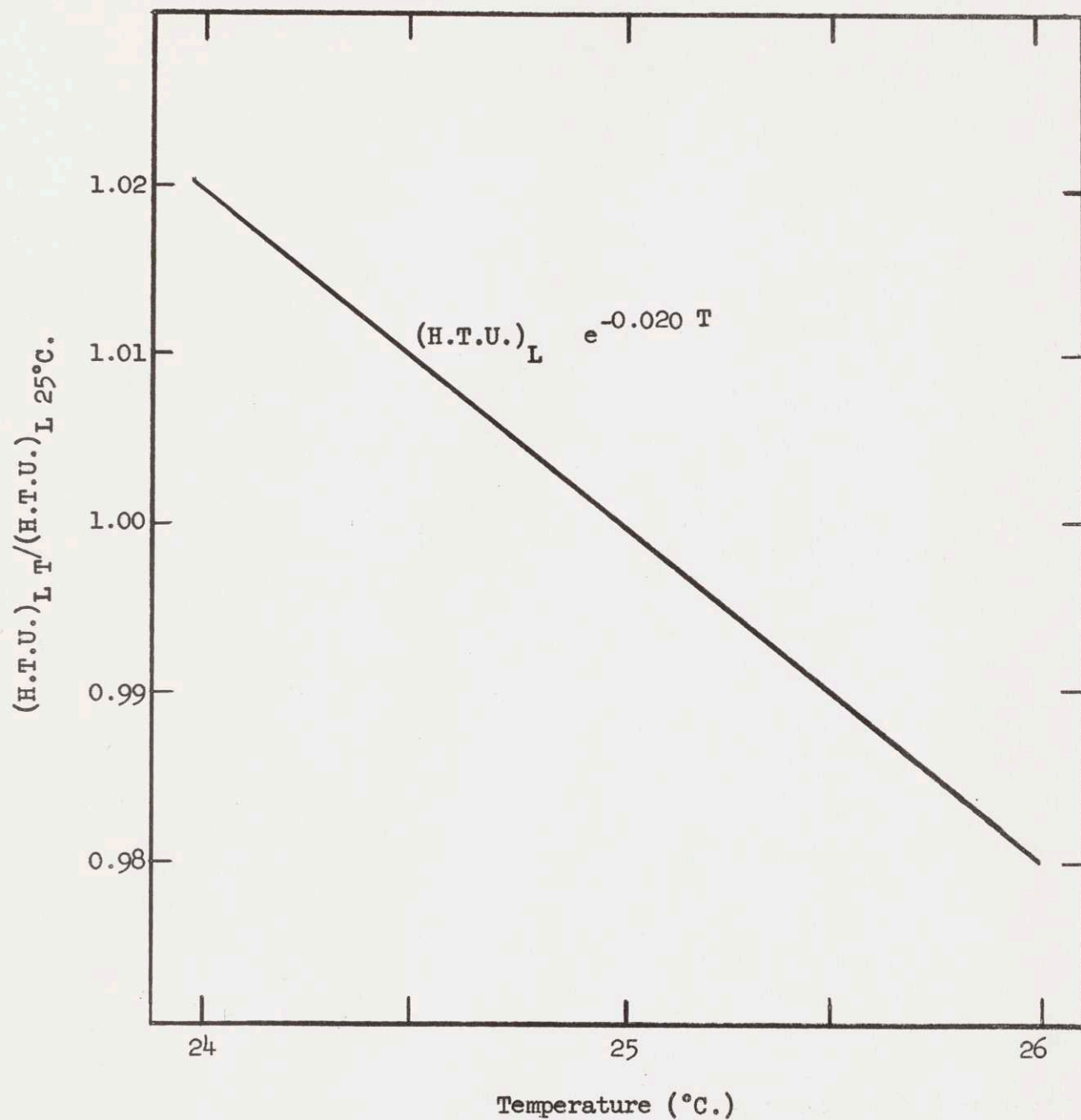
In his Part II studies Holloway measured rates for two different packed heights of 1-1/2 inch Raschig rings: 19 inches and 6.5 inches. As may be seen in Table 15.2, there is no great effect of solubility error on either the slope of H.T.U. vs. L at a particular height or on the relative values at the two heights in comparison with one another.

In the case of 1 inch Raschig rings, Holloway studied packed heights of 49 inches, 17 inches, and 6.5 inches, finding close agreement between the H.T.U.'s at the two larger heights, and 10 - 20% lower H.T.U.'s at the 6.5 inch height. As may be seen in Table 18.2 the principal effect of the solubility error would be to lower the H.T.U.'s for the larger height (49 inches) to values intermediate between those for the 17 inch and the 6.5 inch height. This 9% correction in the results for

49 inches of 1 inch Raschig rings is the largest correction emanating from a 1% solubility error applicable to Holloway's Part II results for various packings.

In summary, then, the main effect of taking C_e variation through the tower into account is to alter the variation of $(H.T.U.)_{OL}$ with temperature as shown in Table 18.1 and Figure 5.6, and the major effect of a -1% error in oxygen solubility is to place the values for a 49 inch height of 1 inch Raschig rings intermediate between those for a 17 inch height and a 6.5 inch height at lower water flow rates.

CHAPTER 19

MISCELLANEOUS PLOTSFIGURE 19.1 TEMPERATURE CORRECTION TO $(H.T.U.)_L$

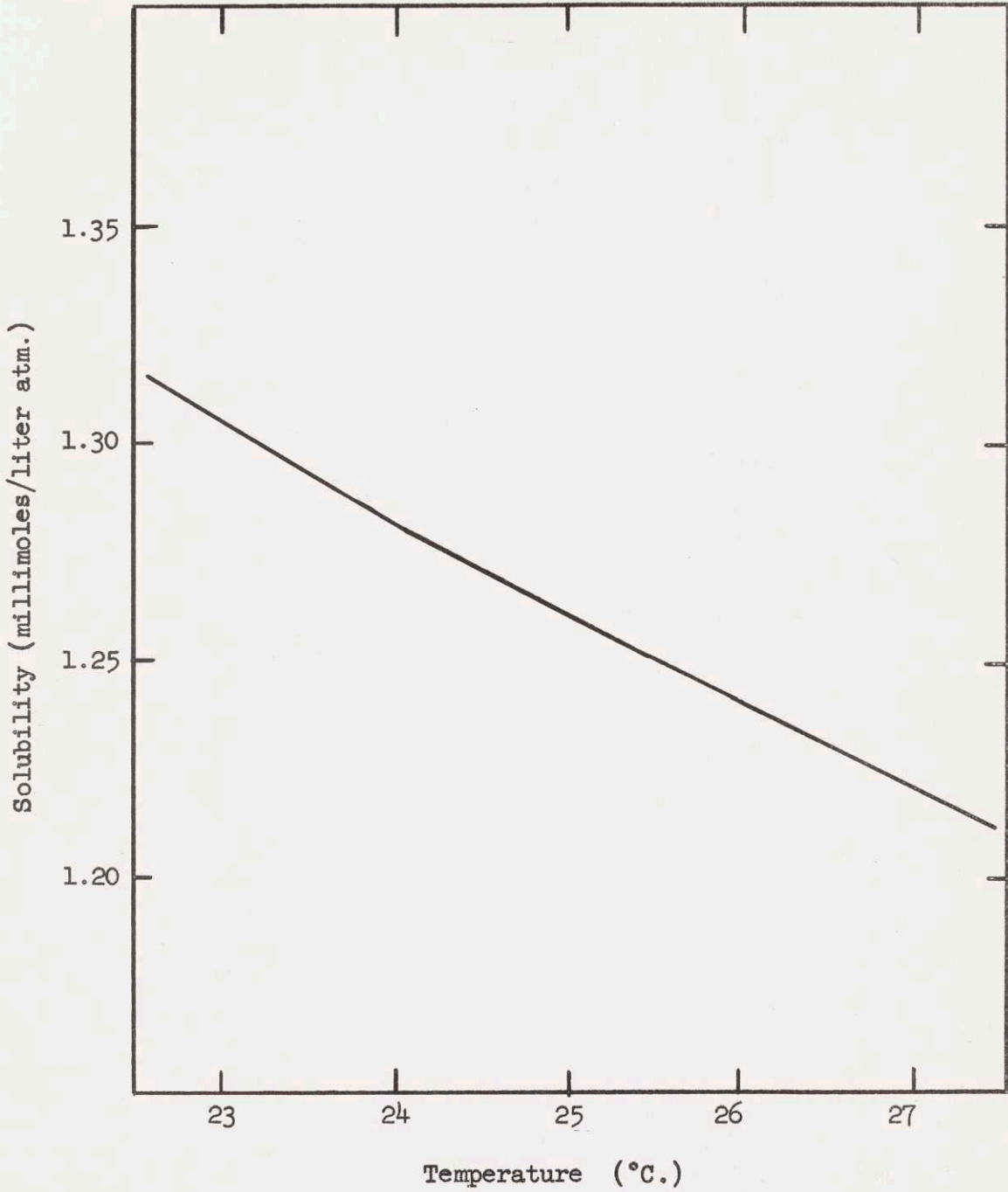


FIGURE 19.2 OXYGEN SOLUBILITY, DATA OF WINKLER (125)

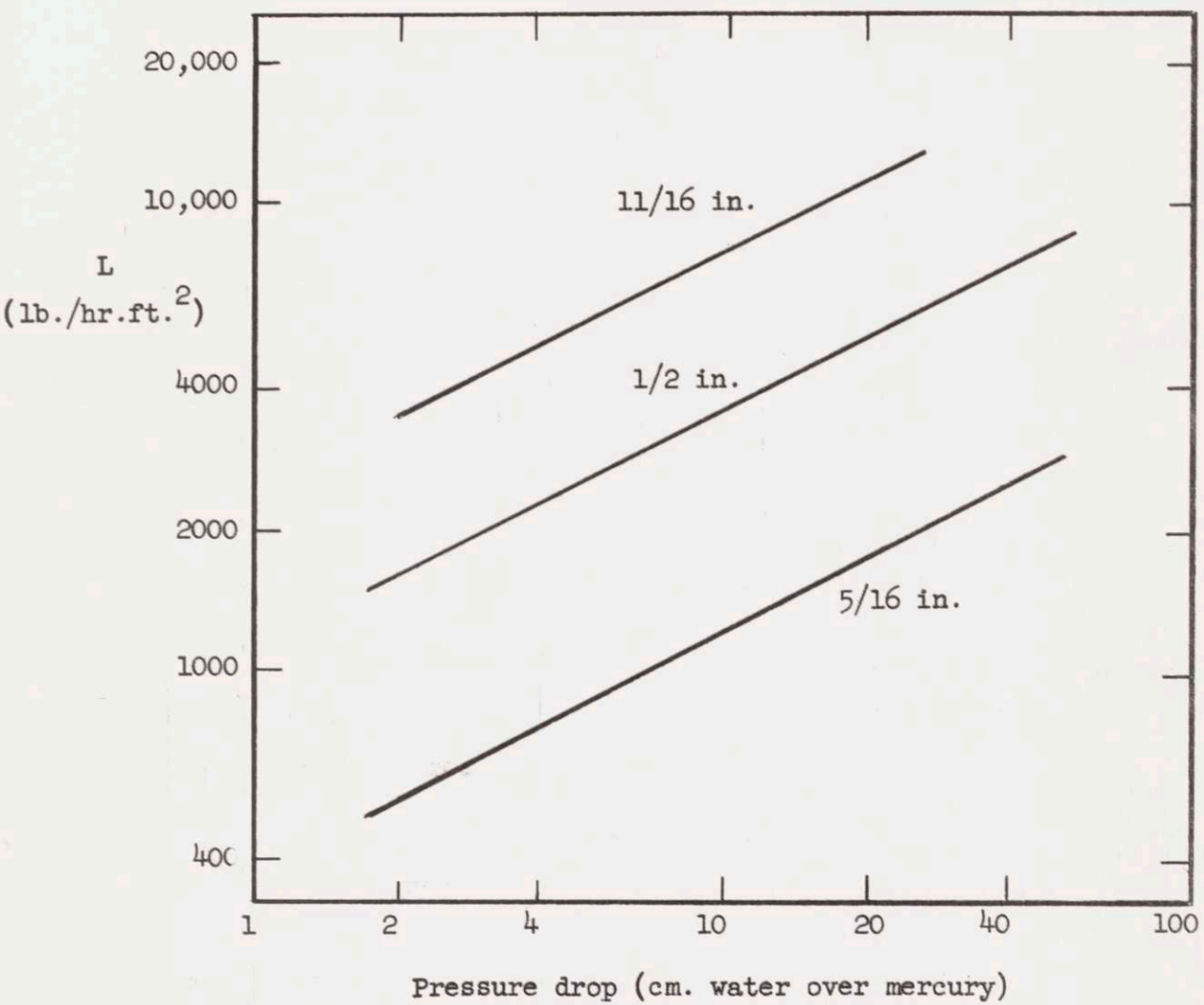


FIGURE 19.3 CALIBRATION OF WATER ORIFICES

CHAPTER 20NOMENCLATURE

- a = Total interfacial area between gas and liquid (area)
 a_e = Effective interfacial area = f_a (area)
 a_t = Total surface area of packing (area)
 A = Reacting solute (see Chapter 10)
 A_T = Cross sectional area of empty tower (area)
 b = Slope of line (see Chapter 16)
 C = Concentration of solute (moles/volume)
 = Orifice discharge coefficient (Section 16.3.6)
 C_1 = Concentration in rich side of diaphragm cell (Chapter 14)
 (moles/volume)
 C_2 = Concentration in lean side of diaphragm cell (Chapter 14)
 (moles/volume)
 C_A = Concentration of physically dissolved reacting solute
 (Chapter 10) (moles/volume)
 C_B = Solute concentration in liquid phase at tower bottom
 (moles/volume)
 C_e = Concentration of solute in liquid in equilibrium with
 solute partial pressure in bulk gas (moles/volume)
 C_G = Concentration of solute in bulk gas (moles/volume)
 C_{Gi} = Concentration of solute in gas at interface (moles/volume)
 C_i = Concentration of solute in liquid at interface (moles/volume)
 C_L = Concentration of solute in bulk liquid (moles/volume)
 C_m = Concentration at distance $m(\Delta y)$ from interface (moles/
 volume)

- C_{m+1} = Concentration at distance $(m+1)(\Delta y)$ from interface (moles/volume)
- C_n = Concentration at time $n(\Delta t)$ (moles/volume)
- C_{n+1} = Concentration at time $(n+1)(\Delta t)$ (moles/volume)
- C_R = Concentration of reactant in bulk liquid (moles/volume)
- C_T = Solute concentration in liquid phase at tower top (moles/volume)
- ΔC_f = Concentration difference in diaphragm cell at conclusion of run (moles/volume)
- ΔC_{lm} = Logarithmic mean concentration difference (moles/volume)
- ΔC_o = Concentration difference in diaphragm cell at initiation of run (moles/volume)
- d = Differential
 = Arbitrary length dimension (length)
- d_p = Nominal packing dimension (length)
- d_w = Tube diameter (length)
- D_A = Diffusivity of physically dissolved reacting solute (area/time)
- D_L = Diffusivity of solute in liquid phase (area/time)
- $D_{L \text{ int}}$ = Integral liquid phase diffusivity (see Section 14.5.2) (area/time)
- D_p = Diameter of sphere of same surface area as packing piece (length)
- D_R = Diffusivity of reactant in solution (area/time)
- D_v = Diffusivity of solute in gaseous phase (area/time)
- D_{2i} = Diameter of orifice (length)

- e = Base of natural logarithms
 $\text{erf}(x)$ = Error function = $\int_0^x \frac{2}{\sqrt{\pi}} e^{-x^2} dx$
 $\text{erfc}(x)$ = Complement of the error function = $1 - \text{erf}(x)$
 $\exp(x)$ = e^x
 E = Solute escape rate (see Chapter 12) (moles/time)
 f = Fraction of more active surface (see Chapter 8)
 = Fraction bulk water is saturated with desorbing solute
 (see Chapter 12)
 $F(x)$ = Function of x
 g = Acceleration due to gravity (length/time²)
 G = Bulk gas flow rate through tower (mass/time · empty tower
 cross sectional area)
 G_m = Bulk gas flow rate through tower (moles/time · empty tower
 cross sectional area)
 h = Tower height (length)
 = Absolute humidity (lb. water/lb. bone dry air)
 h' = Effective free fall height (length)
 h_{25} = Absolute humidity of saturated air at 25°C. (lb. water/
 lb. bone dry air)
 h_G = Gas phase coefficient for heat transfer (flux/degree)
 h_L = Liquid phase coefficient for heat transfer (flux/degree)
 h_o = Operating hold-up (volume/volume)
 h_t = Total hold-up (volume/volume)
 H = Henry's Law constant (atm. volume/moles)
 H_m = Level difference of manometer fluid (length)

- $(H.T.U.)_G$ = Height of individual gas phase transfer unit (length)
 $(H.T.U.)_L$ = Height of individual liquid phase transfer unit (length)
 $(H.T.U.)_{OG}$ = Height of overall gas phase transfer unit (length)
 $(H.T.U.)_{OL}$ = Height of overall liquid phase transfer unit (length)
 i = An individual value in a sequence
 J_D = Gas phase mass transfer factor (defined in Section 8.2.2)
 k = Defined by Equation 16.2.3
 k_G = Individual gas phase mass transfer coefficient (moles/area
time atm.)
 k'_G = Local value of k_G (i.e., at a point)
 k_G^* = k_G measured in the absence or suppression of liquid phase
resistance
 $k_G^{'*}$ = Local value of k_G measured in the absence or suppression
of liquid phase resistance
 k_{Gm} = Mean value of k_G over contact interval
 k_{GF}^a = k_G^a computed from K_G^a by two film additivity
 k_L = Individual liquid phase mass transfer coefficient (length/
time)
 k'_L = Local value of k_L (i.e., at a point)
 k_L^* = k_L measured in the absence or suppression of gas phase
resistance
 $k_L^{'*}$ = Local value of k_L Measured in the absence or suppression
of gas phase resistance
 k_{LS} = Transfer coefficient for surface resistance (length/time)
 k_L^a = k_L^a for infinite tower height
 K_G = Overall gas phase mass transfer coefficient (moles/area time
atm.)

- K'_G = Local value of K_G (i.e., at a point)
- K_L = Overall liquid phase mass transfer coefficient (length/time)
- K'_L = Local value of K_L (i.e., at a point)
- K_{LF} = Value of K_L predicted by two film additivity
- K_w = Range deviation factor
- l = Effective length of frit pores (Chapter 14) (length)
- = Any particular length (length)
- L = Liquid flow rate through tower (mass/ time · empty tower cross sectional area)
- L_m = Liquid flow rate through tower (moles/ time · empty tower cross sectional area)
- m = Solubility of gas in liquid (moles/volume atm.)
- = Quantity defined by Equation 16.2.4
- M = Molecular weight (mass/moles)
- = Dussinberre modulus = $(\Delta y)^2 / D_L \Delta t$
- N = Absorption rate per unit tower volume (moles/ time volume)
- = Biot modulus = $Hk_G \Delta y / D_L$
- N_A = Absorption rate per unit area (moles/time area)
- N'_A = Local value of N_A
- $(N.T.U.)_G$ = Number of transfer units based on individual gas phase driving force
- $(N.T.U.)_L$ = Number of transfer units based on individual liquid phase driving force
- $(N.T.U.)_{OG}$ = Number of transfer units based on overall gas phase driving force

- (N.T.U.)_{OL} = Number of transfer units based on overall liquid phase driving force
- Nu = Nusselt number
- p = Partial pressure (atm.)
- p_A = Partial pressure of reacting solute in gas phase (atm.)
- p_B = Partial pressure of solute at bottom of tower (atm.)
- p_{BM} = Mean pressure of inert gas throughout boundary layer (atm.)
- p_G = Partial pressure of solute in bulk gas (atm.)
- p_i = Partial pressure of solute in gas at interface (atm.)
- p_e = Partial pressure of solute in equilibrium with bulk liquid solute concentration (atm.)
- p_w = Vapor pressure of water (atm.)
- P = Total pressure (atm.)
- Δ P = Pressure drop (atm.)
- q_i = Volumetric flow rate through orifice (volume/time)
- Q = Volumetric flow rate (volume/time)
- r = Radius (length)
- R = Gas constant (atm. volume/moles degrees)
- = Ratio of phase resistances measured separately = $Hk_G a^* / k_L a^*$
- Re = Reynolds Number
- s = Danckwerts renewal rate constant (see Section 2.1.2)
- = Effective cross sectional area of frit pores (Chapter 11)
- (area)
- = Sample estimate of standard deviation
- s² = Sample estimate of variance
- s_m² = Sample estimate of variance from the true mean

s_w^2	= Range estimate of population variance
Sc	= Schmidt Number
t	= Time
	= Liquid surface age (time)
t_f	= Elapsed time during run (Chapter 14)
Δt	= Time increment (time)
T	= Temperature (degrees)
T_B	= Temperature of water at bottom of tower (degrees)
T_T	= Temperature of water at top of tower (degrees)
T_w	= Temperature of water (degrees)
u	= Linear velocity in direction of flow (length/time)
V	= Volume
V_1	= Volume of rich cell side
V_2	= Volume of lean cell side
V_B	= Bubble volume
V_C	= Flask volume (see Chapter 15)
V_s	= Solution sample volume (see Chapter 15)
w	= Range of data
W_i	= Weighting factor (see Chapter 16)
x	= Distance in direction of flow (length)
x_G	= Gas "film" thickness (length)
x_L	= Liquid "film" thickness (length)
X	= Solute concentration (mass of solute/mass of solution)
y	= Distance normal to interfacial surface (length)
Δy	= Increment in distance normal to interface (length)
Y	= Mole fraction in gas phase
	= Expansion factor (Chapter 16)

z = Height of cylinder (length)

Greek

- α = Constant in Equation 9.19 ($\text{ft}^{-1/2}$)
 = Density of air at room temperature & pressure / density
 of air at 25°C. and 1 atm.
- β = Cell constant = $2s / \ell V$
- β' = $\beta (1 - \lambda/6)$
- γ = Surface tension (force/length)
- Γ = Liquid flow rate per unit wetted perimeter (mass/length
 time)
- δ = K_L / K_{LF}
- Δ = An increment
- Δ = Deviation factor (see Chapter 9)
- ϵ = Fraction voidage in packing
 = $C_{eT} - C_{eB}$
- θ = Liquid surface lifetime (time)
- θ_1 = Lifetime of the more active surface (time)
- θ_2 = Lifetime of the less active surface (time)
- θ_i = Lifetime corresponding to a particular point of surface
 (time)
- κ = Thermal diffusivity (area/time)
- λ = $s \ell / V$ (see Chapter 14)
 = $(\theta_2 / \theta_1)^{1/2}$
- μ = Viscosity (mass/time length)
- ν = Kinematic viscosity (area/time)
 = $(1/2)(V_2/V_1 + 1)$ (see Equation 14.5.10)

π	= 3.14159...
ρ	= Density (mass/volume)
ρ_A	= Density of air (mass/volume)
ρ_L	= Liquid phase density (mass/volume)
ρ_M	= Density of manometer fluid (mass/volume)
ρ_{25}	= Density of air at 25°C.
σ	= Standard deviation (population)
σ^2	= Variance (population)
Σ	= Sum
τ	= Residence time of surface elements in tower (time)
φ	= k_L^* for chemical reaction/ k_L^* for physical absorption
Φ	= $k_L a^*$ for desorbing solute/ $k_L a^*$ for air (see Chapter 12)
χ	= Dissociation factor in Equation 14.1.1
ψ_i	= Fraction of surface reaching lifetime between θ_i and $\theta + d\theta_i$
ω	= Frequency of surface temperature disturbance in diaphragm cell
	(time ⁻¹)
ω'	= $(\omega / \kappa)^{1/2}$ (length ⁻¹)

CHAPTER 21REFERENCES

1. Adams, F.W. & R.G. Edmonds, Ind. Eng. Chem., 29, 497 (1937).
2. Aikazyan, E.A. & A.I. Federova, Dokl. Acad. Nauk. S.S.S.R., 86, 1137 (1952). Cited by Chem. Abstr., 47, 5768h (1953).
3. Aladyev, I.T., NACA TM 1356 (1954).
4. Allen, H.V., S.M. Thesis in Chemical Engineering, M.I.T. (1938).
5. Baker, T., T.H. Chilton & H.C. Vernon, Trans. A.I.Ch.E., 31, 296 (1935).
6. Barnes, C., Physics, 5, 4 (1934).
7. Bergholt, J. E., S.M. Thesis in Chemical Engineering, M.I.T. (1959).
8. Berl, W.G., cited by A.M. White, Trans. A.I.Ch.E., 31, 390, (1935).
9. Brauer, H., Chem. Ing. Tech., 29, 785 (1957).
10. Brian, P.L.T., Sc. D. Thesis in Chemical Engineering, M.I.T. (1956).
11. Carlson, T., J. Am. Chem. Soc., 33, 1027 (1911).
12. Carlson, T., J. Chim. Phys., 9, 228 (1911).
13. Carslaw, H.S. & J.C. Jaeger, Conduction of Heat in Solids, 2nd ed., Clarendon Press, Oxford (1959).
 - a. pp. 59 - 62.
 - b. pp. 70 - 73.
 - c. p. 201.
 - d. pp. 282 ff.
14. Chang, S.Y., S.M. Thesis in Chemical Engineering, M.I.T. (1949).
15. Chiang, S. H. & H.L. Toor, A.I.Ch.E. Jour., 5, 165 (1959).
16. Chu, J.C., J. Kalil & W.A. Wetteroth, Chem. Eng. Prog., 49, 141 (1953).
17. Crank, J., The Mathematics of Diffusion, Clarendon Press, Oxford (1956).
18. Cullen, E. J. & J.F. Davidson, Trans. Far. Soc., 53, 113 (1957).
19. Danckwerts, P.V., Trans. Far. Soc., 46, 300 (1950).

20. Danckwerts, P.V., Trans. Far. Soc., 46, 701 (1950).
21. Danckwerts, P.V., Ind. Eng. Chem., 43, 1460 (1951).
22. Danckwerts, P.V., A.I.Ch.E. Jour., 1, 456 (1955).
23. Davidson, J.F. & E.J. Cullen, Trans. Instn. Chem. Eng. (London), 35,
51 (1957).
24. Davies, O.L., ed., Statistical Methods in Research and Production,
Oliver & Boyd, London (1957).
a. pp. 173 - 174.
25. Dawson, C.R., J. Am. Chem. Soc., 55, 432 (1933).
26. Dean, R.B. & W.J. Dixon, Anal. Chem., 23, 4, 636 (1951).
27. Deed, D.W., P.W. Schutz & T.B. Drew, Ind. Eng. Chem., 39, 766 (1947).
28. Deissler, R.G., NACA TN 3016 (1953).
29. Deissler, R.G., NACA TR 1210 (1955).
30. Deissler, R.G. & C.S. Eian, NACA TN 2629 (1952).
31. Deryagin, B.V., P.S. Prokhorov & A.D. Malkina, Zhur. Fiz. Khim., 24,
503 (1950). Cited by Chem. Abstr., 44, 8184h (1950).
32. Dukler, A.E. & O.P. Bergelin, Chem. Eng. Prog., 48, 557 (1952).
33. Dusinberre, G.M., Numerical Analysis of Heat Flow, McGraw-Hill,
New York (1949).
34. Dwight, H.B., Tables of Integrals and Other Mathematical Data, Macmillan,
New York (1947).
35. Dwyer, O.E. & B.F. Dodge, Ind. Eng. Chem., 33, 485 (1941).
36. Emmert, R.E., Sc. D. Thesis in Chemical Engineering, University of
Delaware (1954). Cited by Reference 10.
37. Emmert, R.E. & R.L. Pigford, Chem. Eng. Prog., 50, 87 (1954).
38. Fellingner, L., Sc. D. Thesis in Chemical Engineering, M.I.T. (1941).
39. Garner, F.H., Chem. Ind., 141 (1956).

40. Garner, F.H. & R.D. Suckling, A.I.Ch.E. Jour., 4, 114 (1958).
41. Gertz, K.H. & H.H. Loeschcke, Z. Naturforsch., 9b, 1 (1954);
11b, 61 (1956).
42. Gilliland, E.R., Ind. Eng. Chem., 26, 681 (1934).
43. Gilliland, E.R., R.F. Baddour & P.L.T. Brian, A.I.Ch.E. Jour., 4,
223 (1958).
44. Goldstein, D.J., Sc. D. Thesis in Chemical Engineering, M.I.T. (1956).
45. Goodgame, T.H., Sc. D. Thesis in Chemical Engineering, M.I.T. (1953).
46. Goodgame, T.H. & T.K. Sherwood, Chem. Eng. Sci., 3, 37 (1954).
47. Gordon, A.R., Ann. N.Y. Acad. Sci., 46, 285 (1945).
48. Gordon, K.F. & T.K. Sherwood, Chem. Eng. Prog. Symp. Ser., 10, 15
(1954).
49. Goryunova, N.A. & E.V. Kuvshinsky, Zhur. Tekh. Fiz., 18, 1421 (1948).
Cited by Chem. Abstr., 45, 9957a (1951).
50. Gosting, L.J., J. Am. Chem. Soc., 72, 4418 (1950).
51. Grimley, S.S., Trans. Instn. Chem. Eng. (London), 23, 228 (1945).
52. Habib, A.G., S.M. Thesis in Chemical Engineering, M.I.T. (1957).
53. Hagenbach, A., Wied. Ann., 65, 673 (1898).
54. Hammerton, D. & F.H. Garner, Trans. Instn. Chem. Eng. (London), 32,
s 18 (1954).
55. Handwerk, R.J., S.M. Thesis in Chemical Engineering, M.I.T. (1954).
56. Harned, H.S. & R.L. Nuttal, J. Am. Chem. Soc., 69, 736 (1947); 71,
1460 (1949).
57. Hartley, G.S. & D.F. Runnicles, Proc. Roy. Soc. (London), A168,
401 (1938).
58. Hensel, S.L. & R.E. Treybal, Chem. Eng. Prog., 48, 362 (1952).

59. Higbie, R. , Trans. A.I.Ch.E., 31, 365 (1935).
60. Howkins, J.E. & J.F. Davidson, A.I.Ch.E. Jour., 4, 324 (1958).
61. Holloway, F.A.L., Sc. D. Thesis in Chemical Engineering, M.I.T. (1939)
- a. pp. 179 - 181.
 - b. p. 184.
 - c. pp. 185 - 188.
 - d. p. 189.
 - e. pp. 190 - 191.
 - f. pp. 193 - 204.
 - g. pp. 208 - 209.
 - h. Appendix D.
 - i. Appendix G.
62. Houston, R.W. & C.A. Walker, Ind. Eng. Chem., 42, 1105 (1950).
63. Hufner, G., Wied. Ann., 60, 134 (1897).
64. Humble, L.V., W.H. Lowdermilk & L.G. Desmon, NACA TR 1020 (1951).
65. Hutchings, L.E., L.F. Stutzman & H.A. Koch, Chem. Eng. Prog., 45,
253 (1949).
66. International Critical Tables, U.S. Bureau of Standards (1930).
- a. Volume 4, p. 474.
 - b. Volume 5, p. 21.
67. Ipatieff, V.V. & V.P. Teodorovich, J. Phys. Chem. (U.S.S.R.), 10,
712 (1937).
68. Jenny, F.W., Sc. D. Thesis in Chemical Engineering, M.I.T. (1936).
See also Reference 133, pp. 339 - 342.
69. Johnstone, H.F. & R.L. Pigford, Trans. A.I.Ch.E., 38, 25 (1942).
70. Kafarov, V.V., J. Appl. Chem. (U.S.S.R.), 31, 699 (1958).
71. Kishinevsky, M.K., J. Appl. Chem. (U.S.S.R.), 24, 593 (1951).

72. Kishinevsky, M.K., J. Appl. Chem. (U.S.S.R.), 27, 359 (1954).
73. Kishinevsky, M.K. & M.A. Kerdivarenko, J. Appl. Chem. (U.S.S.R.), 24, 449 (1951).
74. Kishinevsky, M.K. & V.T. Serebryansky, J. Appl. Chem. (U.S.S.R.), 29, 29 (1956).
75. Knudsen, J.G. & D.L. Katz, Fluid Dynamics and Heat Transfer, McGraw-Hill, New York (1958).
- a. pp. 374 - 376.
- b. p. 395, pp. 400 - 403.
76. Koch, H.A., L.F. Stutzman, H.A. Blum & L.E. Hutchings, Chem. Eng. Prog., 45, 677 (1949).
77. Kolthoff, I.M. & C.S. Miller, J. Am. Chem. Soc., 63, 1013 (1941).
78. Kramers, H., R.A. Douglas & R.M. Ullmann, Chem. Eng. Sci., 10, 190 (1959).
79. Kreuzer, F., Helv. Physiol. Pharm. Acta, 8, 505 (1950).
80. Landau, R., C.E. Birchenall, G.G. Joris & J.C. Elgin, Chem. Eng. Prog., 44, 315 (1948).
81. Langmuir, I., Phys. Rev., 34, 421 (1912).
82. Lewis, J.B., J. Appl. Chem. (London), 5, 228 (1955).
83. Lewis, W.K. & W.G. Whitman, Ind. Eng. Chem., 16, 1215 (1924).
84. Littlewood, R. & E. Rideal, Trans. Far. Soc., 52, 1598 (1956).
85. Lorenz, L., Wied. Ann., 13, 582 (1881).
86. Lynch, E.J. & C.R. Wilke, A.I.Ch.E. Jour, 1, 9 (1955).
87. Lynn, S., J.R. Straatemeier & H. Kramers, Chem. Eng. Sci., 4, 58 (1955).
88. Lynn, S., J.R. Straatemeier & H. Kramers, Chem. Eng. Sci., 4, 63 (1955).
89. McAdams, W.H., J.B. Pohlentz & M.A. St. John, Chem. Eng. Prog., 45, 241 (1949).
90. McLachlan, N.W., Bessel Functions for Engineers, 2nd ed., Clarendon Press, Oxford (1955).
- a. pp. 141, 226.

91. Mickley, H.S., T.K. Sherwood & C.E. Reed, Applied Mathematics in Chemical Engineering, McGraw-Hill, New York (1958).
- a. Chapter 2.
 - b. Chapter 10.
92. Molstad, M.C., R.G. Abbey, A.R. Thompson & J.F. McKinney, Trans. A.I.Ch.E., 38, 410 (1942).
93. Molstad, M.C., J.F. McKinney & R.G. Abbey, Trans. A.I.Ch.E., 39, 605 (1943).
94. Molstad, M.C. & L.F. Parsley, Chem. Eng. Prog., 46, 20 (1950).
95. Moore, W., Physical Chemistry, 2nd ed., Prentice-Hall, Englewood Cliffs, N.J. (1955). Chapter 14.
96. Morris, J.C., J. Am. Chem. Soc., 68, 1692 (1946).
97. Morrison, T.J. & F. Billet, J. Chem. Soc. (London), 2033 (1948).
98. Nielson, J.M., A.W. Adamson & J.W. Cobble, J. Am. Chem. Soc., 74, 446 (1952).
99. Nijsing, R.A.T.O., R.N. Hendriksz & H. Kramers, Chem. Eng. Sci., 10, 88 (1959).
100. Northrup, J.N. & M.L. Anson, J. Gen. Physiol., 12, 543 (1928).
101. Olander, D.L., Sc. D. Thesis in Chemical Engineering, M.I.T. (1958).
102. Onda, K., E. Sada & Y. Murase, A.I.Ch.E. Jour., 5, 235 (1959).
103. Othmer, D.F., R.C. Kollman & R.E. White, Ind. Eng. Chem., 36, 963 (1944).
104. Othmer, D.F. & E.G. Scheibel, Trans. A.I.Ch.E., 37, 211 (1941).
105. Othmer, D.F. & M.S. Thakar, Ind. Eng. Chem., 45, 589 (1953).
106. Patterson, A. & H.C. Thomas, Quantitative Analysis, Holt, New York, (1952).
- a. p. 233.
 - b. p. 269.

107. Peaceman, D.W., Sc. D. Thesis in Chemical Engineering, M.I.T. (1951).
- a. Chapter 8.
 - b. Chapter 11.
 - c. Chapter 12.
 - d. Chapter 13.
108. Peclet, J.C.E., Traite de la Chaleur (1844). Chapter 8.
109. Perry, J.H., ed., Chemical Engineers' Handbook, 3rd ed., McGraw-Hill, New York (1950).
- a. p. 175.
 - b. p. 181.
 - c. pp. 400 - 406.
 - d. p. 676.
 - e. pp. 688 - 689.
110. Perry, R.H. & R.L. Pigford, Ind. Eng. Chem., 45, 1247 (1953).
111. Pircher, L., Helv. Physiol. Pharm. Acta, 10, 110 (1952).
112. Potter, O.E., Chem. Eng. Sci., 6, 170 (1957).
113. Quincy, R.R., S.M. Thesis in Chemical Engineering, M.I.T. (1951).
114. Raimondi, P. & H.L. Toor, A.I.Ch.E. Jour., 5, 86 (1959).
115. Rakestraw, N.W. & V.M. Emmel, Ind. Eng. Chem., Anal. Ed., 9, 344 (1937).
116. Reid, R.C. & T.K. Sherwood, The Properties of Gases & Liquids, McGraw-Hill, New York (1958).
- a. pp. 240 - 244.
 - b. Chapter 8.
117. Ringbom, A., Z. Anorg. Allgem. Chem., 238, 94 (1938).
118. Scheibel, E.G., Ind. Eng. Chem., 46, 2007 (1954).
119. Scheibel, E.G. & D.F. Othmer, Trans. A.I.Ch.E., 40, 611 (1944).
120. Schlichting, H., Boundary Layer Theory, Pergamon Press, London (1955).
- a. Chapter 14.

121. Schrage, R.W., A Theoretical Study of Interphase Mass Transfer,
Columbia University Press, New York (1953).
122. Scott, W.W., Standard Methods of Chemical Analysis, 5th ed.,
N.H. Furman, ed., Van Nostrand, New York (1939).
- a. p. 272.
 - b. p. 452.
 - c. p. 2075.
 - d. p. 2079.
123. Scriven, L.E. & R.L. Pigford, A.I.Ch.E. Jour., 4, 382 (1958).
124. Scriven, L.E. & R.L. Pigford, A.I.Ch.E. Jour., 4, 439 (1958).
125. Seidell, A., Solubilities of Inorganic and Metal Organic Compounds,
3rd ed., Van Nostrand, New York (1940).
126. Smerano, G., L. Riccoboni & A. Foffani, Gazz. Chem. Ital., 79, 395
(1949). Cited by Chem. Abstr., 43, 8823h (1949).
127. Sherwood, T.K., Ind. Eng. Chem., 17, 745 (1925).
128. Sherwood, T.K., F.C. Draemel & N.E. Ruckman, Ind. Eng. Chem., 29,
282 (1937).
129. Sherwood, T.K. & K.F. Gordon, A.I.Ch.E. Jour., 1, 129 (1955).
- 130. Sherwood, T.K. & F.A.L. Holloway, Trans. A.I.Ch.E., 36, 21 (1940).
131. Sherwood, T.K. & F.A.L. Holloway, Trans. A.I.Ch.E., 36, 39 (1940).
132. Sherwood, T.K. & A.J. Killgore, Ind. Eng. Chem., 18, 744 (1926).
133. Sherwood, T.K. & R.L. Pigford, Absorption and Extraction, 2nd ed.,
McGraw-Hill, New York (1952).
- a. p. 6.
 - b. p. 10.
 - c. pp. 75 - 80.
 - d. Chapter 5.
 - e. p. 228.

f. Chapter 8.

g. pp. 281 - 283.

h. Chapter 9.

134. Shilov, E.A. & S.N. Solodushenkov, C.R. Acad. Sci. URSS, 3, 17 (1936).
135. Shulman, H.L. & J.J. DeGouff, Ind. Eng. Chem., 44, 1915 (1952).
136. Shulman, H.L., C.F. Ullrich & N. Wells, A.I.Ch.E. Jour., 1, 247 (1955).
137. Shulman, H.L., C.F. Ullrich, A.Z. Proulx & J.O. Zimmerman, A.I.Ch.E. Jour., 1, 253 (1955).
138. Shulman, H.L., C.F. Ullrich, N. Wells & A.Z. Proulx, A.I.Ch.E. Jour., 1, 259 (1955).
139. Shulman, H.L. & J.E. Margolis, A.I.Ch.E. Jour., 3, 157 (1957).
140. Siegel, R. & E.M. Sparrow, A.I.Ch.E. Jour., 5, 73 (1959).
141. Stefan, J., S.B. Akad. Wiss. Wien. Math.-Naturwiss. Kl. Abt. I, 77 II, 371 (1878).
142. Stirba, C. & D.M. Hurt, A.I.Ch.E. Jour., 1, 178 (1955).
143. Stokes, R.H., J. Am. Chem. Soc., 72, 763 (1950).
144. Stokes, R.H., J. Am. Chem. Soc., 72, 2243 (1950).
145. Stokes, R.H., J. Am. Chem. Soc., 73, 3527 (1951).
146. Surosky, A.E. & B.F. Dodge, Ind. Eng. Chem., 42, 1112 (1950).
147. Taecker, R.G. & O.A. Hougen, Chem. Eng. Prog., 45, 188 (1949).
148. Tammann, G. & V. Jessen, Z. Anorg. Allgem. Chem., 179, 125 (1929).
149. Thomas, W.J. & S. Portalski, Ind. Eng. Chem., 50, 1081 (1958).
150. Tillson, P., S.M. Thesis in Chemical Engineering, M.I.T. (1939).
151. Toor, H.L. & J.M. Marchello, A.I.Ch.E. Jour., 4, 97 (1958).
152. Treadwell, F.P. & W.T. Hall, Analytical Chemistry, 9th ed., nvol. 2, John Wiley, New York (1942).

a. p. 521

b. p. 720.

c. p. 735.

153. van Krevelen, D.W. & P.J. Hoftijzer, Chem. Eng. Prog., 44, 529 (1948).
154. Vivian, J.E., Sc. D. Thesis in Chemical Engineering, M.I.T. (1945).
155. Vivian, J.E. & D.W. Peaceman, A.I.Ch.E. Jour., 2, 437 (1956).
156. Vivian, J.E. & R.P. Whitney, Chem. Eng. Prog., 43, 691 (1947);
44, 54 (1948).
157. Wendel, M.M. & R.L. Pigford, A.I.Ch.E. Jour., 4, 249 (1958).
158. Whitman, W. G., Chem. Met. Eng., 29, 146 (1923).
159. Whitman, W. G., & D.S. Davis, Ind. Eng. Chem., 16, 1233 (1924).
160. Whitney, R.P., Sc. D. Thesis in Chemical Engineering, M.I.T. (1945).
161. Whitney, R.P. & J.E. Vivian, Ind. Eng. Chem., 33, 741 (1941).
162. Whitney, R.P. & J.E. Vivian, Chem. Eng. Prog., 45, 323 (1949).
163. Wilke, C.R., Chem. Eng. Prog., 45, 218 (1949).
164. Wilke, C.R. & P. Chang, A.I.Ch.E. Jour., 1, 264 (1955).
165. Wintergerst, E., Ann. Physik., 4, 323 (1930).
166. Wroblewski, S. v., Ann. Phys. Chem., 2, 481 (1877).
167. Yoshida, F., Chem. Eng. Prog. Symp. Ser., 16, 59 (1955).
168. Yoshida, F. & T. Koyanagi, Ind. Eng. Chem., 50, 365 (1958).
169. Zabban, F.W. & B.F. Dodge, Chem. Eng. Prog. Symp. Ser., 10, 61 (1954).
170. Zeisberg, F.C., Chem. Met. Eng., 32, 326 (1925).

CHAPTER 22BIOGRAPHICAL NOTE

The author was born at Fort Monmouth, New Jersey, in September, 1934. He graduated from the Episcopal High School of Alexandria, Virginia, in 1952. From then until 1956 he attended Yale University, from which he obtained a B. E. degree in Chemical Engineering with Highest Honors. While at Yale he resided in Timothy Dwight College, was Managing Editor of The Yale Scientific Magazine, and held the James C. Greenway Scholarship for four years.

He entered M. I. T. in 1956 and was awarded the M. S. degree in Chemical Engineering in February, 1958, after having attended the Oak Ridge Engineering Practice School. Following that he began his doctorate research program. Throughout his graduate work he held fellowships from the General Electric Educational and Charitable Fund.

Since July, 1959, he has been an Assistant Professor of Chemical Engineering at M. I. T. and Director of the Bayway Station of the School of Chemical Engineering Practice, located at the Esso Standard refinery in Linden, New Jersey.

In June, 1957, he and the former Jeanne A. York of Guilford, Connecticut, were married. They have a daughter, Mary Elizabeth, born in March, 1959.